

Dissertation

Lara Schmittmann



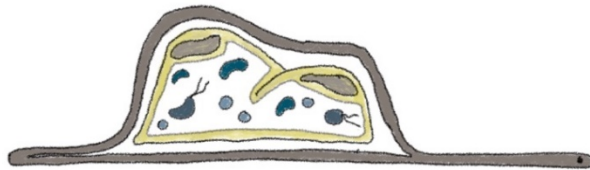
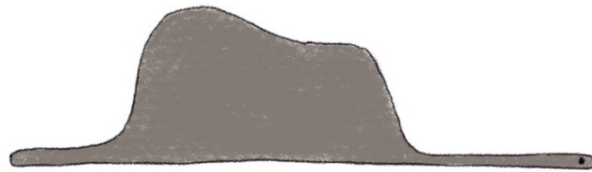
ESTABLISHING THE BREADCRUMB SPONGE
HALICHONDRIA PANICEA
AS AN EXPERIMENTAL MODEL
FOR SPONGE SYMBIOSES

DISSERTATION

zur Erlangung des Doktorgrades
der Mathematisch-Naturwissenschaftlichen Fakultät
der Christian-Albrechts-Universität zu Kiel

vorgelegt von
Lara Schmittmann
Kiel, 2021

L'essentiel est invisible pour les yeux.



inspired by
A. de Saint-Exupéry

Erste Gutachterin: Prof. Dr. Ute Hentschel Humeida

Zweiter Gutachter: Prof. Dr. Sebastian Fraune

Tag der mündlichen Prüfung: 01.02.2022

TABLE OF CONTENTS

Summary.....	2
Zusammenfassung.....	4
Introduction.....	7
Aims and Thesis Outline.....	23
Chapters	
Chapter 1.....	27
Chapter 2.....	47
Chapter 3.....	75
Chapter 4.....	97
Discussion.....	129
Final Conclusions.....	141
References.....	143
Acknowledgements.....	154
Appendix	
Appendix to Chapter 3.....	157
Appendix to Chapter 4.....	199
Eidesstattliche Erklärung	233

SUMMARY

Members of the early divergent metazoan phylum Porifera (sponges) are dependent on interactions with their complex, but stable and specific microbiomes. Sponges can potentially be important emerging model systems to study microbiome stability, colonization and possibly evolutionarily early mechanisms of the communication between animals and microbes. However, experimental approaches that allow the manipulation of sponge microbiomes are practically non-existing and this consequently limits our mechanistic and functional understanding of sponge-microbe symbiosis. Furthermore, gnotobiotic hosts have not been generated and microbial sponge symbionts remain unculturable to this date. In order to fill this gap, the overarching aims of my PhD thesis were to establish an experimental sponge-model using the breadcrumb sponge *Halichondria panicea* and to generate a toolbox to manipulate the host-microbe interaction. *H. panicea* is a promising candidate due to its wide distribution throughout the North Atlantic including the marginal seas and its high abundance in easily accessible coastal areas. Importantly, *H. panicea* is a low microbial abundance sponge with a specific, dominant symbiont, *Candidatus Halichondriabacter symbioticus* (Alphaproteobacteria) that amounts between 20-80% of the microbiome. Targeting the symbiosis between *H. panicea* and its associated bacteria experimentally promises to answer important questions on sponge-microbe interactions.

I approached the sponge holobiont by summarizing current knowledge on multispecies interactions within the host. I focused first on the host-side by exposing sponges to bacterial LPS and characterized their immune repertoire as well as induced immune response by RNAseq. The immune repertoire of *H. panicea* contained a diverse array of potential immune receptors that were expressed either in all sponge individuals or individual-specifically. LPS induced differential expression of genes mainly related to signaling and recognition. We suggest that *H. panicea* has context-dependent strategies of immune gene expression (constitutive vs inducible; ubiquitous vs individual-specific), reflecting the diverse roles of innate immunity in sponges. From the animal's perspective, a basal level of immune gene expression is needed to maintain a stable core microbiome while an inducible response is needed to respond to and distinguish between incoming seawater bacteria and potential pathogens.

I then approached the microbial side of the sponge holobiont. The microbiomes of local *H. panicea* populations were analyzed from different years and their stability in maintenance aquaria was assessed by 16S rRNA amplicon sequencing. The relative abundance of the dominant symbiont varied in wild caught specimens, but a seasonal effect was absent. Upon transfer to maintenance aquaria, microbiomes including the dominant symbiont *Ca. H. symbioticus* remained stable over six months of

cultivation. I then designed an experimental aquarium system in marine gnotobiotic chambers to culture sponges under sterile conditions and to remove sponge-associated bacteria with antibiotics. The experimental system was closed to prevent contamination and allowed exchange of sterile culture water. Bacterial community dynamics after antibiotic treatment were assessed with high temporal resolution both qualitatively (*16S* rRNA amplicon sequencing) and quantitatively (qPCR). Antibiotics induced repeatable shifts in community composition towards a dysbiotic state, that is defined as the disruption of microbiome homeostasis. Dysbiotic microbiomes were characterized by higher relative and absolute abundance of opportunistic, antibiotic-resistant bacteria. We then tested recolonization with the natural microbiome to recover dysbiotic microbiomes. This strategy was not successful, however single bacterial taxa were transferred from the bacterial inoculum to recolonized sponges (termed “recolonizers”). Relative bacterial abundance data suggested a strong decrease of the dominant symbiont after antibiotic treatment. However, together with absolute data we could uncover a high stability of *Ca. H. symbioticus* in spite of dysbiosis at the microbial community level. A core of few other symbionts that were most closely related to sponge- or other host-associated bacteria also persisted throughout dysbiosis (termed “persisters”). Bacterial co-occurrence analysis indicated that *Ca. H. symbioticus* is largely independent of microbe-microbe interactions. Therefore, I speculate that *Ca. H. symbioticus* may be mainly host-dependent and host-controlled. Overall, my findings contribute to an improved understanding of microbiome dynamics, host-microbe and microbe-microbe interactions in the *H. panicea* holobiont and experimentally reveal a stable symbiont core. I conclude that *H. panicea* and its dominant symbiont have the potential to be an experimental model for sponge-symbioses that can be used to disentangle aspects of co-evolution, symbiosis function and adaptation to variable environment.

ZUSAMMENFASSUNG

Porifera (Schwämme) gehören zu den evolutionär ältesten Metazoen und sind auf Interaktionen mit ihren komplexen, aber stabilen und spezifischen Mikrobiomen angewiesen. Schwämme können als Modellsysteme Fragen rund um Mikrobiomstabilität, Kolonisierungsprozesse und möglicherweise evolutionär alte Mechanismen der Kommunikation zwischen Tieren und Mikroben klären. Allerdings gibt es praktisch keine experimentellen Ansätze, um Schwamm-Mikrobiome zu manipulieren. Daher ist unser mechanistisches und funktionelles Verständnis der Schwamm-Mikroben-Symbiose eingeschränkt. Darüber hinaus gibt es bisher keine gnotobiotischen Wirte, und mikrobielle Schwammsymbionten sind bis heute nicht kultivierbar. Um diese Lücke zu schließen, waren die übergeordneten Ziele meiner Doktorarbeit (i) die Etablierung eines experimentellen Schwammmodells anhand des Brotkrumenschwamms *Halichondria panicea*, sowie (ii) die Entwicklung einer Toolbox um Schwamm-Mikroben-Interaktionen zu manipulieren. *H. panicea* bietet vielversprechende Möglichkeiten, da diese Art im gesamten Nordatlantik einschließlich der Rand- und Binnenmeere weit verbreitet ist und häufig in leicht zugänglichen Küstengebieten vorkommt. Eine Besonderheit ist, dass das Mikrobiom von *H. panicea* von einem spezifischen Symbionten dominiert wird, *Candidatus Halichondriabacter symbioticus* (Alphaproteobakterien). Dieser Symbiont macht zwischen 20-80 % des Mikrobioms aus. Experimentelle Ansätze, um den Holobiont *H. panicea* zu manipulieren, versprechen wichtige Fragen zu den Interaktionen zwischen Schwamm und Mikroben zu beantworten.

Ich habe mich zuerst mit dem Schwamm-Holobionten befasst, indem ich den aktuellen Wissensstand über artübergreifende Interaktionen innerhalb des Wirtes zusammengefasst habe. Dann habe ich mich zunächst auf die Wirtsseite konzentriert, und die induzierte Immunantwort von Schwämmen auf bakterielle LPS (Lipopolysaccharide) mittels RNAseq untersucht. Das allgemeine Immunrepertoire von *H. panicea* enthielt eine Vielzahl potenzieller Immunrezeptoren, die entweder in allen Schwammindividuen oder Individuen-spezifisch exprimiert wurden. LPS induzierte die differentielle Expression von Genen, die hauptsächlich eine Rolle in der Signalübertragung und -erkennung spielen. Wir vermuten, dass *H. panicea* über kontextabhängige Strategien der Immunexpression verfügt (konstitutiv vs. induzierbar; ubiquitär vs. Individuum-spezifisch), was die unterschiedlichen Rollen der angeborenen Immunität bei Schwämmen widerspiegelt. Aus der Sicht des Tieres wäre eine Grundexpression von Immungenen erforderlich, um ein stabiles Kernmikrobiom aufrechtzuerhalten, während eine induzierbare Reaktion erforderlich wäre, um auf Meerwasserbakterien und potenzielle Krankheitserreger zu reagieren und zwischen ihnen zu unterscheiden.

Anschließend habe ich mich mit der mikrobiellen Seite des Schwammholobionten befasst. Die Mikrobiome lokaler *H. panicea*-Populationen aus verschiedenen Jahren wurden analysiert, und ihre Stabilität in Hälterungsaquarien durch 16S rRNA-Amplikon-Sequenzierung bewertet. Die relative Häufigkeit des dominanten Symbionten variierte in Exemplaren aus dem Freiland, ein saisonaler Effekt war jedoch nicht zu erkennen. Nach der Überführung in Hälterungsaquarien waren die Mikrobiome einschließlich des dominanten Symbionten *Ca. H. symbioticus* über sechs Monate hinweg stabil. Im nächsten Schritt habe ich ein experimentelles Aquariensystem in marinen, gnotobiotischen Klimakammern entworfen, um Schwämme unter sterilen Bedingungen zu kultivieren und Schwamm-assoziierte Bakterien mit Antibiotika zu entfernen. Das experimentelle Aquariensystem war geschlossen, um Kontamination zu verhindern, und ermöglichte den automatischen Austausch von sterilem Kulturwasser. Änderungen im Mikrobiom nach der Antibiotikabehandlung wurden mit hoher zeitlicher Auflösung sowohl qualitativ (16S rRNA-Amplikon-Sequenzierung) als auch quantitativ (qPCR) untersucht. Antibiotika führten zu replizierbaren Veränderungen in der Mikrobiomzusammensetzung hin zu einem dysbiotischen Zustand, der als Abweichung vom gesunden Zustand des Mikrobioms definiert ist. Dysbiotische Mikrobiome waren durch eine höhere relative und absolute Abundanz opportunistischer, antibiotikaresistenter Bakterien gekennzeichnet. Wir haben versucht, die Dysbiose durch Rekolonisierung mit dem natürlichen Mikrobiom zu reversieren. Diese Strategie war nicht erfolgreich, jedoch wurden einzelne Bakterientaxa aus dem bakteriellen Inokulum auf rekolonisierte Schwämme übertragen (als "recolonizers" bezeichnet). Die relativen Bakterienhäufigkeiten deuteten auf einen starken Rückgang des dominanten Symbionten nach der Antibiotikabehandlung hin. Zusammen mit den absoluten Daten konnten wir jedoch eine hohe Stabilität von *Ca. H. symbioticus* trotz der Dysbiose auf Mikrobiomebene feststellen. Ein Kern bestehend aus wenigen anderen Symbionten, die am engsten mit Schwamm- oder anderen wirtsassoziierten Bakterien verwandt waren, blieb ebenfalls während der Dysbiose bestehen (als "persisters" bezeichnet). Eine Netzwerkanalyse zeigte, dass *Ca. H. symbioticus* weitgehend unabhängig von Mikroben-Mikroben-Interaktionen ist. Daher spekuliere ich, dass *Ca. H. symbioticus* hauptsächlich wirtsabhängig und wirtskontrolliert sein könnte. Insgesamt tragen meine Ergebnisse zu einem besseren Verständnis der Mikrobiomdynamik sowie der Wirt-Mikroben- und Mikroben-Mikroben-Interaktionen im Holobionten *H. panicea* bei und enthüllen experimentell einen stabilen Symbiontenkern. Ich komme zu dem Schluss, dass *H. panicea* und sein Hauptsymbiont das Potenzial haben, ein experimentelles Modellsystem für Schwamm-Symbiosen zu sein, um Aspekte der Koevolution, der Symbiosefunktion und der Anpassung an variable Umgebungen zu enträtseln.

INTRODUCTION

SYMBIOSES AS A PARADIGM OF METAZOAN EVOLUTION

Symbioses with prokaryotes are a key aspect of all life on Earth. Without microbes, multicellular life might have never evolved in the first place (McFall-Ngai *et al.*, 2013; Kolodny *et al.*, 2020). However, unicellular, prokaryotic life in the ocean dominated much of the earth's history after it first appeared ~3.5 billion years ago. Only about 1.5 billion years ago did the first eukaryotic cells evolve as a result of endosymbiosis (Margulis, 1970; Archibald, 2015). However, it was still a long way until the emergence of multicellular organisms. Interestingly, multicellular-like behavior were already detected in prokaryotes, whereby biofilm formation is regulated by genes that are also involved in embryonic development (Futo *et al.*, 2021). Choanoflagellates are the closest unicellular relatives to metazoans (Schalchian-Tabrizi *et al.*, 2008) and are flagellated cells that can switch between their unicellular state and multicellular assemblages. Strikingly, bacterial lipids are involved in both the induction as well as inhibition of rosette formation (Alegado *et al.*, 2012; Woznica *et al.*, 2016). Further, sexual choanoflagellate reproduction is inducible by a bacterial protein (Woznica *et al.*, 2017). Thus, bacteria control key eukaryotic mechanisms that preceded the evolution of multicellular animals.

Its estimated that multicellular eukaryotes evolved comparatively recently in terms of Earths age, somewhere between 600 million years ago (Li *et al.*, 1998) and 890 million years ago (Turner, 2021), but, they were never "alone". All metazoans are considered metaorganisms or holobionts, which acknowledges the permanent association of a metazoan with microorganisms (Bell, 1998; Zilber-Rosenberg and Rosenberg, 2008; Bosch and Mcfall-ngai, 2011). The concept of nested ecosystems (McFall-Ngai *et al.*, 2013; Pita *et al.*, 2018b) expands this to the environmental level and understands a metaorganism as an ecosystem in itself that is nested in its local environment which is again nested in the broader ecosystem.

Intimate symbioses expand the metabolic capacity of the single organism and determine the metaorganism phenotype. From the microbe's perspective, the host provides a protected habitat, nutrients, and other metabolites. From the hosts perspective, microbes provide metabolites and protection from pathogens. Only recently the importance for all aspects of biology has been recognized although symbiosis is a long-known concept (Gilbert *et al.*, 2012) including neurobiology (gut-brain axis) (Sharon *et al.*, 2016), animal metamorphosis (Cavalcanti *et al.*, 2020) and development (Bosch and McFall-Ngai, 2021), host evolution (Kolodny et al 2020), and phenotypic plasticity (Kolodny and Schulenburg, 2020).

Different metaorganisms engage in different types of symbioses. The host-associated microorganisms can include complex communities of bacteria, archaea, fungi, protists and viruses, the composition of which tends to differ between host species. Symbionts can be highly specific for their host as in the

interaction between *Vibrio* bacteria and the Hawaiian bobtail squid (Nyholm and McFall-Ngai, 2021; Visick *et al.*, 2021)). In other cases, symbiont taxonomic affiliation is less strictly controlled and assembly is dependent on the environment (e.g., *Caenorhabditis elegans*, (Johnke *et al.*, 2020)). Diversity of host-associated microbiomes ranges from few taxa (e.g., honeybees (Engel *et al.*, 2012)) to extremely diverse communities that consist of thousands of bacterial species from several phyla (e.g., sponges (Thomas *et al.*, 2016) or human gut (Yatsunenکو *et al.*, 2012)). Each of these metaorganisms needs to maintain homeostasis with a healthy and functional microbiome; thus, both host and microorganisms have to detect and respond to their partners and control population size.

RECOGNITION AND RESPONSE IN HOST-MICROBE INTERACTIONS

Regardless of microbiome diversity and density, the host is required to recognize and respond to microorganisms in order to control microbiome composition and prevent overgrowth of pathogenic bacteria. The host immune system plays a vital role in these processes and, although it was long thought to be a tool for defense against pathogens, evidence suggests that the immune system evolved as a communication tool for microbiome maintenance (Nyholm and Graf, 2012; Bosch, 2014). Innate immunity is shared by all metazoans, whereas the adaptive immune system evolved amongst vertebrates. Immune receptors of the innate immune system play a central role in detecting microbial associated molecular patterns (MAMPs), such as lipopolysaccharides, peptidoglycans, or flagellin unique to prokaryotic organisms (Rosenstiel *et al.*, 2009; Buckley and Rast, 2015). These receptors include pattern recognition receptors (PRRs), such as Toll-like receptors (TLRs), NOD-like receptors, and C-type lectin receptors (Chu and Mazmanian, 2013; Brown *et al.*, 2018). Moreover, other receptor classes, such as G-protein coupled receptors, appear to be responsive to MAMPs (Bufe and Zufall, 2016). Detection of MAMPs generally leads to the initiation of downstream immune responses, mounting differential responses according to the detected bacteria (e.g., defense against pathogens and tolerance against symbionts; (Chu and Mazmanian, 2013; Bi *et al.*, 2015).

Innate immune receptors can be identified based on conserved protein domains, but homology does not necessarily equal function. For example, TLRs are transmembrane receptors characterized by an intracellular Toll/interleukin-1 receptor domain (TIR) and found in many vertebrates and invertebrates (Brennan and Gilmore, 2018). TLRs can bind a diverse array of different MAMPs and initiate downstream signaling via the NF- κ B or MAPK signaling pathways that leads to responses involving inflammatory cytokines or production of antimicrobial peptides. In vertebrates, TLRs are involved in the crosstalk with the microbiome (Rakoff-Nahoum *et al.*, 2016). They can further be involved in developmental processes in, for example, *Drosophila melanogaster* and *C. elegans* (Anderson *et al.*,

1985; Pujol *et al.*, 2001), and in the defense against pathogens (Brennan *et al.*, 2017). TLRs of most invertebrates and vertebrates have extracellular leucine-rich repeats (LRRs), while some early divergent metazoans have other TLR-like putative receptors with other architectures. Sponges have TIR domains homologous to vertebrate TIRs combined with extracellular immunoglobulin domains (Hentschel *et al.*, 2012; Riesgo *et al.*, 2014), and the cnidarian *Hydra* expresses LRR proteins that interact with TIR-domain containing proteins and respond to flagellin (Franzenburg *et al.*, 2012). In sponges, the function TIR-domain containing genes is not yet known, although components of the TLR pathway respond to MAMPs in some species (Wiens *et al.*, 2005; Yuen, 2016).

In addition to host-bacteria interactions, bacteria-bacteria interactions also contribute to holobiont homeostasis across invertebrates and vertebrates (Coyte *et al.*, 2015; Fraune *et al.*, 2015; Mergaert, 2018). Bacteria interact by density-dependent mechanisms, such as quorum-sensing (QS) (Abisado *et al.*, 2018) where N-acyl homoserine lactone (AHL) signaling, is the most studied QS system. It was discovered in the context of bioluminescent symbiosis of the marine bacterium *Vibrio fischeri* and the Hawaiian bobtail squid *Euprymna scolopes* (Fuqua *et al.*, 1994).

Interactions between bacteria can be competitive for resources or cooperative *via* shared metabolic pathways (e.g., in the human gut; (Rakoff-Nahoum *et al.*, 2016; Coyte and Rakoff-Nahoum, 2019). The cumulative interactions result in complex networks that can be predicted by co-occurrence analysis based on community composition data (Faust *et al.*, 2012) and can inform about the relation of bacteria-bacteria interactions during health and disease, as shown in the human gut (Baldassano and Bassett, 2016; Chen *et al.*, 2020). Importantly, experimental approaches and manipulative studies are key to understand how bacterial community dynamics contribute to holobiont homeostasis, and how and to which MAMPs evolutionarily conserved receptor classes respond.

MODEL SYSTEMS FOR SYMBIOSES RESEARCH

The sequencing revolution and the increasing access to diverse *-omics* techniques have led to exciting discoveries in symbioses research. Ranging from *16S rRNA* amplicon sequencing and (meta-)genomics to (meta-)transcriptomics and metabolomics. This has extended most recently to spatial *-omics* approaches (Geier *et al.*, 2020), which have enabled the description and discovery of diverse symbioses and predictions on their functions. The validation of predictions *in vivo* is crucial to understand how symbioses function and respond, and how the phenotype of the host and the symbiont(s) are ultimately affected. Thus, experimental models that can be manipulated under controlled conditions are of key importance.

Introduction

It is crucial to also study non-model animals (Bosch and Mcfall-ngai, 2011; Bosch *et al.*, 2019), where especially aquatic organisms hold a largely unexplored yet ecologically, economically and evolutionarily important holobiont diversity (Dittami *et al.*, 2020). Particularly early diverging marine animals like sponges, ctenophora and cnidaria provide a valuable resource for understanding central mechanisms of animal-microbe interactions. The current methodological advances on aquatic emerging models are summarized in Table 1.

Although the sequencing revolution has generally eased the study of other, non-model organisms and expanded the range of valuable study species, the generation of gnotobiotic animals is challenging and protocols have to be adapted for each species. Especially in aquatic species, an additional challenge is to control bacteria in the culture water. Thus, only few aquatic model organisms for symbioses exist today and the establishment of more model systems across different phyla is currently a major research focus (CRC1182 Origin of Metaorganisms <https://www.metaorganism-research.com/>; Symbioses in Aquatic Systems Initiative by the Gordon and Betty Moore Foundation). Among these, sponges are currently not very amenable to experimentation (Pita *et al.*, 2016) and thus a knowledge gap exists around this highly informative animal phylum for decoding animal-microbe interactions (Schmittmann *et al.*, 2020).

Introduction

TABLE 1 | Emerging marine model organisms for symbioses from sponges (Porifera) to vertebrates (Chordata). Species marked with an asterisk are methodologically advanced and studied extensively in the microbiome context. The extent to which key species fulfil methodological requirements is listed including their advantages and important references.

Phylum	Species	Methodological Requirements								Advantages	References	
		wide natural distribution	long-term culture host	culturability symbionts	gnotobiotic host	reproductive cycle closed	omic information host	omic information symbiont	transgenesis			gene knockdown
Porifera	<i>Amphimedon queenslandica</i>					±	+	+			extensive -omic information, developmental stages	Gauthier <i>et al.</i> , 2016, Song <i>et al.</i> , 2020
	breadcrumb sponge <i>Halichondria panicea</i>	+		±		±	+	+			highly abundant, specific symbiont	Knobloch <i>et al.</i> , 2019a, 2020
	freshwater sponges (e.g., <i>E. muelleri</i>)	+	+			+	+			+	gemmule formation, cryopreservation	Rivera <i>et al.</i> , 2011, Musser <i>et al.</i> , 2021
Ctenophora	sea walnut <i>Mnemiopsis leidyi</i>	+	+		±	+	+	+		+	fast reproduction	Jaspers <i>et al.</i> , 2019
Cnidaria	* <i>Hydra vulgaris</i>	+	+		+	+	+	+	+	+	extensive molecular and genetic toolkit	Augustin <i>et al.</i> , 2017, Franzenburg <i>et al.</i> , 2012
	*starlet sea anemone <i>Nematostella vectensis</i>	+	+	+	+	+	+	+	+	+	simple marine cnidarian, established toolkit	Mortzfeld <i>et al.</i> , 2016, Domin <i>et al.</i> , 2018
	<i>Aiptasia</i>	+	+		±	+	+	+	+	+	photosymbiosis similar to many corals	Bucher <i>et al.</i> , 2016, Costa <i>et al.</i> , 2021
	moon jelly <i>Aurelia aurita</i>	+		+	+	+	+	+			sexual and asexual reproduction	Weiland-Bräuer <i>et al.</i> , 2015, 2019
Annelida	tubeworm <i>Hydroides elegans</i>	+	+			+	+	+			bacteria in metamorphosis well studied	Shikuma <i>et al.</i> , 2016, Ericson <i>et al.</i> , 2019
Mollusca	*Hawaiian bobtail squid <i>Euprymna scolopes</i>		+	+	+	+	+	+			“simple” symbiosis, large toolkit	Visick <i>et al.</i> , 2021, Nyholm <i>et al.</i> , 2021
Echinodermata	sea urchins (e.g., <i>Strongylocentrotus purpuratus</i>)	+	+			+	+	+	+	+	well studied for development	Carrier and Reitzel, 2018
Chordata	sea squirt <i>Ciona intestinalis</i>	+	+		+	+	+	+	+	+	closest relative to vertebrates	Leigh <i>et al.</i> , 2016
	*zebrafish <i>Danio rerio</i>	+	+		+	+	+	+	+	+	vertebrate model with extensive toolkit	Melancon <i>et al.</i> , 2017

SPONGES HELP TO UNDERSTAND EVOLUTIONARILY EARLY SYMBIOSES

The phylum Porifera (sponges) is considered one of the oldest animal phylum ((Simion *et al.*, 2017; Nielsen, 2019; Turner, 2021), but see e.g., (Moroz *et al.*, 2014)). More than 8,500 sponge species (van Soest *et al.*, 2012) of four taxonomic classes have been described so far. Demospongiae are by far the largest class with 83 % of all described species, while Calcarea, Hexactinellida and Homoscleromorpha are much less diverse. Sponges are involved in nutrient cycling (De Goeij *et al.*, 2013) and important members of marine ecosystems in all world oceans. This is especially true in the deep-sea, where sponges are habitat engineers and sponge grounds are considered biodiversity hot-spots (Maldonado *et al.*, 2016) that are crucial to be subjected to conservation efforts (Busch *et al.*, 2020).

Sponges have a simple but highly efficient body plan adapted to their filter-feeding lifestyle (Figure 2). A water current is created by flagellated choanocyte cells and carried through an aquiferous system (Reiswig, 1971; Reiswig, 1975). On the way through the sponge body, nano- and picoplankton (e.g., bacteria, small microalgae, and protists; size-range of 0.2-2 μm ; (Yahel *et al.*, 2006)) are captured by choanocytes and digested by phagocytosis in choanocytes and mobile archaeocytes. Sponges can reach exceptional clearance rates of up to 99 % captured particles (Ribes *et al.*, 1999; Hadas *et al.*, 2009) and filter up to 24,000 l/kg seawater per day (Hentschel *et al.*, 2003). Importantly, sponges do not only feed on microbes from the seawater, but also harbor microbial communities extracellularly in their tissue (Figure 2).

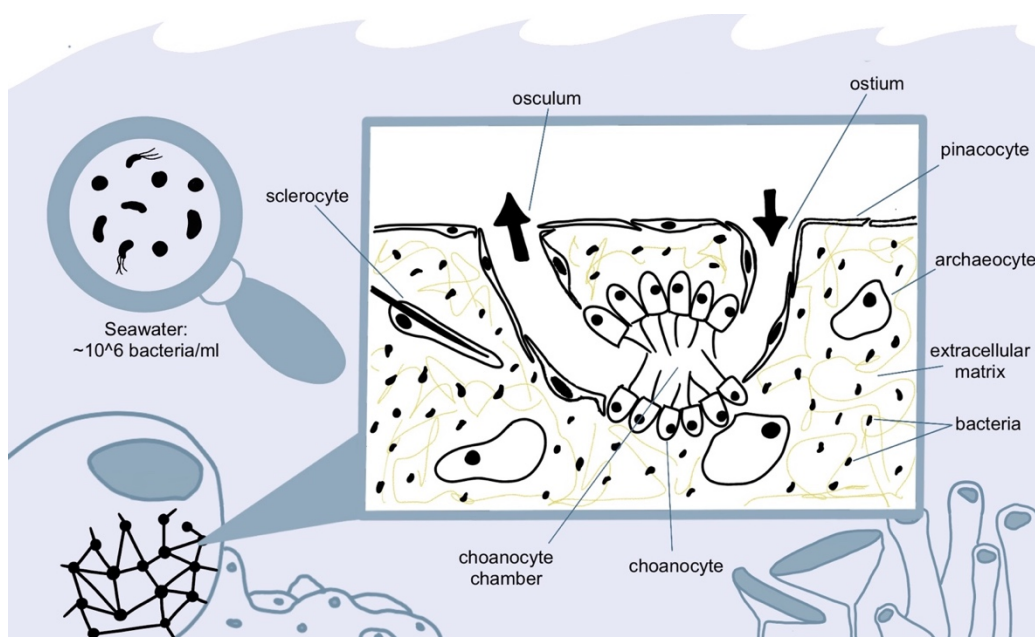


FIGURE 2 | Sponge body plan. Sponges are simple organisms without organs. An overview of their tissue structure is shown including important cell types.

THE MICROBIAL SIDE: DIVERSITY AND DENSITY OF SPONGE MICROBIOMES

Sponge microbiomes are distinct from the surrounding seawater and species-specific (Thomas *et al.*, 2016). Among the 41 detected bacterial phyla in sponges, Proteobacteria (mostly Alpha- and Gammaproteobacteria) and Chloroflexi were particularly abundant. Bacteria fulfil various functions in sponges, ranging from cycling of organic matter (Chloroflexi, (Bayer *et al.*, 2018)) to photosynthesis (Steindler *et al.*, 2005; Bayer *et al.*, 2014) to nitrogen cycling (Bayer *et al.*, 2008; Fan *et al.*, 2012). In addition to bacteria, sponges also harbor associated archaea, fungi, protists, and viruses. However, their role in the sponge microbiome is less understood but it is expected that they also build specific communities adapted to the sponge host environment and contribute to the function of the holobiont (Bayer *et al.*, 2014; Chaib De Mares *et al.*, 2017; Laffy *et al.*, 2018; Jahn *et al.*, 2019).

Not only the bacterial diversity is characteristic for sponge-species, but also the bacterial density in the tissue. Sponges can be classified as low microbial abundance (LMA) or high microbial abundance (HMA) sponges (Gloeckner *et al.*, 2014). Bacterial densities differ by several orders of magnitude, with 10^5 - 10^6 bacteria/g in LMA sponges and 10^8 - 10^{10} bacteria/g in HMA sponges (Hentschel *et al.*, 2006; Bayer *et al.*, 2014; Gloeckner *et al.*, 2014). Additionally, LMA sponge microbiomes are less diverse than those of HMA sponges. Some LMA sponges even have few dominant ASVs (Amplicon sequence variants) that are characteristic for their respective sponge host. Examples are *Amphimedon queenslandica*, dominated by a Gamma- and a Alphaproteobacterium (Gauthier *et al.*, 2016) and *Halichondria panicea*, dominated by the Alphaproteobacterium *Ca. Halichondriabacter symbioticus* (Knobloch *et al.*, 2019a). Interestingly, differences between HMA and LMA sponges are, to some extent, driven by host phylogeny (Gloeckner *et al.*, 2014; Moitinho-Silva *et al.*, 2017), but symbiont density is correlated to several physiological properties. For example, HMA sponges have denser mesohyls than LMA sponges, that are characterized by smaller and fewer choanocyte chambers, longer and thinner water channels, resulting in overall lower pumping rates of HMA sponges (Weisz *et al.*, 2008; Poppell *et al.*, 2014). In consequence, HMA sponges have a more symbiont-driven nutrition mode than LMA sponges and are less dependent on particulate food (Morganti *et al.*, 2017; Rix *et al.*, 2020).

A large knowledge gap in sponge symbioses involves how sponge microbiomes are assembled and maintained. Sponge microbiomes are specific and stable over space and time and considered to be largely stable even in the face of climate change (Bell *et al.*, 2018a; 2018b). Nevertheless, some species do vary with season or due to non-beneficial environmental conditions (reviewed in (Pita *et al.*, 2018b)). In some cases, the microbiomes of sponges are disrupted and enter a state of dysbiosis (disruption of microbiome homeostasis; e.g., during disease) (Angermeier *et al.*, 2011, 2012; Luter *et*

al., 2012; Fan *et al.*, 2013; Lesser *et al.*, 2016; Luter and Webster, 2017). However, it is largely unknown which processes help to maintain a stable sponge microbiome, which role bacteria-bacteria interactions play or if dysbiosis is reversible.

THE HOST SIDE: SPONGE IMMUNE SYSTEMS

Sponges have a diverse repertoire of putative immune receptors that could be involved in detecting, differentiating, and responding to microbes. The first sequenced sponge genome was *Amphimedon queenslandica*, and it revealed putative PRRs identified based on conserved protein domains, such as scavenger receptor cysteine-rich (SRCR) domains, NOD-like receptor (NLR) domains, C-type lectin like domain (CTLD) genes, and TIR domain-containing genes ((Srivastava *et al.*, 2010), reviewed in (Hentschel *et al.*, 2012)). A few other receptor classes beyond PRRs are found in sponges and might be involved in microbial recognition in sponges. These are G-protein coupled receptors (GPCRs) and cytokine receptors (Gardères *et al.*, 2015; Pita *et al.*, 2018a).

The immune repertoire of the earliest metazoan phylum gives insights into which immune pathways are evolutionarily ancient and how they gave rise to the diverse immune systems in other animal phyla. For example, it was long assumed that NLRs originated in teleost fish. Now we know that this receptor class not only originated in sponges and was secondarily lost in other invertebrate phyla, but also that NLRs are especially diverse in sponges compared to vertebrates (Yuen *et al.*, 2014; Ryu *et al.*, 2016; Pita *et al.*, 2018a). Similarly, GPCRs and SRCRs are diversified in sponges (Buckley and Rast, 2015; Ryu *et al.*, 2016; Pita *et al.*, 2018a). Such diverse receptor classes could be one potential innate immune mechanism for sponges to differentiate between microbes and mount specific immune responses (Schulenburg *et al.*, 2007; Buckley and Rast, 2015; Degnan, 2015). However, the extent of within-individual PRR diversity is currently unknown, and also whether these are constitutively expressed or whether they are inducible in response to microbial signals.

However, conserved protein domains do not equal function. The role of the sponge immune system in the crosstalk with microbes has been experimentally shown in different studies, while responses differ between sponge species. Further, it remains elusive which pathways respond to which bacteria, and how the sponge immune system is involved in maintaining the microbiome. SRCRs were found enriched in sponge choanocytes (Sebé-Pedrós *et al.*, 2018) and might therefore be important for selective feeding on symbionts vs. seawater bacteria (Wilkinson *et al.*, 1979; Wehrl *et al.*, 2007). In another sponge species, SRCR expression levels were differentially expressed during photosymbiosis compared to aposymbiotic sponges suggesting their role in maintaining symbiotic cyanobacteria

(Steindler *et al.*, 2007). In *Amphimedon queenslandica*, immune gene expression changed after exposure to symbionts and symbionts from another sponge species (Yuen, 2016). Other studies report the differential gene expression of the TLR pathway (Wiens *et al.*, 2005; Yuen, 2016), NLRs and GPCRs upon microbial encounter (Pita *et al.*, 2018a).

Importantly, the density of sponge symbionts seems to be a relevant factor shaping both the immune response and the immune repertoire. In an HMA sponge, more immune genes were differentially regulated after exposure to MAMPs compared to an LMA sponge, and the responsive PPRs differed (Pita *et al.*, 2018a). The hypothesis is that a higher microbiome density and complexity requires a more complex response to distinguish between MAMPs and symbionts. Additionally, LMA sponges might constitutively need to control their microbiome more strictly in order to maintain less bacterial diversity at a lower density. Interestingly, HMA and LMA sponges do not only differ in their immune responses, but already in their immune repertoire. For example, NLRs seem to be only diversified in LMA sponges, while HMA sponges have zero to few genes (Ryu *et al.*, 2016; Germer *et al.*, 2017; Pita *et al.*, 2018a). The question remains open whether these immune system features are the cause or the consequence of differences in microbial load. It is thus crucial to include more sponge species to broaden our understanding of the diversity of immune repertoires and the responsive immune genes to unravel patterns.

STEPS TOWARDS A SPONGE MODEL FOR HOST-MICROBE INTERACTIONS

Sponges are undoubtedly valuable models for animal-microbe symbiosis due to their phylogenetic position and their unique lifestyle that is dependent on microbes both as a food source and as complex but stable microbiomes. The potential and limitations for sponges as novel experimental models for animal-microbe symbioses have been previously reviewed (Pita *et al.*, 2016) and methodological advances have been made since. Importantly, a vast body of -omic data has been generated for both the host and the associate microbes, although there are gaps in other microbial members than archaea. Host genomes are still limited, but an extensive ongoing sequencing effort will increase the currently available genomes from <10 to >50 (Aquatic Symbiosis Genomics Sponges Project). Further, single cell sequencing technology has recently been applied to sponges in the context of multicellularity and the nervous system (Sebé-Pedrós *et al.*, 2018; Sogabe *et al.*, 2019; Musser *et al.*, 2021) and this opens new doors also for the symbiosis context. Also, genetic manipulation by transfection with plasmids was successful in a *Suberites domuncula* explant culture (Revilla-I-Domingo *et al.*, 2018).

Introduction

The long-term maintenance in aquaria and standing laboratory populations are the first steps to render sponges accessible as experimental models as sponges as organisms are comparatively difficult to cultivate in aquaria. Commercial production of bath sponges is solely done in *in situ* mariculture and not in indoor aquarium systems (Osinga, Tramper, *et al.*, 1999; Duckworth, 2009). The main challenge is nutrition since sponges rely on continuous supply of both DOM and POM, depending on the species in varying ratios, (Osinga, de Beukelaer, *et al.*, 1999), while too high food concentration reduces growth (Osinga *et al.*, 2001; Duckworth and Battershill, 2003). A high flow rate through the aquaria is crucial to continuously mix water and ensure food supply. Due to the extremely high sponge filtration and retention rates, food would need to be added continuously to maintain *ad libitum* levels in a circulating system. The most straight-forward solution to ensure both food supply and current is cultivation in aquaria supplied with natural seawater at a high flow-through rate, which is only feasible in facilities directly at the coast. However, even if this method should ensure a sustainable food composition and density, the natural microbiome composition changes during cultivation in some species (e.g., *Rhopaloeides odorabile* and *Halichondria panicea*; (Webster *et al.*, 2011; Knobloch *et al.*, 2019a)). Cultivating sponges under controlled experimental conditions, such as in closed recirculation systems (Mohamed, Cicirelli, *et al.*, 2008; Mohamed, Rao, *et al.*, 2008) or in small experimental units where food is depleted faster, is an even larger challenge (Knobloch *et al.*, 2019a).

Major challenges still lie in the generation of gnotobiotic/aposymbiotic sponge hosts and cultivation of sponge symbionts, which is the premise for targeted colonization studies to dissect interactions of interest. Different attempts have been made to deplete associated bacteria with antibiotics but have not succeeded yet (Friedrich *et al.*, 2001; De Caralt *et al.*, 2003; Sipkema *et al.*, 2003; Richardson *et al.*, 2012; Gloeckner *et al.*, 2013; Schippers, 2013). Therefore, it is not known whether sponges are viable without their symbionts. Naturally occurring aposymbiotic sponges are being used as an experimental system to study interactions of photosymbionts with sponges and the remaining microbiome (Britstein *et al.*, 2020). Further, experimental manipulation or disturbance of the microbiome can provide answers on the potential recovery of the natural microbiome, host fitness under dysbiosis response to invading bacteria.

Another large knowledge gap are the challenges associated with bacterial isolation and cultivation (“microbial dark matter”; (Rinke *et al.*, 2013)). Novel isolation techniques and co-cultivation with the host and/or other members of the microbiome have been explored while no “true” sponge symbiont (considering here faithful and abundant members of the core microbiome) has yet been cultured (Steinert *et al.*, 2014; Knobloch *et al.*, 2019b; Lewis *et al.*, 2020). The biggest obstacle is probably the complex environment of the sponge mesohyl and the symbiont lifestyle that includes numerous

Introduction

metabolic interactions both not only with the host but also with several other microbial taxa (Pande and Kost, 2017; Gutleben *et al.*, 2018). Despite attempts to simulate the sponge environment under laboratory conditions, cultivation of sponge-specific bacteria has not been successful so far (Sipkema *et al.*, 2011; Steinert *et al.*, 2014; Knobloch *et al.*, 2019b; Gutleben *et al.*, 2020).

Finally, closing the life cycle of sponges remains a major challenge, whereby reproduction, larval culturing, growth of juveniles to adults and spawning of lab-raised adults all occurs in the laboratory. Limitations probably lie in an incomplete understanding of the environmental cues and conditions that are important for spawning, successful larval settlement, and further development (Whalan and Webster, 2014; Ueda *et al.*, 2016). Further, targeted crosses of sponges will require elaborate preparation, because fertilization occurs long before release of larvae for brooding species and sexing of sponges remains laborious (mainly achieved through histological cuts). To control for genetic background of individuals faster, sponges can be divided into clones, taking advantage of the regeneration capacity (e.g., (De Caralt *et al.*, 2003; Webster *et al.*, 2011; Pita *et al.*, 2018a)).

A crucial step in advancing sponges as experimental models is to converge efforts in few, thoroughly chosen sponge species fulfilling basic requirements of experimental models (Figure 3). The most well-described species to date is the Great Barrier Reef sponge *Amphimedon queenslandica*. This species has had a major impact on sponge biology because it was the first full genome sequenced (Srivastava *et al.*, 2010) and this was followed by several -omic based discoveries related to symbioses (Gauthier *et al.*, 2010; Yuen *et al.*, 2014; Degnan, 2015; Fieth *et al.*, 2016; Grice *et al.*, 2017; Williams *et al.*, 2020), development (Conaco *et al.*, 2012; Say and Degnan, 2020), and early metazoan evolution (Krishnan *et al.*, 2014; Yuen *et al.*, 2014; Fernandez-Valverde *et al.*, 2015; Grice *et al.*, 2017; Calcino *et al.*, 2018; Sogabe *et al.*, 2019; Wong *et al.*, 2019; Williams *et al.*, 2020). Its value as a model for metazoan evolution and the origin of multicellularity has already been acknowledged (Degnan *et al.*, 2008), while the knowledge could now be used to expand the system to experimental sponge-microbe studies. The easy access to larvae year-round in clearly visible brood chambers enables the study of all developmental stages (Adamska and Degnan, 2008; Leys *et al.*, 2008) and it has been shown that arginine provided by bacteria is crucial for larval settlement (Song *et al.*, 2020). Despite the knowledge gathered, this species has a rather narrow geographic distribution restricted to the Great Barrier Reef, Australia, limiting access to a wider scientific community.

Introduction

	<i>Amphimedon queenslandica</i>	<i>Halichondria panicea</i>	
Geographic distribution	Coral Sea/Great Barrier Reef	North Atlantic Ocean	
Reproductive mode	Hermaphroditic, viviparous; development in brood chambers	Gonochoristic, viviparous	
Reproductive cycle	Year-round (1)	April-June (7,8)	
In culture	Adults	Yes (1)	Yes (9,10)
	Spawning	Temperature (2)	Light and temp. (11)
	Settlement and metamorphosis	Coralline algae (3,4)	Biofilm (12)
	Maturation	Reared for few weeks (2)	Reared for few days (13)
	Closing life cycle	-	-
Genome	Yes (5)	Yes (14)	
Transcriptome	Yes (6)	Yes (15,16)	
Gnotobiotic host (20)	-	-	
Symbionts in culture	-	Preliminary (17, this thesis)	
Transgenesis (21)	-	-	
Gene knockdown (22)	-	-	
Cell culture (23)	-	-	
Primmorph culture	-	Short-term experiments (18)	
Explant culture	-	Short-term experiments (19)	

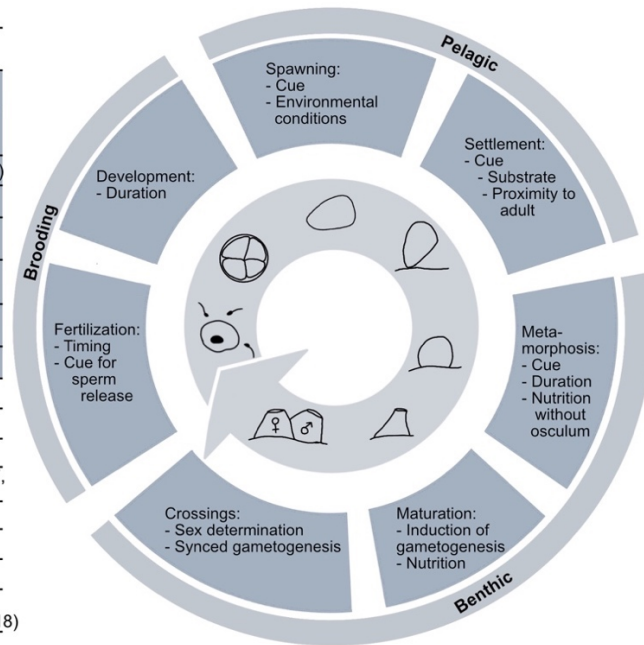


FIGURE 3 | The required properties for an experimental sponge model for symbioses (adapted after (Pita *et al.*, 2016)) and how the two sponge species *Amphimedon queenslandica* and *Halichondria panicea* fulfil these. One important aspect is sponge reproduction under laboratory conditions: based on the sponge life cycle, experimental/technical challenges for each developmental stage are listed. Current limitations for closing the sponge life cycle in the laboratory, i.e., to reproduce lab-spawned and -raised sponges, mainly lie in culturing conditions for post-larvae and during maturation. 1: (Degnan *et al.*, 2008), 2: (Leys *et al.*, 2008), 3: (Degnan and Degnan, 2010), 4: (Jackson *et al.*, 2002), 5: (Srivastava *et al.*, 2010), 6: (Fernandez-Valverde *et al.*, 2015), 7: (Witte and Barthel, 1994), 8: (Witte *et al.*, 1994), 9: (Barthel and Theede, 1986), 10: (Thomassen and Riisgard, 1995), 11: (Amano, 1986), 12: (Barthel, 1986), 13: (Khalaman *et al.*, 2011), 14: (Strehlow *et al.*, 2021), 15: (Vad *et al.*, 2020), 16: (Schmittmann *et al.*, 2021), 17: (Knobloch *et al.*, 2019b), 18: (Lavrov and Kosevich, 2016), 19: (Kumala *et al.*, 2021), 20: (Britstein *et al.*, 2020), 21: (Revilla-I-Domingo *et al.*, 2018), 22: (Rivera *et al.*, 2011), 23: (Conkling *et al.*, 2019)

Another promising candidate on the rise is the breadcrumb sponge *Halichondria panicea* (Figure 4), which inhabits large parts of the North Atlantic (including the North Sea), the environmentally variable Baltic Sea, and the Mediterranean, and an almost global distribution of the other members of the family *Halichondria* (Erpenbeck *et al.*, 2004). This gonochoristic, viviparous sponge is small in size, abundant in coastal areas and amenable to culture under laboratory conditions as adults (Barthel and Theede, 1986), larvae (Khalaman *et al.*, 2011), primmorphs (Lavrov and Kosevich, 2018) and clonal explants (Kumala *et al.*, 2017; Kumala and Canfield, 2018). Spawning time is limited to few weeks in this temperate species (Barthel and Detmer, 1990; Witte *et al.*, 1994) and light and temperature have been proposed as cues to release larvae (Amano, 1986).



FIGURE 4 | *Halichondria panicea* (A) in the field, (B) during transportation to the laboratory (C) and in maintenance aquaria.

A preliminary *H. panicea* genome assembly has recently been assembled from metagenomic data (Strehlow *et al.*, 2021) and *de novo* transcriptomes have been published in the context of responses to microbial elicitors (Schmittmann *et al.*, 2021, in the context of this thesis) and crude oil (Vad *et al.*, 2020). Further, *H. panicea* is particularly interesting from the microbial perspective. It is an LMA sponge (Gloeckner *et al.*, 2014) with a specific, dominant symbiont that amounts between 20-80 % of the microbiome. This symbiont, *Ca. Halichondriabacter symbioticus*, (Alphaproteobacteria) is faithfully associated to its sponge host throughout the North Atlantic and is only found in trace abundances in association with other organisms or free-living (Knobloch *et al.*, 2019a). The closest described bacterial relative is the genus *Amylibacter* of the family Rhodobacteraceae, (92.5 % similarity based on 16S rRNA gene) (Knobloch *et al.*, 2019a). Other host-associated *Amylibacter* are known, for example *A. ulvae* found on green algae and *A. cionae* isolated from a sea squirt (Nedashkovskaya *et al.*, 2016; Wang *et al.*, 2017). Metagenomic information confirm features of a symbiont in *Ca. H. symbioticus* such as a role in ammonia assimilation, vitamin B12 synthesis, and antimicrobial peptide production (Knobloch *et al.*, 2020). However, despite isolation efforts, *Ca. H. symbioticus* remains uncultivated (Knobloch *et al.*, 2019b). Targeting the specific symbiosis between *H. panicea* and *Ca. H. symbioticus* *in vivo* and tracking the response of both host and symbiont to manipulation could answer important questions on sponge-microbe interactions. Improving experimental methods for sponges under laboratory conditions will open a new avenue of research in sponge-microbe symbiosis and bring sponges one step closer to being valuable models for evolutionarily ancient animal-microbe symbiosis.

AIMS AND THESIS OUTLINE

The overall aim of my thesis was to advance the breadcrumb sponge *Halichondria panicea* as an experimental model for sponge-microbe symbioses. Experimental model systems are a key to test and understand mechanisms and functions of host-microbe interactions, such as microbiome stability, colonization dynamics, and immune responses. The sponge *H. panicea* is a potential candidate for an experimental model system to fill a gap in sponge-symbioses research and due to its wide geographic distribution, established methods could serve for the wider scientific community. In my thesis, I have focused on the host-side as well as the bacteria-side of the *H. panicea* holobiont. A general understanding of interactions within sponges (Chapter 1), the local *H. panicea* holobiont (Chapter 3), and the sponge immune system (Chapter 2) was generated. Further, experimental manipulation of the sponge microbiome by antibiotics (Chapter 3) and potential for recolonization was evaluated (Chapter 4). The thesis will finish with an overarching discussion and synthesis of the findings.

For the individual chapters, the following specific research aims were defined:

- Chapter 1:** Summarize current knowledge on interactions within the sponge holobiont.
- Chapter 2:** Characterize the immune repertoire and response to bacterial LPS of *H. panicea*.
- Chapter 3:** Generate knowledge on local sponge population microbiomes, cultivate *H. panicea* under laboratory conditions and evaluate the use of antibiotics to generate gnotobiotic sponges.
- Chapter 4:** Study microbiome dynamics after disturbance with antibiotics and assess recolonization potential.

MAIN CHAPTERS

This thesis is based on the following publications and manuscripts:

CHAPTER 1

Schmittmann L., Jahn M. T., Pita L., Hentschel U. 2020. Decoding cellular dialogues between sponges, bacteria and phages. in Cellular dialogues in the holobiont (Bosch & Hadfield eds.) CRC Press. DOI 10.1201/9780429277375-4.

Participation in	Author initials, responsibility decreasing
Study design	UH/LP, LS
Manuscript writing	LS/LP/UH, MJ
Manuscript reviewing	LS/LP/UH, MJ

CHAPTER 2

Schmittmann L., Franzenburg S., Pita L. 2021. Individuality in the immune repertoire and the induced response of the sponge *Halichondria panicea*. Frontiers in Immunology. 12. 1. DOI 10.3389/fimmu.2021.689051.

Participation in	Author initials, responsibility decreasing
Study design	LP, LS
Experimentation	LS/LP
Molecular lab work	LS
Data analysis, interpretation	LS, LP
Manuscript writing	LS
Manuscript reviewing	LS, LP, SF

CHAPTER 3

Schmittmann L., Pita L. 2021. DNA/RNA extraction and qPCR protocol to assess bacterial abundance in the sponge *Halichondria panicea*. dx.doi.org/10.17504/protocols.io.bxwwppfe

Schmittmann L., Hentschel U. 2021 Antibiotic treatment of the breadcrumb sponge *Halichondria panicea* and subsequent recolonization. dx.doi.org/10.17504/protocols.io.by7hpzj6

Participation in	Author initials, responsibility decreasing
Study design	LS/LP/UH
Method development	LS, LP/UH
Experimentation	LS, LP, TR
Molecular lab work	LS
Data analysis, interpretation	LS, LP/UH
Manuscript writing	LS, LP/UH
Manuscript reviewing	LS, LP/UH

CHAPTER 4

Schmittmann L., Busch K., Rahn T., Wiese J., Pita L., Hentschel U. Submitted to *Environmental Microbiology*. Stability of a dominant sponge-symbiont in spite of antibiotic-induced microbiome disturbance.

Participation in	Author initials, responsibility decreasing
Study design	LS/LP/UH
Method development	LS, LP/UH
Experimentation	LS, LP
Molecular lab work	LS
Data analysis, interpretation	LS, LP/UH, KB
Manuscript writing	LS, UH, LP
Manuscript reviewing	LS, LP/UH, KB, TR

ADDITIONAL SUBMITTED MANUSCRIPTS THAT I CONTRIBUTED TO

Symbiont transmission in marine sponges: embryology, larval ecology and metamorphosis –Carrier T.C., Schmittmann L., Pita L., Bosch T.C.G., Hentschel U. (in revision at *BMC Biology*)

Towards a mechanistic understanding of low salinity acclimation ability in marine invertebrates - a systematic review & meta-analysis – Podbielski I., Schmittmann L., Sanders T., Melzner F. (in revision at *Biological Reviews*)

CHAPTER 1

DECODING CELLULAR DIALOGUES BETWEEN SPONGES, BACTERIA AND PHAGES

Chapter reproduced with permission of The Licensor through PLSclear.

Original publication by *CRC Press*, Taylor & Francis Group, LLC.

Schmittmann L., Jahn M. T., Pita L., Hentschel U. 2020. Decoding cellular dialogues between sponges, bacteria and phages. in Cellular dialogues in the holobiont (Bosch & Hadfield eds.) *CRC Press*. DOI 10.1201/9780429277375-4.

DECODING CELLULAR DIALOGUES BETWEEN SPONGES, BACTERIA AND PHAGES

Schmittmann L.¹, Jahn M. J.¹, Pita L.¹, Hentschel U.^{1,2}

¹*Research Unit Marine Symbioses, GEOMAR Helmholtz Centre for Ocean Research, Kiel, Germany,*

²*Christian-Albrechts-University Kiel, Germany*

INTRODUCTION

The evolution of multicellularity has not only enabled the specialization of eukaryote cell types, but also provided stable confined habitats for microbes to engage in symbiotic associations with metazoans. Animal-microbe interactions presented new challenges, such as self/non-self-recognition, but also new opportunities that have shaped the evolution and diversification of holobionts. Sponges (Porifera), as one of the most basal animals, provide a fundamental resource to decipher key mechanisms of animal-microbe interactions with implications for more complex invertebrates and vertebrates. In this chapter we aim to summarize the current knowledge on cellular dialogues within sponge holobionts by taking a close look at the different players and interactions that make sponges one of the most diverse and successful marine animal groups.

Sponges have a fossil record dating back to ~ 600 Mya (Yin et al. 2015) and around 9,000 extant species have been described (Van Soest et al. 2012). Despite their high taxonomic diversity, all sponges possess a sessile, filter-feeding adult lifestyle (exceptions: carnivorous sponges and the pelagic larval phase). Sponges continuously pump water and consume large amounts of microbial cells as well as dissolved carbon. Specialized flagellated cells (choanocytes) capture particles from the surrounding water and transfer them into the mesohyl. Once inside the sponge interior, the particles are digested by phagocytotically active, amoeboid cells (archaeocytes). While seawater bacteria constitute one of the main sponge food sources, the mesohyl also harbors dense bacterial symbiotic communities with the sponge host (Moitinho-Silva et al. 2017b; Thomas et al. 2016).

Comprehensive knowledge on sponge microbiome diversity and functions has been gained from 16S rRNA gene sequencing and high-throughput sequencing technologies such as metagenomics, metatranscriptomics and single-cell genomics (Horn et al. 2016; Moitinho-Silva et al. 2017a; Podell et al. 2019; Slaby et al. 2017; Thomas et al. 2016). A comparative study showed that, depending on the sponge species, the sponge microbiome comprised 50 up to 3,820 genetically unique operational taxonomic units (OTUs) belonging to at least 13 different phyla (Fan et al. 2013; Thomas et al. 2016).

Although a fraction of sponge-associated microbes also occurs in the surrounding environment, each sponge species maintains a specific and stable microbial community (Thomas et al. 2016). Notably, the sponge-specific symbionts are adapted to live within the sponge habitat (Jahn et al. 2016; Siegl et al. 2011), making sponges a refuge for novel biodiversity. The symbionts are either maintained by vertical transmission from adults to offspring (Björk et al. 2018; Russell, 2019; Schmitt et al. 2008; Sharp et al. 2007; Sipkema et al. Webster et al. 2010; 2015) or are acquired horizontally from the seawater environment (Björk et al. 2018). Based on the composition and abundance of microbes in their tissues, sponges can be differentiated in high and low microbial abundance (HMA/LMA) sponges (Gloeckner et al. 2014). Those two lifestyles can be differentiated based on microbial microscopy and taxonomy (Gloeckner et al. 2014; Moitinho-Silva et al. 2017c) as well as on sponge physiology and pumping rates (Weisz et al. 2008).

In contrast to most other animals, microbes in sponges mainly occur extracellularly, in close vicinity to sponge cells (but note exceptions where bacteria are enclosed in bacteriocytes e.g. Burgsdorf et al. 2019; Tianero et al. 2019). Bacterial cell densities can reach up to 10^9 cells per cm^3 of sponge tissue and outnumber sponge cell abundance by orders of magnitude (Taylor et al. 2007). Thus, these morphological basal animals constitute one of the most complex holobionts with several types of sponge cells and a large diversity of microbial symbiont lineages coexisting in the same matrix. In this chapter, we focus on three main types of interactions: (i) the dialogue between sponge cells and bacteria, (ii) the dialogue between bacterial cells and (iii) the tripartite interaction between sponge cells, bacteria and bacteriophages (Figure 1). In the first section, we will discuss the current knowledge on host mechanisms for microbial recognition as well as microbial features to promote tolerance. In the second section, we will present recent literature on bacteria-bacteria interactions in the context of quorum sensing/quenching. In the third section, we will present a recent discovery on how bacteriophages can foster sponge-bacteria symbiosis. Finally, we will highlight emerging topics in sponge-microbe research.

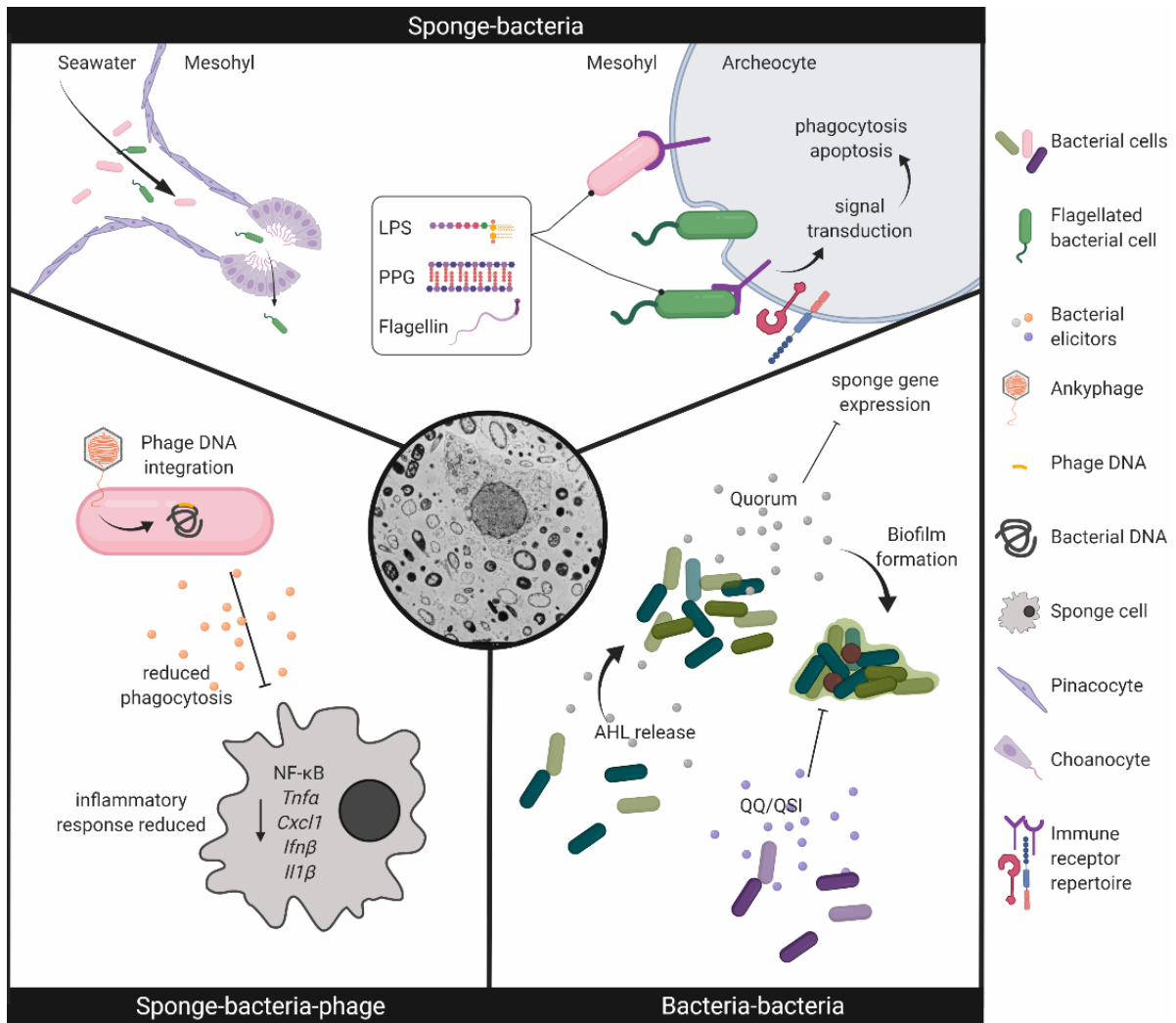


FIGURE 1 | Schematic presentation of the cellular interactions on the platform that the sponge mesohyl provides (central circle): sponge and bacterial cells (upper panel); bacterial cells (right panel); sponge and bacterial cells with bacteriophages (left panel; adapted from Jahn et al. 2019). LPS – lipopolysaccharides; PPG – peptidoglycan; AHL - N-acyl homoserine lactones; QQ/QSI – quorum sensing/quorum sensing inhibition. The figure was created with the visualization tool BioRender.com.

HOST-MICROBE DIALOGUE

Already in the early 80's, Wilkinson et al. (1979) reported that sponges can distinguish between seawater bacteria and their symbionts by feeding tritium-labelled bacteria to sponges followed by high-resolution radioautography of sponge tissue. While most cells of the bacterial symbionts passed through the sponge unharmed and were expelled via the exhalant water, the seawater bacteria (*Vibrio alginolyticus*) were retained by the sponge and were digested. Later, Wehrl et al. (2007) confirmed that feeding rates of sponges on seawater bacteria are higher than on sponge symbionts. How does the sponge differentiate between food bacteria and symbionts?

To address this question in an experimental way, differential gene expression analyses was used to characterize the molecular response of sponges towards microbial elicitors. Two sponges that are representatives of the HMA/LMA dichotomy (*Aplysina aerophoba*, HMA, *Dysidea avara*, LMA) were exposed to a cocktail of lipopolysaccharide and peptidoglycan as signals (Pita et al. 2018). We hypothesized that the different microbial densities in these sponges would affect the host's responses towards bacterial elicitors. Both species responded to microbial stimuli by increasing the expression of a subset of immune receptors (such as NLRs in *D. avara*, SRCR and GPCRs in *A. aerophoba*) and activating kinase cascades likely yielding apoptotic and phagocytotic processes (Figure 2). Moreover, the magnitude of the transcriptionally-regulated response (in terms of number of differentially expressed genes) was more complex in *A. aerophoba* (HMA) than in *D. avara* (LMA). We propose that the HMA species requires a more fine-tuned regulated response to deal with conflicting signals coming from the microbial stimuli vs those from the symbionts.

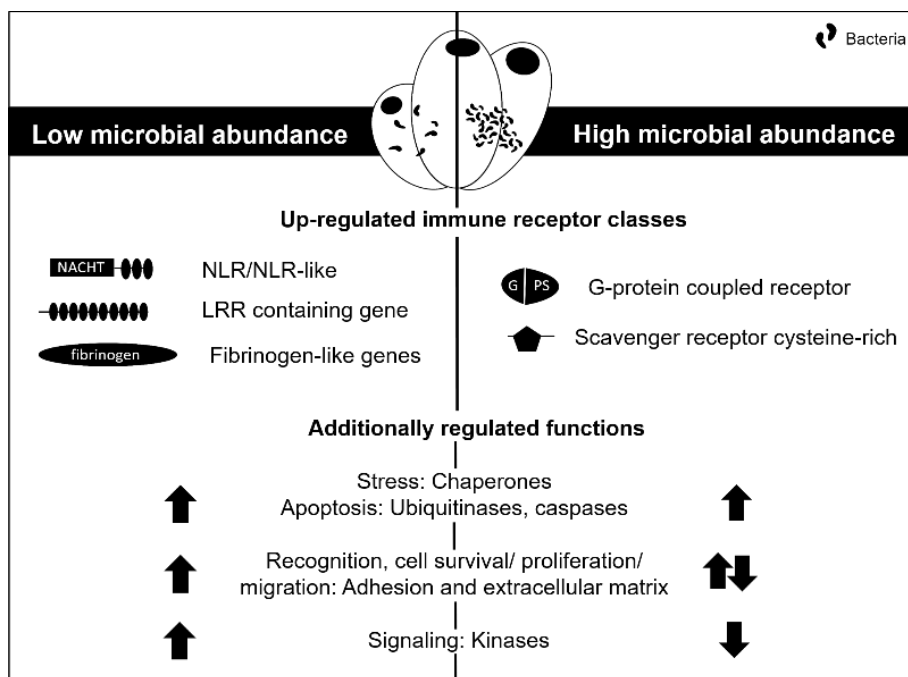


FIGURE 2 | Differentially expressed genes in *Dysidea avara* (LMA sponge, left side) and *Aplysina aerophoba* (HMA sponge, right side) after exposure to bacterial elicitors (LPS and peptidoglycan) (adapted from Pita et al. 2018). The up-regulated immune receptors with characteristic, conserved domains are depicted, as well as additional regulated functions (up- and/or down-regulation represented by arrows).

Other studies support the role of the sponge immune system in the crosstalk with microbes. The sponge *Petrosia ficiformis* displayed an increased expression of a gene containing the conserved SRCR domain when living in symbiosis with a cyanobacterium, in comparison to the aposymbiotic status

(Steindler et al. 2007). In juvenile *Amphimedon queenslandica*, bacterial encounter involved regulation of SRCR-containing genes, but the downstream signaling response differed depending on the origin of the bacteria (Yuen, 2016). In particular, the transcription factors *FoxO* and *NFκB* were up-regulated upon exposure to own symbionts, but not to a bacterial fraction from another sponge species (Yuen, 2016). Finally, the components of the TLR pathway such as *MyD88* were activated in response to microbial signals in different sponge species (Wiens et al. 2005; Yuen, 2016).

SPONGE-IMMUNE RECEPTORS

The sponge cellular immune response was studied already in the 19th century by Nobel laureate Elias Metchnikoff and colleagues (Metchnikoff, 1893). While these first studies were not focused on the sponge's response to microbes, the observed cell behaviors suggested that two cell types are the key players for mediating in the interactions with microbes: choanocytes (representing the first barrier for external microbes) and archeocytes (representing the patrol of the sponge matrix). Despite this promising takeoff, our understanding of sponge cellular immunity is still at the beginning. The publication of the first sponge genome, that of the Great Barrier Reef species *Amphimedon queenslandica*, brought a complex and expanded repertoire of immune receptors into light (Srivastava et al. 2010). This repertoire included several extracellular (i.e., scavenger receptor cystein-rich, SRCR, domain), membrane-bound (immunoglobulin-like domains), and intracellular (NOD-like receptor, NLR, domains) receptors (Srivastava et al. 2010; reviewed in Hentschel et al. 2012). These gene families were identified at sequence level because the domains (sequence patterns) were arranged in a particular architecture that is conserved from early metazoans to vertebrates. The conserved gene structure suggests a conserved function, which is not always clear. For example, Toll-like receptors (TLRs) are transmembrane receptors characterized by several extracellular leucine-rich repeat (LRR) motifs and an intracellular Toll/interleukin-1 receptor (TIR) domain. In vertebrates the extracellular LRR motifs recognize the ligand (e.g. bacteria) and transduce the signal via the TIR domain. All components of the signaling cascade induced by TLRs are present in *A. queenslandica*, but not the conventional TLR. The genome of *A. queenslandica* contained a TIR domain-containing gene, homolog of the TIR-domain in vertebrates TLRs, which was combined with extracellular Ig domains rather than LRR motifs. Therefore, its role in bacteria recognition remains to be validated.

A striking feature of the *A. queenslandica* genome was the high diversification of two other immune receptor families (Hentschel et al. 2012). The NLR family are defined according to the presence of a nucleotide-binding domain combined with a leucine-rich repeat domain (Ting et al. 2008). The genetic animal models *Drosophila melanogaster* and *C. elegans* lost this receptor family and, therefore, it was

long thought that these receptors had their origin in the teleost. An interesting feature of *A. queenslandica* NLRs is their enormous diversity: *A. queenslandica* genome comprises 135 genes, which is in stark contrast to 20 NLR genes in humans. Similarly, the family of scavenger receptors cysteine rich (SRCRs) in *A. queenslandica* is also highly expanded (ca. 300 genes) when compared to vertebrates (e.g. 16 genes in humans) and other invertebrates (Buckley and Rast, 2015). All cell types in *A. queenslandica* adult express genes with SRCR domains, but they are significantly enriched in choanocytes (Sebé-Pedrós et al. 2018). The evolutionary forces driving a high diversity of pattern recognition receptors (PRRs) are suggested to be related to the specific recognition of a wide variety of microbial compounds and has been proposed as a mechanism for specificity in sponges and other invertebrates (Schulenburg et al. 2007; Messier-Solek et al. 2010; Buckley and Rast, 2015; Degnan, 2015).

Since the publication of *A. queenslandica* genome in 2010, further sponges have been sequenced at genome and transcriptome level. Most of these reference genomes and transcriptomes are incomplete, yet they are adding new knowledge to our understanding on sponge molecular repertoire of immunity. Poriferan TLR/IL-1R-like receptors as well as their downstream signaling cascades were detected in other sponge genomes and transcriptomes (Riesgo et al. 2014; Germer et al. 2017; Pita et al. 2018). These new data confirmed the complex and expanded repertoire of Poriferan immune receptors, notably NLRs and SRCRs (Germer et al. 2017; Pita et al. 2018). However, there are also differences among sponge species that may be related to their symbiotic status (HMA or LMA). Ryu et al. (Ryu et al. 2016) detected different enrichment in immune domains depending on symbiont densities within the mesohyl when comparing the genomes of LMA sponges *A. queenslandica* and *Stylissa carteri* vs the HMA sponge *Xestospongia testudinaria*. Along similar lines, we detected 80 *bona fide* NLRs in the reference transcriptome of the LMA sponge *D. avara*; whereas, using the same experimental setup, we found only one *bona fide* NLR gene in *A. aerophoba* (HMA) reference transcriptome (Pita et al. 2018). The reference transcriptome of the HMA sponge *Vaceletia* sp. contained no NLR (Germer et al. 2017). These distinct signatures in the HMA and LMA genomic repertoires of immune receptors support the different evolutionary trajectories imposed by the symbiosis with microbes.

Apart from the above-mentioned receptors, lectins are also diversified in sponges. This class of soluble or membrane-bound proteins recognizes carbohydrates and mediates cell adherence, self/non-self-recognition and symbiotic relationships (Brown et al. 2018; Dinh et al. 2018). A few dozen lectins from sponges are known so far of which some may aid in bacterial recognition by responding to carbohydrates from gram positive (peptidoglycan) as well as from gram negative (lipopolysaccharides)

bacteria (reviewed in Gardères et al. 2012). In a growth assay, a lectin from *Halichondria panicea* stimulated bacterial proliferation of sponge derived bacterial strains (Müller et al. 1981).

MICROBE-ASSOCIATED MOLECULAR PATTERNS (MAMPs)

Immune receptors detect microorganisms via molecules that are present in prokaryotes but absent in eukaryotes, the so-called “pathogen associated molecular patterns” (PAMPs). PAMPs include components of bacterial cell walls and membranes such as peptidoglycans (PPGs) of gram-positive bacteria and lipopolysaccharides (LPS) from gram negative bacteria. If such PAMPs are recognized by an immune receptor, they will trigger a signaling cascade yielding the elimination of the microbial invader (e.g. via phagocytosis). It was soon recognized that PAMPs are not exclusive for pathogens, but are also present in bacterial symbionts (Koropatnick et al. 2004), leading to the alternative use of the term „microbe associated molecular patterns“ or MAMPs. Therefore, host recognition of microorganisms must be specific enough to yield an appropriate response, which may be either to eliminate or tolerate microorganisms.

We have limited experimental evidence for which symbiont MAMPs may be recognized by poriferan receptors. However, genetic features enriched or depleted in sponge-associated versus free-living bacteria revealed interesting patterns. In this context, it is remarkable that sponge-associated microbes lack flagella (Siegl et al. 2011). Flagellin is known as a powerful immune stimulator that initiated e.g. signal transduction mediated by TLR5 receptors (Hayashi et al. 2001). The absence of flagella (thus, flagellin) could allow microbes to evade host immunity and persist within the sponge holobiont. On a different note, a common sponge symbiont, “*Candidatus Synechococcus spongiarum*” (Cyanobacteria) presents a modified O-antigen in its LPS, as compared to free-living *Synechococcus* relatives (Burgsdorf et al. 2015). This modification could represent another mechanism for recognition. Thus, modifications in MAMP structure could help microbes to escape recognition as “non-self” by the host. Altogether, these studies provide evidence of adaption to symbiosis in both the host and the microbial side.

BACTERIA-BACTERIA DIALOGUE

Within the sponge holobiont, bacterial cells do not only interact with the sponge cells, but also with bacteria of the same or other species. Figure 3 is an illustration of the density of microbes within the sponge mesohyl matrix. Competition for space and resources or initiation of biofilm formation, as well

as secondary metabolite production are among the well-studied topics of bacterial communication (Abisado et al. 2018). Thereby, competition and cooperation are facilitated within the proximity of micrometers and are often a matter of balance (Nadell et al. 2016; Rakoff-Nahoum et al. 2016). Modeling can aid in predicting the metabolic interactions between bacteria, either based on co-occurrence models from relative abundance data (Thomas et al. 2016) or from metabolic models as inferred from metagenomic data (Slaby et al. 2017).

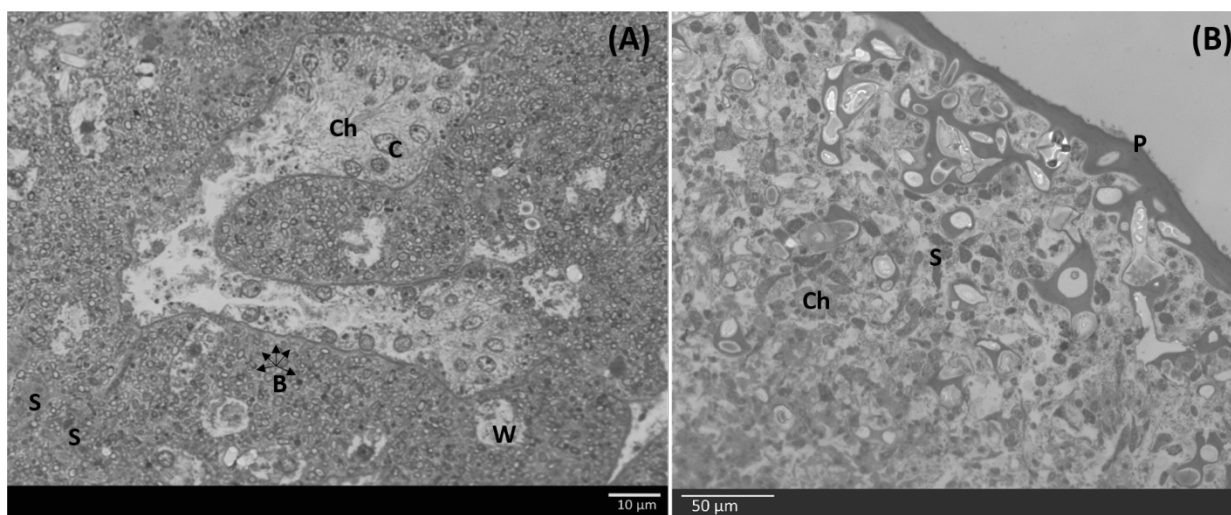


FIGURE 3 | The sponge extracellular matrix is densely populated by sponge cells as well as by diverse and abundant bacterial symbionts. Light microscopy images of semi-thin sponge tissue sections **(A)** of *Plakortis simplex* stained with Richardson solution and **(B)** of *Acantheurypon spinispinosum*. An epithelium-like outer cell layer, (pinacoderm, visible in (B)) surrounds the extracellular matrix (mesohyl) and the inorganic skeleton made up of spicules. Only pinacocytes are connected by tight junctions (Draper et al. 2019). C – choanocytes in Ch - choanocyte chamber; P – pinacoderm; B – bacterial cells in mesohyl; S – sponge cell; W – water canal. Images kindly provided by Kathrin Busch (GEOMAR Helmholtz Centre for Ocean Research Kiel).

QUORUM SENSING

Bacteria-bacteria communication within the sponge extracellular matrix is mediated by quorum-sensing (QS). QS is a universal principle that aids inter-bacterial communication and is known from free-living as well as host-associated marine bacteria (reviewed in Hmelo, 2017). Quorum sensing relies on the use of diffusible chemical signals in a population density-dependent manner. With increasing bacteria population size, the concentration of released QS molecules increases accordingly and eventually reaches a level (quorum) that initiates coordinated responses at the population level. QS mediates cellular mechanisms such as cell division, secondary metabolite production, plasmid transfer, and biofilm formation (Fuqua et al. 1994; Venturi and Subramoni, 2009).

One of the most studied QS active molecule classes are N-acyl homoserine lactones (AHLs). AHLs are produced via the synthase LuxI family and interact with the LuxR cognate receptor proteins to initiate transcriptional activators and gene expression (Fuqua et al. 1994). The AHLs were first discovered in the marine bacterium *Vibrio fischeri* (Fuqua et al. 1994) and were detected in bacteria isolated from sponges for the first time in 2004 (Taylor et al. 2004). A great variety of AHLs have been recovered from sponge-derived bacterial isolates of different phylogenetic affiliations, including Gammaproteobacteria, Alphaproteobacteria, Firmicutes and Flavobacteria (Bin Saidin et al. 2017; Mohamed et al. 2008; Mangano et al. 2018).

While bacterial isolates allow a thorough characterization of AHLs and their producers, only a small fraction of the sponge symbionts is cultivable, making it difficult to interpret the relevance of AHLs within the holobiont. Metagenomic data from *Theonella swinhoei* revealed an AHL synthase of an uncultured member of the Rhodobacterales family (Britstein et al. 2016). When heterologously expressed in *E. coli*, the synthase produced three different AHLs, demonstrating its function *in vitro* (Britstein et al. 2016). The first *in vivo* evidence of AHL production within the sponge comes from a study on *Suberites domuncula* (Gardères et al. 2012). AHLs were found in extracts of the whole sponge but not in extracts from the sponge cells, suggesting that the sponge itself does not produce AHLs (Gardères et al. 2012).

AHL production seems to be dependent on host-species and varies over time (Britstein et al. 2018). Out of four investigated sponge species, one showed AHL production year-round, one showed no production at all, and two species displayed periodic production of AHLs (Britstein et al. 2018). For the sponge with constant AHL production, 14 different AHL molecules were identified, while only 9 were present in the three replicate individuals. However, it is still unclear what drives this diversity. AHL patterns were neither related to LMA/HMA dichotomy nor correlated to microbiome composition (Britstein et al. 2018). One possibility is that constantly expressed AHLs derive from the core microbiome while varying AHL molecules result from transient seawater bacteria. Britstein et al. (2018) propose that microbial activity (i.e. gene expression) rather than microbial composition could account for AHL variability.

On the contrary, a single sponge-associated bacterium can produce a high diversity of AHLs, as in the case of a member of the family Rhodobacteraceae (Alphaproteobacteria), *Paracoccus sp.* Ss63 isolated from *Sarcotragus sp.* (Saurav et al. 2016). *Paracoccus sp.* Ss63 is present in low abundances in seawater, sediment and other sponges. A diverse array of AHL molecules may provide the possibility to sense various environmental cues aiding the free-living versus host-associated life-style (Girard et al. 2019). For example, the pH gradient between seawater and sponges might benefit the

accumulation of AHLs within the host and thus aid symbiosis establishment (Saurav et al. 2016). The clear role of AHLs within the sponge holobiont remains unknown, however, they are likely relevant for the bacteria-bacteria dialogue within the sponge holobiont.

QUORUM QUENCHING

Quorum quenching (QQ) and quorum sensing inhibition (QSI) refer to mechanisms by which QS molecules are degraded or inactivated and communication is interrupted (reviewed in Borges and Simoes, 2019). Sponges have recently been mined for both, QSI and QQ molecules (reviewed in Saurav et al. 2017) while several sponge extracts showed QSI or QQ activity which inhibited biofilm formation and/or population growth (Annapoorani et al. 2012; Mai et al. 2015; Britstein et al. 2016, Gutiérrez-Barranquero et al. 2017). In some cases, these molecules were able to disrupt established biofilms (Gutiérrez-Barranquero et al. 2017). Plakofuranolactone (γ -lactone) is one of the few well described QQ active molecules and was isolated from the sponge *Plakortis cf. lita* (Costantino et al. 2017). The bacterial origin of this molecule has been proven, but the microbial producer remains unidentified. A dual QS/QSI activity was described for bacteria isolated from sponges (Gutiérrez-Barranquero et al. 2017) highlighting the complexity of bacterial interactions within the sponge holobiont.

The exchange of molecules between bacteria might ultimately interfere with the communication between sponge cells or between sponge and bacteria. QS was shown to not only to work in bacteria-bacteria interactions, but also to be involved in inter-kingdom communication in both animals and plants (González and Venturi, 2013; Pietschke et al. 2017; Weiland-Bräuer et al. 2019). In primmorph-cultures and adult *Suberitus domuncula* sponges, short-term stimulation with bacterial N-3-oxododecanoyl-L-homoserine lactone affected gene expression of the sponge-host, while cell viability and morphology remained unaffected (Gardères et al. 2014). More specifically, genes related to immunity and apoptosis were downregulated as assessed by qRT-PCR, potentially aiding the sponge to monitor and regulate bacterial populations (Gardères et al. 2014). This is a fascinating example of the interlinked dialogue between sponges and bacteria as molecules that have originally evolved for bacteria-bacteria interactions may eventually be adopted by the sponge as a means to detect and respond to microorganisms.

PHAGE-BACTERIA-HOST DIALOGUE

Phages are the most abundant and diverse entities in the oceans (Rohwer, 2003) and, along with their role as major bacterial killers, significantly impact global biochemical cycles (Suttle, 2007), bacterial fitness and diversity (King et al. 2018). In terms of numbers, each millilitre of seawater contains on average about 10 million virus particles. As filter-feeding animals, sponges pump up to 24,000 litres of seawater through their system per day (Weisz et al. 2008), exposing them to up to an estimated $\sim 2.4 \times 10^{13}$ viruses daily. The very high exposure to viruses prompts the question whether viruses interact in any way with either the sponge host or with its associated microbial symbionts. Interestingly, defence mechanisms against invading phages were identified previously as enriched features of microbial sponge symbionts by metagenomics (Fan et al. 2012; Slaby et al. 2017). These defence mechanisms are based on self–non-self-discrimination (i.e., restriction-modification system) or prokaryotic adaptive immunity (i.e., CRISPR-Cas system), representing major strategies against viral infection. While sponges are clearly exposed to massive amounts of viruses, little is known about their potential dialogue with the sponges and its associated microbial symbionts.

PHAGE-DIVERSITY AND HOST-SPECIFICITY

The presence of virus-like particles within sponge tissues was already described in 1978 (Vacelet and Gallissian, 1978) and was confirmed recently by electron-microscopy (Pascelli et al. 2018). In order to capture the molecular diversity of the viral associates, sponge virome sequencing was performed on several Great Barrier Reef sponges (Laffy et al. 2018). Interestingly, the identified patterns indicated species-specific viral signatures. Taxonomically, many of the recovered sponge associated viruses were dominated by clades of bacteriophages such as by tailed bacteriophages of the order *Caudovirales* (dsDNA) and *Microviridae* (ssDNA) as well as viruses including members of *Megavirales* and *Parvoviridae* (Laffy et al. 2018). High viral diversity and novelty was also found in a recent study by Jahn et al. (2019) who used metagenomics to characterize the viral diversity of three Mediterranean sponge species along with seawater controls. The extent of novelty in the sponge viromes was astonishing: only 3 % were known on the taxonomic family level. The identified virome signatures (“fingerprints”) were highly specific to their host sponges in that each individual displayed its own unique virome signature (Jahn et al. 2019). The observation of viruses being individual specific is consistent with similar findings in humans (Moreno-Gallego et al. 2019).

ANKYPHAGES AID SYMBIONTS IN IMMUNE EVASION

Jahn et al. (2019) further described a group of phages (hereafter termed “Ankyphages”) that suppresses immune cell function and phagocytosis in eukaryotic cells (reviewed in Leigh, 2019). These Ankyphages encode a novel symbiont phage-encoded protein, ANKp, that modulates eukaryote-bacterium interaction by altering the eukaryotes’ physiology in response to bacteria. Specifically, it appears that the phage-encoded Ankyrin protein is secreted from the bacterial cell and downregulates eukaryotic pro-inflammatory cytokines and phagocytosis in response to ANKp. These experiments were performed in murine cell lines as an experimentally tractable model for sponge-microbe interactions is still lacking. Murine macrophages display many features of a major class of sponge cells (archaeocytes) which, much like macrophages, are single, amoeboid cells that patrol the sponge matrix in search for bacteria to be phagocytosed. Moreover, the major elements involved in mammalian immune signalling were found to be present in sponges. The resulting data show, to our knowledge for the first time, that phage ANKp modulates the eukaryote response to bacteria by downregulating pro-inflammatory signalling along with reduced phagocytosis rates.

Surprisingly, homology searches revealed that Ankyphages are widely distributed in host-associated environments, including the human oral cavity, gut and stomach. It is thus tempting to speculate that the role of Ankyphages in mediating the dialogue between bacteria and animal hosts is much more widespread than in the context of marine sponges. In summary, ANKp represents the first secreted phage effector protein that downregulates eukaryote immunity upon exposure to bacteria. This is of relevance to host-microbe symbiosis research in that it provides the functional underpinnings for tripartite phage-bacteria-eukaryote dialogue. Moreover, this finding is of interest in the context of phage therapy as mechanisms to temper host immune responses are urgently sought-after in clinical and medical settings.

CONCLUSIONS AND FUTURE PERSPECTIVES

Sponge holobionts represent astonishingly complex ecosystems that consist of different types of host cells and a high diversity of microbes existing in close proximity to each other. We suggest phagocytizing cells, like choanocytes and archaeocytes, to be of special interest to unravel the sponge-microbe dialogue on the cellular level. Current efforts to develop experimental models for sponge symbioses promise a more functional understanding of the cellular interactions in the sponge holobiont. Further, they will inform how sponge-microbe interactions shape and maintain the performance of the holobiont and allow evolutionary insights.

ACKNOWLEDGEMENTS: We thank the members of the CRC1182 for stimulating discussions on metaorganism research. Funding was provided by the DFG CRC1182 “Origin and Function of Metaorganisms” to U. H. (TPB1) and to M. T. J. (Young Investigator Award). L. S. was funded by the IMPRS for Evolutionary Biology.

REFERENCES

- Abisado, R. G., Benomar, S., Klaus, J. R., Dandekar, A. A., and Chandler, J. R. 2018. Bacterial quorum sensing and microbial community interactions. *mBio* 9: 1–13.
- Annapoorani, A., Jabbar, A. K. K. A., Musthafa, S. K. S., Pandian, S. K., and Ravi, A. V. 2012. Inhibition of quorum sensing mediated virulence factors production in urinary pathogen *Serratia marcescens* PS1 by marine sponges. *Indian Journal of Microbiology* 52: 160–166.
- Bin Saidin, J., Abd Wahid, M. E., and Le Pennec, G. 2017. Characterization of the in vitro production of N-acyl homoserine lactones by cultivable bacteria inhabiting the sponge *Suberites domuncula*. *Journal of the Marine Biological Association of the United Kingdom* 97: 119–127.
- Björk, J. R., Díez-Vives, C., Astudillo-Garcia, C., Archie, E., and Montoya, J. M. 2018. Vertical transmission of sponge microbiota is inconsistent and unfaithful. *BioRxiv* 425009.
- Borges, A., and Simoes, M. 2019. Quorum sensing inhibition by marine bacteria. *Marine Drugs* 17: 1–25.
- Britstein, M., Devescovi, G., Handley, K. M., et al. 2016. A new N-Acyl homoserine lactone synthase in an uncultured symbiont of the red sea sponge *Theonella swinhoei*. *Applied and Environmental Microbiology* 82: 1274–1285.
- Britstein, M., Saurav, K., Teta, R., et al. 2018. Identification and chemical characterization of N-acyl-homoserine lactone quorum sensing signals across sponge species and time. *FEMS Microbiology Ecology* 94: 1–7.
- Brown, G. D., Willment, J. A., and Whitehead, L. 2018. C-type lectins in immunity and homeostasis. *Nature Reviews Immunology* 18: 374–389.
- Buckley, K. M., and Rast, J. P. 2015. Diversity of animal immune receptors and the origins of recognition complexity in the deuterostomes. *Developmental & Comparative Immunology* 49: 179–189.
- Burgsdorf, I., Handley, K. M., Bar-Shalom, R., Erwin, P. M., and Steindler, L. 2019. Life at home and on the roam: genomic adaptations reflect the dual lifestyle of an intracellular, facultative symbiont. *mSystems* 4.
- Burgsdorf, I., Slaby, B. M., Handley, K. M., et al. 2015. Lifestyle evolution in cyanobacterial symbionts of sponges. *mBio* 6: e00391-15.
- Costantino, V., Sala, G. D., Saurav, K., et al. 2017. Plakofuranolactone as a quorum quenching agent from the Indonesian sponge *Plakortis cf. lita*. *Marine Drugs* 15: 1–12.
- Degnan, S. M. 2015. The surprisingly complex immune gene repertoire of a simple sponge, exemplified by the NLR genes: A capacity for specificity? *Developmental & Comparative Immunology* 48: 269–274.
- Dinh, C., Farinholt, T., Hirose, S., Zhuchenko, O., and Kuspa, A. 2018. of Social Amoebae. *Science* (80). 406: 402–406.
- Draper, G. W., Shoemark, D. K., and Adams, J. C. 2019. Modelling the early evolution of extracellular matrix from modern ctenophores and sponges. *Essays in Biochemistry* EBC20180048.
- Fan, L., Liu, M., Simister, R., Webster, N. S., and Thomas, T. 2013. Marine microbial symbiosis heats up: the phylogenetic and functional response of a sponge holobiont to thermal stress. *ISME Journal* 7: 991–1002.

- Fan, L., Reynolds, D., Liu, M., et al. 2012. Functional equivalence and evolutionary convergence in complex communities of microbial sponge symbionts. *Proceedings of the National Academy of Sciences* 109: E1878–E1887.
- Fuqua, W. C., Winans, S. C., and Greenberg, E. P. 1994. Quorum sensing in bacteria: The LuxR-LuxI family of cell density-responsive transcriptional regulators. *Journal of Bacteriology* 176: 269–275.
- Gardères, J., Henry, J., Bernay, B., et al. 2014. Cellular effects of bacterial N-3-oxo-dodecanoyl-L-homoserine lactone on the sponge *Suberites domuncula* (Olivi, 1792): Insights into an intimate inter-kingdom dialogue. *PLoS One* 9: 1–10.
- Gardères, J., Taupin, L., Bin-Saïdin, J., Dufour, A., and Le Pennec, G. 2012. N-acyl homoserine lactone production by bacteria within the sponge *Suberites domuncula* (Olivi, 1792) (Porifera, Demospongiae). *Marine Biology* 159: 1685–1692.
- Germer, J., Cerveau, N., and Jackson, D. J. 2017. The holo-transcriptome of a calcified early branching metazoan. *Frontiers in Marine Science* 4: 1–19.
- Girard, L., Lantoine, F., Lami, R., Vouvé, F., Suzuki, M. T., and Baudart, J. 2019. Genetic diversity and phenotypic plasticity of AHL-mediated quorum sensing in environmental strains of *Vibrio mediterranei*. *ISME Journal* 13: 159–169.
- Gloeckner, V., Wehrl, M., Moitinho-Silva, L., et al. 2014. The HMA-LMA dichotomy revisited: an electron microscopical survey of 56 sponge species. *Biological Bulletin* 227: 78–88.
- González, J. F., and Venturi, V. 2013. A novel widespread interkingdom signaling circuit. *Trends in Plant Science* 18: 167–174.
- Gutiérrez-Barranquero, J. A., Reen, F. J., Parages, M. L., McCarthy, R., Dobson, A. D. W., O’Gara, F. 2017. Disruption of N-acyl-homoserine lactone-specific signalling and virulence in clinical pathogens by marine sponge bacteria. *Microbial Biotechnology* 12: 1049–1063.
- Hayashi, F., Smith, K. D., Ozinsky, A., et al. 2001. The innate immune response to bacterial flagellin is mediated by Toll-like receptor 5. *Nature Letters* 410: 1–6.
- Hentschel, U., Piel, J., Degnan, S. M., and Taylor, M. W. 2012. Genomic insights into the marine sponge microbiome. *Nature Reviews Microbiology* 10: 641–654.
- Hmelo, L. R. 2017. Quorum sensing in marine microbial environments. *Annual Review of Marine Science* 9: 257–281.
- Horn, H., Slaby, B. M., Jahn, M. T., et al. 2016. An enrichment of CRISPR and other defense-related features in marine sponge-associated microbial metagenomes. *Frontiers in Microbiology* 7.
- Jahn, M. T., Arkipova, K., Markert, S. M., et al. 2019. A phage protein aids bacterial symbionts in eukaryote immune evasion. *Cell Host Microbe* 26: 542-550.e5.
- Jahn, M. T., Markert, S. M., Ryu, T., et al. 2016. Shedding light on cell compartmentation in the candidate phylum Poribacteria by high resolution visualisation and transcriptional profiling. *Scientific Reports* 6: 1–9.
- King, K. C., Zelek, M., Gray, C., Betts, A., and MacLean, R. C. 2018. High parasite diversity accelerates host adaptation and diversification. *Science* 360: 907–911.
- Koropatnick, T. A., Engle, J. T., Apicella, M. A., Stabb, E. V., Goldman, W. E., and McFall-Ngai, M. J. 2004. Microbial factor-mediated development in a host-bacterial mutualism. *Science* 306: 1186–1188.
- Laffy, P. W., Wood-Charlson, E. M., Turaev, D., et al. 2018. Reef invertebrate viromics: diversity, host specificity and functional capacity. *Environmental Microbiology* 20: 2125–2141.
- Leigh, B. A. 2019. Cooperation among conflict: prophages protect bacteria from phagocytosis. *Cell Host Microbe* 26: 450–452.
- Mai, T., Tintillier, F., Lucasson, A., et al. 2015. Quorum sensing inhibitors from *Leucetta chagosensis* Dendy, 1863. *Letters in Applied Microbiology* 61: 311–317.
- Mangano, S., Caruso, C., Michaud, L., Lo Guidice, A. 2018. First evidence of quorum sensing activity in bacteria associated with Antarctic sponges. *Polar Biology* 41: 1435–1445.
- Messier-Solek, C., Buckley, K. M., Rast, J. P. 2010. Highly diversified innate receptor systems and new forms of animal immunity. *Seminars in Immunology* 22: 39–47.

- Metchnikoff, E. 1893. *Lectures on the comparative pathology of inflammation*. London, Kegan Paul, Trench, Trubner & Co.
- Mohamed, N. M., Cicirelli, E. M., Kan, J., Chen, F., Fuqua, C., and Hill, R. T. 2008. Diversity and quorum-sensing signal production of Proteobacteria associated with marine sponges. *Environmental Microbiology* 10: 75–86.
- Moitinho-Silva, L., Díez-Vives, C., Batani, G., Esteves, A. I. S., Jahn, M. T., and Thomas, T. 2017a. Integrated metabolism in sponge-microbe symbiosis revealed by genome-centered metatranscriptomics. *ISME Journal* 11: 1651–1666.
- Moitinho-Silva, L., Nielsen, S., Amir, A., et al. 2017b. The sponge microbiome project. *GigaScience* 6: 1–7.
- Moitinho-Silva, L., Steinert, G., Nielsen, S., et al. 2017c. Predicting the HMA-LMA status in marine sponges by machine learning. *Frontiers in Microbiology* 8: 1–14.
- Moreno-Gallego, J. L., Chou, S.-P., Di Rienzi, S. C., et al. 2019. Virome diversity correlates with intestinal microbiome diversity in adult monozygotic twins. *Cell Host Microbe* 25: 261–272.
- Müller, W. E., Zahn, R. K., Kurelec, B., Lucu, C., Müller, I., and Uhlenbruck, G. 1981. Lectin, a possible basis for symbiosis between bacteria and sponges. *Journal of Bacteriology* 145: 548–558.
- Nadell, C. D., Drescher, K., and Foster, K. R. 2016. Spatial structure, cooperation and competition in biofilms. *Nature Reviews Microbiology* 14: 589–600.
- Pascelli, C., Laffy, P. W., Kupresanin, M., Ravasi, T., and Webster, N. S. 2018. Morphological characterization of virus-like particles in coral reef sponges. *PeerJ* 6: e5625.
- Pietschke, C., Treitz, C., Forêt, S., et al. 2017. Host modification of a bacterial quorum-sensing signal induces a phenotypic switch in bacterial symbionts. *Proceedings of the National Academy of Sciences* 201706879.
- Pita, L., Hoepfner, M. P., Ribes, M., and Hentschel, U. 2018. Differential expression of immune receptors in two marine sponges upon exposure to microbial-associated molecular patterns. *Scientific Reports* 8: 1–15.
- Podell, S., Blanton, J. M., Neu, A., et al. 2019. Pangenomic comparison of globally distributed Poribacteria associated with sponge hosts and marine particles. *ISME Journal* 13: 468–481.
- Rakoff-Nahoum, S., Foster, K. R., and Comstock, L. E. 2016. The evolution of cooperation within the gut microbiota. *Nature* 533: 255–259.
- Riesgo, A., Farrar, N., Windsor, P. J., Giribet, G., and Leys, S. P. 2014. The analysis of eight transcriptomes from all poriferan classes reveals surprising genetic complexity in sponges. *Molecular Biology and Evolution* 31: 1102–1120.
- Rohwer, F. 2003. Global phage diversity. *Cell* 113(2): 141.
- Russell, S. L. 2019. Transmission mode is associated with environment type and taxa across bacteria-eukaryote symbioses: a systematic review and meta-analysis. *FEMS Microbiology Letters* 366: 430–439.
- Ryu, T., Seridi, L., Moitinho-Silva, L., et al. 2016. Hologenome analysis of two marine sponges with different microbiomes. *BMC Genomics* 17: 1–11.
- Saurav, K., Burgsdorf, I., Teta, R., et al. 2016. Isolation of marine *Paracoccus* sp. Ss63 from the sponge *Sarcotragus* sp. and characterization of its quorum-sensing chemical-signaling molecules by LC-MS/MS analysis. *Israel Journal of Chemistry* 56: 330–340.
- Saurav, K., Costantino, V., Venturi, V., and Steindler, L. 2017. Quorum sensing inhibitors from the sea discovered using bacterial N-acyl-homoserine lactone-based biosensors. *Marine Drugs* 15(53).
- Schmitt, S., Angermeier, H., Schiller, R., Lindquist, N., and Hentschel, U. 2008. Molecular microbial diversity survey of sponge reproductive stages and mechanistic insights into vertical transmission of microbial symbionts. *Applied and Environmental Microbiology* 74: 7694–7708.
- Schulenburg, H., Boehnisch, C., and Michiels, N. K. 2007. How do invertebrates generate a highly specific innate immune response? *Molecular Immunology* 44: 3338–3344.
- Sebé-Pedrós, A., Chomsky, E., Pang, K., et al. 2018. Early metazoan cell type diversity and the evolution of multicellular gene regulation. *Nature Ecology & Evolution* 2: 1176–1188.

- Sharp, K. H., Eam, B., Faulkner, D. J., and Haygood, M. G. 2007. Vertical transmission of diverse microbes in the tropical sponge *Corticium sp.* *Applied and Environmental Microbiology* 73: 622–629.
- Siegl, A., Kamke, J., Hochmuth, T., et al. 2011. Single-cell genomics reveals the lifestyle of Poribacteria, a candidate phylum symbiotically associated with marine sponges. *ISME Journal* 5: 61–70.
- Sipkema, D., de Caralt, S., Morillo, J. A., et al. 2015. Similar sponge-associated bacteria can be acquired via both vertical and horizontal transmission. *Environmental Microbiology* 17: 3807–3821.
- Slaby, B. M., Hackl, T., Horn, H., Bayer, K., and Hentschel, U. 2017. Metagenomic binning of a marine sponge microbiome reveals unity in defense but metabolic specialization. *ISME Journal* 11: 2465–2478.
- Srivastava, M., Simakov, O., Chapman, J., et al. 2010. The *Amphimedon queenslandica* genome and the evolution of animal complexity. *Nature* 466: 720–726.
- Steindler, L., Schuster, S., Ilan, M., Avni, A., Cerrano, C., Beer, S. 2007. Differential gene expression in a marine sponge in relation to its symbiotic state. *Marine Biotechnology* 9: 543–549.
- Suttle, C. A. 2007. Marine viruses — major players in the global ecosystem. *Nature Reviews Microbiology* 5: 801.
- Taylor, M. W., Schupp, P. J., Baillie, H. J., et al. 2004. Evidence for acyl homoserine lactone signal production in bacteria associated with marine sponges. *Applied and Environmental Microbiology* 70: 4387–4389.
- Taylor, M. W., Thacker, R. W., and Hentschel, U. 2007. Evolutionary insights from sponges. *Science* 316: 1854–1855.
- Thomas, T., Moitinho-Silva, L., Lurgi, M., et al. 2016. Diversity, structure and convergent evolution of the global sponge microbiome. *Nature Communications* 7: 11870.
- Tianero, M. D., Balaich, J. N., and Donia, M. S. 2019. Localized production of defence chemicals by intracellular symbionts of *Haliclona* sponges. *Nature Microbiology* 4: 1149–1159.
- Ting, J. P. Y., Lovering, R. C., Alnemri, E. S., et al. 2008. The NLR gene family: a standard nomenclature. *Immunity* 28: 285–287.
- Vacelet, J., and Gallissian, M. F. 1978. Virus-like particles in cells of the sponge *Verongia cavernicola* (Demospongiae, Dictyoceratida) and accompanying tissues changes. *Journal of Invertebrate Pathology* 31: 246–254.
- Van Soest, R. W. M., Boury-Esnault, N., Vacelet, J., et al. 2012. Global diversity of sponges (Porifera). *PLoS One* 7: e35105.
- Venturi, V., and Subramoni, S. 2009. Future research trends in the major chemical language of bacteria. *HFSP Journal* 3: 105–116.
- Webster, N. S., Taylor, M. W., Behnam, F., et al. 2010. Deep sequencing reveals exceptional diversity and modes of transmission for bacterial sponge symbionts. *Environmental Microbiology* 12: 2070–2082.
- Wehrl, M., Steinert, M., and Hentschel, U. 2007. Bacterial uptake by the marine sponge *Aplysina aerophoba*. *Microbial Ecology* 53: 355–365.
- Weiland-Bräuer, N., Fischer, M. A., Pinnow, N., and Schmitz, R. A. 2019. Potential role of host-derived quorum quenching in modulating bacterial colonization in the moon jellyfish *Aurelia aurita*. *Scientific Reports* 9: 1–12.
- Weisz, J. B., Lindquist, N., and Martens, C. S. 2008. Do associated microbial abundances impact marine demosponge pumping rates and tissue densities? *Oecologia* 155: 367–376.
- Wiens, M., Korzhev, M., Krasko, A., et al. 2005. Innate immune defense of the sponge *Suberites domuncula* against bacteria involves a MyD88-dependent signaling pathway: Induction of a perforin-like molecule. *Journal of Biological Chemistry* 280: 27949–27959.
- Wilkinson, C. R., Garrone, R., and Vacelet, J. 1979. Marine sponges discriminate between food bacteria and bacterial symbionts: electron microscope radioautography and in situ evidence. *Proceedings of the Royal Society B* 205: 519–528.

Yin, Z., Zhu, M., Davidson, E. H., Bottjer, D. J., Zhao, F., and Tafforeau, P. 2015. Sponge grade body fossil with cellular resolution dating 60 Myr before the Cambrian. *Proceedings of the National Academy of Sciences* 1453-1460.

Yuen, B. 2016. Deciphering the genomic toolkit underlying animal-bacteria interactions-insights through the demosponge *Amphimedon queenslandica*. PhD diss., University of Queensland.

Copyright © 2021 Taylor & Francis Group, LLC

CRC Press is an imprint of Taylor & Francis Group, LLC

Reproduced with permission of The Licensor through PLSclear.

CHAPTER 2

INDIVIDUALITY IN THE IMMUNE REPERTOIRE AND INDUCED RESPONSE OF THE SPONGE *HALICHONDRIA PANICEA*

Chapter published under the terms of the Creative Commons Attribution License (CC-BY 4.0).

Original publication by *Frontiers in Immunology*

Schmittmann L., Franzenburg S., Pita L. 2021. Individuality in the immune repertoire and the induced response of the sponge *Halichondria panicea*. *Frontiers in Immunology*. 12. 1. DOI 10.3389/fimmu.2021.689051.

INDIVIDUALITY IN THE IMMUNE REPERTOIRE AND INDUCED RESPONSE OF THE SPONGE *HALICHONDRIA PANICEA*

Schmittmann L.^{1*}, Franzenburg S.², Pita L.^{1*}

¹Research Unit Marine Symbioses, GEOMAR Helmholtz Centre for Ocean Research, Kiel, Germany,

²Research Group Genetics & Bioinformatics / Systems Immunology, Institute of Clinical Molecular Biology, Christian-Albrechts-University of Kiel, Germany, *correspondence authors

ABSTRACT

The animal immune system mediates host-microbe interactions from the host perspective. Pattern recognition receptors (PRRs) and the downstream signaling cascades they induce are a central part of animal innate immunity. These molecular immune mechanisms are still not fully understood, particularly in terms of baseline immunity vs induced specific responses regulated upon microbial signals. Early-divergent phyla like sponges (Porifera) can help to identify the evolutionarily conserved mechanisms of immune signaling. We characterized both the expressed immune gene repertoire and the induced response to lipopolysaccharides (LPS) in *Halichondria panicea*, a promising model for sponge symbioses. We exposed sponges under controlled experimental conditions to bacterial LPS and performed RNA-seq on samples taken 1h and 6h after exposure. *H. panicea* possesses a diverse array of putative PRRs. While part of those PRRs was constitutively expressed in all analyzed sponges, the majority was expressed individual-specific and regardless of LPS treatment or timepoint. The induced immune response by LPS involved differential regulation of genes related to signaling and recognition, more specifically GTPases and post-translational regulation mechanisms like ubiquitination and phosphorylation. We have discovered individuality in both the immune receptor repertoire and the response to LPS, which may translate into holobiont fitness and susceptibility to stress. The three different layers of immune gene control observed in this study, - namely constitutive expression, individual-specific expression, and induced genes -, draw a complex picture of the innate immune gene regulation in *H. panicea*. Most likely this reflects synergistic interactions among the different components of immunity in their role to control and respond to a stable microbiome, seawater bacteria, and potential pathogens.

Keywords: innate immunity, Porifera, LPS, host-microbe interaction, early-diverging metazoa, gene expression, RNA-seq, holobiont

INTRODUCTION

The core function of immunity is shared across animals: to differentiate between self and non-self, to maintain homeostasis, and to interact with microbes (1, 2). Immunity accompanied the evolution of multicellularity in response to the coexistence with microbial life, which already dominated our planet when animals emerged (3). Innate immunity is the most ancient and universal mechanism for host-microbe interactions and, even if vertebrates evolved adaptive immunity, they also strongly rely on their innate immunity (4). A key component of innate immunity is a variety of pattern-recognition receptors (PRRs), which detect microbes via conserved microbial-associated molecular patterns (MAMPs) like lipopolysaccharides (LPS), peptidoglycan, or flagellin (5). Among the most studied PRRs are: TLRs (Toll-like receptors), NLRs (nucleotide binding and leucine-rich repeat receptors), CTLD genes (C-type lectin like domain genes), and SRCRs (scavenger receptor cysteine-rich). In addition to classical PRRs, other receptor classes can detect microbial signals, among them GPCRs (G protein-coupled receptors) and cytokine receptors (6, 7). Some PRR families are highly diversified in invertebrates suggesting their potential for specific recognition (reviewed in 8). Traditionally, the evolution of PRR diversity has been seen as an “arms race” against pathogens (4, 9). But since recent, evidence suggests that PRRs also detect commensal microbes, promoting homeostasis (reviewed in 10).

The signals detected by PRRs are amplified *via* signaling cascades in order that the corresponding immune response can be mounted. Upon MAMP binding, induced transcriptomic responses can either intensify or also dampen the immune response, in a context-dependent manner (11, 12). It remains largely unknown which transcriptional mechanisms of signal transduction respond to different MAMPs, how they determine the specific response to pathogens or commensals, and how they might differ between and within animal phyla. On the one hand, the genetically available immune repertoire will determine the potential response of an animal. On the other hand, the realized (expressed) immune repertoire often differs from the potential repertoire and the expressed genes prior to microbe encounter are relevant to the response that is mounted (13). It is thus important to characterize the molecular components of the baseline immunity and the induced responses to get a comprehensive picture of the mechanisms mediating animal- microbe interactions.

Sponges (phylum Porifera) as early-diverging metazoans provide information about the origin and early evolution of innate immunity. They harbor a specific and stable microbiome (14) while feeding on microbes from the seawater (15, 16). Intriguingly, only one opportunistic sponge pathogen has been discovered so far (17). The first sponge genome, that of the Great Barrier reef sponge

Amphimedon queenslandica (18), revealed a complex repertoire of immune receptors, including NLRs, SRCRs, and non-canonical TLRs (19). Canonical TLRs are comprised of an intracellular TIR domain and extracellular LRRs (leucine-rich repeats), but sponge TLR-like receptors consist of the TIR domain [homologous to the TIR domain in vertebrate TLRs (20)], combined with extracellular immunoglobulin domains (19). Importantly, the PRR families NLR, GPCR, and SRCR are diversified in *A. queenslandica* (21–23) suggesting their potential for microbial differentiation (24). The genomes and transcriptomes generated so far confirmed that the diverse repertoire of PRRs and presence of TLR-mediated signaling cascades occur in other sponge species, too (20, 25, 26). However, the diversification of certain families and the induced response upon MAMP challenge may as well depend on the microbial density associated with sponges (26, 27). Based on the microbial density, sponges are classified as either high or low microbial abundance sponges (HMA or LMA, respectively) (28, 29). LMA sponges harbor two to four orders of magnitude less bacteria than HMA sponges (30). Still, the field of sponge immunity is at its infancy. It is largely unclear how sponges recognize and respond to bacteria and whether those mechanisms are conserved across this phylum, are linked to the HMA-LMA dichotomy, or are rather species-specific.

We aim to characterize the expressed immune repertoire and the induced response in the breadcrumb sponge *Halichondria panicea*, a promising model for sponge symbioses (31), by ways of RNA-seq. We explored both the repertoire and gene expression patterns of PRRs, as well as the induced immune response to bacterial LPS. *H. panicea* is an LMA sponge and is dominated by an extracellular alphaproteobacterial symbiont that is unique to this sponge species (32, 33). Our results provide a first understanding on the innate immune system of *H. panicea* in the context of sponge-microbe interactions.

MATERIALS AND METHODS

SPONGE COLLECTION AND LPS CHALLENGE

Twelve individuals of the breadcrumb sponge *H. panicea* were collected close to the shore at ~2 m depth in Kiel, Germany (54.424278, 10.175794) on 10.07.2018 and directly transferred to an open flow-through aquarium system at KIMMOCC facilities in GEOMAR Helmholtz Centre for Ocean Research, Kiel, Germany. We defined sponge individuals as these were collected from the same location but from distinct rocky crevices. Four weeks prior to the experiment, sponges were transferred to a closed re-circulation aquarium system with a mechanical and biological filter unit and thus reduced bacterial load. Each sponge individual was placed in separate 12 L aquariums and

divided into 2 equally sized clones (~2x2x3 cm). In the closed system, sponges were fed five times a week with powdered *Nannochloropsis salina* algae in sterile filtered saltwater (~ 6000 cells/mL, Algova, Germany). Water was constantly mixed by pressurized air supplied through 2 mL serological glass pipets. For the duration of the experiment on the 25.09.2018, the recirculation was stopped and experiments were performed at 15.1°C and a salinity of 15.4 PSU. The treatment was started by either injecting sponges with 500 µL of LPS at a concentration of 1 mg/mL (*Escherichia coli* O55:B5, Sigma L2880) in filtered sterile artificial seawater (LPS treatment), or with 500 µL filtered sterile artificial seawater as sham control (ASW control treatment). LPS or ASW were injected by piercing the sponges at 5 different locations with a syringe and needle (diameter 0.45 mm) and injecting 100 µL each time. This way, the treatment was distributed through the tissue and a local response prevented. Samples were taken 1 h and 6 h after treatment. Importantly, the same sponge individual was sampled at both time points (clones of the same individual), but not from both treatments (different individuals per treatment). The sponge tissue samples were cleaned from algae and rinsed with sterile filtered ASW before preservation in RNAlater. Samples were first stored at 4°C overnight and subsequently frozen at -80°C until RNA extraction. This experimental design consisted of 2 treatments x 2 time points x 6 replicates (5 replicates in the LPS treatment at 6 h due to poor RNA quality).

EUKARYOTIC TOTAL RNA EXTRACTION AND SEQUENCING

Eukaryotic total RNA was extracted from ~70-80 mg tissue with the AllPrep DNA/RNA Mini Kit (Qiagen, Netherlands) according to the manufactures' protocol. Degradation of RNA was inhibited by application of SUPERase-IN (Thermo Fisher Scientific, USA) at 1 U/µL and genomic DNA was removed post extraction (DNA-free DNA removal Kit, Thermo Fisher Scientific, USA). Successful removal of prokaryotic and eukaryotic DNA was verified by PCR and gel electrophoresis [18S rRNA primer Sp18aF 5'CCTGCCAGTAGTCATATGCTT, Sp18gR 5'CCTTGTTACGACTTTTACTTCCT (34), 16S rRNA gene primers Eco8F 5'AGAGTTTGATCCTGGCTCAG, 1492R 5'GGTTACCTTGTTACGACTT (35)]. RNA was quantified in Qubit (RNA BR Kit, Thermo Fisher Scientific, USA) and its quality checked spectrophotometrically (NanoDrop, Thermo Scientific, USA) and with automated electrophoresis (Experion, Bio-Rad, USA). RNA extracts were normalized to 50 ng/µL per sample by dilution with the Qiagen elution buffer. Library preparation (TruSeq stranded mRNA kit with poly-A enrichment, Illumina, USA) and paired-end sequencing (NovaSeq S1 2x150 bp, Illumina, USA) were performed at the IKMB Kiel, Germany.

DE NOVO TRANSCRIPTOME ASSEMBLY AND ANNOTATION

Adapter trimming and quality filtering of the raw sequencing reads was performed with Trimmomatic (36) (version 0.35, parameters LEADING:3 TRAILING:3 MINLEN:120). The read quality was manually checked in FastQC (version 0.11.8). Prokaryotic and microbial eukaryotic reads were removed with Kaiju (37) (version 1.7.2) in greedy-5 mode. Due to the lack of a reference genome for *H. panicea*, *de novo* transcriptome assembly was performed in Trinity (38) (version 2.8.5). The assembly was analyzed for completeness by comparing the longest isoforms of each Trinity component to the metazoan reference database for conserved genes with the BUSCO approach (39) (version 3.0.1). Annotation was performed with Trinotate (40) (version 3.2.0) by comparison to publicly available data (Blast+, SwissProt), protein domain identification (HMMER, Pfam), protein signal peptide and transmembrane domain prediction (signalP, tmHMM), as well as eggnog, GO and KEGG annotation. Contigs matching bacteria, archaea and viruses (based on blast results) were removed. The transcripts and the translated coding regions predicted by TransDecoder as part of the Trinotate pipeline (> 100 amino acids) were compared to the proteome of the sponge *A. queenslandica* (Uniprot UP000007879_444682) by blastx and blastp, respectively (e-value < 1e-5).

IDENTIFICATION OF GENES RELATED TO IMMUNITY

KEGG pathways were reconstructed with KEGG Mapper (41) (version 4.3) based on K numbers identified from the Trinotate blastp annotation. Genes mapping to KEGG pathways within the category “Organismal systems: Immune system” were considered as immune genes. Putative cytokine receptors were identified from KEGG pathways reconstructed based on the *A. queenslandica* blastp annotation (aqu04050 Cytokine receptors). In addition, we screened the reference transcriptome for immune receptors according to the presence of conserved domains (i.e., Pfam domains). In particular, we searched for the presence of TIR domains (PF1582), also in combination with Ig-like domains (PF00047), NACHT domains (PF05729), also in combination with leucine-rich repeat (LRR) domains (PF13516), GPS motifs (PF01825) and seven transmembrane domain (“7TM”), C-type lectin (PF00059) and Scavenger receptor cysteine-rich (SRCR) domains (PF00530 or PF15494). Protein visualization and arrangement of domains was manually checked for identified receptor proteins with SMART (42).

QUANTIFICATION OF CONSTITUTIVELY EXPRESSED GENES

Constitutively expressed genes were defined as expressed in all 23 samples (i.e., expression level >0 in RSEM expression matrix), regardless of the treatment. TMM (trimmed mean of M values) (43) normalized TPM (transcripts per million) expression was used to explore expression patterns among all sampled sponges (threshold > 10 TMM normalized TPM). Further, the average expression of constitutively expressed genes related to immunity was compared to other genes and differentially expressed genes. Plotting was performed in R with the packages ggplot2 and ComplexHeatmap (version R3.5.1 and 3.6.0) (44, 45).

DIFFERENTIAL GENE EXPRESSION ANALYSIS

Gene abundances (Trinity components) were quantified with RSEM (version 1.3.3) for each sample.

Differential gene expression between the control and LPS treatment was analyzed in DESeq2 (within Trinity version 2.8.5 run with R version 3.6.0) For this study, we defined differentially expressed genes (DEGs) as detected by DESeq2 with an FDR p-value < 0.005 and log₂-fold change ≥ 2. The DEGs were further assigned to different clusters based on expression pattern similarity (within Trinity version 2.8.5, tree height cut-off 40%) (for more details see Supplementary Figures 1, 2). We observed that in some clusters the expression levels were consistent among the replicates of the same treatment, whereas others showed more variability in the response depending on the individual. Therefore, for further analyses, DEGs were subset into *consistent* and *variable* based on expression clusters (Supplementary Figures 1, 2). Plotting was performed in R with the packages ggplot2 and ComplexHeatmap (version R3.5.1 and 3.6.0) (44, 45).

Gene ontology (GO) enrichment analysis was performed using GOseq for all genes that were found to be significantly up- or down-regulated (46, 47). KEGG pathways were reconstructed with KEGG Mapper (41) (version 4.3) based on K numbers identified from the Trinotate blastp annotation. A protein interaction network analysis was performed in STRING (48) (version 11.0) (default settings with high confidence interaction score 0.700). The network was built on the Clusters of Orthologous Groups of proteins (COG) annotations of the top blastp hit from the *A. queenslandica* proteome. Protein interaction networks were generated with STRING and prettified in Inkscape (version 0.92).

RESULTS

DE NOVO TRANSCRIPTOME ASSEMBLY AND ANNOTATION

In total, the sequencing approach yielded 2135.98 million paired- end Illumina reads from the 23 sponge samples, which resulted in ~25 million reads per sample after trimming, quality filtering and removal of prokaryotic reads (Supplementary Table 1). The generated reference transcriptome showed a high completeness regarding conserved BUSCO genes with 93.5% of the 978 metazoan genes detected while only 4.8% and 1.6% were fragmented or missing, respectively (Supplementary Table 2). In total, we identified > 400,000 Trinity components from which 26.7% had an open reading frame (ORF) translating into a protein longer than 100 amino acids. The *de novo* assembly most likely contains several fragments per gene, resulting in an overestimation of total gene number (a common issue in *de novo* assemblies). Thus, one Trinity component does not necessarily correspond to one single gene, and whenever we refer to “genes” in the *H. panicea* transcriptome, we refer to Trinity components or “assembled genes” as identified in the Trinity pipeline. After gene quantification within each sample, on average $80.87 \pm 1.63\%$ (average \pm standard error) of reads mapped to the reference transcriptome. More details on the *de novo* transcriptome assembly statistics can be found in the supplementary material (Supplementary Table 2).

DIVERSITY OF PATTERN RECOGNITION RECEPTORS IN *H. PANICEA*

To gain an overview of the microbial recognition potential of *H. panicea*, we screened the reference transcriptome for putative PRRs (i.e., non-canonical TLRs, NLRs, CTLD genes, SRCRs and GPCRs) based on conserved protein domains (Pfam annotations) (Figure 1 and Supplementary Table 3). We found one complete non-canonical TLR in *H. panicea* (17215_c0_g2), and as expected (19), no canonical TLRs. We also detected twenty *bona fide* NLRs with a NACHT-domain in combination with LRR domains. Additionally, 181 NACHT-domain containing genes pointed to an even larger variety of NLRs. The reference transcriptome contained a total of 157 CTLD genes and a diverse set of > 600 SRCRs. The characteristic SRCR domains were associated to other domains like Sushi repeats, fibronectin III or epidermal growth factor-like domains like already described for SRCRs in other sponge species (26). 333 GPCR genes contained the distinctive seven transmembrane domains (7tm domain). Due to their extremely diverse domain structure, we focused here on the 57 GPCRs additionally containing a GPCR proteolytic site domain (GPS) (Figure 1). Additionally, we detected almost 200 cytokine receptors. Compared to the other receptor classes that can be clearly identified by characteristic, conserved protein domains, cytokine receptors are more heterogeneous. The dominant conserved protein

domains among the putative sponge cytokine receptors were tyrosine kinase domains, immunoglobulin domains and fibronectin III, and receptors were classified as receptor tyrosine kinases and TGF- beta receptors. Among all receptor classes we found both membrane-bound (with transmembrane domain), and cytosolic and/or secreted receptors. For the latter, the sequences might be incomplete, and the number of membrane-bound receptors thus underestimated.

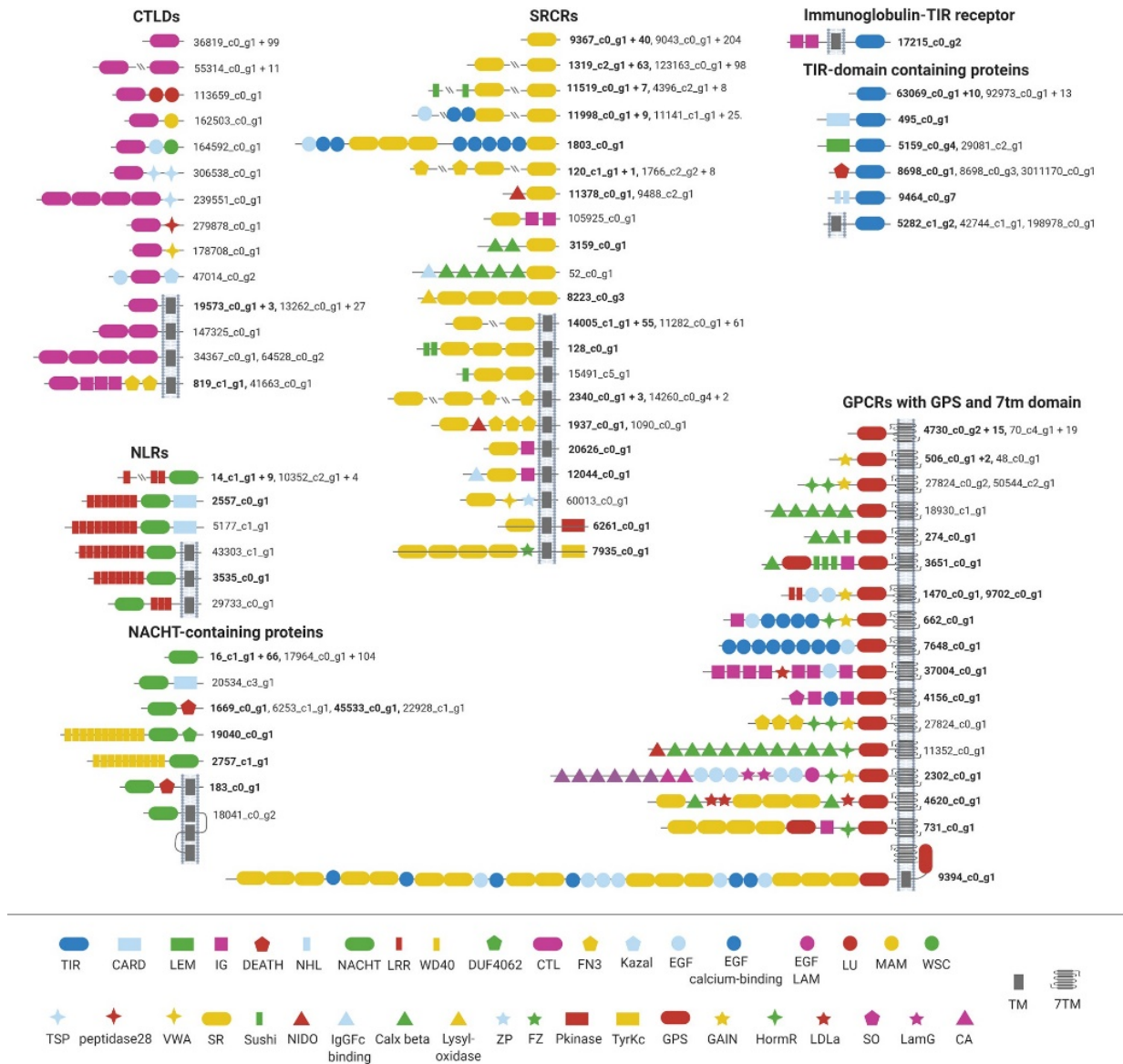


FIGURE 1 | The repertoire of pattern recognition receptors in *Halichondria panicea*. The PRR families GPCRs, SRCRs, CTLD genes, NLRs and TIR-domain receptors were identified based on conserved Pfam domains. Identification numbers of representative transcripts are shown next to protein models, and bold IDs indicate constitutive expression (i.e. present in each analyzed sponge). The number of additional transcripts with the same protein domain architecture is given behind the representative ID. TIR, Toll/interleukine-1 receptor; CARD, caspase recruitment domain; LEM, in nuclear membrane associated proteins; IG, immunoglobulin; NHL, repeat; LRR, leucine-rich repeat; WD40, repeat of 40 amino acids typically terminating in Trp-Asp; DUF4062, conserved domain of

unknown function; CTL, C-type lectin; FN3, fibronectin III; Kazal, part of serine protease inhibitors; EGF, epidermal growth factor; EGF-calcium-binding, epidermal growth factor calcium-binding; EGF-LAM, Laminin-type epidermal growth factor-like; LU, Ly-6 antigen/uPA receptor-like; TSP, Thrombospondin domain; peptidase28; VWA, von Willebrand factor; SR, scavenger receptor cysteine-rich; ZP, zona pelludica; FZ, frizzled domain; Pkinase, phosphate kinase; TyrKc, tyrosine-specific kinase; GPS, G-protein-coupled receptor proteolytic site; HormR, present in hormone receptors; LDLa, low density lipoprotein receptor class A repeat; SO, somatomedin B- like; LamG, laminin G; CA, cadherin repeat; TM, transmembrane region; 7TM, 7 helix transmembrane domain. Other domains: DEATH, NACHT, MAM, WSC, Sushi, NIDO, IgGFc-binding, Calx-beta, Lysyl-oxidase, GAIN. The Figure was created with BioRender.com.

PRR EXPRESSION PATTERNS AND CONSTITUTIVE IMMUNE COMPONENTS

Each sponge individual expressed all PRR families but only about 50% of all putative PRR genes detected in the reference transcriptome. Overall, one third of the putative PRRs in *H. panicea* were constitutively expressed, which we defined as expressed in all 23 analyzed samples (Figure 2A). The constitutively expressed PRRs covered all PRR families. However, CTLD genes are underrepresented (3% constitutive), whereas GPCRs, *bona fide* NLRs and TIR-domain containing proteins (including the non-canonical TLR) are overrepresented (~50-60% constitutive, respectively). The expression levels of constitutive PRRs were similar across replicate samples (Figure 2B). In contrast, we also detected plasticity in PRR expression patterns within the same individual. This was most apparent in one individual expressing an extremely diverse CTLD gene repertoire at 1 h after LPS treatment (125 CTLD genes) compared to 6 h (< 10 CTLD genes) (Figure 2C). Nevertheless, the majority of PRRs followed an individual-specific expression pattern (Figure 2C).

Then, we examined genes that are constitutively expressed and play a potential role in immunity. Among all 23 analyzed sponge transcriptomes, we identified 28,466 constitutively expressed genes (7% of all genes) (Supplementary Figure 3A). From those, we classified a set of 441 genes with a potential function in immunity based on the KEGG mapping results from protein annotations (Supplementary Table 4). 61 constitutively expressed genes were related to 19 KEGG orthology (KO) terms relevant for the Toll-like receptor signaling pathway, like NF- κ B (K02580) or toll-like receptor 2 (K10159), as well as for the TGF- β signaling pathway (e.g. K13375), MAPK signaling (e.g. K04427), apoptosis and TNF signaling like tumor necrosis factor receptor-associated factors (TRAFs) (e.g. K03173), and caspases (e.g. K02187).

The median expression level of constitutively expressed immune genes was ~35% higher than the median of all other constitutive genes (Supplementary Figure 3A). We further investigated the subset of constitutive immune genes with higher expression levels (Supplementary Figure 3B). As for the PRRs, expression patterns of each of these constitutive immune genes were homogenous across

replicates (Supplementary Figure 3B). Among these, we highlight those with higher expression levels: two GPCRs (18879_c0_g2, 12713_c0_g1), a cytokine receptor (3010_c1_g1), a nuclear receptor (22428_c0_g1) and a RIG-I-like receptor retinoic acid-inducible gene-I-like receptors) (14596_c0_g1). Further, NF- κ B (6780_c0_g1), MyD88 (3294_c2_g1), and several tumor necrosis factor (TNF) receptor-associated factor (TRAF) genes (e.g. 8577_c0_g1, 54071_c0_g1, 196_c1_g1) were also constantly expressed at high levels. The constitutive immune genes with the highest expression were a protease (19175_c0_g1) and two actin binding proteins (91189_c0_g1, 169038_c0_g1).

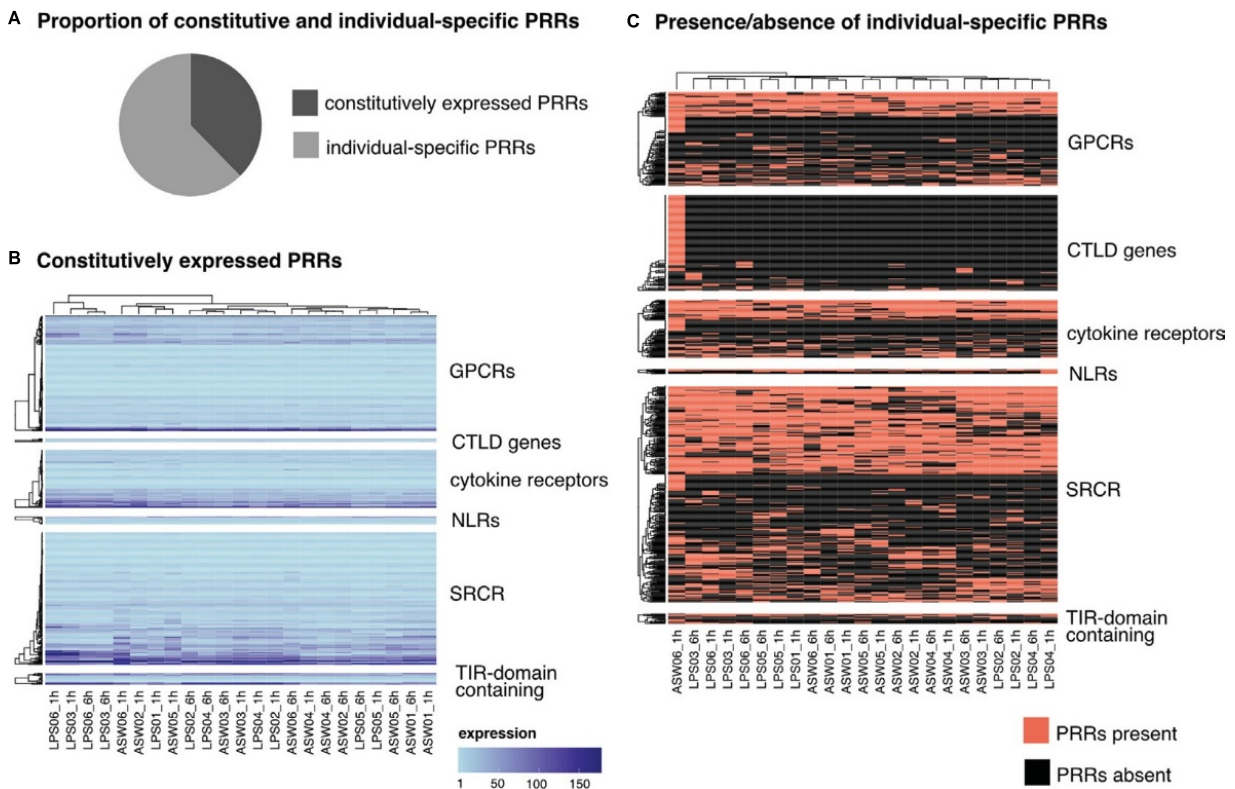


FIGURE 2 | Expression patterns of PRRs. **(A)** 38% of the identified PRRs were constitutively expressed (present in all samples), 62% were expressed individual specific (PRRs present in only some samples). **(B)** Expression levels of constitutively expressed PRRs. Each row represents one gene and each column one sponge sample. The color gradient indicates the expression level (TMM normalized TPM). **(C)** Presence/absence of individual-specific PRRs. Each row represents one gene and each column one sponge sample. Note the clustering of individuals independent of the timepoint (LPS01 was only sampled at 1h and not at 6h). PRR, pattern recognition receptor; GPCR, G-protein coupled receptor; CTLD, C-type lectin like domain; NLR, nucleotide-binding domain and leucine-rich repeat containing receptors; SRCR, scavenger receptor cysteine-rich; TIR, Toll/interleukin-1 receptor.

TRANSCRIPTOMIC RESPONSE TO BACTERIAL LPS IS HIGHLY INDIVIDUAL

We compared the gene expression levels in samples exposed to either LPS or sham (control) at two time points (1 h post treatment and 6 h post treatment) with 6 replicates (but 5 replicates in the LPS treatment at 6 h). The time points were chosen based on results from a similar study in sponges (26). Response to bacterial elicitors is expected to happen and change within a short time frame, where 1 h represents an immediate response, and 6 h a delayed response. Significant differential expression was defined as FDR p-value < 0.005 and $\log_2|FC| \geq 2$. Overall, LPS induced more down- than up-regulation of gene expression (Figure 3A). The proportion of shared genes between timepoints was larger for the down-regulated genes (~ 40%) than for the up-regulated genes (~ 30%) (Figure 3A). DEGs detected at both time points always had the same direction of differential expression and similar expression levels.

We realized that not all DEGs show a consistent expression pattern across all replicates (Figure 4 and Supplementary Figures 1, 2). Variability was mainly driven by two individuals in the LPS treatment that seem more responsive to the treatment (Figure 4, individual 3 and 6 in LPS treatment). In addition, the control treatment showed high individual variability with individuals 2 and 4 following a similar expression pattern at both timepoints (Figure 4). Importantly, some genes identified as differentially expressed were highly expressed in these two control sponges, while they were absent from all other replicates. Because of this individual variability, we clustered DEGs according to their expression patterns (Figures S1, S2) and, thus, distinguished between *consistent* and *variable* DEGs. DEGs were considered *variable* when they were only regulated in 2 out of the 5/6 replicates per treatment. In contrast, DEGs were considered *consistent* when they showed a similar expression pattern in more than half of the replicates. At 1 h post treatment, 52% of the DEGs were *consistently* regulated, and 48% of the DEGs at the 6 h timepoint (Figure 3B).

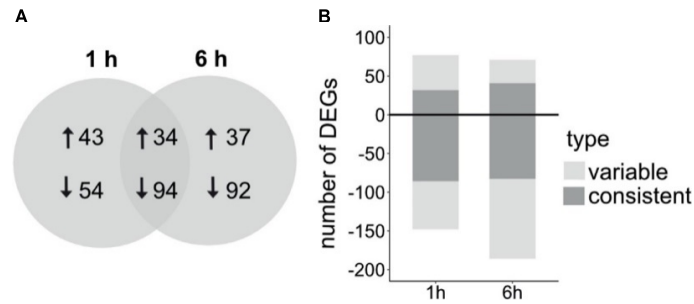


FIGURE 3 | (A) Number of DEGs comparing LPS treated versus control sponges and the overlap between the two time points after LPS exposure, 1 h and 6 h after treatment. Arrows indicate up- and downregulation in comparison to control treatment. **(B)** Proportion of consistent and variable DEGs (with consistent/variable expression patterns across replicate samples, see Methods). Total DEGs 1 h: 225, total DEGs 6 h: 257 (genes defined as differentially expressed with FDR p-value < 0.005 and $\log_2|\text{FC}| \geq 2$).

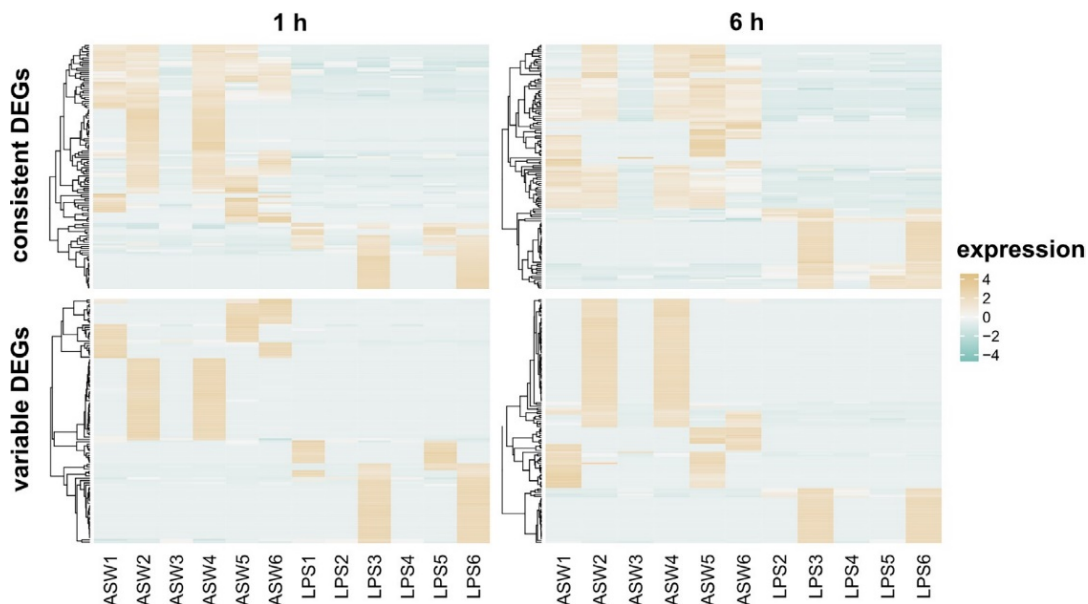


FIGURE 4 | Differentially expressed genes at 1 h and 6 h after LPS exposure. The heatmap shows the TMM-normalized relative expression per DEG (rows) for control and LPS treated samples (columns). DEGs are divided according to expression pattern in consistent and variable expressed (see Methods). Genes were defined as differentially expressed with FDR p-value < 0.005 and $\log_2|\text{FC}| \geq 2$.

TRANSCRIPTOMIC RESPONSE TO BACTERIAL LPS INVOLVES GENES RELATED TO SIGNALING AND RECOGNITION

A limiting factor in the functional interpretation of the response of *H. panicea* to LPS is the annotation. No genome for this sponge species is currently available and only about 27% of the DEGs could be annotated based on public databases and conserved protein domains. With additional information

retrieved from blastp comparison to the proteome of *Amphimedon queenslandica* (Uniprot UP000007879_444682), we could increase the proportion of annotated DEGs from 27% to ~ 37% (Supplementary Table 5). At 1 h post LPS treatment most DEGs were functionally related to i) recognition and protein binding, ii) signaling and iii) metabolism and transport (Figure 5). Notably, at 6 h post LPS treatment, the same main functional categories were regulated but in varying abundance (Figure 5). When considering only the *consistent* DEGs, we detected the same functional categories and temporal differences.

Within genes related to signaling, we found regulation of GTPase activity and GTP binding proteins in response to bacterial LPS. Among the *consistently* up-regulated genes, was a small GTPase with a BTB domain at both timepoints. At 6 h post LPS treatment, two genes involved in semaphorin signaling were also *consistently* upregulated (49): a putative semaphorin receptor (18299_c0_g2) belonging to the plexin group and with a homolog in *A. queenslandica*, and a Sema domain-containing gene that could either function as a semaphorin receptor binding protein or be a receptor itself (8862_c0_g1). Down-regulated genes related to G- Proteins contain several GTPase binding or activating proteins including different septins and small GTPases. We did not detect any G-Protein coupled receptors (GPCRs) among the DEGs.

Several DEGs had typical protein domains involved in recognition, cell adhesion or protein binding: such as ankyrin repeats, Sushi domains, immunoglobulin domains and fibrinogen-like domains. At both timepoints, a gene of the collagen superfamily was *consistently* up-regulated at similar logFC. The signaling response to LPS was also characterized by the regulation of genes annotated as putative tyrosine and serine/ threonine kinase activity were differentially expressed at both timepoints, while some of those had homologs in the *A. queenslandica* genome. The majority had *consistent* expression patterns. Genes with kinase activity had different conserved domains including sushi, DEATH or LRR domains. Another *consistent* pattern included the regulation of genes related to ubiquitination, like ubiquitin protein ligases.

Several genes related to the Tumor Necrosis Factor (TNF) signaling pathway were differentially expressed at both timepoints. However, most of these DEGs showed *variable* expression patterns and were only regulated in some of the replicates.

To aid further interpretation of differentially regulated processes after exposure to LPS, we performed a GO-term enrichment analysis and KEGG mapping. The enrichment analysis revealed no significantly enriched GO-terms (FDR corrected p-value < 0.05). *Consistent* DEGs with KEGG annotation were associated to, among others, the KEGG pathways NF- κ B signaling (04064), NOD like receptor signaling (04621), IL-17 signaling, TNF signaling (04668) and apoptosis (04210). More specifically, this included

genes annotated as TNF receptor-associated factor (TRAF2, TRAF5 and TRAF6), receptor-interacting serine/threonine-protein kinase 1 (RIPK1), and PKR-like endoplasmic reticulum kinases (PERK).

At 1h after LPS exposure, the COG association network with the most interactions was centered around leucine-rich repeat proteins and multiple interactions among serine-threonine kinases, GTPases, and ankyrin repeat-containing proteins (Figure 6). Distinct networks related to apoptosis (proteases, TNF receptor-associated factors, Zinc-finger proteins) and C- type lectins interacting with proteinases were also identified. At 6 h after LPS exposure, a network showed ankyrin repeat-containing proteins interacting with serine proteases, GTPases, and molecular chaperones. We also observed a network related with apoptosis similar to the one at 1 h, but this time with more connections and centered around TNF receptor-associated factors interacting with caspases, ubiquitin ligases, plexins and WD-40 proteins.

In summary, the main regulated pathways in *H. panicea* upon LPS exposure were related to signaling, recognition, and protein binding, with a large overlap between the timepoints. Despite the variable expression patterns across individuals, all sponges regulated genes in similar functions. The differences lied in the number of regulated genes within each functional category. We did not identify any PRR as differentially expressed. The induced immune response consisted of a network relying predominantly on down-regulation of genes. The transcriptomic response to LPS involved GTP-binding proteins, post-translational regulatory mechanism like ubiquitination, and genes involved in apoptosis.

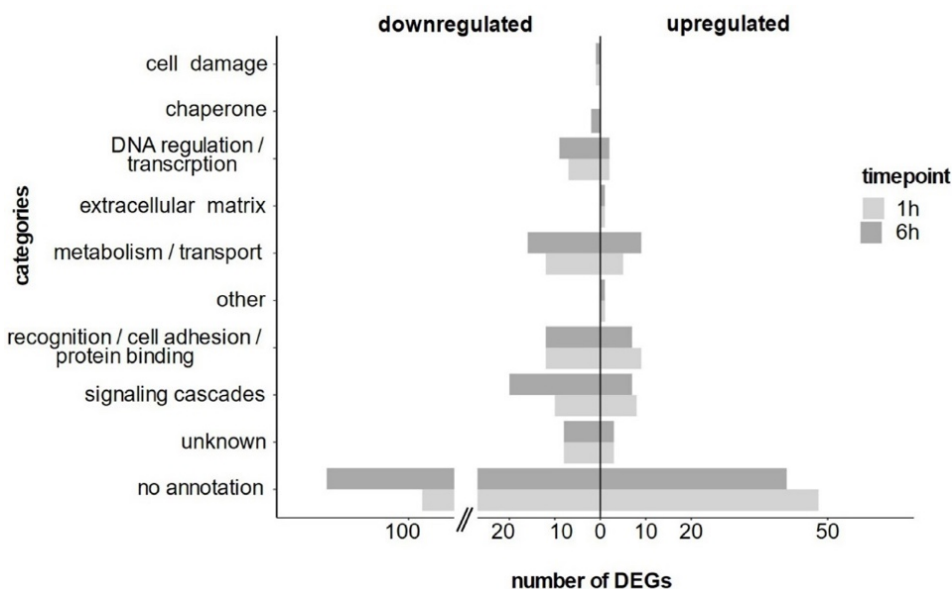


FIGURE 5 | Annotated differentially expressed genes at 1 h and 6 h after LPS exposure separated into functional categories based on their annotation.

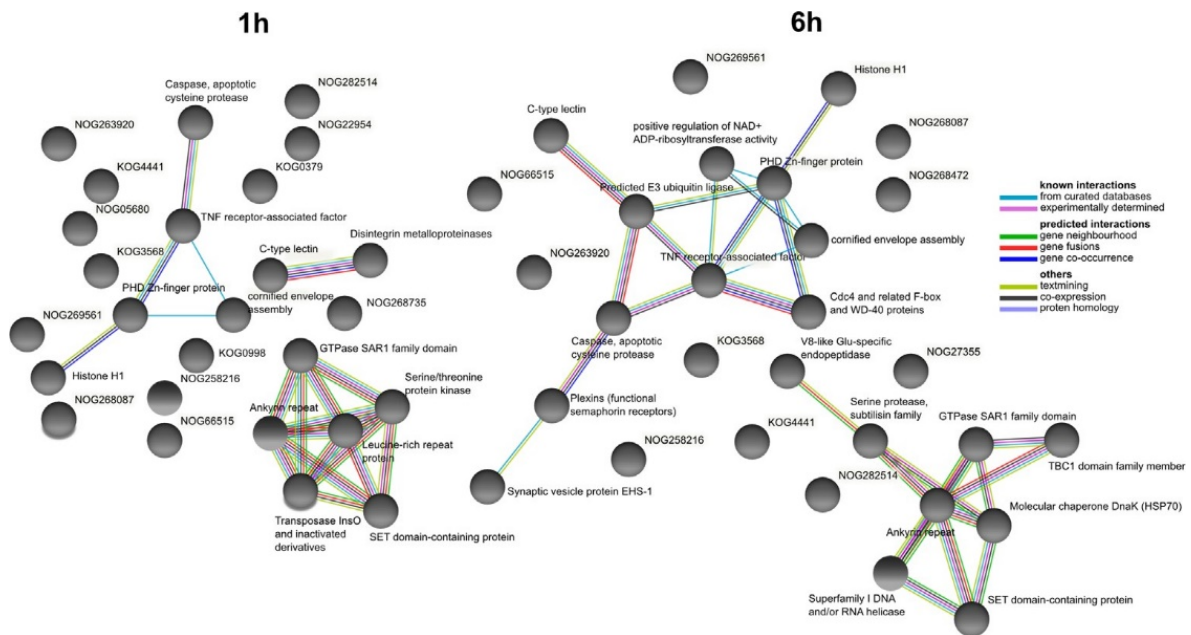


FIGURE 6 | COG association network analysis from DEGs at 1 h and 6 h after LPS exposure identified from closest annotated proteins in *Amphimedon queenslandica*. Created with STRING. Edges represent protein-protein associations coded by color according to the type of evidence for the shown interaction.

DISCUSSION

In this study, we explored the expression patterns of PRRs and characterized the transcriptomic response to LPS challenge in the LMA sponge *H. panicea*. We identified a diverse array of putative PRRs, GPCRs and cytokine receptors. One third of the genes coding for these receptors were expressed at similar levels in all samples (i.e., constitutive PRRs), but each individual also expressed a unique array of PRRs. We further observed high variability between individuals in the genes responding to LPS, although the regulated genes fell under similar functional categories. The differentially expressed genes were predominantly downregulated and involved genes related to signaling and recognition, such as GTPases, and serine/threonine kinases.

The reference transcriptome assembly of *H. panicea* contained a large diversity of PRRs (Figure 1), confirming previous findings based on genomic and transcriptomic information of other sponge species (18, 20, 26, 27). The PRR repertoire in *H. panicea* also agrees with the patterns observed for other LMA sponges, which harbor a more expanded NLR repertoire than HMA sponges (this study, 22, 26, 50). GPCRs and cytokine receptors are not typically considered PRRs, but recent evidence demonstrates their role in recognizing microbial signals (6, 51). Interestingly, the high diversity of cytokine receptors remained hidden with annotation in the standard pipeline (i.e., Trinotate), and was only detected when comparing our dataset to the proteome of the sponge *A. queenslandica*. This

lineage-specific annotation suggests a Porifera-specific superfamily of cytokine receptors, as suggested for *A. queenslandica* tyrosine-kinase receptors (52). Most likely, the diversity of cytokine receptors is also large in other sponges and currently underestimated due to the underrepresentation of this phylum in public genomic databases. Further, cytokine receptors do not have a characteristic protein domain in common. Rather, the receptor classes summarized as cytokine receptors are both variable in their architecture and functions [e.g. TGF- β in wounding (53), Eph receptors in cell-cell communication (52)], while their role in immunity is increasingly recognized (54). Cytokine receptors of sponges provide interesting targets for further exploration and promise to harbor novelty.

We evaluated how the PRR diversity and immune-related genes were expressed across samples. Importantly, each individual transcriptome contains representative genes of all PRR families. Moreover, one third of the detected PRR genes were constitutively expressed in all 23 samples (Figure 2B). The constitutive immune repertoire of *H. panicea* showed consistent expression levels across samples, suggesting a tight transcriptional regulation and might thus be obligatory for protein function/activity (55, 56). Thus, modulation of these constitutive components could happen *via* post-translational mechanisms like phosphorylation status or binding of adapters. This constitutive and elevated expression is quite intriguing. In plants, overexpression of NLRs negatively affected host health and fitness (reviewed in 57). In the coral *Acropora millepora*, higher disease susceptibility was attributed to elevated constitutive immunity (58). In contrast, we propose that the constitutively expressed genes in *H. panicea* contribute to maintaining microbiome homeostasis and, thus, require sustained expression levels. In LMA sponges, constitutive expression could be higher than in HMA sponges and crucial to maintain a constantly lower microbial load. Jahn et al. recently identified a mechanism for symbionts to silence host immune genes (59). We hypothesize that symbiotic-mediated silencing signals are weaker in the LMA sponges, compared to HMA sponges, allowing the former an elevated constitutive expression. Then, LMA sponges would need to regulate less genes than HMA sponges in response to MAMPs, a pattern observed in two Mediterranean sponges (26). How the density of the microbiome shapes sponge immunity needs to be tested.

The largest proportion of PRR genes showed an individual-specific expression, independent of the timepoint and the treatment (Figure 2C). A similar pattern was also found in the purple sea urchin *Strongylocentrotus purpuratus*, where coelomocyte SRCR expression changed on an individual basis (13). The benefit of individual PRR diversity might contribute to the successful response to potential pathogens on the population level by reducing the probability for infection of all individuals simultaneously. For example, in *Drosophila*, individual differences in immune genes are correlated to infection with a gram-negative pathogen (60). Here, differences in the immune repertoire leading to an advantage on the population level (61, 62). This concept has been described in host-pathogen

interactions but it may as well apply in the context of proliferation of opportunistic microbes, which seems the real threat for sponges upon environmental stress (17, 63–65).

Variability in PRR diversity occurs at the level of the individual sponge, and thus we argue that the injection with LPS/sham control and a potential associated injury was not the reason for variability. Instead, we propose three possible sources of individual variability. First, variability could result from different genetic backgrounds (e.g., 60). Second, previous exposure and environmental conditions could account for differences between individuals (66). However, in our case all sponges were collected at once from the same location and animals were kept for 2 months in a controlled aquarium system prior to the experiment, further reducing variability. Nevertheless, we cannot discard that previous encounters with microbes have long-term effects or even act over generations, for example, in insects, maternal exposure to pathogens can determine the gene expression of its offspring (67). Third, the potential costs of PRR expression might result in an individual balance between costs and benefit of active immunity in relation, for example, to fitness, as observed in plants (57). We attributed the observed variability mainly to the genotype, as this is rising as a common pattern in other systems, such as for induced immune responses in corals (68).

The individuality observed in the PRR repertoire was also evident in the induced response of *H. panicea* to bacterial LPS, in terms of number of DEGs across individuals. However, the functional categories of the annotated DEGs were consistent and mainly included signaling, recognition, and metabolism (Figure 5). We observed the intricate differential expression of multiple GTPases, related to cell-cell interaction *via* G-proteins (69). A particular pathway, *consistently* activated at 6h after LPS exposure, was semaphorin signaling. This pathway is involved in immunity and has its origin in the last common ancestor of choanoflagellates (71). In mice macrophages, semaphorin positively regulated phagocytosis and the inflammatory response after LPS treatment (72). In invertebrates, semaphorins are likely involved in detection and phagocytosis of photosymbionts [in cnidarians (73), in sea slugs (74)]. Sponges rely on phagocytosis for food uptake while depending on differential recognition of their symbionts. Here, semaphorins could also be involved in the discrimination between bacteria. We hypothesize that this function might be conserved from early metazoans to vertebrates.

We see similarities in the transcriptomic response of *H. panicea* to LPS (this study) and the response of Mediterranean sponges *Aplysina aerophoba* (HMA) and *Dysidea avara* (LMA) in response to exposure to LPS and peptidoglycan (26). These similarities are independent of the HMA/LMA dichotomy and the experimental conditions that differed between experiments, and rather reflect a universal response to MAMPs. The three sponge species regulated multiple genes in the category recognition/cell adhesion/protein binding (e.g., immunoglobulin-, leucine-rich repeat- and ankyrin

repeat containing genes), and signaling (e.g. TRAFs, protein kinases). GTPases were also regulated in response to MAMPs, but only in *A. aerophoba* we detected regulation of a GPCR. In all three sponges, the gene expression patterns suggest the regulation of apoptosis (e.g. TRAFs, ubiquitination-related genes, proteases). Apoptosis is indeed a common response to microbial elicitation as a mechanism to maintain tissue homeostasis and to restrain infection spread (75, 76). Genes like caspases and ubiquitin ligases, which trigger and regulate apoptosis (77–79), are often activated by LPS in different animal groups like in *C. elegans* (80) and mollusks (81, 82). Apoptosis emerges as a common response to bacterial elicitors in sponges (25, 26, this study), as well as in cnidarians (83, 84) and mollusks (81, 82).

Thus, the gene expression patterns observed in the LMA sponge *Halichondria panicea* show three layers of immune control: (i) a constitutive expression of a subset of PRRs and immune-related genes, (ii) an individual repertoire that expands the constitutive immune array, and (iii) an induced response that acts mainly at the level of signaling cascades (via GTPases) and post-translational regulation of immune components (e.g. *via* ubiquitination and phosphorylation). We propose that the first layer of constitutive genes reflects the low dense *H. panicea* microbiome. We hypothesize that symbiotic-mediated silencing signals (59) are weaker in the LMA sponges, compared to HMA sponges, allowing the former an elevated constitutive expression. The second layer of an individual immune repertoire reflects an individually-determined aspect of immunity. This is an emerging trend in many other organisms and, in fact, this individual variability is well recognized in human medicine and translated increasingly into personalized treatments (85–87). A big question remains: how this individuality may translate into different fitness of marine holobionts upon disturbances (58, 88, 89). The third layer of immunity, i.e. the induced response to LPS, did reflect this individuality. This is a pattern also found in other marine invertebrates like sea urchins and corals (68, 90–92). However, we would like to highlight here the common induced responses, which are differential regulation of signaling by GTPases and post-translational regulation mechanisms, like ubiquitination and protein kinase-mediated phosphorylation. In summary, the discussed layers of immunity would interact with each other in order to determine the specific adequate response. A complex picture of the innate immune control in *H. panicea* emerges, where the different layers act in synergy to maintain a stable microbiome and at the same time mount a flexible response to microbe encounter.

CONCLUSION

Here we characterized the patterns of immune gene expression in the emerging LMA sponge model *H. panicea*. We have discovered individuality in both the expressed immune receptor repertoire and

the response to the bacterial elicitor LPS. We propose that this individualized immunity may maximize the potential to detect and respond to microbes on the population-level. Our observations further raise the question on how this individualized expressed immune repertoire determines protein function and holobiont fitness in response to a stressor, and whether the amplitude of the induced response affect its costs. The three different layers of immune gene control observed in this study, namely constitutive expression, individual-specific expression, and induced genes, illustrate the complex innate immune gene regulation in *H. panicea*. Most likely this reflects the diverse roles of immunity in sponges interacting with a stable microbiome, seawater bacteria and potential pathogens, and may as well apply to other marine holobionts.

DATA AVAILABILITY STATEMENT: The raw reads, metadata and transcriptome assembly for this study have been deposited in the European Nucleotide Archive (ENA) at EMBL-EBI under the accession number PRJEB43257 (<https://www.ebi.ac.uk/ena/browser/view/PRJEB43257>). The full annotation of the de novo transcriptome can be found in Supplementary Table 6.

AUTHOR CONTRIBUTIONS: LP and LS conceived the idea, planned and conducted the experiment. LS performed molecular laboratory work. SF coordinated and performed RNA-seq at the IKMB Kiel. LS and LP analyzed sequencing data and wrote the manuscript. All authors contributed to the article and approved the submitted version.

FUNDING: LS and LP were supported by the DFG (CRC1182-B1). LP is also funded by the DFG “Comparative immunogenomics of basal marine metazoans” (IMMUBASE) (project 417981041). This work was supported by the DFG Research Infrastructure NGS_CC (project 407495230) as part of the Next Generation Sequencing Competence Network (project 423957469). NGS analyses were carried out at the Competence Centre for Genomic Analysis (Kiel). LS is supported by the International Max Planck Research School for Evolutionary Biology.

ACKNOWLEDGMENTS: We are grateful to Prof. Dr. Ute Hentschel for helpful discussions and to Angela M. Marulanda for feedback on preliminary results. We acknowledge the staff from CCGA Kiel for cDNA library preparation and sequencing. We are grateful to Dr. Felix Mittermayer for the field collection support, and to Fabian Wendt for support with the sponge aquarium system.

SUPPLEMENTARY MATERIAL: The Supplementary Material for this article can be found online at: <https://www.frontiersin.org/articles/10.3389/fimmu.2021.689051/full#supplementary-material>

REFERENCES

1. Chu H, Mazmanian SK. Innate Immune Recognition Promotes Symbiosis. *Nat Immun* (2013) 14:668–75. doi: 10.1038/ni.2635
2. Gerardo NM, Hoang KL, Stoy KS. Evolution of Animal Immunity in the Light of Beneficial Symbioses. *Philos Trans R Soc Lond B Biol Sci* (2020) 375:20190601. doi: 10.1098/rstb.2019.0601
3. McFall-Ngai M, Hadfield MG, Bosch TCG, Carey HV, Domazet-Los T, Douglas AE, et al. Animals in a Bacterial World, a New Imperative for the Life Sciences. *Proc Natl Acad Sci* (2013) 110:3229–36. doi: 10.1073/pnas.1218525110
4. Janeway CA, Medzhitov R. Innate Immune Recognition. *Annu Rev Immunol* (2002) 20:197–216. doi: 10.1146/annurev.immunol.20.083001.084359
5. Medzhitov R, Janeway CA. Innate Immunity: The Virtues of a Nonclonal System of Recognition. *Cell* (1997) 91:295–8. doi: 10.1016/S0092-8674(00) 80412-2
6. Reboul J, Ewbank JJ. Gpcrs in Invertebrate Innate Immunity. *Biochem Pharmacol* (2016) 114:82–7. doi: 10.1016/j.bcp.2016.05.015
7. Liongue C, Sertori R, Ward AC. Evolution of Cytokine Receptor Signaling. *J Immunol* (2016) 197:11–8. doi: 10.4049/jimmunol.1600372
8. Schulenburg H, Boehnisch C, Michiels NK. How do Invertebrates Generate a Highly Specific Innate Immune Response? *Mol Immunol* (2007) 44:3338–44. doi: 10.1016/j.molimm.2007.02.019
9. Akira S, Uematsu S, Takeuchi O. Pathogen Recognition and Innate Immunity. *Cell* (2006) 124:783–801. doi: 10.1016/j.cell.2006.02.015
10. Dierking K, Pita L. Receptors Mediating Host-Microbiota Communication in the Metaorganism: The Invertebrate Perspective. *Front Immunol* (2020) 11: 1–17. doi: 10.3389/fimmu.2020.01251
11. Mu Y, Ding F, Cui P, Ao J, Hu S, Chen X. Transcriptome and Expression Profiling Analysis Revealed Changes of Multiple Signaling Pathways Involved in Immunity in the Large Yellow Croaker During *Aeromonas Hydrophila* Infection. *BMC Genomics* (2010) 11:1–14. doi: 10.1186/1471-2164-11-506
12. Saco A, Rey-Campos M, Novoa B, Figueras A. Transcriptomic Response of Mussel Gills After a *Vibrio Splendidus* Infection Demonstrates Their Role in the Immune Response. *Front Immunol* (2020) 11: 1–18. doi: 10.3389/fimmu.2020.615580
13. Pancer Z. Dynamic Expression of Multiple Scavenger Receptor Cysteine-Rich Genes in Coelomocytes of the Purple Sea Urchin. *Proc Natl Acad Sci U S A* (2000) 97:13156–61. doi: 10.1073/pnas.230096397
14. Thomas T, Moitinho-Silva L, Lurgi M, Bj rk JR, Easson C, Astudillo-Garc a C, et al. Diversity, Structure and Convergent Evolution of the Global Sponge Microbiome. *Nat Commun* (2016) 7:11870. doi: 10.1038/ncomms11870
15. Reiswig H. Particle Feeding in Natural Populations of Three Marine Demosponges. *Biol Bull* (1971) 141:568–91. doi: 10.2307/1540270
16. Wehrl M, Steinert M, Hentschel U. Bacterial Uptake by the Marine Sponge *Aplysina Aerophoba*. *Microb Ecol* (2007) 53:355–65. doi: 10.1007/s00248-006- 9090-4
17. Webster NS, Negri AP, Webb RI, Hill RT. A Spongian-Boring α - Proteobacterium is the Etiological Agent of Disease in the Great Barrier Reef Sponge *Rhopaloeides Odorabile*. *Mar Ecol Prog Ser* (2002) 232:305–9. doi: 10.3354/meps232305
18. Srivastava M, Simakov O, Chapman J, Fahey B, Gauthier MEA, Mitros T, et al. The *Amphimedon Queenslandica* Genome and the Evolution of Animal Complexity. *Nature* (2010) 466:720–6. doi: 10.1038/nature09201
19. Hentschel U, Piel J, Degnan SM, Taylor MW. Genomic Insights Into the Marine Sponge

- Microbiome. *Nat Rev Microbiol* (2012) 10:641–54. doi: 10.1038/nrmicro2839
20. Riesgo A, Farrar N, Windsor PJ, Giribet G, Leys SP. The Analysis of Eight Transcriptomes From All Poriferan Classes Reveals Surprising Genetic Complexity in Sponges. *Mol Biol Evol* (2014) 31:1102–20. doi: 10.1093/molbev/msu057
 21. Krishnan A, Dnyansagar R, Almén MS, Williams MJ, Fredriksson R, Manoj N, et al. The GPCR Repertoire in the Demosponge *Amphimedon Queenslandica*: Insights Into the GPCR System at the Early Divergence of Animals. *BMC Evol Biol* (2014) 14:1–16. doi: 10.1186/s12862-014-0270-4
 22. Yuen B, Bayes JM, Degnan SM. The Characterization of Sponge Nlrs Provides Insight Into the Origin and Evolution of This Innate Immune Gene Family in Animals. *Mol Biol Evol* (2014) 31:106–20. doi: 10.1093/molbev/mst174
 23. Buckley KM, Rast JP. Diversity of Animal Immune Receptors and the Origins of Recognition Complexity in the Deuterostomes. *Dev Comp Immunol* (2015) 49:179–89. doi: 10.1016/j.dci.2014.10.013
 24. Degnan SM. The Surprisingly Complex Immune Gene Repertoire of a Simple Sponge, Exemplified by the NLR Genes: A Capacity for Specificity? *Dev Comp Immunol* (2015) 48:269–74. doi: 10.1016/j.dci.2014.07.012
 25. Wiens M, Korzhev M, Perović-Ottstadt S, Luthringer B, Brandt D, Klein S, et al. Toll-Like Receptors Are Part of the Innate Immune Defense System of Sponges (Demospongiae: Porifera). *Mol Biol Evol* (2007) 24:792–804. doi: 10.1093/molbev/msl208
 26. Pita L, Hoepfner MP, Ribes M, Hentschel U. Differential Expression of Immune Receptors in Two Marine Sponges Upon Exposure to Microbial-Associated Molecular Patterns. *Sci Rep* (2018) 8:1–15. doi: 10.1038/s41598-018-34330-w
 27. Ryu T, Seridi L, Moitinho-Silva L, Oates M, Liew YJ, Mavromatis C, et al. Hologenome Analysis of Two Marine Sponges With Different Microbiomes. *BMC Genomics* (2016) 17:1–11. doi: 10.1186/s12864-016-2501-0
 28. Gloeckner V, Wehrl M, Moitinho-silva L, Schupp P, Pawlik JR, Lindquist NL, et al. The HMA-LMA Dichotomy Revisited : An Electron Microscopical Survey of 56 Sponge Species. *Biol Bull* (2014) 227:78–88. doi: 10.1086/BBLv227n1p78
 29. Moitinho-Silva L, Steinert G, Nielsen S, Haroim CCP, Wu YC, McCormack GP, et al. Predicting the HMA-LMA Status in Marine Sponges by Machine Learning. *Front Microbiol* (2017) 8: 1–14. doi: 10.3389/fmicb.2017.00752
 30. Hentschel U, Usher KM, Taylor MW. Marine Sponges as Microbial Fermenters. *FEMS Microbiol Ecol* (2006) 55:167–77. doi: 10.1111/j.1574-6941.2005.00046.x
 31. Pita L, Fraune S, Hentschel U. Emerging Sponge Models of Animal-Microbe Symbioses. *Front Microbiol* (2016) 7: 1–8. doi: 10.3389/fmicb.2016.02102
 32. Knobloch S, Jóhannsson R, Marteinson V. Bacterial Diversity in the Marine Sponge *Halichondria Panicea* From Icelandic Waters and Host-Specificity of its Dominant Symbiont “*Candidatus Halichondriabacter Symbioticus*”. *FEMS Microbiol Ecol* (2018) 95:1–13. doi: 10.1093/femsec/fiy220
 33. Knobloch S, Jóhannsson R, Marteinson VP. Genome Analysis of Sponge Symbiont ‘*Candidatus Halichondriabacter Symbioticus*’ Shows Genomic Adaptation to a Host-Dependent Lifestyle. *Environ Microbiol* (2020) 22:483–98. doi: 10.1111/1462-2920.14869
 34. Redmond NE, Morrow CC, Thacker RW, Diaz MC, Boury-Esnault N, Cárdenas P, et al. Phylogeny and Systematics of Demospongiae in Light of New Small-Subunit Ribosomal DNA (18S) Sequences. *Integr Comp Biol* (2013) 53:388–415. doi: 10.1093/icb/ict078
 35. Lane DJ. 16S/23S Rrna Sequencing. In: E Stackebrandt, M Goodfellow, editors. *Nucleic Acid Techniques in Bacterial Systematics*. New York: John Wiley & Sons (1991). p. 115–75.
 36. Bolger AM, Lohse M, Usadel B. Trimmomatic: A Flexible Trimmer for Illumina Sequence Data. *Bioinformatics* (2014) 30:2114–20. doi: 10.1093/bioinformatics/btu170
 37. Menzel P, Ng KL, Krogh A. Fast and Sensitive Taxonomic Classification for Metagenomics With Kaiju. *Nat Commun* (2016) 7:1–9. doi: 10.1038/ncomms11257

38. Haas BJ, Papanicolaou A, Yassour M, Grabherr M, Philip D, Bowden J, et al. *De Novo* Transcript Sequence Reconstruction From RNA-Seq: Reference Generation and Analysis With Trinity. *Nat Protoc* (2013) 8:1–43. doi: 10.1038/nprot.2013.084.De
39. Simão FA, Waterhouse RM, Ioannidis P, Kriventseva EV, Zdobnov EM. BUSCO: Assessing Genome Assembly and Annotation Completeness With Single-Copy Orthologs. *Bioinformatics* (2015) 31:3210–2. doi: 10.1093/bioinformatics/btv351
40. Bryant DM, Johnson K, DiTommaso T, Tickle T, Couger MB, Payzin-Dogru D, et al. A Tissue-Mapped Axolotl *De Novo* Transcriptome Enables Identification of Limb Regeneration Factors. *Cell Rep* (2017) 18:762–76. doi: 10.1016/j.celrep.2016.12.063
41. Kanehisa M, Sato Y. KEGG Mapper for Inferring Cellular Functions From Protein Sequences. *Protein Sci* (2020) 29:28–35. doi: 10.1002/pro.3711
42. Letunic I, Khedkar S, Bork P. SMART: Recent Updates, New Developments and Status in 2020. *Nucleic Acids Res* (2021) 49:D458–60. doi: 10.1093/nar/gkaa937
43. Robinson MD, Oshlack A. A Scaling Normalization Method for Differential Expression Analysis of RNA-Seq Data. *Genome Biol* (2010) 11:R25. doi: 10.1186/gb-2010-11-3-r25 Wickham H. *Ggplot2: Elegant Graphics for Data Analysis*. New York: Springer-Verlag (2016). Available at: <https://ggplot2.tidyverse.org>.
44. Gu Z, Eils R, Schlesner M. Complex Heatmaps Reveal Patterns and Correlations in Multidimensional Genomic Data. *Bioinformatics* (2016) 32:2847–9. doi: 10.1093/bioinformatics/btw313
45. Consortium TGO, Ashburner M, Ball C, Blake J, Botstein D, Butler H, et al. Gene Ontology: Tool for the Unification of Biology. *Nat Genet* (2000) 25:25–9. doi: 10.1038/75556
46. Consortium TGO. The Gene Ontology Resource: Enriching a Gold Mine. *Nucleic Acids Res* (2021) 49:D325–34. doi: 10.1093/nar/gkaa1113
47. Szklarczyk D, Gable AL, Lyon D, Junge A, Wyder S, Huerta-Cepas J, et al. STRING V11: Protein-Protein Association Networks With Increased Coverage, Supporting Functional Discovery in Genome-Wide Experimental Datasets. *Nucleic Acids Res* (2019) 47:D607–13. doi: 10.1093/nar/gky1131
48. Jackson RE, Eickholt BJ. Semaphorin Signalling. *Curr Biol* (2009) 19:504–7. doi: 10.1016/j.cub.2009.04.055
49. Germer J, Cerveau N, Jackson DJ. The Holo-Transcriptome of a Calcified Early Branching Metazoan. *Front Mar Sci* (2017) 4:81. doi: 10.3389/fmars.2017.00081
50. DeFilippo J, Beck G. Cytokines of Invertebrate Immunity. *Ref Modul Life Sci Elsevier* (2018). doi: 10.1016/b978-0-12-809633-8.90751-9
51. Krishnan A, Degan BM, Degan SM. The First Identification of Complete Eph-Ephrin Signalling in Ctenophores and Sponges Reveals a Role for Neofunctionalization in the Emergence of Signalling Domains. *BMC Evol Biol* (2019) 19:1–17. doi: 10.1186/s12862-019-1418-z
52. Pozzolini M, Gallus L, Ghignone S, Ferrando S, Candiani S, Bozzo M, et al. Insights Into the Evolution of Metazoan Regenerative Mechanisms: Roles of TGF Superfamily Members in Tissue Regeneration of the Marine Sponge *Chondrosia Reniformis*. *J Exp Biol* (2019) 222:1–17. doi: 10.1242/jeb.207894
53. Darling TK, Lamb TJ. Emerging Roles for Eph Receptors and Ephrin Ligands in Immunity. *Front Immunol* (2019) 10:1–15. doi: 10.3389/fimmu.2019.01473
54. Inoue M, Horimoto K. Relationship Between Regulatory Pattern of Gene Expression Level and Gene Function. *PLoS One* (2017) 12:1–14. doi: 10.1371/journal.pone.0177430
55. Hickmann MJ, Jackson A, Smith A, Thornton J, Tursi A. Gene Function Contributes to Gene Expression Levels in *s. Cerevisiae*. *bioRxiv Prepr* (2018), 1–36. doi: 10.1101/330365
56. Lai Y, Eulgem T. Transcript-Level Expression Control of Plant NLR Genes. *Mol Plant Pathol* (2018) 19:1267–81. doi: 10.1111/mpp.12607
57. Wright RM, Kenkel CD, Dunn CE, Shilling EN, Bay LK, Matz MV. Intraspecific Differences in Molecular Stress Responses and Coral Pathobiome Contribute to Mortality Under Bacterial

- Challenge in Acropora Millepora. *Sci Rep* (2017) 7:1–13. doi: 10.1038/s41598-017-02685-1
58. Jahn MT, Arkhipova K, Markert SM, Stigloher C, Lachnit T, Pita L, et al. A Phage Protein Aids Bacterial Symbionts in Eukaryote Immune Evasion. *Cell Host Microbe* (2019) 26:542–50. doi: 10.1016/j.chom.2019.08.019
 59. Lazzaro BP. Genetic Basis of Natural Variation in *D. Melanogaster* Antibacterial Immunity. *Science* (2004) 303:1873–6. doi: 10.1126/science.1092447
 60. Muraille E. Generation of Individual Diversity: A Too Neglected Fundamental Property of Adaptive Immune System. *Front Immunol* (2014) 5: 1–7. doi: 10.3389/fimmu.2014.00208
 61. Bouso P, Casrouge A, Altman JD, Haury M, Kanellopoulos J, Abastado JP, et al. Individual Variations in the Murine T Cell Response to a Specific Peptide Reflect Variability in Naive Repertoires. *Immunity* (1998) 9:169–78. doi: 10.1016/S1074-7613(00)80599-3
 62. Blanquer A, Uriz MJ, Cebrian E, Galand PE. Snapshot of a Bacterial Microbiome Shift During the Early Symptoms of a Massive Sponge Die- Off in the Western Mediterranean. *Front Microbiol* (2016) 7: 1–10. doi: 10.3389/fmicb.2016.00752
 63. Luter HM, Bannister RJ, Whalan S, Kutti T, Pineda MC, Webster NS. Microbiome Analysis of a Disease Affecting the Deep-Sea Sponge *Geodia Barretti*. *FEMS Microbiol Ecol* (2017) 93:1–6. doi: 10.1093/femsec/fix074
 64. Belikov S, Belkova N, Butina T, Chernogor L, Kley, Van AM, et al. Diversity and Shifts of the Bacterial Community Associated With Baikal Sponge Mass Mortalities. *PLoS One* (2019) 14:1–19. doi: 10.1371/journal.pone.0213926
 65. Greenwood JM, Milutinović B, Peuß R, Behrens S, Esser D, Rosenstiel P, et al. Oral Immune Priming With *Bacillus Thuringiensis* Induces a Shift in the Gene Expression of *Tribolium Castaneum* Larvae. *BMC Genomics* (2017) 18:1–14. doi: 10.1186/s12864-017-3705-7
 66. Barribeau SM, Schmid-Hempel P, Sadd BM. Royal Decree: Gene Expression in Trans-Generationally Immune Primed Bumblebee Workers Mimics a Primary Immune Response. *PLoS One* (2016) 11:1–13. doi: 10.1371/journal.pone.0159635
 67. Connelly MT, McRae CJ, Liu PJ, Traylor-Knowles N. Lipopolysaccharide Treatment Stimulates Pocillopora Coral Genotype-Specific Immune Responses But Does Not Alter Coral-Associated Bacteria Communities. *Dev Comp Immunol* (2020) 109:103717. doi: 10.1016/j.dci.2020.103717
 68. Etienne-Manneville S, Hall A. Rho Gtpases in Cancer Cell Biology. *Nature* (2008) 582:2093–101. doi: 10.1016/j.febslet.2008.04.039
 69. Takamatsu H, Kumanogoh A. Diverse Roles for Semaphorin-Plexin Signaling in the Immune System. *Trends Immunol* (2012) 33:127–35. doi: 10.1016/j.it.2012.01.008
 70. Junqueira Alves C, Yotoko K, Zou H, Friedel RH. Origin and Evolution of Plexins, Semaphorins, and Met Receptor Tyrosine Kinases. *Sci Rep* (2019) 9:1–14. doi: 10.1038/s41598-019-38512-y
 71. Mohammed A, Okwor I, Shan L, Onyilagha C, Uzonna JE, Gounni AS. Semaphorin 3E Regulates the Response of Macrophages to Lipopolysaccharide- Induced Systemic Inflammation. *J Immunol* (2020) 204:128–36. doi: 10.4049/jimmunol.1801514
 72. Neubauer E-F, Poole AZ, Neubauer P, Detournay O, Tan K, Davy SK, et al. A Diverse Host Thrombospondin-Type-1 Repeat Protein Repertoire Promotes Symbiont Colonization During Establishment of Cnidarian-Dinoflagellate Symbiosis. *Elife* (2017) 6:1–26. doi: 10.7554/elife.24494
 73. Melo Clavijo J, Frankenbach S, Fidalgo C, Serôdio J, Donath A, Preisfeld A, et al. Identification of Scavenger Receptors and Thrombospondin-Type-1 Repeat Proteins Potentially Relevant for Plastid Recognition in *Sacoglossa*. *Ecol Evol* (2020) 10:12348–63. doi: 10.1002/ece3.6865
 74. Negroni A, Cucchiara S, Stronati L. Apoptosis, Necrosis, and Necroptosis in the Gut and Intestinal Homeostasis. *Mediators Inflamm* (2015) 2015:1–10. doi: 10.1155/2015/250762
 75. Chan FKM, Siegel RM, Lenardo MJ. Signaling by the TNF Receptor Superfamily and T Cell Homeostasis. *Immunity* (2000) 13:419–22. doi: 10.1016/S1074-7613(00)00041-8
 76. Liebl MP, Hoppe T. It's All About Talking: Two-Way Communication Between Proteasomal and Lysosomal Degradation Pathways via Ubiquitin. *Am J Physiol - Cell Physiol* (2016) 311:C166–78.

- doi: 10.1152/ajpcell.00074.2016
77. Lee JC, Peter ME. Regulation of Apoptosis by Ubiquitination. *Immunol Rev* (2003) 193:39–47. doi: 10.1034/j.1600-065X.2003.00043.x
 78. Creagh EM, Conroy H, Martin SJ. Caspase-Activation Pathways in Apoptosis and Immunity. *Immunol Rev* (2003) 193:10–21. doi: 10.1034/j.1600-065X.2003.00048.x
 79. De Arras L, Seng A, Lackford B, Keikhaee MR, Bowerman B, Freedman JH, et al. An Evolutionarily Conserved Innate Immunity Protein Interaction Network. *J Biol Chem* (2013) 288:1967–78. doi: 10.1074/jbc.M112.407205
 80. Lv Z, Song X, Xu J, Jia Z, Yang B, Jia Y, et al. The Modulation of Smac/ DIABLO on Mitochondrial Apoptosis Induced by LPS in *Crassostrea Gigas*. *Fish Shellfish Immunol* (2019) 84:587–98. doi: 10.1016/j.fsi.2018.10.035
 - Nguyen TV, Alfaro AC, Merien F, Young T. *In Vitro* Study of Apoptosis in Mussel (*Perna Canaliculus*) Haemocytes Induced by Lipopolysaccharide. *Aquaculture* (2019) 503:8–15. doi: 10.1016/j.aquaculture.2018.12.086
 81. Seneca F, Davtian D, Boyer L, Czerucka D. Gene Expression Kinetics of *Exaiptasia Pallida* Innate Immune Response to *Vibrio Parahaemolyticus* Infection. *BMC Genomics* (2020) 21:1–16. doi: 10.1186/s12864-020-07140-6
 82. Fuess LE, Pinzón CJH, Weil E, Mydlarz LD. Associations Between Transcriptional Changes and Protein Phenotypes Provide Insights Into Immune Regulation in Corals. *Dev Comp Immunol* (2016) 62:17–28. doi: 10.1016/j.dci.2016.04.017
 83. Dayan AD. The Immune Response is Subject to Individual Variability at All Levels. *Environ Toxicol Pharmacol* (1996) 2:177–80. doi: 10.1016/S1382-6689(96)00051-8
 84. Duffy D. Understanding Immune Variation for Improved Translational Medicine. *Curr Opin Immunol* (2020) 65:83–8. doi: 10.1016/j.coi.2020.06.005
 85. Moyer AM, Matey ET, Miller VM. Individualized Medicine: Sex, Hormones, Genetics, and Adverse Drug Reactions. *Pharmacol Res Perspect* (2019) 7: e00541. doi: 10.1002/prp2.541
 86. Nichols HL, Goldstein EB, Ziabari OS, Parker BJ. Intraspecific Variation in Immune Gene Expression and Heritable Symbiont Density. *bioRxiv* (2020), 1–31. doi: 10.1101/2020.12.17.420083
 87. Sackton TB, Lazzaro BP, Clark AG. Genotype and Gene Expression Associations With Immune Function in *Drosophila*. *PLoS Genet* (2010) 6:1–15. doi: 10.1371/journal.pgen.1000797
 88. Nair SV, Del Valle H, Gross PS, Terwilliger DP, Smith LC. Microarray Analysis of Coelomocyte Gene Expression in Response to LPS in the Sea Urchin. Identification of Unexpected Immune Diversity in an Invertebrate. *Physiol Genomics* (2005) 22:33–47. doi: 10.1152/physiolgenomics.00052.2005
 89. Terwilliger DP, Buckley KM, Brockton V, Ritter NJ, Courtney LC. Distinctive Expression Patterns of 185/333 Genes in the Purple Sea Urchin, *Strongylocentrotus Purpuratus*: An Unexpectedly Diverse Family of Transcripts in Response to β -1,3-Glucan, and Dsrna. *BMC Mol Biol* (2007) 8:1–16. doi: 10.1186/1471-2199-8-16
 90. Terwilliger DP, Buckley KM, Mehta D, Moorjani PG, Smith LC. Unexpected Diversity Displayed in Cdnas Expressed by the Immune Cells of the Purple Sea Urchin, *Strongylocentrotus Purpuratus*. *Physiol Genomics* (2006) 26:134–44. doi: 10.1152/physiolgenomics.00011.2006

Conflict of Interest: The authors declare that the research was conducted in the absence of any commercial or financial relationships that could be construed as a potential conflict of interest.

Copyright © 2021 Schmittmann, Franzenburg and Pita. This is an open-access article distributed under the terms of the Creative Commons Attribution License (CC BY). The use, distribution or reproduction in other forums is permitted, provided the original author(s) and the copyright owner(s) are credited and that the original publication in this journal is cited, in accordance with accepted academic practice. No use, distribution or reproduction is permitted which does not comply with these terms.

CHAPTER 3

THE SPONGE *HALICHONDRIA PANICEA* AS AN EXPERIMENTAL MODEL FOR HOST-MICROBE SYMBIOSES: ESTABLISHING A TOOL-BOX

This chapter is presented as a summary of the efforts to establish a basic tool-box for experimental work with *H. panicea*. Protocols are published under the terms of the Creative Commons Attribution License (CC-BY 4.0) and can be found in the appendix 3.8 and 3.9:

Schmittmann, L., U. Hentschel. 2021. Antibiotic treatment of the sponge *Halichondria panicea* and subsequent recolonization. dx.doi.org/10.17504/protocols.io.by7hpzj6

Schmittmann, L., L. Pita. 2021. DNA/RNA extraction and qPCR protocol to assess bacterial abundance in the sponge *Halichondria panicea*. dx.doi.org/10.17504/protocols.io.bxwwppfe

INTRODUCTION

The interaction with microbes has shaped the evolution of multicellular organisms since their first appearance about 600 million years ago (Kolodny et al. 2020). Experimental model systems are a crucial tool to understand the many ways microbes and multicellular host organisms interact (Douglas 2019). Well established models like *Drosophila melanogaster*, *C. elegans*, *Mus musculus* and *Hydra* have been studied for decades in different biological disciplines, ranging from development to cell biology and medicine. Methods, specifically omics ((meta)genomics, (meta)transcriptomics, proteomics, single-cell omics), were adapted and expanded to study host-microbe interactions in these model organisms (e.g. Zhang et al. 2017). Yet, the overwhelming wealth of animal symbioses calls for the establishment of new model systems covering the animal tree of life (Bosch et al. 2019). A central tool is the generation of axenic/gnotobiotic host organisms to simplify complex host-microbe communities to few players in a controlled environment (Douglas 2019), however it has proved to be challenging and methods are only available for few organisms. Especially gnotobiotic culture methods for aquatic organisms are difficult to achieve and maintain due to the increased contamination risk by culture water (Marques et al. 2006). Efforts to generate gnotobiotic hosts have focused on raising animals directly in a sterile environment, or on the application of antibiotics to remove the natural microbiome in later life stages. Only recently, methods have been optimized for members of the basal phylum Cnidaria, like the anemones *Hydra vulgaris* (Augustin et al. 2012), *Nematostella vectensis* (Domin et al. 2018), the jellyfish *Aurelia aurita* (Weiland-Bräuer et al. 2015), and, to some extent *Aiptasia sp.* (Costa et al. 2021).

The phylum Porifera (sponges) is one of the closest extant phyla to the last common ancestor of all metazoans and originated about 600 mya (Li et al. 1998). For this reason, mechanisms of sponge-symbioses can give insights into ancestral symbioses. Yet, so far, no experimentally tractable sponge model system has been established. Sponges are sessile filter-feeders that are able to filter vast amounts of water through their porous body while taking up small food particles such as bacteria or unicellular algae by phagocytosis. Their lifestyle makes sponges comparatively difficult to maintain in aquaria and experimental set-ups require continuous water exchange of large water volumes (Osinga et al. 1999; Webster et al. 2011). Moreover, sponge-associated microbial communities represent one of the most diverse and stable microbiomes (Thomas et al. 2016).

The aim of this chapter was to establish a suitable marine sponge as an experimental model for host-microbe symbioses. The tools and techniques considered essential for a model organism (Pita et al. 2016), include the availability of genomic and transcriptomic data with a well annotated genome, cultivability under laboratory conditions, wide natural distribution, easy access to wildtype specimens,

a closed life-cycle in the lab and continuous lab culture, cultivation of abundant symbionts, gnotobiotic hosts and amenability for genetic manipulation. In the emerging field of aquatic symbioses models no sponge species fulfills all of these requirements yet, while the marine sponge *Amphimedon queenslandica* and the freshwater sponge *Ephydatia muelleri* are currently the most advanced (Srivastava et al. 2010; Gauthier et al. 2016; Kenny et al. 2020; Hall et al. 2021). The genome of *A. queenslandica* was the first sponge genome to be sequenced (Srivastava et al. 2010) and experimentation with adults and developmental stages from larva to juveniles is possible under laboratory conditions (Leys et al. 2008). However, the life cycle cannot be closed (i.e. reproduction of lab-spawned sponges), and the sponges's distribution is restricted to the Great Barrier Reef in Australia. The freshwater sponge *E. muelleri* has the capacity to produce gemmules by asexual reproduction (Leys et al. 2019), which allows developing clones from a single individual and the shipment of samples across labs. However, *E. muelleri* is a freshwater sponge, and its microbiome has not been described yet. We chose the marine shallow water breadcrumb sponge *Halichondria panicea* (Demospongiae). It is widely distributed in the North Atlantic, including the Baltic Sea, with a closely related sister species in the North Pacific (Erpenbeck et al. 2004) allowing access to wildtype specimens throughout the Northern hemisphere and thus, many laboratories. *H. panicea* is comparatively resistant to environmental conditions like low oxygen concentrations (Mills et al. 2014) and thrives in brackish conditions in the Baltic Sea. Here, it is often the dominant sponge in coastal systems where only few other sponge species are able to survive. *H. panicea* can be studied in aquaria as adults (Riisgård et al. 2016) and as explant cultures (Kumala et al. 2017), and reproduces in the lab (unpublished data, Carrier, Pita and Schmittmann). A preliminary sponge genome has been sequenced (Strehlow et al. 2021), while a high-quality genome is currently in preparation (ASG Sponges Project <https://www.sanger.ac.uk/collaboration/aquatic-symbiosis-genomics-project/>) and *de novo* transcriptomes have been generated in the context of immune responses (Chapter 2; (Schmittmann et al. 2021)) and in response to crude oil (Vad et al. 2020). *H. panicea* is a low microbial abundance sponge (Gloeckner et al. 2014) and its microbiome is dominated by a novel Alphaproteobacterium, *Ca. Halichondribacter symbioticus* that is highly specific to its sponge host (Knobloch et al. 2019a). This novel symbiotic clade is only 92.7 % related to the closed cultivated representative, called *Amylibacter sp.*, indicating that this the sponge lineage has evolved to a symbiotic lifestyle within Halichondria. The monodominance of a single bacterial clade in *H. panicea* offers a simplified version of the otherwise extremely complex sponge microbiomes known today. As for other sponge symbionts, *Ca. H. symbioticus* has not been isolated and knowledge on the symbioses comes exclusively from metagenomic data (Knobloch et al. 2019b, 2020).

The goals of this chapter were (i) to understand the natural variability of wildtype *H. panicea* microbiomes, (ii) to evaluate the culturing conditions and methodology that enable *in vivo* work with *H. panicea*, (iii) the design of an experimental set-up for working in sterile conditions and that allows the manipulation of sponge microbiomes by antibiotics, and (iv) to get a better understanding of the dominant symbiont *Ca. H. symbioticus*. The relative abundance and natural diversity of the dominant symbiont *Ca. Halichondriabacter symbioticus* was assessed in wild populations collected during different seasons and years. Maintenance aquaria were set up to culture the sponges under close-to natural conditions, and changes in the microbiome assessed after several months of culture. An experimental aquarium system was designed to culture sponges under controlled conditions and two antibiotic cocktails tested to manipulate the sponge microbiome. Lastly, the diversity of closely related bacteria to *Ca. H. symbioticus* was assessed. In addition, a bacteria strain collection from *H. panicea* was constructed and the cultured diversity compared to the culture-independent sponge microbiome. This bacterial strain collection serves as a resource for further experimentation with *H. panicea* under controlled laboratory conditions.

METHODS

COLLECTION OF *H. PANICEA* FROM THE FIELD

The sponge *Halichondria panicea* can be found year-round along the West Baltic on hard substratum like rocks, wooden piers, *Mytilus* mussels and perennial algae such as *Fucus vesiculosus*. The animals can be accessed easily by snorkeling in shallow water (1-3 m) while they are mostly found sheltered from direct light, e.g., under rocks or between algae. Sponges were found reliably in suitable habitat given the substratum was old enough. For example, in a newly built sailing harbor wall in Mönkeberg (2018), no sponges were found within the same year. Samples can be best collected by carefully scraping sponges off with a spatula close the substratum, while individuals should never be removed completely, to allow the remaining tissue to recover in the wild. *H. panicea* co-occurs with two other sponge species around Kiel, mainly *Haliclona* sp. and rarely *Chalinula limbata* (Figure 1). The species can be distinguished by their spicules, sometimes color (*Haliclona* sp. is mostly red to purple but can be orange as well), and perceived density of the tissue. *H. panicea* is the densest sponge of the three and appears harder/sturdier when touched.

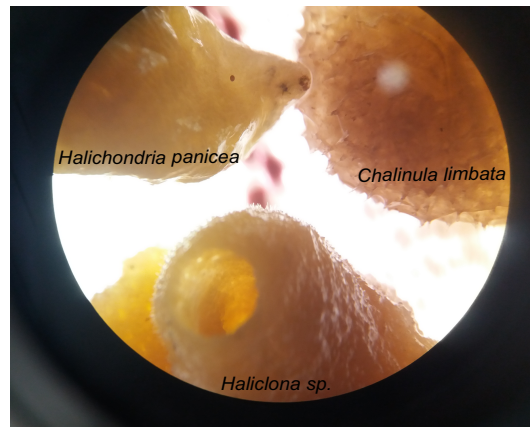


FIGURE 1 | The three sponge species commonly co-occurring on rocks in Schilksee (Kiel, Germany). Upper left: *Halichondria panicea*, smooth surface and dense tissue. Upper right: presumably *Chalinula limbata*, very hispid surface, tissue is spongy and resilient to compression. Down: presumably *Haliclona sp.*, smooth surface with very thin needles sticking out, much softer tissue than *H. panicea*.

The relative abundance of *Ca. H. symbioticus* in *Halichondria panicea* microbiomes was monitored in different years and seasons. Sponges were sampled in June 2017 from three different locations along the West Baltic in June 2017 by Yazmin Zurita-Gutiérrez, and from Schilksee in November 2018, 2019 and June 2020 (Figure 2). Tissue was sampled directly in the field or after 2-7 days maintenance in semi-flow-through maintenance aquaria at the institute. Samples were preserved in RNAlater until analysis (stored overnight at 4°C and subsequently frozen at -80°C).

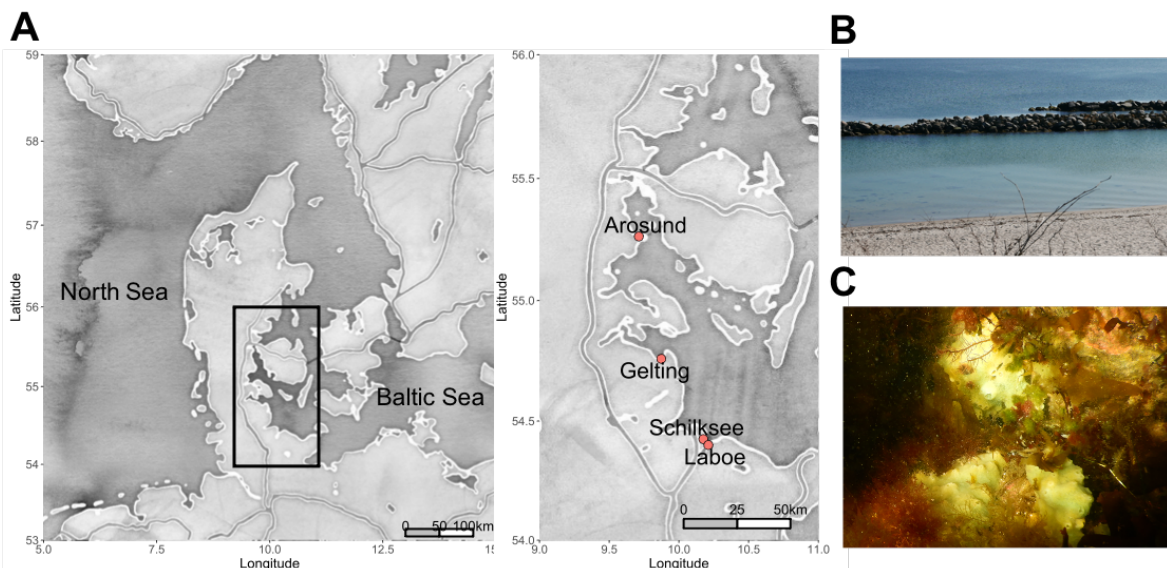


FIGURE 2 A-C | Sampling locations in the West Baltic Sea. **(A)** Overview and close-up map of the sampling locations Schilksee, Laboe and Gelting (Germany), and Arosund (Denmark). **(B)** “Hausgarten” sponge sampling location in Schilksee, close to Kiel in Germany. Sponges are collected close to the beach from below rocks. Picture taken by Andrea Hethke. **(C)** Underwater picture of *H. panicea* between algae. Two sponge individuals are depicted, both about 10 cm in diameter.

DESIGN OF AN SPONGE MAINTENANCE AQUARIUM SYSTEM

Sponges from Schilksee, Germany were collected by snorkeling in late July 2018 and November 2018 (Figure 2). They were individually transported in 500 ml bottles and brought to Baltic semi-flow-through maintenance aquaria at the institute within 2 hours after collection. The aquaria system consisted of 20 x 8 l tanks supplied from a source tank where fresh Baltic seawater (> 10 l / min) is constantly mixed with recirculating water from the aquaria (100 mL / min) (Figure 3). Water temperature and salinity follow the ambient conditions in the Baltic Sea. To assess stability of sponge microbiomes in maintenance aquaria, sponge tissue was sampled after 3 and 6 months in aquaria (n=6 and 3, respectively) and preserved in RNAlater (stored overnight at 4°C and subsequently frozen at -80°C). Aquarium water was filtered in triplicates (1 l filtered each onto 0.22 µm filter). For comparison, sponges were sampled from three different locations along the West Baltic in June 2017 (Figure 2), and both tissue (n=5 per location) and seawater (n=3 per location) were preserved directly in the field.

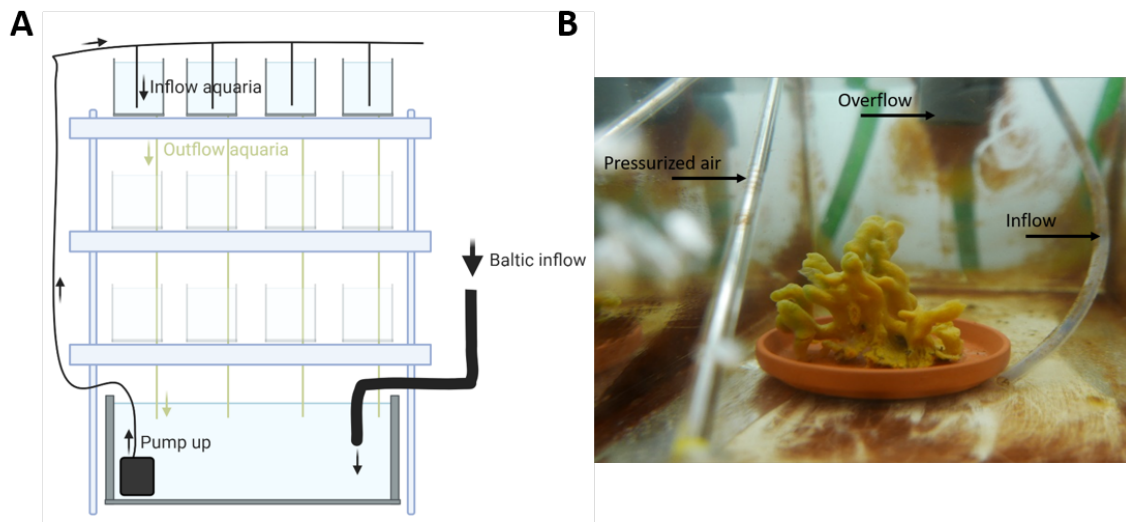


FIGURE 3 A-B | *Halichondria panicea* maintenance aquaria set-up. **(A)** Schematic of the semi flow-through aquarium system. Each aquarium is supplied from a source tank where fresh Baltic seawater is mixed with recirculating water from the aquaria. **(B)** Close-up of a sponge in a single aquarium (picture taken by Andrea Hethke). The water in each aquarium is constantly mixed by pressurized air.

DESIGN OF AN EXPERIMENTAL AQUARIUM SYSTEM TO STUDY SPONGE-MICROBE SYMBIOSIS UNDER CONTROLLED CONDITIONS

A custom experimental aquarium system was manufactured to automate water exchange and create a flow-through system in a sterile environment. The basis was 500 mL Erlenmeyer Flasks (NS 45/40 and hollow glass stopper) with a glass olive attached to a 6 mm glass tube for water inflow directly to

the bottom of the flask, and a glass olive for water outflow (Figure 4) (EYDAM Labortechnik und Lehrmittel, Germany). To allow sterile sampling of water with syringe and needles, a thread (GL 14) with screw cap and silicone septum was installed. All parts can be re-used and autoclaved.

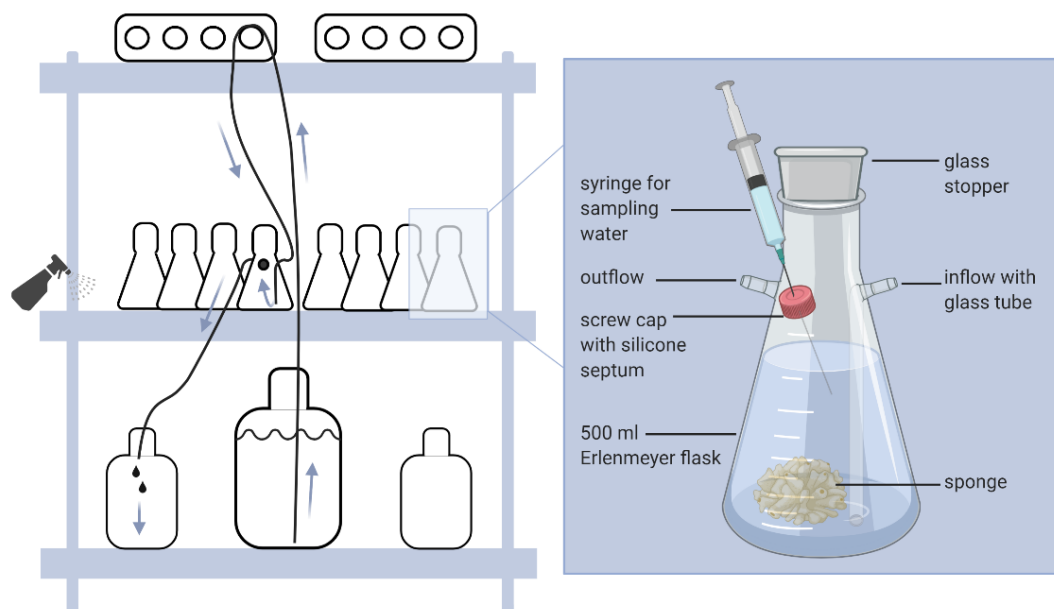


FIGURE 4 | Experimental set-up in gnotobiotic chambers at GEOMAR Kiel, Germany. For more information see Schmittmann & Hentschel 2021 or appendix 3.8.

The gnotobiotic system consists of four shelves with eight flasks each, a total of 32 individually supplied flasks (Figure 4). The eight flasks per shelf are supplied from one 20 L source tank (Nalgene, PP) filled with sterile filtered ASW and waste water was collected from four flasks at a time into 10 L chemical waste canisters. The waste water during the antibiotic treatment is disposed as pesticide waste and afterwards as medical waste containing potentially antibiotic resistant bacteria in high abundances. The shelves, room and material is surface sterilized with soaked wipes (Curacid Medical wipes, PICO-Medical, Germany) regularly and the air is continuously sterilized (CP Type 500 NATURE SYSTEM, Expansion Electronic SRL, Italy). Contamination by scientists is prevented by wearing protection consisting of lab coat that is exclusively used inside the gnotobiotic chambers, disposable gloves and shoe covers. Successful reduction of bacteria in the air was tested by placing open bacterial culture plates for three hours in the gnotobiotic chambers compared to the hallway and other climate chambers (MarineBroth Difco 2216).

The flasks (Figure 4) can be completely closed by compressing the in- and outflow tube close to the bottle with screw clamps. By carefully topping up the bottle afterwards with sterile filtered ASW and

inserting the glass stopper without formation of air bubbles, a completely water filled and airtight system is created. This offers the possibility for respiration measurements mid-experiment with non-invasive sensors (OXY4-mini and sensorspots, PreSens, Germany) and was tested in a pilot test for two different sponge individuals in comparison to empty controls.

ANTIBIOTIC EXPOSURE EXPERIMENTS

Two different antibiotic treatments were tested to remove bacteria associated to *H. panicea*. The first experiment was performed in 500 ml glass beakers and water was exchanged manually twice a day (methods below). The second experiment was performed with automatic aquaria pumps exchanging water continuously. Details on the materials and methods can be found online (Schmittmann and Hentschel 2021) and in appendix 3.8.

Halichondria panicea individuals were collected by snorkeling from Schilksee, Germany in late July 2018. Sponges were individually transported in 500 ml bottles and brought to Baltic flow-through tanks at the institute within 2 hours after collection for a 1-week acclimation period prior to experiments. The experimental set-up consisted of 800 ml glass beakers filled with autoclaved (15 min, 121°C) artificial seawater with *Nannochloropsis salina* algae as a food source (Algova, solution from freeze dried powder, $\sim 10^5$ cells/ml). For the preliminary antibiotic exposure experiment, three sponge individuals were each cut into five clones with a sterile scalpel. One clone per individual was immediately preserved in RNAlater (incubated overnight at 4°C and stored at -80°C) and serves as the start sample T0 (n=3). The other four clones per individual were placed in separate glass beakers and either treated with an antibiotic cocktail, or served as a control. The antibiotic protocol to generate germ-free *Hydra* was tested (Franzenburg et al. 2012): rifampicin (50 mg/L in DMSO), ampicillin (50 mg/ml in water), streptomycin (50 mg/ml in water), neomycin (50 mg/ml in water). Half the water volume was exchanged manually twice a day. Experiments were performed with stable temperatures and salinities according to the environmental conditions at the time of the experiment (18°C, 15 PSU). Samples were taken at day T2 and day T7, tissues were preserved in RNAlater (n=3).

DNA, RNA EXTRACTIONS, QPCR AND AMPLICON SEQUENCING

Please see the published protocol (Schmittmann and Pita, 2021 or appendix 3.9) for details regarding sample processing, qPCR and bioinformatic analysis of 16S rRNA amplicon sequences. In short, DNA was extracted from sponge tissue with the DNeasy PowerSoil Kit (Qiagen, Netherlands) and the V3-V4 variable regions of the 16S rRNA gene amplified and sequenced at the CCGA Kiel (MiSeqFGx, Illumina,

USA). Sequences were processed bioinformatically within QIIME2 (Bolyen et al. 2019) and taxonomically classified based on the online reference database (Silva132) (Quast et al. 2013). Statistics and diversity indices were calculated within QIIME2 and data was visualized in R (version 3.5.1 and 4.0.2) and finalized in Inkscape (version 0.92). RNA was extracted from sponge tissue with the RNeasy Mini Kit (Qiagen, Netherlands) and reverse transcribed to cDNA. QPCR was run on both gDNA and cDNA with primers for eubacteria, *Ca. H. symbioticus* and the sponge house-keeping genes *18S rRNA* (gDNA) and β -tubulin (cDNA). Copynumbers were calculated with standard curves for each gene.

RESULTS AND DISCUSSION

SEASONAL VARIATION OF *CA. H. SYMBIOTICUS*

H. panicea sampled in different seasons and years were dominated by a single ASV (on average 46 %) identified as *Ca. H. symbioticus* (Figure 5). The abundance varied from a minimum of 18 % to a maximum of 66 %. The average abundance was highest in June 2020, while no obvious trend is visible depending on the season or the year. Monthly monitoring would be needed to determine whether *Ca. H. symbioticus* abundance is correlated to season, environmental factors (e.g., temperature or pH) or biotic factors (e.g., reproduction or morphology). Sampling the same sponge individuals over time would reveal whether *Ca. H. symbioticus* abundance is variable only within the population, or also within the same individual. Further, important questions remain whether differences in relative abundance are reflected in absolute abundances, and whether abundances are linked to sponge performance and physiology.

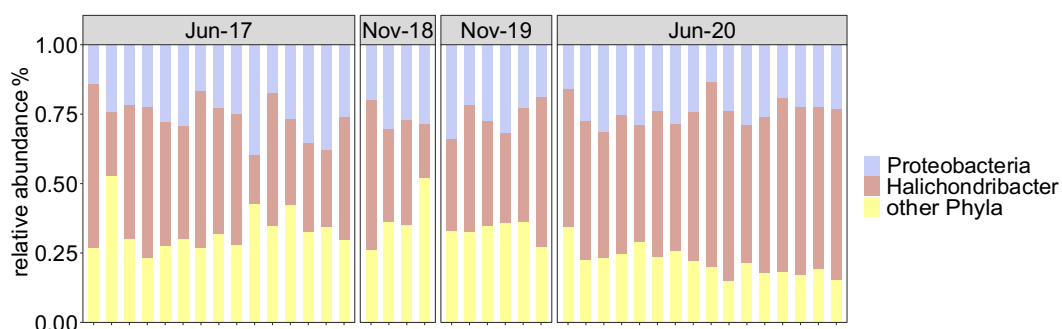


FIGURE 5 | Relative contribution of *Ca. Halichondribacter symbioticus* to the bacterial community of *H. panicea* collected in different seasons and years. Sponges were wild caught in June 2017, or kept in maintenance aquaria for up to one week prior to sampling for the remaining time points. Proteobacteria are resolved in the Alphaproteobacterium *Ca. Halichondribacter symbioticus* and

other Proteobacteria. Average relative abundance Jun17: 41 %, Nov18: 36 %, Nov19: 40 %, Jun20: 54 %.

COMPARISON BETWEEN SPONGE MICROBIOMES COLLECTED FROM THE WILD AND FROM MAINTENANCE AQUARIA

A semi-flow-through aquarium system supplied with natural Baltic seawater was set-up to maintain *H. panicea* and have sponges readily accessible for experimentation (KIMOCC, GEOMAR Helmholtz Center for Ocean Research). Changes in the microbiome after long-term culture in aquaria (3 and 6 months) was assessed by 16S rRNA amplicon sequencing. Importantly, the dominant symbiont *Ca. H. symbioticus* was maintained in high abundances regardless of cultivation in aquaria (Figure 6A), and alpha-diversity was not affected (Figure 6C). Beta-diversity of sponges collected directly from the field did not differ between sites, while sponges maintained for 3 and 6 months in aquaria differed to some of the field sponges (Figure 6B, appendix 3.1). Compositional differences included, for example, the loss of photosynthetic Cyanobacteria in sponges kept in aquaria. This might be due to the light in the aquaria system that does not reflect wavelength and intensity of light found in the field, and should be improved in the future. The microbiome of sponges kept in aquaria for 3 and 6 months was similar, suggesting that any changes due to maintenance in aquaria happened early upon transplantation, and then remained stable over several months. It is known that sponges in cultivation tend to change their microbiome, including *H. panicea* (Mohamed et al. 2008; Webster et al. 2011; Knobloch et al. 2019a,b). Importantly, in the semi-flow-through system tested here, the dominant symbiont remained in high abundances suggesting adequate conditions to maintain this symbiosis. Compared to other culturing methods for *H. panicea* where the dominant symbiont reduced in relative abundance after 6 months in a recirculating seawater aquaria (Knobloch et al. 2019a) and flow-through aquaria (Knobloch et al. 2019b), a semi-flow-through system with a large continuous input of fresh ambient seawater seems appropriate to maintain a comparatively stable microbiome with high proportions of *Ca. H. symbioticus*.

Morphologically, the sponges tended to grow thinner in aquaria and optically “shrink”. This might be because of different current conditions in the aquaria compared to the exposed rocky shore where they are found. For *H. panicea* it is known that the morphology varies strongly with the habitat (Barthel 1991). Knobloch et al. reported that some individuals shrank in captivity, while others grew without an indication what favored growth (Knobloch et al. 2019a). Most likely, sponges are food-limited in the aquaria system due to and shrinking is a sign of starvation. It has to be determined in the future how the sponge hosts are performing and whether there is an impact on the host performance after long-term culture. Food uptake and basic physiological measurements like respiration will be a good

starting point. Further, it should be determined if the visual shrinking of the tissue is as expected a loss of organic matter, or a reorganization of the tissue without a reduction in organic mass.

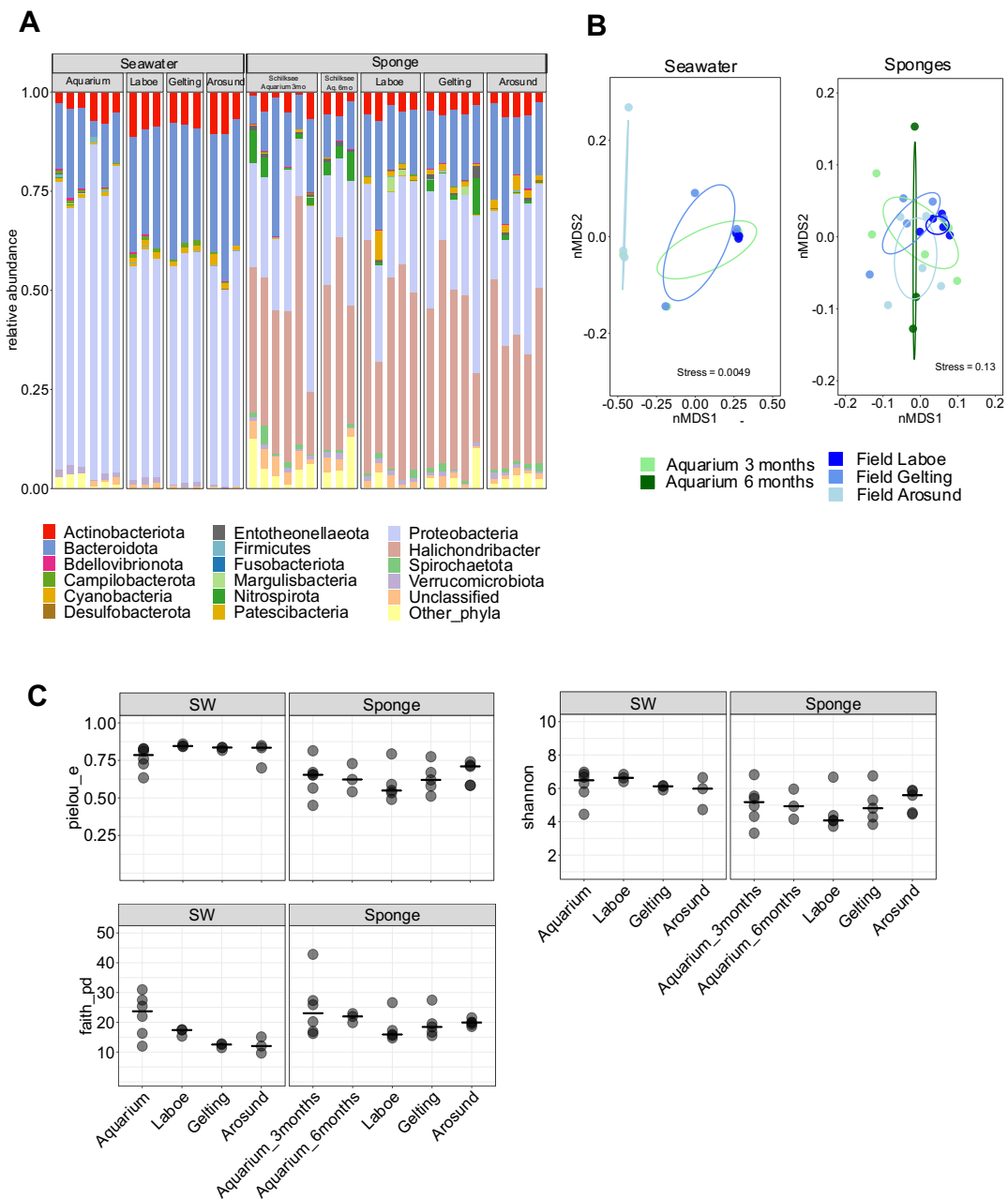


FIGURE 6 A-C | Bacterial community composition and diversity of sponges and seawater from maintenance aquaria and directly from the field. Sponges were sampled from Schilkesee and maintained in aquaria, or directly sampled from the field (Laboe, Gelting, Arosund). **(A)** Relative bacterial community composition shown on phylum level (top 15 phyla) separated by sample type (seawater or sponge), and sample location. Proteobacteria are resolved in the Alphaproteobacterium *Ca. Halichondribacter symbioticus* and other Proteobacteria. **(B)** Beta diversity of microbial communities (non-metric multidimensional scaling plot on weighted UniFrac distances). Sample locations are represented by color. For results of pairwise PERMANOVA on beta diversity see appendix 3.1. **(C)** Alpha-diversity of microbial communities (pielou-evenness, Shannon-diversity and Faith's phylogenetic diversity).

EXPERIMENTAL AQUARIUM SET-UP AND ANTIBIOTIC TREATMENT TO MANIPULATE THE SPONGE MICROBIOME

Sponge maintenance aquaria are suitable for maintaining sponges and making them readily available for experimentation, but they do not allow to control or manipulate the bacterial community. Thus, a controlled experimental system was set-up that allows sponge culturing in an environment without contamination of microbes from the environment. The system is closed and exchanges sterile water automatically. By the application of antibiotics, the sponge microbiome can be manipulated and hypothesis on assembly and recolonization can be tested (Chapter 4). Further, oxygen uptake of the sponges can be assessed within the experimental aquarium system. Trial runs were performed with two sponge individuals measured twice each and show that dissolved oxygen decreases over time compared to an empty control (appendix 3.2). The system is appropriate to perform closed respiration measurements and has to be evaluated during longer experiments.

Two antibiotic treatments were tested to reduce bacteria associated to *H. panicea*. The first resulted in only slightly shifted bacterial community composition after seven days of treatment and *Ca. H. symbioticus* was not reduced in terms of relative abundance (Figure 7A+B). The second antibiotic treatment shifted the bacterial community composition significantly from the start conditions at T0 and control (untreated) sponges and reduced *Ca. H. symbioticus* to ~3% (Figure 7C+D, for more details see Chapter 4).

To assess whether bacteria were actually reduced by the antibiotic treatment, qPCR was performed for bacterial gDNA and cDNA. *16S* rRNA qPCR primers specific for *Ca. H. symbioticus* were designed and tested for specificity by sequencing the PCR product (Schmittmann and Pita, 2021). After antibiotic treatment, *Ca. H. symbioticus* was decreased by several orders of magnitude, confirming the relative decrease in terms of absolute numbers (appendix 3.3). Nevertheless, the effect was variable between sponge individuals, for example both data from gDNA as well as cDNA indicate that there was no reduction of *Ca. H. symbioticus* in individual 1 (appendix 3.3, pink). Unexpectedly, both after antibiotic treatment and in the control treatment eubacterial abundance increased. This was accompanied by an increase in *Ca. H. symbioticus* in the control treatment, suggesting an overall growth of the sponge microbiome in experimental beakers under control conditions. The agreement of RT-qPCR results from gDNA and cDNA confirm that the detected bacteria are indeed active, including *Ca. H. symbioticus*. In this way, bacteria load in the sponge were calculated both as copy numbers, as well as relative changes compared to a stable sponge gene (*18S* rRNA gene for gDNA and β -tubulin for cDNA). Since there were no differences in the patterns reported, for further studies results were presented as copy numbers only.

The combination of relative and absolute measures of bacterial communities was absolutely crucial to interpret the effect of antibiotics on sponge microbiomes. Even though overall bacteria were not reduced, antibiotics can be used to manipulate the sponge microbiome and alter the healthy community composition. The reduction of the dominant and faithfully associated symbiont *Ca. H. symbioticus* presents a starting point for further experimentation and study recolonization processes of the natural microbiome (see Chapter 4). Additionally, the increase of *Ca. H. symbioticus* in control sponges after eleven days in experimental beakers suggests potential to manipulate the symbiosis also in this direction and generate *H. panicea* with a significantly increased symbiont load.

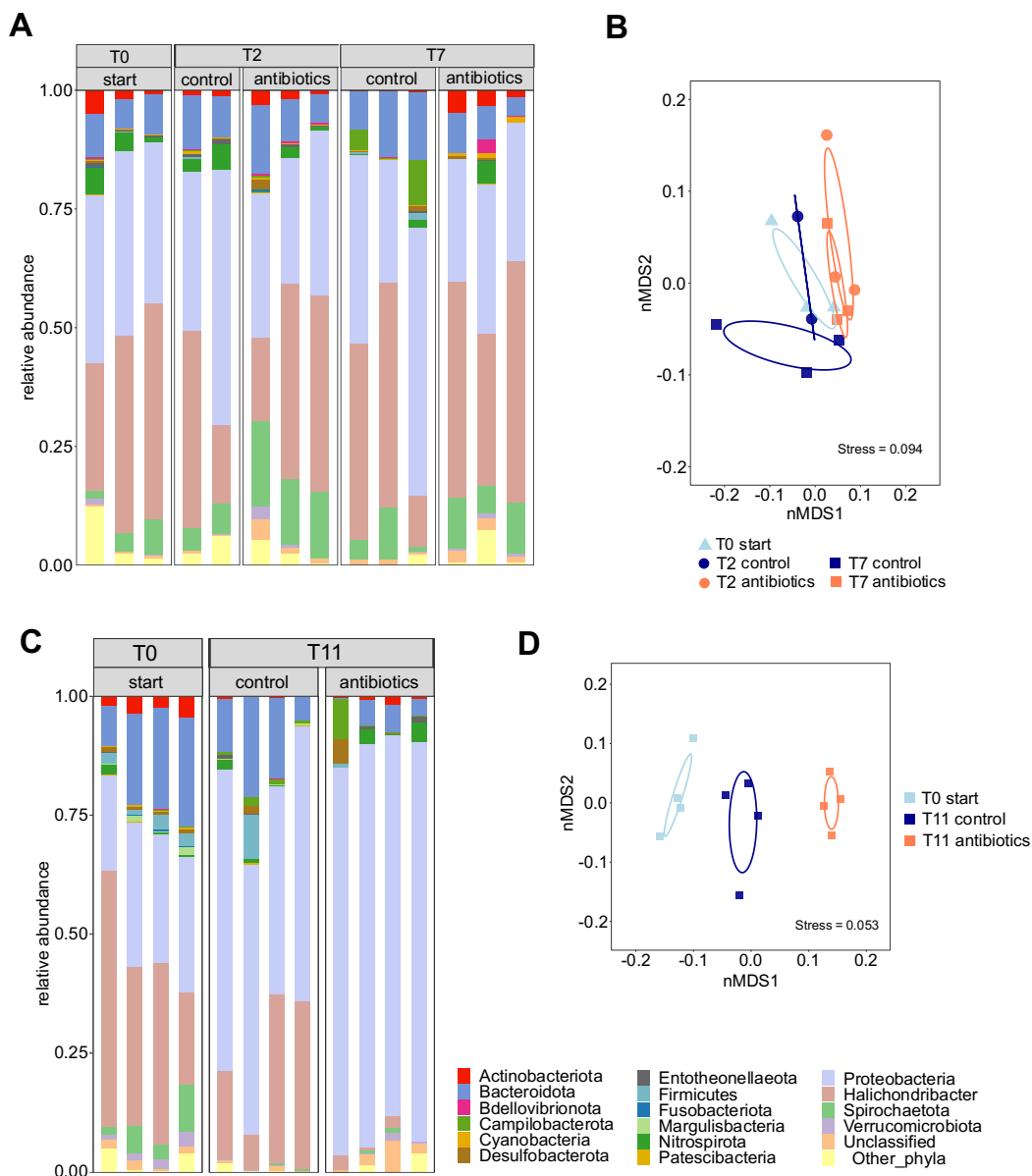


FIGURE 7 A-D | Antibiotic exposure experiments I (**A+B**) and II (**C+D**): Relative bacterial community composition shown on phylum level (top 15 phyla) across time and separated by treatment. Proteobacteria are resolved in the Alphaproteobacterium *Ca. Halichondriabacter symbioticus* and

other Proteobacteria. Beta diversity of microbial communities (non-metric multidimensional scaling plot on weighted UniFrac distances). Treatments are represented by color, with increasing color intensity representing progressing time.

UNDERSTANDING THE DIVERSITY OF THE *CA. H. SYMBIOTICUS* CLADE

Interestingly, among the other Proteobacteria associated with *H. panicea* (e.g. Figure 5), I detected a diverse array of ASVs assigned to the genus *Amylibacter* that represent the closest relatives to *Ca. Halichondribacter symbioticus*. Taking together all 16S rRNA amplicon data generated from *H. panicea* in this thesis (219 samples), 326 ASVs were annotated as *Amylibacter*. From here on, I will refer to them as *Ca. H. symbioticus*-related. Interestingly, 15 % of the bacteria involved in bacteria-bacteria interactions in healthy sponges, belonged to the *Ca. H. symbioticus*-related (Figure 8A, appendix 3.4). Those 17 ASVs vary in their sequence similarity to the dominant ASV 01, ranging from 1 bp difference (of 270 bp ASV) to 35 bp differences (Figure 8B, appendix 3.4). The dominant ASVs found in this and other studies cluster in a monophyletic group together with few other related ASVs (Althoff et al. 1998; Wichels et al. 2006; Naim et al. 2014; Knobloch et al. 2019a) (Figure 8B). The *Ca. H. symbioticus*-related ASVs A03 and A04 were present in almost all analyzed sponges and thus the most common next to the dominant symbiont (appendix 3.4). Despite their frequency, they were not the closest relatives (Figure 8B). Besides the common *Ca. H. symbioticus*-related ASVs like A01, A03 and A04, each sponge individual has its individual composition of this taxonomic clade.

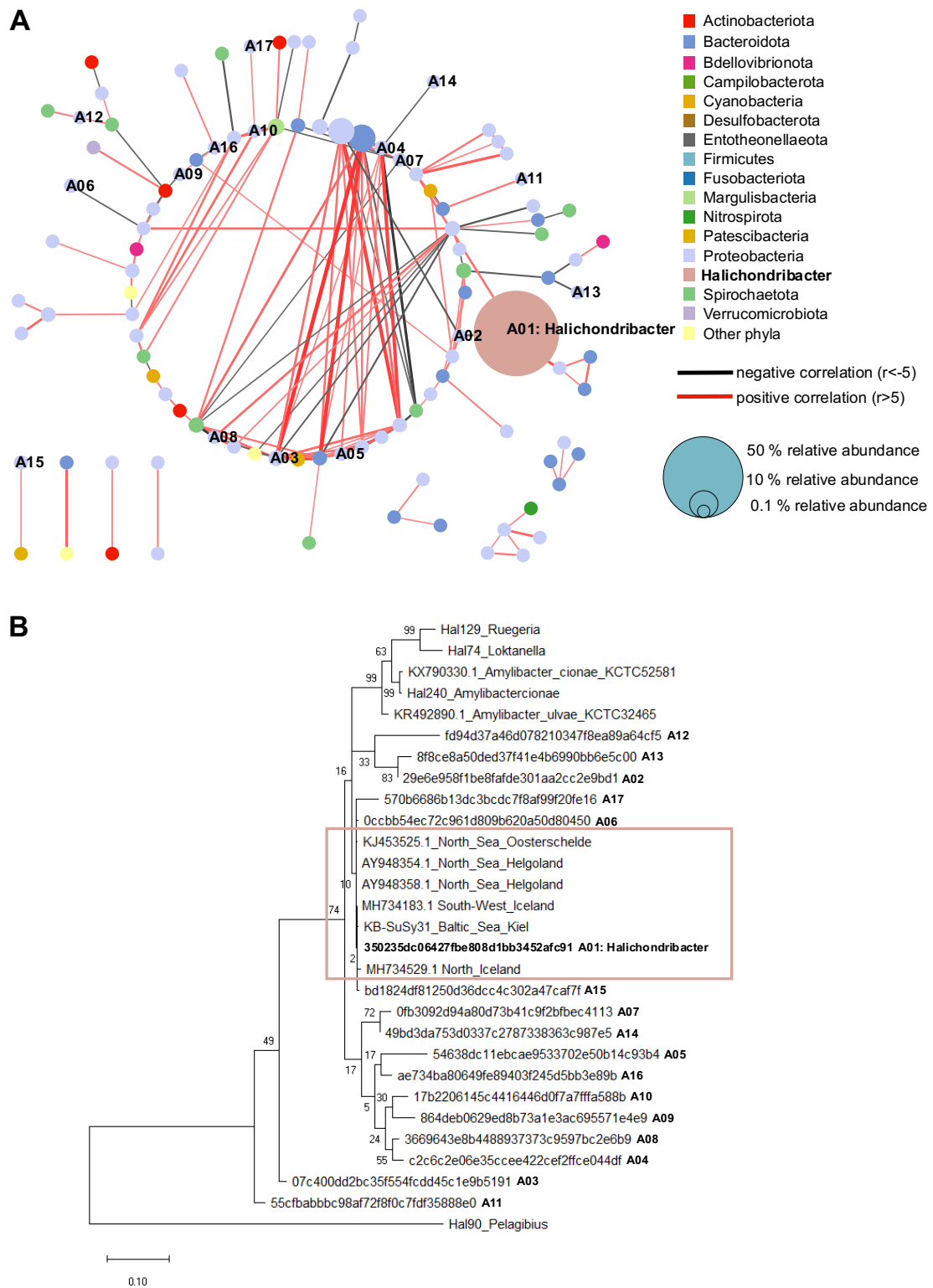


FIGURE 8 A+B | **(A)** Bacterial co-occurrence network for healthy wildtype sponges (see Chapter 4 for more details). Co-occurrences between ASVs ($-0.5 < R < 0.5$, p -value < 0.05) are displayed by edges (interaction) connecting nodes (ASVs). The color of the edges depicts the direction of the correlation (negative or positive), and thickness the interaction strength. The size of the nodes is proportional to the relative abundance of ASVs and the color represents taxonomic affiliation. ASVs affiliated to the family *Amylibacter* are labelled “A”. **(B)** Maximum-Likelihood phylogeny (bootstrap 500) of *Ca. Halichondribacter symbioticus* and related ASVs. Box highlights the dominant ASVs in this study (A01)

and previous studies (Knobloch et al. 2019, Naim et al. 2014, Althoff et al. 1998). Accession numbers of *Ca. H. symbioticus* sequences obtained from NCBI are given; isolates from *H. panicea* indicated by “Hal”; for details on ASVs see appendix 3.4. Alignment (ClustalW) and phylogeny were calculated in MEGA (version 10.0.5).

Overall, the group of *Ca. H. symbioticus*-related ASVs seems to hold a lot of unknown diversity. While *H. panicea* specimens from North and South-West Island had different *Ca. H. symbioticus*-related ASVs (Knobloch et al. 2019a), some were identical with bacteria identified in the North Sea (Naim et al 2014, Althoff et al 1998) and this study. The dominant ASV detected in this study might itself be more diverse than currently estimated, and its true diversity cannot be resolved with the V3-V4 16S rRNA region. Longer markers or metagenomic approaches would offer a much greater resolution and might reveal potential physiological differences of this clade. It is not clear whether the fragmented *Ca. H. symbioticus* genome (Knobloch et al. 2019c) is actually a composition of different *H. panicea* adapted symbionts. Deep sequencing will open the door to a new clade of sponge symbionts, and reveal their specialization to the sponge environment.

The variable presence of most *Ca. H. symbioticus*-related ASVs indicates either stochastic processes, or growth and diversification of this symbiont clade within their host over time. This system could be an interesting model for observing ‘evolution in action’ and tracking variation over time, potentially even within the same sponge individual. It remains an open question whether the diversity has an advantage for the sponge host, and if the different symbionts fulfil specialized roles or if they are functionally redundant. The key question is what makes one strain more successful than close relatives within the same environment.

Considerable efforts to isolate *Ca. H. symbioticus* from *H. panicea* tissue were not successful (personal communication, Tanja Rahn, see appendix 3.5 and 3.6 for methods and results, respectively). Nevertheless, 25 % of all isolated bacterial strains (335 isolates) belonged to the *Rhodobacteraceae* family that *Ca. H. symbioticus* is affiliated to. One *Amylibacter* strain was isolated (Hal240, Figure 8B, appendix 3.6) that had 90.4 % similarity to the dominant ASV in this study (based on 270 bp). Hal240 was isolated on solid medium based on Baltic Seawater, biotin and tryptophan, which was the medium most effective at selecting for *Rhodobacteraceae*. This isolate is the closest *Ca. H. symbioticus*-related bacterium in culture and *in vivo* tests can be performed in the future on the differential uptake (phagocytosis) of symbiont-related bacteria vs. environmental bacteria.

CONCLUSION AND OUTLOOK

In this chapter, the basis for experimentation with the Baltic *H. panicea* and its dominant symbiont *Ca. H. symbioticus* was established. First, the natural variability of local wildtype *H. panicea* microbiomes was assessed. The relative abundance of the dominant symbiont varies but there was no effect attributed to the season or the year. As a next step, maintenance aquaria were set up that allow the culturing of sponges over several months with minor microbiome changes and importantly preserving the natural dominance of *Ca. H. symbioticus*. However, in order to test functions of symbionts *in vivo* and their effect on the sponge we need experimental set-ups to manipulate sponge microbiomes. One future option would be the generation of axenic/gnotobiotic sponge hosts to test the effect of single bacteria in a controlled environment. Therefore, an experimental system was set-up and an antibiotic cocktail identified that reduces the dominant symbiont *Ca. H. symbioticus* in terms of both relative and absolute numbers. Additionally, a large diversity within the *Ca. H. symbioticus*-related bacteria raise the question whether there is diversity hidden within the dominant ASV that cannot be resolved by 16S rRNA amplicon sequencing. Efforts to construct a metagenome and to resolve the diversity further were only partially met with success so far and need to be continued (Knobloch et al. 2019c, Beate Slaby, personal communication). Lastly, a bacterial strain collection isolated from *H. panicea* provides a resource for experimentation. For example, the currently closest isolated relative to the dominant symbiont Hal240 could be used to test whether *H. panicea* can differentiate between environmental and symbiont-related bacteria.

Other experimental approaches utilizing different sponge life stages (larvae or juveniles) or primmorphs (aggregated sponge cells after cell dissociation) offer complementing routes to manipulate the sponge microbiome. Efforts by Carrier, Pita and Schmittmann show that *H. panicea* larvae settlement is possible under laboratory and sterile conditions, while metamorphosis into a functional sponge (with an osculum) has not happened yet. A co-occurring sponge species *Haliclona* sp. might offer experimental accessibility of early life stages that develop into adult sponges and have visible egg clusters (appendix 3.7). A window of opportunity could here be the very early larvae phase during which different larvae have not yet developed self-self recognition and different individuals would fuse together (Gauthier and Degnan 2008)). The role of the microbiome during this time is not understood yet, and manipulating the bacteria here could interfere with the establishment of a specific and stable microbiome. Similarly, primmorph cultures with and without bacteria could help understand the role of bacteria in aggregation and formation of a new sponge.

Sponges represent challenges as experimental models for symbioses, in terms of cultivation and large water volumes, but with *H. panicea* I believe we have a promising candidate at hand. The comparative

simplicity of the microbiome is a unique access point to manipulate specifically the interaction between the host and the dominant symbiont and study the effect on host performance. A key question is why and how the dominant symbiont reaches higher abundances than closely related bacteria and which advantage it provides to its host.

REFERENCES

- Althoff, K., C. Schütt, R. Steffen, R. Batel, and W. E. G. Müller. 1998. Evidence for a symbiosis between bacteria of the genus *Rhodobacter* and the marine sponge *Halichondria panicea*: harbor also for putatively toxic bacteria? *Mar. Biol.* 130:529–536.
- Augustin, R., S. Fraune, S. Franzenburg, and T. C. G. Bosch. 2012. Where simplicity meets complexity: *Hydra*, a model for host – microbe interactions. In *Recent Advances on Model Hosts* (eds. E. Mylonakis et al.). Springer. Pp. 71–81.
- Barthel, D. 1991. Influence of different current regimes on the growth form of *Halichondria panicea* (Pallas). *Foss. Recent sponges* 387–394.
- Bolyen, E., J. R. Rideout, M. R. Dillon, N. A. Bokulich, C. C. Abnet, G. A. Al-Ghalith, et al. 2019. Reproducible, interactive, scalable and extensible microbiome data science using QIIME 2. *Nat. Biotechnol.* 37:852–857.
- Bosch, T. C. G., K. Guillemin, and M. McFall-Ngai. 2019. Evolutionary “experiments” in symbiosis: the study of model animals provides insights into the mechanisms underlying the diversity of host–microbe interactions. *BioEssays* 41:1–8.
- Costa, R. M., A. Cárdenas, C. Loussert-Fonta, G. Toullec, A. Meibom, and C. R. Voolstra. 2021. Surface topography, bacterial carrying capacity, and the prospect of microbiome manipulation in the sea anemone coral model *Aiptasia*. *Front. Microbiol.* 12:1–16.
- Domin, H., Y. H. Zurita-Gutiérrez, M. Scotti, J. Buttler, U. Hentschel Humeida, and S. Fraune. 2018. Predicted bacterial interactions affect *in vivo* microbial colonization dynamics in *Nematostella*. *Front. Microbiol.* 9:1–12.
- Douglas, A. E. 2019. Simple animal models for microbiome research. *Nat. Rev. Microbiol.* 17:764–775.
- Erpenbeck, D., A. L. Knowlton, S. L. Talbot, R. C. Highsmith, and R. W. Van Soest. 2004. A molecular comparison of Alaskan and Northeast Atlantic *Halichondria panicea* (Pallas 1766) (Porifera: Demospongiae) populations. *Boll. Mus. Ist. Univ. Genova* 61:319–325.
- Franzenburg, S., S. Fraune, S. Kunzel, J. F. Baines, T. Domazet-Lošo, and T. C. G. Bosch. 2012. MyD88-deficient *Hydra* reveal an ancient function of TLR signaling in sensing bacterial colonizers. *Proc. Natl. Acad. Sci.* 109:19374–19379.
- Gauthier, M. A., J. R. Watson, and S. M. Degnan. 2016. Draft genomes shed light on the dual bacterial symbiosis that dominates the microbiome of the coral reef sponge *Amphimedon queenslandica*. *Front. Mar. Sci.* 3:1–18.
- Gauthier, M., and B. M. Degnan. 2008. Partitioning of genetically distinct cell populations in chimeric juveniles of the sponge *Amphimedon queenslandica*. *Dev. Comp. Immunol.* 32:1270–1280.
- Gloeckner, V., M. Wehrl, L. Moitinho-silva, P. Schupp, J. R. Pawlik, N. L. Lindquist, et al. 2014. The HMA-LMA dichotomy revisited : an electron microscopical survey of 56 sponge species. *Biol. Bull.* 227:78–88.
- Hall, C., S. Camilli, H. Dwaah, B. Kornegay, C. Lacy, M. S. Hill, and A. L. Hill. 2021. Freshwater sponge hosts and their green algae symbionts: a tractable model to understand intracellular symbiosis. *PeerJ* 9:1–28.
- Kenny, N. J., W. R. Francis, R. E. Rivera-Vicéns, K. Juravel, A. de Mendoza, C. Díez-Vives, et al. 2020. Tracing animal genomic evolution with the chromosomal-level assembly of the freshwater

- sponge *Ephydatia muelleri*. Nat. Commun. 11:1–11.
- Knobloch, S., R. Jóhannsson, and V. Marteinson. 2019a. Bacterial diversity in the marine sponge *Halichondria panicea* from Icelandic waters and host-specificity of its dominant symbiont “*Candidatus Halichondriabacter symbioticus*”. FEMS Microbiol. Ecol. 95:1–13.
- Knobloch, S., R. Jóhannsson, and V. Marteinson. 2019b. Co-cultivation of the marine sponge *Halichondria panicea* and its associated microorganisms. Sci. Rep. 9:1–11.
- Knobloch, S., R. Jóhannsson, and V. Marteinson. 2019c. Genome analysis of sponge symbiont “*Candidatus Halichondriabacter symbioticus*” shows genomic adaptation to a host-dependent lifestyle. Environ. Microbiol. 1462-2920.14869.
- Kolodny, O., B. J. Callahan, and A. E. Douglas. 2020. The role of the microbiome in host evolution. Philos. Trans. R. Soc. Lond. B. Biol. Sci. 375:20190588.
- Kumala, L., H. U. Riisgard, and D. E. Canfield. 2017. Osculum dynamics and filtration activity in small single-osculum explants of the demosponge *Halichondria panicea*. Mar. Ecol. Prog. Ser. 572:117–128.
- Leys, S., L. Grombacher, and A. Hill. 2019. Hatching and freezing gemmules from the freshwater sponge *Ephydatia muelleri* v1 (protocols.io.863hzgn). Protocols.io 1:2–7.
- Leys, S. P., C. Larroux, M. Gauthier, M. Adamska, B. Fahey, G. S. Richards, S. M. Degnan, and B. M. Degnan. 2008. Isolation of *Amphimedon* developmental material. Cold Spring Harb. Protoc. 3:1–5.
- Li, C. W., J. Y. Chen, and T. E. Hua. 1998. Precambrian sponges with cellular structures. Science 279:879–882.
- Marques, A., F. Ollevier, W. Verstraete, P. Sorgeloos, and P. Bossier. 2006. Gnotobiotically grown aquatic animals: opportunities to investigate host-microbe interactions. J. Appl. Microbiol. 100:903–918.
- Mills, D. B., L. M. Ward, C. Jones, B. Sweeten, M. Forth, and A. H. Treusch. 2014. Oxygen requirements of the earliest animals. Proc. Natl. Acad. Sci. 111:4168–4172.
- Mohamed, N. M., V. Rao, M. T. Hamann, M. Kelly, and R. T. Hill. 2008. Monitoring bacterial diversity of the marine sponge *Ircinia strobilina* upon transfer into aquaculture. Appl. Environ. Microbiol. 74:4133–4143.
- Naim, M. A., J. A. Morillo, S. J. Sørensen, A. A. S. Waleed, H. Smidt, and D. Sipkema. 2014. Host-specific microbial communities in three sympatric North Sea sponges. FEMS Microbiol. Ecol. 90:390–403.
- Osinga, R., J. Tramper, and R. H. Wijffels. 1999. Cultivation of marine sponges. Mar. Biotechnol. 1:509–532.
- Pita, L., S. Fraune, and U. Hentschel. 2016. Emerging sponge models of animal-microbe symbioses. Front. Microbiol. 7:1–8.
- Quast, C., E. Pruesse, P. Yilmaz, J. Gerken, T. Schweer, P. Yarza, J. Peplies, and F. O. Glöckner. 2013. The SILVA ribosomal RNA gene database project: Improved data processing and web-based tools. Nucleic Acids Res. 41:590–596.
- Riisgård, H. U., L. Kumala, and K. Charitonidou. 2016. Using the F/R-ratio for an evaluation of the ability of the demosponge *Halichondria panicea* to nourish solely on phytoplankton versus free-living bacteria in the sea. Mar. Biol. Res. 12:907–916.
- Schmittmann, L., U. Hentschel. 2021. Antibiotic treatment of the sponge *Halichondria panicea* and subsequent recolonization. dx.doi.org/10.17504/protocols.io.by7hpzj6
- Schmittmann, L., L. Pita. 2021. DNA/RNA extraction and qPCR protocol to assess bacterial abundance in the sponge *Halichondria panicea*. dx.doi.org/10.17504/protocols.io.bxwwppfe
- Schmittmann, L., L. Pita, and S. Franzenburg. 2021. Individuality in the immune repertoire and induced response of the sponge *Halichondria panicea*. Front. Immunol. 12:1–13.
- Srivastava, M., O. Simakov, J. Chapman, B. Fahey, M. E. A. Gauthier, T. Mitros, et al. 2010. The *Amphimedon queenslandica* genome and the evolution of animal complexity. Nature 466:720–726.
- Strehlow, B. W., A. Schuster, W. R. Francis, and D. E. Canfield. 2021. Metagenomic data for

- Halichondria panicea* from Illumina and Nanopore sequencing and preliminary genome assemblies for the sponge and two microbial symbionts. bioRxiv 1–8.
- Thomas, T., L. Moitinho-Silva, M. Lurgi, J. R. Björk, C. Easson, C. Astudillo-García, et al. 2016. Diversity, structure and convergent evolution of the global sponge microbiome. *Nat. Commun.* 7:11870.
- Vad, J., F. Dunnett, F. Liu, C. C. Montagner, J. M. Roberts, and T. B. Henry. 2020. Soaking up the oil: biological impacts of dispersants and crude oil on the sponge *Halichondria panicea*. *Chemosphere* 257:127109.
- Webster, N. S., R. E. Cobb, R. Soo, S. L. Anthony, C. N. Battershill, S. Whalan, and E. Evans-Illidge. 2011. Bacterial community dynamics in the marine sponge *Rhopaloeides odorabile* under *in situ* and *ex situ* cultivation. *Mar. Biotechnol.* 13:296–304.
- Weiland-Bräuer, N., S. C. Neulinger, N. Pinnow, S. Künzel, J. F. Baines, and R. A. Schmitz. 2015. Composition of bacterial communities associated with *Aurelia aurita* changes with compartment, life stage, and population. *Appl. Environ. Microbiol.* 81:6038–6052.
- Wichels, A., S. Würtz, H. Döpke, C. Schütt, and G. Gerds. 2006. Bacterial diversity in the breadcrumb sponge *Halichondria panicea* (Pallas). *FEMS Microbiol. Ecol.* 56:102–118.
- Zhang, F., M. Berg, K. Dierking, M. A. Félix, M. Shapira, B. S. Samuel, and H. Schulenburg. 2017. *Caenorhabditis elegans* as a model for microbiome research. *Front. Microbiol.* 8:1–10

CHAPTER 4

STABILITY OF A DOMINANT SPONGE-SYMBIONT IN SPITE OF ANTIBIOTIC-INDUCED MICROBIOME DISTURBANCE

Chapter submitted to *Environmental Microbiology*: **Schmittmann L.**, Busch K., Rahn T., Pita L., Hentschel U. Sponge symbiont stability in spite of antibiotic-induced microbiome disturbance.

STABILITY OF A DOMINANT SPONGE-SYMBIONT IN SPITE OF ANTIBIOTIC-INDUCED MICROBIOME DISTURBANCE

Schmittmann L.^{1*}, Rahn T.¹, Busch K.¹, Pita L.^{1,2}, Hentschel U.^{1,3*}

¹Research Unit Marine Symbioses, GEOMAR Helmholtz Centre for Ocean Research, Kiel, Germany,

²Institut de Ciències del Mar – CSIC, Barcelona, Spain, ³Christian-Albrechts-Universität Kiel, Germany,

*correspondence authors

ABSTRACT

Marine sponges are known for complex and stable microbiomes. However, aspects of microbiome assembly and colonization remain understudied due to the difficulty to manipulate sponge holobionts in the laboratory. We aimed to understand compositional and structural changes in the sponge microbiome after disturbance by antibiotics and asked whether the microbiome can be rescued via recolonization with the natural microbiome. We have used the widely distributed sponge *Halichondria panicea* as an emerging experimental model for host-microbe interactions. Marine gnotobiotic facilities were set up with a closed, sterile flow-through aquarium system. Bacterial abundance dynamics were monitored qualitatively and quantitatively over time by 16S rRNA amplicon sequencing and qPCR, respectively. Antibiotics induced dysbiosis by favoring the growth of opportunistic, antibiotic-resistant bacteria. The dominant symbiont, *Ca. H. symbioticus*, remained overall unchanged, reflecting its obligately symbiotic nature. Recolonization with the natural microbiome could not rescue the microbiome from dysbiosis, however single bacterial taxa were transferred and successfully re-colonized the host sponge. By experimentally manipulating microbiome composition, we could show the stability of a sponge-symbiont clade despite microbiome dysbiosis. Our findings suggest that the fate of *Ca. H. symbioticus* is tightly linked to

Keywords: Breadcrumb sponge, *Halichondria panicea*, metaorganism/holobiont, host-microbe interaction, early-diverging metazoa, emerging model-system

INTRODUCTION

Microbiome homeostasis and stable species interactions among and across kingdoms are a key requirement for animal health (Manor *et al.*, 2020; Peixoto *et al.*, 2021). From an ecological perspective, animals and their associated microbes are considered ecosystems and ecological concepts on species interactions and dynamics apply (Costello *et al.*, 2012; Fierer *et al.*, 2012). Accordingly, in health, animal microbiomes are in a dynamic equilibrium and resistant to disturbance within a certain range. Beyond that threshold, disturbances, for example warming in the marine environment (Fan *et al.*, 2013) or antibiotics in the human gut (Strati *et al.*, 2021), can result in dysbiosis, which is defined as divergence from healthy microbiome. In a dysbiotic state, species interactions are altered, and the function of the healthy symbiosis is lost, which often translates to disease (Cho and Blaser, 2012). In some cases, the microbiome is resilient and the state of dysbiosis is reversible, while in other cases the dysbiosis becomes a new stable state of the microbiome (Sarker *et al.*, 2017). Species interactions (host-microbe and microbe-microbe) are crucial during both, microbiome homeostasis and disturbance, and may determine how dysbiosis can be prevented or reversed.

Model systems offer experimental routes to simplify processes and approaching questions that are too complex in the environmental context of the organism. Especially gnotobiotic (i.e., germ-free or reduced, defined microbiome) or aposymbiotic (i.e., without a certain symbiont) model systems are crucial to decipher the contribution of specific members of the microbiome. For example, mice gnotobiotic models have long been used in human medicine to understand the role of the microbiome in gastric disease (Rooks *et al.*, 2014), or the side effects of antibiotics (Ng *et al.*, 2013; Lange *et al.*, 2016). Experimental models also allow to test the effectiveness of microbiome-based treatments, such as fecal transplants to treat gastric diseases (Ianiro *et al.*, 2020) and to restore dysbiosis after antibiotic treatment (Le Bastard *et al.*, 2018). Traditional symbioses model systems (Douglas, 2019), such as mice, *C. elegans*, *Hydra*, or *Drosophila melanogaster*, offer established protocols, ease of manipulation and cost-efficiency, but lack ecological relevance. Several emerging models can increase our understanding across animal evolution or in an environmental context (Bosch *et al.*, 2019). Life and much later multicellularity evolved in the ocean, and aquatic ecosystems harbor diverse symbioses across all animal phyla. One of the most advanced marine symbioses models is the *Vibrio*-squid system that is prominent for its simplicity of few interacting players and the possibility for investigating symbiotic colonization in the naturally symbiont-free juveniles (Nyholm and McFall-Ngai, 2021; Visick *et al.*, 2021). Beyond that, few aquatic model systems of evolutionarily early metazoans for symbioses are the Cnidarians *Hydra vulgaris* (Augustin *et al.*, 2012), *Nematostella vectensis*

(Mortzfeld *et al.*, 2016), and *Aiptasia sp.* for the *Symbodinium*-Cnidarian interactions (Bucher *et al.*, 2016; Costa *et al.*, 2021).

The phylum Porifera (sponges) dates back to the Precambrian (Li *et al.*, 1998) and sponge models would allow to study symbioses at the base of animal evolution (Pita *et al.*, 2016). Shallow water sponges harbor one of the most complex microbiomes in the marine environment, with dozens of bacterial phyla, translating to thousands of bacterial clades (Thomas *et al.*, 2016), a diversity much exceeding the one in the human gut (King *et al.*, 2019). Sponge microbiome composition is first and foremost determined by sponge host species (Easson and Thacker, 2014; Thomas *et al.*, 2016; Steinert *et al.*, 2017) and is thought to be comparatively resilient to environmental conditions (Bell *et al.*, 2018; Campana *et al.*, 2021). However, cases of dysbiosis in sponges have been reported during disease (Blanquer *et al.*, 2016; Luter *et al.*, 2017), and also in the context of climate change (Fan *et al.*, 2013; Posadas *et al.*, 2021), that correlate with altered/decreased physiological performance of the sponge host.

An experimental sponge model system would facilitate our understanding of host-microbe interactions, microbiome stability, microbe-microbe interactions and colonization dynamics (Pita *et al.*, 2016). A promising candidate is the widely distributed shallow water sponge *Halichondria panicea*. *H. panicea* is a low microbial abundance sponge (Gloeckner *et al.*, 2014) with a unique monodominance of a single bacterial species (25 - 80 % relative abundance in 16S rRNA amplicon data), recently described as *Candidatus Halichondribacter symbioticus* (Knobloch *et al.*, 2019a). This alphaproteobacterium has key genomic features of a sponge-symbiont, e.g., its role in ammonia assimilation, vitamin B12 synthesis and antimicrobial peptide production (Knobloch *et al.*, 2019b). The sponge host has been studied in its natural environment (e.g., (Barthel, 1986, 1988; Lüsckow, Kløve-Mogensen, *et al.*, 2019; Lüsckow, Riisgård, *et al.*, 2019)) including the reproductive cycle (Witte *et al.*, 1994). It is amenable to aquarium maintenance and experimentation with adults, explant cultures and primmorphs (e.g. (Lavrov and Kosevich, 2016; Riisgård *et al.*, 2016; Kumala *et al.*, 2021)) and spawns in captivity. A preliminary host genome assembly is available (Strehlow *et al.*, 2021) and *de novo* transcriptomes have been published in the context of responses to microbial elicitors (Schmittmann *et al.*, 2021) and crude oil (Vad *et al.*, 2020).

We evaluated the use of antibiotics to generate gnotobiotic or aposymbiotic (i.e., *Ca. H. symbioticus*-lacking) sponges in newly built, germ-free facilities for marine organisms at the Kiel Marine Organism Culture Centre (KIMOCC). We aimed to understand compositional and structural changes in the sponge microbiome after disturbance by antibiotics and assessed bacterial communities both

quantitatively (qPCR) and qualitatively (16S rRNA amplicon sequencing) over time. We further asked whether the microbiome can be rescued via recolonization with the natural sponge microbiome.

METHODS

EXPERIMENTAL OVERVIEW

Three experiments were performed: first, the ‘antibiotic test experiment’ was run to test an antibiotic cocktail for its efficacy to reduce the *H. panicea* microbiome. Second, the ‘recolonization by incubation experiment’ was performed to study bacterial community dynamics after antibiotic treatment and recolonization where the natural sponge microbiome was administered to the incubation water (see appendix 4.1 and 4.2 for methods and results). Third, in the ‘recolonization by injection experiment’ recolonization was performed where the natural microbiome was injected directly to the sponge tissue with a syringe. In the main manuscript, we focus on the recolonization by injection experiment due to higher sampling resolution and replication. More details on the materials and methods are deposited on the online platform protocols.io (Schmittmann and Hentschel 2021 or appendix 3.8).

SPONGE COLLECTION

Halichondria panicea individuals were collected by snorkeling from Kiel, Germany (54.424705 N, 10.175133 E) in late October 2018 (antibiotic exposure experiment), and in June 2020 (recolonization by injection experiment). Sponges were individually transported in 500 ml bottles and brought to Baltic flow-through tanks at the institute within 2 hours after collection for a 1-week acclimation period prior to experiments.

EXPERIMENTAL CONDITIONS

The set-up consisted of 500 ml glass flow-through beakers, that were individually connected to aquarium pumps (GHL Doser2) for water exchange (twice the volume per day, 10 ml every ~15 min) with sterile filtered (0.22 µm) artificial seawater. Artificial seawater (TropicMarine) was sterile filtered with a 0.22 µm membrane (Sartorius SM 162 75, 142 mm) into autoclaved 20 l carboys (Nalgene) and regularly plated on MB agar to test sterility. Autoclaved *Nannochloropsis salina* algae were added at a concentration of ~10⁵ cells/ml as a food source (Algova, solution from freeze dried powder). For the antibiotic treatment, an antibiotic cocktail was added to the source water from T0 to T4 of the experiment: rifampicin (50 mg/L in DMSO), Nalidixic acid (50 mg/ml in 0.3 M NaOH), ampicillin (50

mg/ml in water), neomycin (50 mg/ml in water), polymyxin B (2 mg/ml in water). From day T4 on, the antibiotic treatment was stopped, and the residual antibiotics were washed out within one day (the estimated concentration was monitored by pigmentation of rifampicin). Fresh artificial seawater was prepared every day during the antibiotic treatment and every alternating day afterwards. Experiments were performed with stable temperatures and salinities according to the environmental conditions at the time of the respective experiment (appendix 4.1). In order to control the efficacy of the antibiotic treatment, colony forming units were counted from the seawater. Water from four replicates per treatment was sampled several times throughout the recolonization experiments via a sterile serological 10 ml pipet permanently inserted in the culture units. Dilutions were prepared 1:1000 in sterile 1.5 % NaCl, and 100 μ L plated onto MarineBroth (Difco2216) agar plates in triplicates. After incubation at 28°C for 7 days, colony forming units were counted.

GNOTOBIOTIC EXPERIMENTAL FACILITIES

Experiments were performed in marine gnotobiotic chambers that are inspired by gnotobiotic mouse facilities. Briefly, they consist of a restricted transitioning area, a preparation climate chamber, and an experimental climate chamber permanently equipped with an air filtration system (CP Type 500 NATURE SYSTEM, Expansion Electronic SRL, Italy) that successfully removes microbes from the air. Further, surfaces were sterilized daily (Curacid Medical wipes, PICO-Medical, Germany), and all materials were either sterile packed, autoclaved or sterilized with ethanol. An experimental aquarium set-up was custom made that enables a sterile flow-through of water and automatic water exchange. For details please see additional information published on the online platform protocols.io (Schmittmann and Hentschel 2021).

ANTIBIOTIC EXPOSURE EXPERIMENT

For the antibiotic exposure experiment, four sponge individuals were each cut into three clones with a sterile scalpel (each about 2x2x2 cm). One clone per individual was immediately preserved in RNAlater (incubated overnight at 4°C and stored at -80°C) and serves as the start sample T0 (n=4). The other two clones per individual were placed in separate glass beakers and either treated with an antibiotic cocktail from T0 to T4 or served as a control. After a recovery phase of 7 days, tissues were preserved in RNAlater (T11, n=4).

RECOLONIZATION EXPERIMENT

Sixteen sponge individuals were each cut in three clones with a sterile scalpel (each about 4x4x4 cm). One clone per individual was immediately preserved in RNAlater and serves as the start sample T0 (n=16). The other two clones per individual were each placed in separate glass beakers and all were treated with the antibiotic cocktail described above. DNA extraction and qPCR were performed on the sampling day allowing a real-time tracking of bacterial and *Ca. H. symbioticus* abundances. Therefore, after the antibiotic treatment, daily biopsy samples were taken from 6 random tanks by cutting a small tissue piece (~5x5x5 mm) with sterile scissors while the individual remained within the experiment. On day T12 and T13, half of the sponges were recolonized three times within 36 h. For each recolonization, 2 ml freshly prepared *H. panicea* symbiont inoculum was injected with a sterile syringe (0.6 mm diameter, 80 mm length). The bacterial inoculum was prepared by differential centrifugation from several fresh and healthy sponges kept in a Baltic flow-through system with a modified protocol after (Wehrl *et al.*, 2007) (for further details see appendix 4.1). The volume of the sponge tissue used to prepare the inoculum was equivalent to the volume of the sponges to be recolonized (estimated by size). For DNA extraction, the inoculum was pelleted and flash frozen, and filtered 2 ml filtered on a 0.22 µm filter (PVDF 25 mm Merck Millipore, USA) and flash frozen. After recolonization, biopsy samples of sponges were taken daily (n=3), and a larger sampling size 2 days and 6 days after recolonization (n=8).

DNA/RNA EXTRACTION

DNA was extracted from ~25 mg sponge tissue or half of the water filters with the DNeasy PowerSoil Kit (Qiagen, Netherlands). The pelleted inoculum was extracted with the Blood+Tissue Kit (Qiagen, Netherlands) following the manufacturers protocol with proteinase K incubation for 30 min. The DNA was eluted in 50 µl elution buffer. Total RNA from 70-80 mg sponge tissue was extracted with the RNeasy Mini Kit (Qiagen, Netherlands) and RNA eluted in 60 µl. Degradation of RNA was inhibited (1 U/µl SUPERase-IN, Thermo Fisher Scientific, USA) and genomic DNA was removed after extraction (DNA-free DNA removal Kit, Thermo Fisher Scientific, USA). DNA and RNA were quantified in Qubit (DNA and RNA BS and HS Kits, Thermo Fisher Scientific, USA) and their quality checked (NanoDrop, Thermo Fisher Scientific, USA, some RNA samples additionally with Experion, Bio-Rad, USA). For additional information on DNA and RNA extractions, as well as qPCR (next section), refer to the information published on the online platform protocols.io (Schmittmann and Pita 2021 or appendix 3.9).

QUANTITATIVE PCR (QPCR)

Overall eubacterial abundance as well as *Ca. H. symbioticus* abundance was estimated by qPCR based on the 16S rRNA gene (appendix 4.1). Analysis was run on both gDNA and cDNA (RNA transcribed with iScript cDNA synthesis kit, Bio-Rad). For quantification of gene copy numbers, dilutions of purified PCR products in tRNA solution (10 ng/μl Sigma Aldrich, Germany) were used as standards. The concentration of the highest standard of each dilution series was measured with Qubit (DNA and RNA HS Kits, Thermo Fisher Scientific, USA) and copy numbers calculated based on concentration and fragment length. Quantitative PCRs were performed in a CFX96 real-time detection system (Bio-Rad, Germany) with the Maxima SYBR Green 2x Master Mix (Thermo Fisher Scientific, USA) (appendix 4.1). Standards were run in duplicates and samples in triplicates. Efficiencies and copy numbers were calculated with the Bio-Rad CFX Manager Software (version 3.1) and data analysis was performed in R (version 3.5.1). Generalized linear models or linear mixed effect models were applied according to the tested data set.

AMPLICON SEQUENCING

The V3-V4 variable regions of the 16S rRNA gene were amplified in a one-step PCR using the primer pair 341F-806R (dual-barcoding approach (Kozich *et al.*, 2013); primer sequences: 5'-CCTACGGGAGGCAGCAG-3' & 5'-GGACTACHVGGGTWTCTAAT-3'). After verification of the presence of PCR-products by gel electrophoresis, normalisation (SequalPrep Normalisation Plate Kit; ThermoFisher Scientific, Waltham, USA) and equimolar pooling was performed. Sequencing was conducted on the MiSeq platform (MiSeqFGx; Illumina, San Diego, USA) with v3 chemistry. The settings for demultiplexing were 0 mismatches in the barcode sequences.

AMPLICON BIOINFORMATIC AND STATISTICAL ANALYSES

For computation of microbial core-diversity metrics, sequences were processed within the QIIME2 environment (version 2018.11, (Bolyen *et al.*, 2019)). Amplicon Sequence Variants (ASVs) were generated from forward reads (truncated to 270nt) with the DADA2 algorithm (Callahan *et al.*, 2016). Phylogenetic trees were calculated based on resulting ASVs with the FastTree2 plugin. Representative ASVs were classified using the Silva 132 99 % OTUs 16S database (Quast *et al.*, 2013) with the help of a primer-specific trained Naive Bayes taxonomic classifier. Mitochondrial and chloroplast reads were removed. The data were rarefied to a sampling depth of 3300 reads per sample (appendix 4.4, 4.5, 4.10). Alpha and beta diversity indices (e.g., Faith's Phylogenetic Diversity and weighted UniFrac

distances, respectively) were calculated within QIIME2. To evaluate sample separation in ordination space, non-metric multidimensional scaling (NMDS) was performed on weighted UniFrac distances. Alpha diversity was analyzed in R (version 3.5.1) with generalized linear or linear mixed models depending on the dataset. Beta diversity (weighted unifracs) were tested for dissimilarity by PERMANOVA with 999 permutations and for homogeneity by PERMDISP within QIIME2 (version 2018.11). The dataset was analyzed as a whole (T0-T19), as well as a subset only including control and recolonized sponge samples after recolonization (T14-T19).

To assess the effect of recolonization on microbiome community composition, significantly different abundance of ASVs between recolonized and control sponges was assessed for the end of the experiment at T19 (LEfSe in Galaxy version 1.0) (Segata *et al.*, 2011). With an UpSetR analysis “persister” ASVs (present throughout the whole experiment), and potential “recolonizer” ASVs (present in inoculum and recolonized sponges only) were identified (UpSetR version 1.4.0) (Conway *et al.*, 2017). The ASV sequences were compared to the GenBank standard database (with BLASTN, August 2021). If there were several closest hits with the same similarity, the results were screened for host-association and the closest host-associated hit was reported.

BACTERIAL CO-OCCURRENCE NETWORKS

Bacterial co-occurrence networks were calculated based on relative abundances with the SparCC methodology (Friedman and Alm, 2012) in SCNIC (version 2020.10) (Shaffer *et al.*, 2020) within QIIME2 (version 2020.8). Significant interactions were defined as $-0.5 < R < 0.5$. Networks were calculated from data subsets to represent different states of the *H. panicea* microbiome: i) *healthy* from the wildtype start samples T0, and ii) *recolonized* from the recolonized sponges T14-T19, compared to *control* from the non-recolonized control sponges.

DATA VIZUALIZATION

Plots were generated in R (version 3.5.1 and 4.0.2), but the fluid barplots were prepared in RawGraphs (version 2.0 beta) (Mauri *et al.*, 2017) and the co-occurrence networks were visualized and annotated in Cytoscape (version 3.8.2) (Shannon *et al.*, 2003). If necessary, figure layouts were finalized in Inkscape (version 0.92). The schemes for experimental timelines were generated with BioRender.com.

RESULTS

In this study we aimed at modifying the bacterial microbiome of *H. panicea*, targeting specifically the dominant symbiont *Ca. Halichondriabacter symbioticus*. The *Ca. H. symbioticus* amplicon sequence identified in this study (ASV 350235dc06427fbe808d1bb3452afc91) is identical to most published sequences from previous studies (0-1 bp difference from 270 bp), (Althoff *et al.*, 1998; Naim *et al.*, 2014; Knobloch *et al.*, 2019a). We designed specific 16S rRNA gene primers for *Ca. H. symbioticus* to assess absolute abundance via qPCR and used universal eubacterial 16S rRNA primers to quantify total bacterial abundance. The relative proportion of *Ca. H. symbioticus* 16S rRNA gene in the total eubacterial 16S rRNA gene pool estimated by both qPCR and 16S rRNA amplicon sequencing was highly correlated (appendix 4.3, $R^2 = 0.87-0.93$). Further, qPCR results from both gDNA and cDNA (synthesized from RNA) revealed similar trends throughout the experiments (Figure 1 B+C, appendix 4.9), suggesting that the *Ca. H. symbioticus* symbionts and eubacteria were active.

ANTIBIOTIC EXPOSURE EXPERIMENT

Microbiome changes in *H. panicea* were assessed seven days after antibiotic treatment (Figure 1 A). The absolute abundance of the dominant symbiont *Ca. H. symbioticus* increased in the control treatment, respective to T0, while it decreased by 2-3 orders of magnitude after antibiotic treatment, as assessed by qPCR (Figure 1 B). The absolute abundance of eubacteria increased significantly, by 1-2 orders of magnitude, in control and antibiotic treated sponges. Results from cDNA followed similar patterns (Figure 1 C). With respect to the relative abundance (amplicon sequencing), *Ca. H. symbioticus* ASV numbers decreased from 36.2 ± 7.1 % to 1.6 ± 0.7 % (average \pm standard error) after antibiotic exposure while relative numbers remained at an average of 24.1 ± 6.9 % in controls (n=4, Figure 1 D). Other Proteobacteria (including *Alteromonadales* and *Vibrionales*) increased in relative abundance over time (from 26.5 ± 2.3 % to 82.5 ± 1.1 %), regardless the treatment. The composition and beta-diversity of the microbial communities shifted in the control sponges, and even more so, in the antibiotic treated sponges (Figure 1 E, appendix 4.11). The alpha-diversity in terms of evenness (Pilou) and richness (Shannon) did not change throughout the experiment, whereas phylogenetic diversity decreased significantly in control and antibiotic treatment (appendix 4.4).

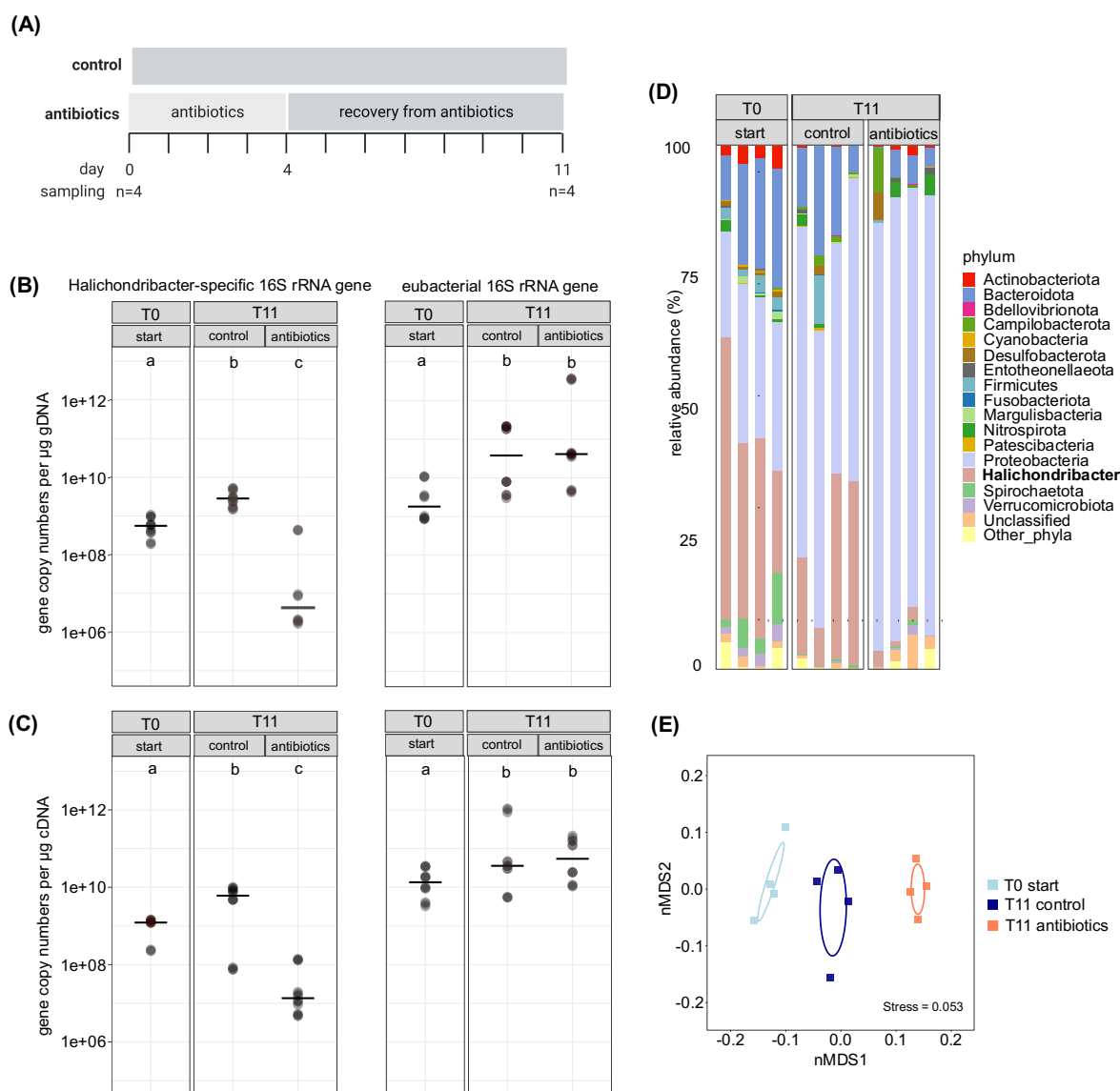


FIGURE 1 A-E | Antibiotic exposure experiment: absolute and relative bacterial abundance after antibiotic treatment. **(A)** Timeline of antibiotic exposure experiment. Sponges were either treated with antibiotics for four days or left untreated as a control. Samples were taken prior to the experiment at T0, and after a recovery phase at T11. $n=4$. **(B+C)** Absolute bacterial abundance estimated by RT-qPCR. 16S rRNA gene copy numbers per μg genomic DNA **(B)** and per μg cDNA **(C)** at the start (T0) and after the recovery phase (T11). Left: gene copy numbers for *Ca. Halichondribacter*-specific 16S rRNA gene, right: gene copy numbers for total bacterial 16S rRNA gene. Values with different letters are significantly different ($p > 0.05$), and black lines represent median. **(D)** Relative microbial community composition on phylum level (top 15 phyla) across timepoints and treatments. Proteobacteria are resolved in the Alphaproteobacterium *Ca. Halichondribacter symbioticus* and other Proteobacteria. **(E)** Non-metric multidimensional scaling plot on weighted UniFrac distances. Color indicates the treatment and timepoint.

RECOLONIZATION EXPERIMENT

Based on the results from the antibiotic exposure experiment, we performed two follow-up experiments to test whether *Ca. H. symbioticus* numbers could be recovered after antibiotic treatment by recolonization with the natural sponge microbiome. The two experiments differed in the mode of recolonization. In the first experiment, the symbiont inoculum was added to the incubation water while in the second, the symbiont was injected into the sponge tissue. We will focus on the injection experiment here (Figure 2 A), since the mode of recolonization did not affect the main outcome of the experiments (see appendix 4.9 for details on the recolonization by incubation experiment), and the temporal resolution and replication is much higher for the recolonization by injection experiment.

When looking at absolute bacteria numbers over time (qPCR), the absolute abundance of *Ca. H. symbioticus* was lower and more variable across individuals than at T0 (Figure 2 B). The abundance of *Ca. H. symbioticus* significantly decreased between T10 and T14; but, it dropped, at maximum, by one-two orders of magnitude, which is less than the change by two-three orders of magnitude observed in the antibiotic exposure experiment (Figure 1 B). From T14 onwards, *Ca. H. symbioticus* absolute numbers recovered to T0 levels, regardless of whether the sponges were recolonized or not (Figure 1 B). In contrast, the total bacterial abundance increased during the experiment by three orders of magnitude. In particular, bacterial *16S* rRNA gene copy numbers steeply rose in the time frame from T07 to T15, after which a new, stable carrying capacity was reached, independently of whether the sponges were recolonized or not.

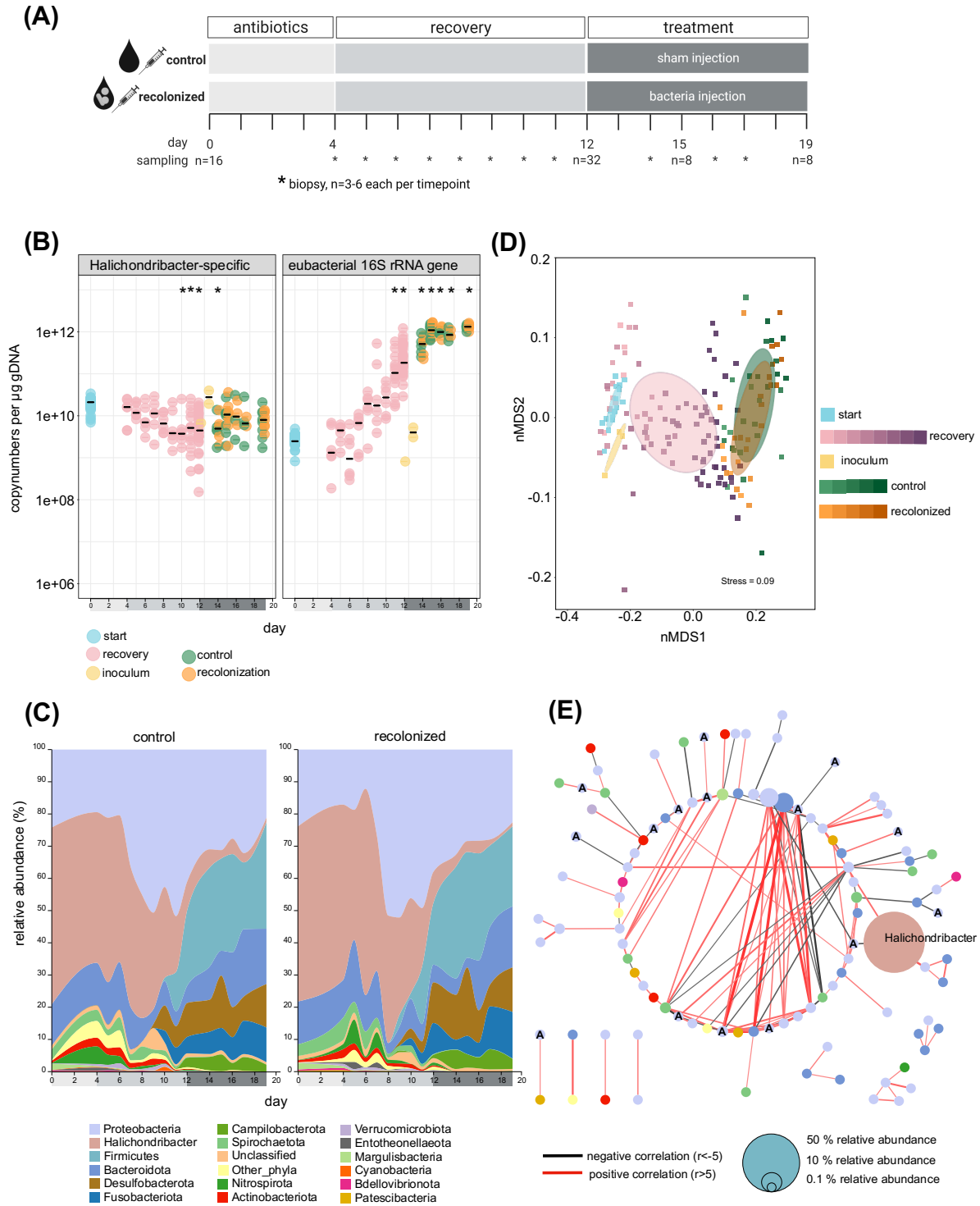


FIGURE 2 A-E | Recolonization experiment: absolute and relative bacterial abundance before and after recolonization by injecting the natural microbiome of *H. panicea* to antibiotic treated sponges. **(A)** Timeline of recolonization by injection experiment. All sponges were treated with antibiotics for four days and recovered in sterile filtered artificial seawater for 7 days. Then, sponges were either injected three times with a bacterial inoculum, or with a sham control. Samples were taken prior to the experiment at T0 (n=16), after a recovery phase at T12 (n=32), from the bacterial inoculum, and 2 and 6 days after recolonization (n=8). In between major samplings, daily biopsy samples were taken (n=3-6). **(B)** Absolute bacterial abundance estimated by RT-qPCR. 16S rRNA gene copy numbers per µg

genomic DNA throughout the experiment. Results for total 16S rRNA genes (left) and *Ca. Halichondribacter*-specific 16S rRNA genes (right). Different treatment groups are indicated by color. Black lines represent median per day. Significant differences between the start (T0) and the respective days are indicated by asterisks above the days (ANOVA or Schreier-Ray-Hare test). Recolonization had no effect on copy numbers, while the sponge individual did affect *Halichondribacter*-specific copy numbers ($p = 0.00017$) (appendix 4.17). **(C)** Relative bacterial community composition shown on phylum level (top 15 phyla) across time and separated by treatment. Proteobacteria are resolved in the Alphaproteobacterium *Ca. Halichondribacter symbioticus* and other Proteobacteria. **(D)** Betadiversity of microbial communities (non-metric multidimensional scaling plot on weighted UniFrac distances). Treatments are represented by color, with increasing color intensity representing progressing time. For results of pairwise PERMANOVA on beta diversity see appendix 4.13. **(E)** Bacterial co-occurrence network for healthy wildtype (T0) sponges. Co-occurrences between ASVs ($-0.5 < R > 0.5$, $p\text{-value} < 0.05$) are displayed by edges (interaction) connecting nodes (ASVs). The color of the edges depicts the direction of the correlation (negative or positive) and thickness the interaction strength. The size of the nodes is proportional to the relative abundance of ASVs and the color represents taxonomic affiliation (as in Figure 2D). ASVs that have the family *Amylibacter* as the closest known relative are labelled "A".

When looking at relative microbial community compositions over time (amplicon sequencing), no differences between recolonized sponges and control sponges were observed (Figure 2 C). Both profiles changed in similar manner throughout the experiment. The relative abundance of *Ca. H. symbioticus* decreased from $54 \pm 1.8\%$ at T0 ($n=16$) to $1.4 \pm 0.4\%$ and $1.2 \pm 0.2\%$ in the control and recolonized treatment ($n=9$), respectively, in the end of the experiment. Certain microbial phyla (mainly Proteobacteria, followed by the phyla Firmicutes, Desulfobacteria, Campilobacteria and Fusobacteria) took over other bacterial phyla that almost disappeared (among them Actinobacteria, Verrucomicrobiota and Cyanobacteria). Overall, the microbial community was dominated by several phyla at the end of both treatments rather than the monodominance of Proteobacteria at T0, which was reflected in higher evenness (appendix 4.5). Both Shannon diversity (richness) and phylogenetic diversity (phylogenetic richness) were more variable after antibiotic treatment than at T0. Shannon diversity increased until the end of the experiment, while phylogenetic diversity decreased over time. The microbial community compositions (beta-diversity) shifted from the start to the recovery phase to the treatment, where control and recolonized samples overlapped (Figure 2 D). Noteworthy, the inocula were most similar to the starting sponge microbiomes, reflecting a high proportion of *Ca. H. symbioticus* in these samples.

Bacterial co-occurrence networks indicate that *Ca. H. symbioticus* is largely independent from the remaining microbiome (3 from total 151 interactions) in healthy sponges (Figure 2 E). About 15 % of all nodes in the bacterial co-occurrence network were annotated as *Amylibacter*, the closest known relative of *Ca. H. symbioticus*. Some of *Amylibacter* ASVs were among the most connected, while others had only one or few interactions. We also compared the differences between treatments on a sponge individual basis (appendix 4.6). This was possible because the same individual was split into

two clones that were subjected to either control or recolonized treatment. Interestingly, even after 19 days of experimentation, the abundance of *Ca. H. symbioticus* was nearly identical between clones, and regardless of treatment. Moreover, the sponge individuals followed different trajectories over time: while symbiont populations remained stable in some individuals, they were either increasing or decreasing in others. Notably, the clones of the same individual followed the same trend, which was independent of the treatment regime.

In addition to cultivation-independent analyses (amplicon sequencing, qPCR), we monitored the culturable microbial fraction (appendix 4.7). First, we checked for bacterial growth in the culture seawater by counting colony forming units (CFU's). Colony growth was absent during the antibiotic treatment, however bacterial numbers increased in the recovery phase until they reached a plateau of $\sim 10^5$ CFUs/ml at T11. There was no difference between control and recolonized treatments. Secondly, we separately tested the five antibiotics of the cocktail for their inhibition of bacterial growth. Isolates obtained from antibiotic-treated sponges had developed more resistances than those isolated from sponges not treated with antibiotics. These antibiotic-resistant isolates were mainly affiliated to Flavobacteria. All isolated strains remained sensitive to rifampicin, one of the five components of the treatment cocktail.

IDENTIFICATION OF PERSISTERS AND RECOLONIZERS

We then inspected the overlap of ASVs that were shared between experimental groups (Figure 3). We defined “persisters” as those ASVs that were present in all experimental groups. Altogether 13 such persister ASVs were identified that were present either in all groups (11 ASVs) or in all groups except inoculum (2 ASVs). Cumulatively, these were also the most abundant ASVs. It is noteworthy that persisters were detected in more sponge individuals at the end compared to the beginning of the experiment. Interestingly, the closest relatives of the persister ASVs were found to be host-associated, and majorly sponge-associated (Table 1). As expected, *Ca. Halichondriabacter symbioticus* (P1) belonged to the persisters and was identified in all analyzed samples. Two additional persisters (P2, P3) were present in more than half of the replicate sponges throughout the entire experiment.

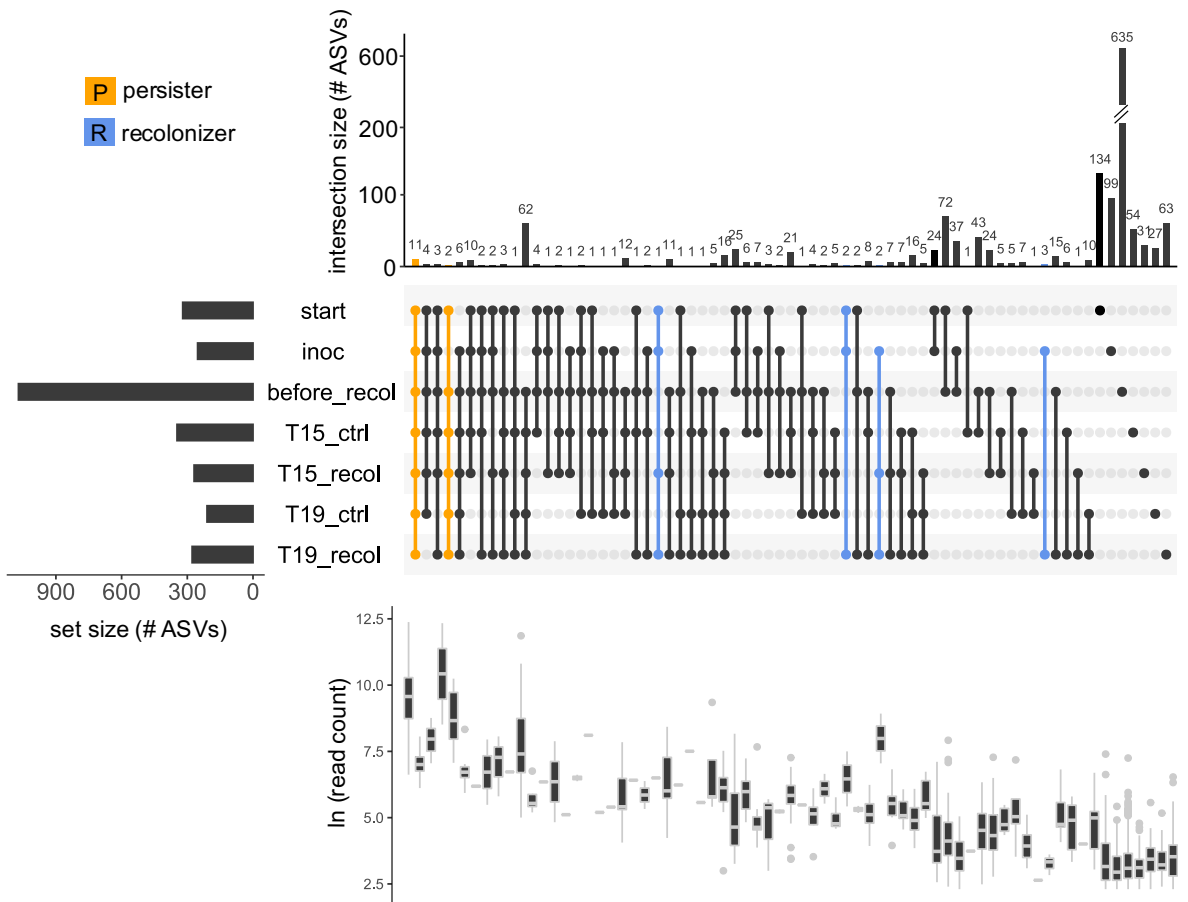


FIGURE 3 | Recolonization experiment: shared ASVs between experimental groups. UpSetR analyses depicts the intersection of ASVs between experimental groups. “Persister” ASVs that remain throughout the experiment are marked in yellow, and potential “recolonizers” transmitted from inoculum to recolonized sponges are marked in blue. The set size (number of ASVs) is shown in horizontal bars, the intersection size is shown in vertical bars above the respective intersection. The boxplot represents the ASV abundance as In-transformed read counts.

We defined the group of “recolonizers” as those ASVs that occurred both in the inoculum and the recolonized sponges, while being absent in the control sponges (Figure 3). Eight such recolonizer ASVs were identified. The corresponding ASVs represented moderate to low proportions in the read counts. Four potential recolonizers were detected in more than half of the replicate sponges (Table 1, appendix 4.8). Recolonizers were affiliated with marine, environmental taxa members of the Bacteroidota, Campilobacteria, and Desulfobacteria.

TABLE 1 | Recolonization experiment: affiliation and presence/absence of persistent ASVs, and potential recolonizers transmitted from inoculum to recolonized sponges. Recolonizer in bold also appeared in *recolonized* bacterial co-occurrence network (Figure 4B). ASVs were compared to GenBank database (BLASTN) and the closest hit was reported.

PERSISTER	taxonomy	presence T0	presence T19 ctrl	presence T19 recol	NCBI	Similarity	Source	ASV
P1	Proteobacteria (Halichondriabacter)	16/16	8/8	8/8	Ca. Halichondriabacter symbioticus MH734183.1	100	Halichondria panicea	350235dc06427fbe8 08d1bb3452afc91
P2	Bacteroidota (Cyclobacteriaceae)	16/16	5/8	6/8	uncultured FJ393780.1	97.4	Stichopus mollis (echinoderm)	cdf31677e0019171c 637774ded46a19d
P3	Proteobacteria (HOC36)	16/16	6/8	7/8	Gammaproteobacterium KT880336.1	94.4	Hymeniacidon heliophila (sponge)	5517e82f0118eaf02c 2c08d15c54fd41
P4	Spirochaetota (Spirochaetaceae)	16/16	3/8	1/8	uncultured Spirochaetales FN424158.1	90	Clathrina clathrus (sponge)	b59335a4fffbb1846d b5cfa20309b5a8
P5	Proteobacteria (Vibrio)	3/16	6/8	5/8	Vibrio sp. MT484171.1	100	Hymeniacidon perlevis (sponge)	5950c0e71fea54a0e a4a20b8a92357b5
P6	Nitrospirota (Nitrospira)	1/16	1/8	1/8	Nitrospira sp. JF802723.1	100	cold-water sponge	1594bb9f6e95a0b91 bf7da9d083e55b3
P7	Bacteroidota (Flavobacterium)	2/16	5/8	6/8	uncultured HQ203853.1	100	seawater	838f2180a057d71e9 6a64cb64296df0b
P8	Proteobacteria (Pseudoalteromonas)	1/16	2/8	4/8	uncultured DQ274152.1	97.4	Dysidea avara (sponge)	cc9c276056e8a3d12 92597378f5128da
P9	Proteobacteria (Shewanella)	4/16	5/8	8/8	Shewanella sp. KT583451.1	100	soft coral	3d56fd9774125a927 d7e3142d542144f
P10	Proteobacteria (Vibrio)	2/16	6/8	5/8	Vibrio sp. MN974025.1	100	seawater	801f55a4831a1d3ba 3eca43803ec88c3
P11	Bacteroidota (Flavobacterium)	1/16	5/8	3/8	Flavobacteriaceae DQ660391.1	99.26	sponge (Korea)	b5f8481ab1741f39cf f72fb2289d7c7a
P12	Firmicutes (Clostridiaceae)	3/16	8/8	8/8	uncultured KP684471.1	99.6	Halichondria panicea;	5b4a1fd9e459b1fe6 de448175250ba66
P13	Proteobacteria (Pseudoalteromonas)	1/16	8/8	8/8	Pseudoalteromonas sp. CP041330.1	100	Sycon capricorn (sponge)	17753a04c358b6597 2ce4531833fcc1
RECOLONIZER	taxonomy	presence T0	presence T19 ctrl	presence T19 recol	NCBI	Similarity	Source	ASV
R1	Bacteroidota (Marinifiliaceae)	0/8	0/8	8/8	Labilibaculum antarcticum LC085518.1	96.3	marine sediment;	fc9547cd146cb7db 87c7405ac268abb
R2	Campilobacterota (Arcobacter)	0/8	0/8	7/8	Arcobacter sp AJ866949.1	99.6	marine sediment	19da1f623abc338a0f cca317ffdb984
R3	Campilobacterota (Pseudoarcobacter)	1/16	0/8	4/8	uncultured bacterium GU451405.1	100	macroalga	c463a879fa5cba0fca 7210e19c696094
R4	Desulfobacteria (Desulfofrigus)	4/16	0/8	5/8	Desulfofrigus AJ630195.1	97.9	marine sediment	7ded0311410334d54 b8dda089ef372db
R5	Gammaproteobacteria (Vibrio)	0/8	0/8	1/8	Vibrio anguillarum MK967051.1	100	Aurelia aurita	14f78e83791c069d4 99bdf618c7b7b73
R6	Bacteroidota	0/8	0/8	1/8	uncultured bacterium AB779896	100	freshwater sediment	6dcc6b264cc78f903 a9c11f80a3010a
R7	Bacteroidota (Flavobacteriales)	0/8	0/8	1/8	uncultured bacterium LC465504.1	100	seagrass	b74009ee162d508ba c3435a12b73b0cd
R8	Gammaproteobacteria (Thiotrichaceae)	16/16	0/8	1/8	Pelagibaculum spongiae MG877746.1	100	Halichondria panicea	76df9929de34e15c0 0f74819ffd363ab

Chapter 4

We investigated if and how recolonizers affected bacteria-bacteria interactions by calculating bacterial co-occurrence networks for control and recolonized sponge microbiomes separately. In the control treatment, 126 ASVs were correlated, and 81 % of the bacteria-bacteria interactions were positive (Figure 4 A). The four potential recolonizers, R1-R4, affected bacteria-bacteria interactions (Figure 4 B). Recolonizers R1 and R2 had several interactions (9 and 10, respectively) with other ASVs and a positive correlation among them. They were negatively correlated to other ASVs, including a highly abundant *Pseudoalteromonas* and *Halodesulfobivrio*. The recolonized network was more complex than the control network with 16 % more nodes and 28 % more interactions, specifically 50 % more negative and 15 % more positive interactions.

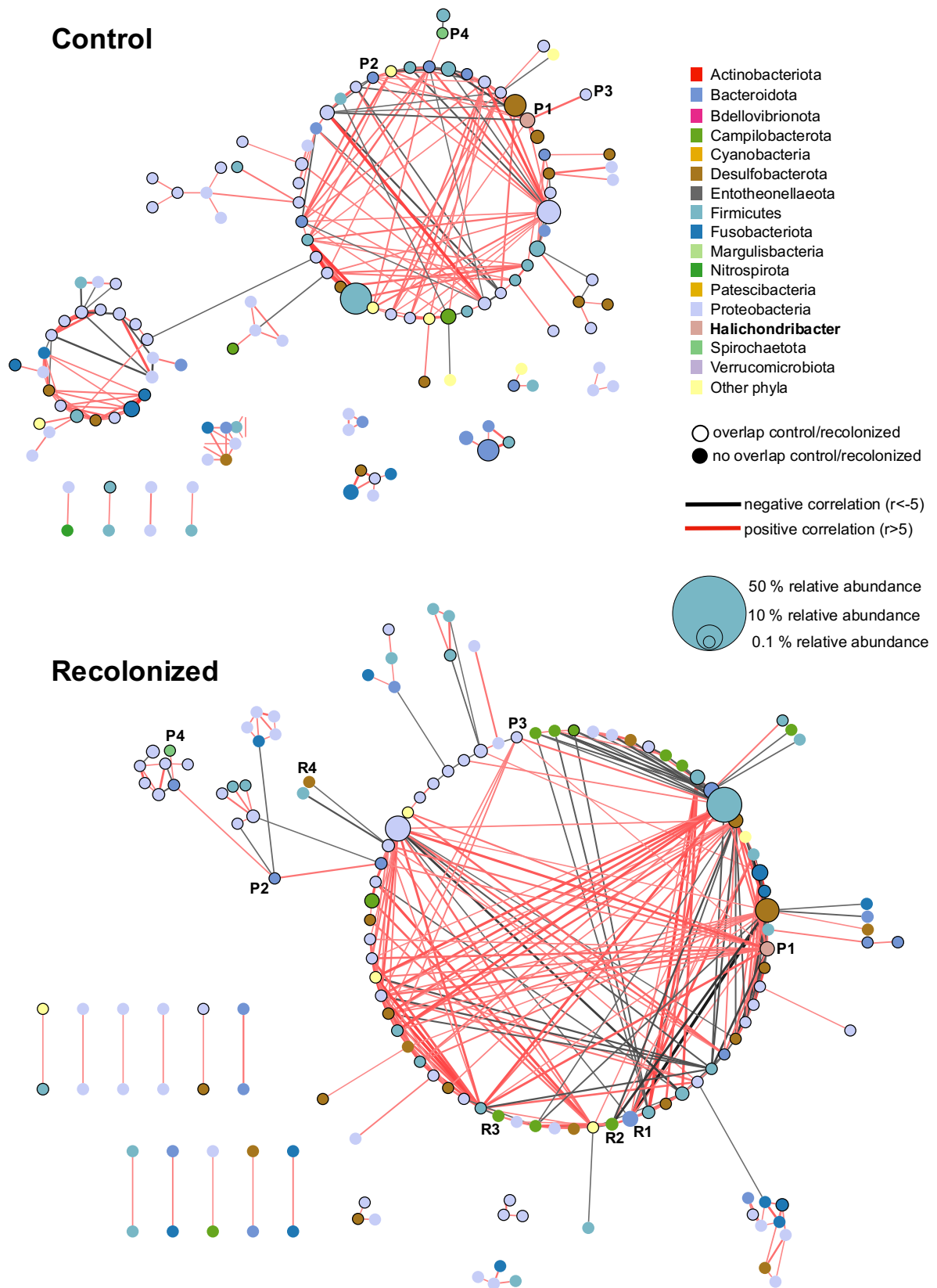


FIGURE 4 A+B | Recolonization experiment: Bacterial co-occurrence networks for **(A)** control (T14-T19) and **(B)** recolonized *H. panicea* microbiomes (T14-T19). Co-occurrences between ASVs ($-0.5 < R < 0.5$, p -value < 0.05) are displayed by edges (interactions) connecting nodes (ASVs). The color of the

edges depicts the direction of the correlation (negative or positive), and the thickness the interaction strength. The size of the nodes is proportional to the relative abundance of ASVs and the color represents taxonomic affiliation. Nodes with a black outline are also present in the respective other treatment network. R1-R4 and P1-P4 indicate recolonizer and persister ASVs as defined in Table 1.

DISCUSSION

In this study, we explored microbial community dynamics in the microbiome of the sponge *Halichondria panicea* after disturbance by antibiotics and evaluated the potential for reversing changes via recolonization. Antibiotics exposure induced a strong dysbiosis that was characterized by higher relative and absolute abundances of opportunistic microbes and concomitantly, a reduced dominance of *Ca. Halichondriabacter symbioticus*. Interestingly, the absolute abundances of *Ca. H. symbioticus* decreased only temporarily after antibiotic treatment and recovered to initial levels regardless of recolonization, implying a high stability and underlining the obligate nature of this sponge symbiont. Other symbionts, most closely related to sponge- and other host-associated bacteria, also persisted in the microbiome in spite of the antibiotic treatment. Overall, dysbiosis resulted in more complex, but less specific bacteria-bacteria interactions than in healthy sponges. Recolonization with the natural microbiome had no effect on overall microbiome composition and diversity, but single bacterial taxa were transferred and successfully colonized the sponge. These recolonizers negatively affected the abundance of opportunistic bacteria, but the effects were not strong enough to recover the microbiome.

EXPOSURE TO ANTIBIOTICS PROMOTES GROWTH OF OPPORTUNISTIC BACTERIA

We were unable to create aposymbiotic sponges, which is consistent with previous studies that have applied antibiotics in sponges so far (Friedrich et al. 2001; De Caralt et al. 2003; Sipkema et al. 2003; Richardson et al. 2012; Gloeckner et al. 2013; Schippers 2013). However, there is one exception where the continuous exposure to ampicillin and gentamycin led to a decreased microbial load in *Haliclona cnidata* (Schellenberg *et al.*, 2020). Contrary to our expectations, antibiotics resulted in an increase in total bacterial abundance in our study (Figure 2). Prolonged antibiotic exposure can favor the growth of resistant bacteria (Callens *et al.*, 2018) as was indeed observed in our study (appendix 4.7) and would explain the increased carrying capacity. Nevertheless, our antibiotic tests showed that all culturable bacteria including those isolated from antibiotic treated sponges remained sensitive to rifampicin throughout the experiment. We thus speculate that the sponge extracellular matrix might

provide a protective barrier for the sponge-associated bacteria similar to mucus in the human gut or biofilms, (Samad *et al.*, 2019; Yan and Bassler, 2019), that prevent antibiotics to reach their bacterial target. Additionally, antibiotics are known to be less effective at high bacterial cell densities (Udekwo *et al.*, 2009), which might further decrease their efficacy inside the sponge tissue. Completely eradicating sponge-associated bacteria by antibiotics continues to be a challenge and alternative methods like i.e., rearing of sterile sponge larvae or eradicating selected sponge symbionts by phage therapy should be explored.

CA. HALICHONDRIABACTER SYMBIOTICUS REMAINS STABLE IN SPITE OF DYSBIOSIS

The increase of antibiotic resistant, opportunistic bacteria correlated with a relative decrease of the dominant symbiont *Ca. H. symbioticus* (Figure 2 C). In terms of absolute numbers however, *Ca. H. symbioticus* numbers remained surprisingly unaffected in most sponge individuals, and overall returned to initial levels regardless of recolonization (Figure 2 B). Together with twelve other bacterial taxa, *Ca. H. symbioticus* comprises what we define as a “core microbiome” that persisted throughout the experiment. Intriguingly, most persisters were related to sponge-associated microbes, providing strong evidence that these are true sponge symbionts (Table 1). In healthy sponges at T0, some persisters appear to be part of the rare biosphere of the sponge and occur at low concentrations. Since they were found in an increasing number of sponge individuals over time, it is conceivable that they grow inside of the sponge, which would however need to be verified by qPCR in future studies. Thus, their abundances are more dynamic and flexible than that of *Ca. H. symbioticus* which could be a reflection of different processes controlling their abundance. When looking at bacterial activity (i.e., qPCR on cDNA), we showed that at least the *Ca. H. symbioticus* clade remained transcriptionally active during dysbiosis. This finding is consistent with Schellenberg *et al.* (2020) who have described that a resilient portion of the sponge microbiome remains metabolically active after antibiotic treatment.

Surprisingly, the absolute abundance of *Ca. H. symbioticus* did not decrease in all sponge individuals. Inter-individual differences were detected by both 16S rRNA amplicon sequencing and qPCR (appendix 4.6). Genotyping sponges would elucidate whether host-genetics correlate to symbiont abundance, similarly as to what has been reported in humans (Tavalire *et al.*, 2021). The low number of bacteria-bacteria interactions with the dominant symbiont in healthy sponge microbiomes let us speculate that *Ca. H. symbioticus* might be mainly host-dependent. One possible explanation could be that the hosts immune system controls symbiont abundance on an individual level. Indeed, *H. panicea* possesses an individual-specific immune repertoire (Schmittmann *et al.*, 2021), that could be involved in controlling

symbiont populations. The symbiosis between *H. panicea* and its dominant symbiont is highly specific and may have evolved over evolutionarily long periods of time.

In terms of taxon level diversity, the *Ca. Halichondriabacter* clade appears to be more diverse than previously appreciated (Knobloch *et al.*, 2019a). Amplicon sequencing revealed a high diversity of ASVs classified as *Amylibacter*, which is the closest known related clade to *Ca. H. symbioticus*. Surprisingly, 15 % of the interacting ASVs in healthy sponge microbiomes were associated to the *Amylibacter* family (Figure 2E). Some of those ASVs were highly similar to the *Ca. H. symbioticus* ASV (up to 99.6%), while others were less similar (>87 %). An in-depth phylogenomic analysis of this extended sponge symbiont taxon would be required to understand the diversity and host-specificity of this conspicuous clade. When looking at full length 16S rRNA gene phylogenies, *Ca. H. symbioticus* is only distantly related to the genus *Amylibacter* (92.5 %, unpublished data), indicating that the sponge symbiont lineage has diversified within its sponge host over evolutionary times. Whether and to what extent the phylogenetic differences translated into functional differences and adaptations remains to be investigated.

DYNAMICS AND CHARACTERISTICS OF DYSBIOSIS

The application of antibiotics induced a strong disturbance of the sponge microbiome. The microbiome composition reached a new configuration consisting of increased bacterial abundance (Figure 2), reduced phylogenetic diversity, and higher evenness (appendix 4.5). Overall, the response on the bacterial community level to antibiotics was consistent between replicate sponges and also between experiments in terms of diversity and compositional changes. Similarly, in complex human gut communities, antibiotic exposure leads to a restructuring of the microbiome driven by antibiotic resistant, opportunistic bacteria (Francino, 2016; Gaulke *et al.*, 2016) and can induce reversible but also long-lasting dysbioses (Lange *et al.*, 2016). Increases in alpha- and beta-diversity and compositional shifts towards opportunistic microbes are similar to environmental induced dysbiosis in other sponges ((Luter *et al.*, 2012; Lesser *et al.*, 2016) and reviewed in (Pita *et al.*, 2018)).

Importantly, the combination of amplicon sequencing and qPCR in our study has been key to interpret the microbial patterns of dysbiosis. Without qPCR data, we would have concluded that *Ca. H. symbioticus* numbers were decreasing after antibiotic treatment. However, qPCR data clearly reveals that numbers of *Ca. H. symbioticus* remain constant whereas the microbiome shifts by an increased number of opportunists. Few studies reported bacterial change in absolute numbers during dysbiosis. As one example, increases in absolute bacterial abundances were linked to disease in corals (Luna *et*

al., 2010; Smith *et al.*, 2015). Most other studies have so far relied on amplicon sequencing as a marker of relative community changes, although relative data alone can mask underlying community dynamics (Rao *et al.*, 2021). Our study again highlights the importance to interpret microbial community shifts in the context of both, relative and absolute bacterial abundances.

Bacteria-bacteria interactions could be one important indicator of sponge microbiome condition and health. Indeed, changes in microbiome diversity and composition during dysbiosis were reflected in bacteria-bacteria co-occurrence networks. In healthy sponges, few ASVs were had several bacteria-bacteria interactions (Figure 2), whereas the connectivity increased after disturbance (Figure 4). Similar patterns were observed in zebra fish microbiomes after exposure to antibiotics (Gaulke *et al.*, 2016). We could clearly identify the loss of bacterial players (e.g., highly connected *Spirochaeta*) and the reduction of negative interactions during the transition from a healthy to a disturbed state. During dysbiosis, an opportunistic *Pseudoalteromonas* was among the most abundant and connected ASVs and as such a potential driver of microbiome dysbiosis. Crucial microbial players of sponge microbiome homeostasis in comparison to the transition to dysbiosis can principally be identified and may be used as indicators to predict microbiome stability and health, also in other host or environmental contexts.

SINGLE BACTERIAL TAXA RECOLONIZE WITH BACTERIA-BACTERIA INTERACTIONS

Recolonization experiments of animal hosts are generally met with mixed success. In corals, the microbiome of antibiotic-treated animals was recovered by simple exposure to natural water (Bent *et al.*, 2021). In another study, microbiome recolonization (“coral microbiome transplantation”, CMT) of two coral species yielded a heat-resistant phenotype (Doering *et al.*, 2021). However, one coral species was less flexible to integrate bacteria than the other. In our study, recolonization had no effect on the bacterial community composition and diversity and could not reverse the antibiotic-induced dysbiosis. One reason might be that the dysbiotic state is too stable for new bacteria to alter the community (Sommer *et al.*, 2017). Another reason could be that the *H. panicea* symbionts cannot be transferred horizontally, for example, if they were vertically transmitted through the reproductive stages. It remains unclear why recolonization had no effect on the bacterial community composition. Yet, the successful transfer of single bacterial taxa opens a window of opportunity for rescue from dysbiosis.

Four bacterial taxa were transferred with the inoculum and consistently recolonized sponges (Figure 3, Table 1). In both recolonization experiments, transferred ASVs seem to establish with a delay after recolonization. Thus, potential changes on the community level might only become visible after a longer time than monitored in our experiments. The transferred taxa are affiliated to general marine

bacteria and the question remains, whether they are opportunists that happen to benefit from the conditions in the sponge, or whether they would enable long-term restructuring of the healthy microbiome. Bacteria-bacteria co-occurrence networks on recolonized and control sponges indicate that transferred bacteria have strong, and partly negative correlations to other ASVs including those that became highly abundant after antibiotic treatment (Figure 4). Frequently negative, competitive correlations are related to network stability and thus homeostasis, through negative feedback loops (Coyte *et al.*, 2015). Such negative interactions can be mediated by properties such as antimicrobial defense, host colonization and quorum sensing, which are frequently found on sponge symbiont genomes (Fan *et al.*, 2012; Slaby *et al.*, 2017). This stabilizing effect may be reflected in the intra-specific beta-diversity that recovers to T0 levels after recolonization (appendix 4.5). This effect could provide for a mechanistic explanation for the general success of microbial recolonization/transplantation experiments in many different contexts ranging from fecal transplantation to coral probiotics.

CONCLUSIONS AND OUTLOOK

This present study is among the first to experimentally manipulate marine sponge microbiomes by controlled experimentation in gnotobiotic chambers and application of antibiotics. We report the following findings: (i) The dominant symbiont in *H. panicea*, *Ca. H. symbioticus*, remained largely unchanged in spite of dysbiosis caused by growth of opportunistic bacteria following antibiotic treatment. This finding could only be uncovered by combination of quantitative (qPCR) with relative (amplicon sequencing) bacterial abundance analyses. ((ii) Next to the dominant symbiont, several other ASVs were permanently associated with the sponge (“persisters”) that are known as from other sponge- and host-contexts. (iii) Recolonization of the sponge with its native microbiome did not rescue the microbiome from the dysbiotic state. Still, we discovered bacterial ASVs from the inoculum that could be successfully transferred (“recolonizers”). This study contributes to ongoing efforts to unearth evolutionarily ancient mechanisms of microbiome dynamics and host-microbe as well as microbe-microbe interactions in the sponge holobiont.

ACKNOWLEDGEMENTS: We acknowledge Andrea Hethke and Ina Clefsen for technical assistance in the lab and the students Julius Krebs, Ashley Coons and Violeta Albacete for their experimental support. We thank Kristina Bayer, Sebastian Fraune and the CRC1182 community for stimulating

discussions. We acknowledge the Competence Center for Genomic Analysis (CCGA) Kiel for amplicon sequencing. Further, we are grateful to Felix Mittermayer for sponge collections and to Claas Hiebenthal for technical support in the gnotobiotic chambers.

FINANCE STATEMENT: This project is supported by funding of the DFG (“Origin and Function of Metaorganisms”, CRC1182-TP B01) and the Gordon and Betty Moore Foundation (“Symbiosis in Aquatic Systems Initiative”, GBMF9352) to UH. LS is further supported by the International Max Planck Research School for Evolutionary Biology, and LP receives funding by the DFG (“IMMUBASE”, 417981041) and is currently supported by “la Caixa” Foundation (ID 10010434) and from the European Union’s Horizon 2020 research and innovation program under the Marie Skłodowska-Curie grand agreement (No 847648, fellowship code is 104855).

DATA DEPOSITION: All 16S rRNA gene amplicon reads and the sample metadata and attributes are available in the National Center for Biotechnology Information (NCBI) Sequence Read Archive (SRA): PRJNA786895; BioSample accessions: SAMN23732322- SAMN23732615. Data is currently under embargo and will be made publicly available once manuscript is published.

CONFLICT OF INTEREST: The authors declare that the research was conducted in the absence of any commercial or financial relationships that could be construed as a potential conflict of interest.

REFERENCES

- Althoff, K., Schütt, C., Steffen, R., Batel, R., and Müller, W.E.G. (1998) Evidence for a symbiosis between bacteria of the genus *Rhodobacter* and the marine sponge *Halichondria panicea*: Harbor also for putatively toxic bacteria? *Mar Biol* **130**: 529–536.
- Augustin, R., Fraune, S., Franzenburg, S., and Bosch, T.C.G. (2012) Recent Advances on Model Hosts, Mylonakis, E., Ausubel, F.M., Gilmore, M., and Casadevall, A. (eds) New York, NY: Springer.
- Barthel, D. (1986) On the ecophysiology of the sponge *Halichondria panicea* in Kiel Bight. I. Substrate specificity, growth and reproduction. *Mar Ecol Prog Ser* **32**: 291–298.
- Barthel, D. (1988) On the ecophysiology of the sponge *Halichondria panicea* in Kiel Bight. II. Biomass, production, energy budget and integration in environmental processes. *Mar Ecol* **43**: 87–93.
- Le Bastard, Q., Ward, T., Sidiropoulos, D., Hillmann, B.M., Chun, C.L., Sadowsky, M.J., et al. (2018) Fecal microbiota transplantation reverses antibiotic and chemotherapy-induced gut dysbiosis in mice. *Sci Rep* **8**: 1–11.
- Bell, J.J., Bennett, H.M., Rovellini, A., and Webster, N.S. (2018) Sponges to Be Winners under Near-Future Climate Scenarios. *Bioscience* **68**: 955–968.
- Bent, S.M., Miller, C.A., Sharp, K.H., Hansel, C.M., and Apprill, A. (2021) Differential Patterns of Microbiota Recovery in Symbiotic and Aposymbiotic Corals following Antibiotic Disturbance. *mSystems* **6**: 1–18.

- Blanquer, A., Uriz, M.J., Cebrian, E., and Galand, P.E. (2016) Snapshot of a bacterial microbiome shift during the early symptoms of a massive sponge die-off in the western Mediterranean. *Front Microbiol* **7**: 1–10.
- Bolyen, E., Rideout, J.R., Dillon, M.R., Bokulich, N.A., Abnet, C.C., Al-Ghalith, G.A., et al. (2019) Reproducible, interactive, scalable and extensible microbiome data science using QIIME 2. *Nat Biotechnol* **37**: 852–857.
- Bosch, T.C.G., Guillemin, K., and McFall-Ngai, M. (2019) Evolutionary “Experiments” in Symbiosis: The Study of Model Animals Provides Insights into the Mechanisms Underlying the Diversity of Host–Microbe Interactions. *BioEssays* **41**: 1–8.
- Bucher, M., Wolfowicz, I., Voss, P.A., Hambleton, E.A., and Guse, A. (2016) Development and Symbiosis Establishment in the Cnidarian Endosymbiosis Model *Aiptasia* sp. *Sci Rep* **6**: 1–11.
- Callahan, B.J., McMurdie, P.J., Rosen, M.J., Han, A.W., Johnson, A.J.A., and Holmes, S.P. (2016) DADA2: High-resolution sample inference from Illumina amplicon data. *Nat Methods* **13**: 581–583.
- Callens, M., Watanabe, H., Kato, Y., Miura, J., and Decaestecker, E. (2018) Microbiota inoculum composition affects holobiont assembly and host growth in *Daphnia*. *Microbiome* **6**: 56.
- Campana, S., Hudspeth, M., Lankes, D., de Kluijver, A., Demey, C., Schoorl, J., et al. (2021) Processing of Naturally Sourced Macroalgal- and Coral-Dissolved Organic Matter (DOM) by High and Low Microbial Abundance Encrusting Sponges. *Front Mar Sci* **8**: 1–13.
- De Caralt, S., Agell, G., and Uriz, M.J. (2003) Long-term culture of sponge explants: Conditions enhancing survival and growth, and assessment of bioactivity. *Biomol Eng* **20**: 339–347.
- Cho, I. and Blaser, M.J. (2012) The human microbiome: At the interface of health and disease. *Nat Rev Genet* **13**: 260–270.
- Conway, J.R., Lex, A., and Gehlenborg, N. (2017) UpSetR: An R package for the visualization of intersecting sets and their properties. *Bioinformatics* **33**: 2938–2940.
- Costa, R.M., Cárdenas, A., Loussert-Fonta, C., Toullec, G., Meibom, A., and Voolstra, C.R. (2021) Surface Topography, Bacterial Carrying Capacity, and the Prospect of Microbiome Manipulation in the Sea Anemone Coral Model *Aiptasia*. *Front Microbiol* **12**: 1–16.
- Costello, E.K., Stagaman, K., Dethlefsen, L., Bohannan, B.J.M., and Relman, D.A. (2012) The application of ecological theory toward an understanding of the human microbiome. *Science (80-)* **336**: 1255–1262.
- Coyte, K.Z., Schluter, J., and Foster, K.R. (2015) The ecology of the microbiome: Networks, competition, and stability. *Science (80-)* **350**: 663–666.
- Doering, T., Wall, M., Putschim, L., Rattanawongwan, T., Schroeder, R., Hentschel, U., and Roik, A. (2021) Towards enhancing coral heat tolerance: a “microbiome transplantation” treatment using inoculations of homogenized coral tissues. 1–16.
- Douglas, A.E. (2019) Simple animal models for microbiome research. *Nat Rev Microbiol* **17**: 764–775.
- Easson, C.G. and Thacker, R.W. (2014) Phylogenetic signal in the community structure of host-specific microbiomes of tropical marine sponges. *Front Microbiol* **5**: 1–11.
- Fan, L., Liu, M., Simister, R., Webster, N.S., and Thomas, T. (2013) Marine microbial symbiosis heats up: the phylogenetic and functional response of a sponge holobiont to thermal stress. *ISME J* **7**: 991–1002.
- Fan, L., Reynolds, D., Liu, M., Stark, M., Kjelleberg, S., Webster, N.S., and Thomas, T. (2012) Functional equivalence and evolutionary convergence in complex communities of microbial sponge symbionts. *Proc Natl Acad Sci* **109**: E1878–E1887.
- Fierer, N., Ferrenberg, S., Flores, G.E., González, A., Kueneman, J., Legg, T., et al. (2012) From animalcules to an ecosystem: Application of ecological concepts to the human microbiome. *Annu Rev Ecol Evol Syst* **43**: 137–155.
- Francino, M.P. (2016) Antibiotics and the human gut microbiome: Dysbioses and accumulation of resistances. *Front Microbiol* **6**: 1–11.
- Friedman, J. and Alm, E.J. (2012) Inferring Correlation Networks from Genomic Survey Data. *PLoS Comput Biol* **8**: 1–11.
- Friedrich, A.B., Fischer, I., and Proksch, P. (2001) Temporal variation of the microbial community associated with the mediterranean sponge *Aplysina aerophoba*. *FEMS Microbiol Ecol* **38**: 105–113.
- Gaulke, C.A., Barton, C.L., Proffitt, S., Tanguay, R.L., and Sharpton, T.J. (2016) Triclosan exposure is associated with rapid restructuring of the microbiome in adult zebrafish. *PLoS One* **11**: 1–20.
- Gloeckner, V., Lindquist, N., Schmitt, S., and Hentschel, U. (2013) *Ectyoplasia ferox*, an Experimentally Tractable Model for Vertical Microbial Transmission in Marine Sponges. *Microb Ecol* **65**: 462–474.
- Gloeckner, V., Wehrl, M., Moitinho-silva, L., Schupp, P., Pawlik, J.R., Lindquist, N.L., et al. (2014) The HMA-LMA Dichotomy Revisited: an Electron Microscopical Survey of 56 Sponge Species. *Biol Bull* **227**: 78–88.
- Ianiro, G., Segal, J.P., Mullish, B.H., Quraishi, M.N., Porcari, S., Fabiani, G., et al. (2020) Fecal microbiota transplantation in gastrointestinal and extraintestinal disorders. *Future Microbiol* **15**: 1173–1186.

- King, C.H., Desai, H., Sylvestsky, A.C., Id, J.L., Ayanyan, S., Carrie, J., et al. (2019) Baseline human gut microbiota profile in healthy people and standard reporting template. 1–25.
- Knobloch, S., Jóhannsson, R., and Marteinson, V. (2019a) Bacterial diversity in the marine sponge *Halichondria panicea* from Icelandic waters and host-specificity of its dominant symbiont “*Candidatus Halichondriabacter symbioticus*.” *FEMS Microbiol Ecol* **95**: 1–13.
- Knobloch, S., Jóhannsson, R., and Marteinson, V. (2019b) Genome analysis of sponge symbiont “*Candidatus Halichondriabacter symbioticus*” shows genomic adaptation to a host-dependent lifestyle. *Environ Microbiol* 1462-2920.14869.
- Kozich, J.J., Westcott, S.L., Baxter, N.T., Highlander, S.K., and Schloss, P.D. (2013) Development of a dual-index sequencing strategy and curation pipeline for analyzing amplicon sequence data on the miseq illumina sequencing platform. *Appl Environ Microbiol* **79**: 5112–5120.
- Kumala, L., Larsen, M., Glud, R.N., and Canfield, D.E. (2021) Spatial and temporal anoxia in single-ostium *Halichondria panicea* demosponge explants studied with planar optodes. *Mar Biol* **168**: 1–13.
- Lange, K., Buerger, M., Stallmach, A., and Bruns, T. (2016) Effects of Antibiotics on Gut Microbiota. *Dig Dis* **34**: 260–268.
- Lavrov, A.I. and Kosevich, I.A. (2016) Sponge cell reaggregation: Cellular structure and morphogenetic potencies of multicellular aggregates. *J Exp Zool Part A Ecol Genet Physiol* **325**: 158–177.
- Lesser, M.P., Fiore, C., Slattery, M., and Zaneveld, J. (2016) Climate change stressors destabilize the microbiome of the Caribbean barrel sponge, *Xestospongia muta*. *J Exp Mar Bio Ecol* **475**: 11–18.
- Li, C.W., Chen, J.Y., and Hua, T.E. (1998) Precambrian sponges with cellular structures. *Science (80-)* **279**: 879–882.
- Luna, G.M., Bongiorno, L., Gili, C., Biavasco, F., and Danovaro, R. (2010) *Vibrio harveyi* as a causative agent of the White Syndrome in tropical stony corals. *Environ Microbiol Rep* **2**: 120–127.
- Lüskow, F., Kløve-Mogensen, K., Tophøj, J., Pedersen, L.H., Riisgård, H.U., and Eriksen, N.T. (2019) Seasonality in Lipid Content of the Demosponges *Halichondria panicea* and *H. bowerbanki* at Two Study Sites in Temperate Danish Waters. *Front Mar Sci* **6**: 1–7.
- Lüskow, F., Riisgård, H.U., Solovyeva, V., and Brewer, J.R. (2019) Seasonal changes in bacteria and phytoplankton biomass control the condition index of the demosponge *Halichondria panicea* in temperate Danish waters. *Mar Ecol Prog Ser* **608**: 119–132.
- Luter, H.M., Bannister, R.J., Whalan, S., Kutti, T., Pineda, M.C., and Webster, N.S. (2017) Microbiome analysis of a disease affecting the deep-sea sponge *Geodia barretti*. *FEMS Microbiol Ecol* **93**: 1–6.
- Luter, H.M., Whalan, S., and Webster, N.S. (2012) Thermal and sedimentation stress are unlikely causes of brown spot syndrome in the Coral Reef sponge, *Ianthella basta*. *PLoS One* **7**: 1–9.
- Manor, O., Dai, C.L., Kornilov, S.A., Smith, B., Price, N.D., Lovejoy, J.C., et al. (2020) Health and disease markers correlate with gut microbiome composition across thousands of people. *Nat Commun* **11**: 1–12.
- Mauri, M., Elli, T., Caviglia, G., Uboldi, G., and Azzi, M. (2017) RAWGraphs: A visualisation platform to create open outputs. *ACM Int Conf Proceeding Ser Part F1313*:
- Mortzfeld, B.M., Urbanski, S., Reitzel, A.M., Künzel, S., Technau, U., and Fraune, S. (2016) Response of bacterial colonization in *Nematostella vectensis* to development, environment and biogeography. *Environ Microbiol* **18**: 1764–1781.
- Naim, M.A., Morillo, J.A., Sørensen, S.J., Waleed, A.A.S., Smidt, H., and Sipkema, D. (2014) Host-specific microbial communities in three sympatric North Sea sponges. *FEMS Microbiol Ecol* **90**: 390–403.
- Ng, K.M., Ferreyra, J.A., Higginbottom, S.K., Lynch, J.B., Kashyap, P.C., Gopinath, S., et al. (2013) Microbiota-liberated host sugars facilitate post-antibiotic expansion of enteric pathogens. *Nature* **502**: 96–99.
- Nyholm, S. V. and McFall-Ngai, M.J. (2021) A lasting symbiosis: how the Hawaiian bobtail squid finds and keeps its bioluminescent bacterial partner. *Nat Rev Microbiol* **10**:
- Peixoto, R.S., Harkins, D.M., and Nelson, K.E. (2021) Advances in Microbiome Research for Animal Health. *Annu Rev Anim Biosci* **9**: 289–311.
- Pita, L., Fraune, S., and Hentschel, U. (2016) Emerging sponge models of animal-microbe symbioses. *Front Microbiol* **7**: 1–8.
- Pita, L., Rix, L., Slaby, B.M., Franke, A., and Hentschel, U. (2018) The sponge holobiont in a changing ocean: from microbes to ecosystems. *Microbiome* **6**: 46.
- Posadas, N., Baquiran, J.I.P., Nada, M.A.L., Kelly, M., and Conaco, C. (2021) Microbiome diversity and host immune functions influence survivorship of sponge holobionts under future ocean conditions. *ISME J* 1–10.
- Quast, C., Pruesse, E., Yilmaz, P., Gerken, J., Schweer, T., Yarza, P., et al. (2013) The SILVA ribosomal RNA gene database project: Improved data processing and web-based tools. *Nucleic Acids Res* **41**: 590–596.

- Rao, C., Coyte, K.Z., Bainter, W., Geha, R.S., Martin, C.R., and Rakoff-Nahoum, S. (2021) Multi-kingdom ecological drivers of microbiota assembly in preterm infants. *Nature* **591**: 633–638.
- Richardson, C., Hill, M., Marks, C., Runyen-Janecky, L., and Hill, A. (2012) Experimental manipulation of sponge/bacterial symbiont community composition with antibiotics: Sponge cell aggregates as a unique tool to study animal/microorganism symbiosis. *FEMS Microbiol Ecol* **81**: 407–418.
- Riisgård, H.U., Kumala, L., and Charitonidou, K. (2016) Using the F/R-ratio for an evaluation of the ability of the demosponge *Halichondria panicea* to nourish solely on phytoplankton versus free-living bacteria in the sea. *Mar Biol Res* **12**: 907–916.
- Rooks, M.G., Veiga, P., Wardwell-Scott, L.H., Tickle, T., Segata, N., Michaud, M., et al. (2014) Gut microbiome composition and function in experimental colitis during active disease and treatment-induced remission. *ISME J* **8**: 1403–1417.
- Samad, T., Co, J.Y., Witten, J., and Ribbeck, K. (2019) Mucus and Mucin Environments Reduce the Efficacy of Polymyxin and Fluoroquinolone Antibiotics against *Pseudomonas aeruginosa*. *ACS Biomater Sci Eng* **5**: 1189–1194.
- Sarker, S.A., Ahmed, T., and Brüßow, H. (2017) Persistent diarrhea: a persistent infection with enteropathogens or a gut commensal dysbiosis? *Environ Microbiol* **19**: 3789–3801.
- Schellenberg, J., Reichert, J., Hardt, M., Klingelhöfer, I., Morlock, G., Schubert, P., et al. (2020) The Bacterial Microbiome of the Long-Term Aquarium Cultured High-Microbial Abundance Sponge *Haliclona cnidata* – Sustained Bioactivity Despite Community Shifts Under Detrimental Conditions. *Front Mar Sci* **7**.
- Schippers, K.J. (2013) Sponge cell culture.
- Schmittmann, L., Franzenburg, S., and Pita, L. (2021) Individuality in the Immune Repertoire and Induced Response of the Sponge *Halichondria panicea*. *Front Immunol* **12**: 1–13.
- Schmittmann, L., Hentschel, U. (2021) Antibiotic treatment of the sponge *Halichondria panicea* and subsequent recolonization. [dx.doi.org/10.17504/protocols.io.by7hpzj6](https://doi.org/10.17504/protocols.io.by7hpzj6).
- Schmittmann, L., Pita, L. (2021) DNA/RNA extraction and qPCR protocol to assess bacterial abundance in the sponge *Halichondria panicea*. [dx.doi.org/10.17504/protocols.io.bxwwppfe](https://doi.org/10.17504/protocols.io.bxwwppfe).
- Segata, N., Izard, J., Waldron, L., Gevers, D., Miropolsky, L., Garrett, W.S., and Huttenhower, C. (2011) Metagenomic biomarker discovery and explanation. *Genome Biol* **12**.
- Shaffer, M., Thurimella, K., and Lozupone, C.A. (2020) SCNIC: Sparse Correlation Network Investigation for Compositional Data. *bioRxiv* 2020.11.13.380733.
- Shannon, P., Markiel, A., Ozier, O., Baliga, N.S., Wang, J.T., Ramage, D., et al. (2003) Cytoscape: A Software Environment for Integrated Models of Biomolecular Interaction Networks. *Genome Res* **13**: 426.
- Sipkema, D., M, A.A., and Tramper, J. (2003) Primmorphs from seven marine sponges : formation and structure. *J Biotechnol* **100**: 127–139.
- Slaby, B.M., Hackl, T., Horn, H., Bayer, K., and Hentschel, U. (2017) Metagenomic binning of a marine sponge microbiome reveals unity in defense but metabolic specialization. *ISME J* **11**: 2465–2478.
- Smith, D., Leary, P., Craggs, J., Bythell, J., and Sweet, M. (2015) Microbial Communities associated with healthy and white syndrome-affected *Echinopora lamellosa* in aquaria and experimental treatment with the antibiotic ampicillin. *PLoS One* **10**: 1–17.
- Sommer, F., Anderson, J.M., Bharti, R., Raes, J., and Rosenstiel, P. (2017) The resilience of the intestinal microbiota influences health and disease. *Nat Rev Microbiol* **15**: 630–638.
- Steinert, G., Rohde, S., Janussen, D., Blaurock, C., and Schupp, P.J. (2017) Host-specific assembly of sponge-associated prokaryotes at high taxonomic ranks. *Sci Rep* **7**: 1–9.
- Strati, F., Pujolassos, M., Burrello, C., Giuffrè, M.R., Lattanzi, G., Caprioli, F., et al. (2021) Antibiotic-associated dysbiosis affects the ability of the gut microbiota to control intestinal inflammation upon fecal microbiota transplantation in experimental colitis models. *Microbiome* **9**: 1–15.
- Strehlow, B.W., Schuster, A., Francis, W.R., and Canfield, D.E. (2021) Metagenomic data for *Halichondria panicea* from Illumina and Nanopore sequencing and preliminary genome assemblies for the sponge and two microbial symbionts. *bioRxiv* 1–8.
- Tavalire, H.F., Christie, D.M., Leve, L.D., Ting, N., Cresko, W.A., and Bohannan, B.J.M. (2021) Shared environment and genetics shape the gut microbiome after infant adoption. *MBio* **12**.
- Thomas, T., Moitinho-Silva, L., Lurgi, M., Björk, J.R., Easson, C., Astudillo-García, C., et al. (2016) Diversity, structure and convergent evolution of the global sponge microbiome. *Nat Commun* **7**: 11870.
- Udekwi, K.I., Parrish, N., Ankomah, P., Baquero, F., and Levin, B.R. (2009) Functional relationship between bacterial cell density and the efficacy of antibiotics. *J Antimicrob Chemother* **63**: 745–757.
- Vad, J., Dunnett, F., Liu, F., Montagner, C.C., Roberts, J.M., and Henry, T.B. (2020) Soaking up the oil: Biological impacts of dispersants and crude oil on the sponge *Halichondria panicea*. *Chemosphere* **257**: 127109.

Chapter 4

- Visick, K.L., Stabb, E. V., and Ruby, E.G. (2021) A lasting symbiosis: how *Vibrio fischeri* finds a squid partner and persists within its natural host. *Nat Rev Microbiol* **0123456789**:
- Wehrl, M., Steinert, M., and Hentschel, U. (2007) Bacterial uptake by the marine sponge *Aplysina aerophoba*. *Microb Ecol* **53**: 355–365.
- Witte, U., Barthel, D., and Tendal, O. (1994) The reproductive cycle of the sponge *Halichondria panicea* Pallas (1766) and its relationship to temperature and salinity. *J Exp Mar Bio Ecol* **183**: 41–52.
- Yan, J. and Bassler, B.L. (2019) Surviving as a Community: Antibiotic Tolerance and Persistence in Bacterial Biofilms. *Cell Host Microbe* **26**: 15–21.

DISCUSSION

In the present PhD thesis, I evaluated the use of the breadcrumb sponge *Halichondria panicea* as an experimental model for sponge-symbioses. I targeted both the host-side as well as the bacteria-side of the sponge holobiont by experimental approaches. Thereby, I identified different levels of immune gene control in the host *H. panicea*, and bacterial community dynamics during dysbiosis. For the latter, the integration of absolute and relative bacterial abundance data was crucial and revealed the high stability of the dominant symbiont of *H. panicea*. My findings contribute to an understanding of the *H. panicea*-specific core microbiome and demonstrate its persistence in spite of dysbiosis. I conclude that *H. panicea* and its dominant symbiont have the potential to be an experimental model for sponge-symbioses that can be used to disentangle aspects of coevolution, symbiosis function and adaptation to variable environments. However, technical challenges remain, e.g., the generation of gnotobiotic sponges by antibiotic treatment was not successful. In the following, I will discuss and synthesize the findings of my PhD thesis and their implications and provide ideas for future research.

HALICHONDRIA PANICEA AS AN EXPERIMENTAL MODEL FOR HOST-MICROBE INTERACTIONS

SPONGE CULTIVATION IN MAINTENANCE AQUARIA

Maintenance aquaria for *H. panicea* were set up with a semi-flow through of natural seawater and thus fluctuating water parameters following the seasonal ambient temperature, salinity and pH cycles (Chapter 3). This maintenance system is intended to culture *H. panicea* for a few months and perform experiments under natural environmental conditions. Importantly, the dominant symbiont was maintained at high abundances over six months, which was not achieved in other cultivation attempts of adult *H. panicea* (Knobloch *et al.*, 2019b). Thus, from the microbiome perspective, the maintenance system provides access to adult sponges for at least 6 months. From the host perspective however, it is less clear that sponges can be maintained under such conditions in the long-term. The tissue seems to shrink, which was also reported previously for *H. panicea* in aquaria (Knobloch *et al.*, 2019a). It is not related to an infection that is usually characterized by white or grey mats of bacterial growth that is reported as signs of disease from other sponges (Luter and Webster, 2017). So far, it is not clear what exactly is required for successful growth in aquaria.

Important next steps are to evaluate the food composition and sponge feeding rates in maintenance aquaria and compare them to the natural environment. Whether sponges receive sufficient food with fresh seawater can be assessed via filtration rates (energy uptake), respiration rates (energy expenditure) in maintenance aquaria (Reiswig, 1971; Reiswig, 1981). If food is limiting, the gap should

be filled by providing additional food. Here, it is important to differentiate between particulate organic matter (POM) and dissolved organic matter (DOM) as a food source that both probably plays a role for the LMA sponge *H. panicea* (Reiswig, 1981; De Goeij *et al.*, 2013; Rix *et al.*, 2020).

Additionally, the position of sponges in aquaria could be re-considered in an effort to improve culturing. In aquaculture, sponges are most often cultivated hanging in the water column to ease access to food, either threaded on ropes or in net bags (Van Treeck *et al.*, 2003; Gökalp *et al.*, 2021). Previously, hanging has been found the best for *H. panicea* (Barthel and Theede, 1986). Further, *H. panicea* was already successfully grown on ropes in outdoor mesocosms that harbored benthic communities including sponges (Kristina Bayer, unpublished), where water-flow and thus food supply was also much higher than in our maintenance aquaria. So far, we have placed sponges directly in the maintenance aquaria or on clay tiles and readily attached to plastic, glass, PVC and clay. Hanging them would prevent sedimentation of debris on/around the sponges, which can impair filtration capacity and survival (Maldonado *et al.*, 2008; Bannister *et al.*, 2012). Bubble formation in the sponge aquiferous system was identified as an additional threat during sponge cultivation. This happened when either the water pipe system was drawing air or water pumps were not submersed, resulting in micro air bubbles entering the aquaria. Sponges were subsequently covered in air bubbles and ultimately died or were left with severe tissue damage. Importantly, larger air bubbles that were constantly used to create a water current did not affect sponges negatively. In an effort to ensure long-term cultivation of *H. panicea* in aquaria, access to food and cultivation method should be re-evaluated and optimized.

GENERATION OF GNOTOBIOTIC SPONGES REMAINS A CHALLENGE

Since the maintenance aquaria are not suitable for controlled experiments with sponge holobionts I developed a unique experimental aquarium system intended to culture sponges under controlled and sterile conditions with an automated water exchange and enable gnotobiotic cultivation of sponges (Chapter 3). The set-up is closed in order to avoid bacterial contamination while sterile seawater is exchanged continuously. Gnotobiotic facilities are best established for mice where they are elaborate and highly technological while the staff is specifically trained (Faith *et al.*, 2010). Cultivation of aquatic organisms under gnotobiotic conditions is even more challenging, due to the large volumes of sterile water that have to be produced to maintain aquatic animals (Marques *et al.*, 2006; Zhang *et al.*, 2020). For gnotobiotic zebrafish cultures, extensive protocols and commercial cultivation supply exist (Pham *et al.*, 2008). I made the first attempt to design an experimental aquarium system for sponges. Although it could not be tested under gnotobiotic conditions, it is suitable to perform experiments

Discussion

(tested for up to 3 weeks), measure respiration and take water samples during the running experiment without opening the aquaria.

Few studies so far have assessed the potential of reducing sponge-associated bacteria by exposure to antibiotics (Friedrich *et al.*, 2001b; De Caralt *et al.*, 2003; Sipkema *et al.*, 2003; Richardson *et al.*, 2012; Gloeckner *et al.*, 2013; Schippers, 2013). None of them have succeeded in removing the host-associated bacteria while Schellenberg *et al.* (Schellenberg *et al.*, 2020) noticed a reduction after continuous exposure to ampicillin and gentamicin for four weeks. Within the context of this thesis, an antibiotic cocktail was identified that reduces absolute numbers of *Ca. H. symbioticus* by up to 2-3 orders of magnitude (Chapter 3, 4). However, this effect could not be repeated in all sponge individuals with high confidence. Inter-individual variability was extremely high and independent from the season when experiments were performed. Already in the first antibiotic test experiment where the effect of antibiotics was strongest, one individual showed no reduction of the dominant symbiont while the other three were heavily reduced. It is unclear what determines a successful reduction of the dominant symbiont and it can only be speculated at this point. The host probably plays a role since both, relative and absolute of *Ca. H. symbioticus* were linked to the sponge host individual. Specifically, two clones of the same sponge individual had similar abundances regardless of experimental treatment or timepoint, while abundances differed between individuals. These intriguing patterns suggest *Ca. H. symbioticus* abundance might have a host individual specific, probably genetic underpinning as was shown previously for human symbionts (Tavalire *et al.*, 2021). It is less likely that bacteria-bacteria interactions are important for the successful reduction since *Ca. H. symbioticus* abundance is mostly independent from other ASVs.

Contrary to my expectations, the total bacterial abundance increased strongly after antibiotic treatment in all experiments (Chapter 3, 4). It was shown in mice that opportunistic bacteria grow on nutritional resources that become available after microbial disruption due to antibiotic treatment. Opportunists merely exploit the opening niche (Ng *et al.*, 2013). I suspect that this happened in our system as well. Additionally, selection for antibiotic-resistant bacteria was observed, that sponges are known to harbor naturally (Versluis *et al.*, 2016). Antibiotic tests with over 60 bacterial isolates from *H. panicea* and 29 antibiotics showed that rifampicin was the most effective antibiotic, and all tested strains were sensitive to this antibiotic. Taking everything into consideration, it appears rather unlikely that the highly diverse sponge microbiome can be eliminated by antibiotic treatment in adult sponges. Thus, alternative or additional approaches should be considered. Sponge larvae could be a promising starting point since they are smaller, and antibiotics could potentially penetrate easier into the tissue. First qPCR results from trials with *H. panicea* show that total bacteria are reduced by some antibiotic cocktails but not by others (Carrier *et al.* unpublished). Interestingly, the dominant symbiont remains

Discussion

stable also in larvae. Along similar lines, sponge explants or sponge primmorphs would provide a smaller biomass and may be more amenable to antibiotic treatment than adult tissue. First tests on sponge primmorphs show promising morphological differences between *H. panicea* primmorphs with and without antibiotic treatment, and further, with and without recolonization (Hethke and Schmittmann, unpublished). As an alternative to antibiotics, phage treatment could be tested to remove bacteria (Kim *et al.*, 2020). However, phages are often highly specific to their bacterial host and thus not entirely appropriate to remove bacteria completely, although there are exceptions (Kauffman *et al.*, 2018; de Jonge *et al.*, 2019). Ideally, a *Ca. H. symbioticus*-specific phage would be used to eliminate the dominant symbiont, but for the lack of a culturable symbiont, phage isolation remains elusive.

Another promising avenue is to artificially enriching the dominant symbiont *in vivo*. We could show that the numbers of eubacteria and of *Ca. H. symbioticus* in particular increased by 1-2 orders of magnitude in healthy *H. panicea* sponges maintained in experimental aquaria. In a co-cultivation approach intended to enrich *Ca. H. symbioticus* in order to increase chances of isolation, relative abundances were increased from 60 % to 80 % (Knobloch *et al.*, 2019b). However, it was not tested whether the symbiont increased in terms of absolute numbers as well. Sponge individuals with varying levels of symbiont abundance could be then tested for their physiological performance and nutrient assimilation to understand whether symbiont load correlates to host fitness and phenotype, and whether there is any fitness cost associated with high *Ca. H. symbioticus* abundance. In doing so, the function of the symbiosis between *H. panicea* and *Ca. H. symbioticus* could be revealed.

However, the challenge remains to choose the appropriate phenotypic measurements that will change in response to altered symbiont load. The published *Ca. H. symbioticus* metagenome is highly fragmented and only 87.6 % complete (Knobloch *et al.*, 2020). The genome comparison with the closest known relatives *Amylibacter cionae* and *Amylibacter kogurei* and other sponge symbionts revealed common but no unique, surprising features of a sponge-symbiont. *Ca. H. symbioticus* seems involved in ammonia assimilation, vitamin B12 synthesis and antimicrobial defense *via* a bacteriocin cluster. This bacteriocin is not specific for *Ca. H. symbioticus* but is also found in the *Amylibacter* strains (Knobloch *et al.*, 2020). It remains unclear which features make this bacterium unique compared to others in their function for the sponge host and why it is so successful in this environment. We currently do not fully understand the hidden diversity behind the dominant *Ca. H. symbioticus* ASV. There are different 16S rRNA gene variants ((Knobloch *et al.*, 2019a); Kristina Bayer unpublished data) and in I have also detected several closely related ASVs as well as a high diversity of the wider group. A combination of long-read sequencing (e.g., Nanopore) with high depth short-read sequencing will hopefully provide a better coverage. On the other side, we only have transcriptomic data on the host

H. panicea (Vad *et al.*, 2020; Schmittmann *et al.*, 2021) and a preliminary genome assembly from metagenomic data (Strehlow *et al.*, 2021). We urgently need to improve the availability of genomic information on both the dominant symbiont and the host in order to generate hypothesis what the function of the symbiosis is and to plan informed experiments and phenotypic measurements, e.g., nutrient assimilation experiments.

RECOLONIZATION DID NOT REVERSE DYSBIOSIS

Recolonization did not recover dysbiotic sponge microbiomes after antibiotic treatment, whether performed by incubation with or injection of the natural sponge microbiome into sponge tissue (Chapter 4). Both approaches did not lead to a recovery of the microbiome composition or diversity, while single ASVs were transferred with the inoculum. These recolonizers were of marine origin, and are best classified as opportunists. This is not surprising since the dysbiotic microbiome community and the distressed host were probably not able anymore to select for beneficial microbes. However, recolonization studies from the cnidarian *Nematostella* showed that establishing a mature microbiome takes seven days and that the microbiome passes through a certain compositional dynamic until the final state is reached (Domin *et al.*, 2018). Thus, recolonization is a dynamic process and it is not clear if the sponge microbiome in our experiments would have changed in terms of diversity after recolonization. Differences in the bacteria-bacteria networks and on intra-specific beta-diversity in our recolonization experiment suggest an ongoing restructuring at the end of the experiment that might have progressed further. In the future, alternative experimental approaches should include earlier recolonization timepoints and recolonization with single isolates. It would be interesting to monitor absolute abundance of the dominant symbiont to test whether it remains stable regardless of shifts in the remaining microbiome.

IDENTIFICATION OF PERSISTENT BACTERIA AND RECOLONIZERS

Although the elimination of sponge-associated bacteria by antibiotics was not achieved, important knowledge was generated on the *H. panicea* holobiont. With an antibiotic treatment we could repeatedly manipulate the sponge microbiome and identified a persistent symbiont core in spite of dysbiosis. Further, the unexpected stability of *Ca. H. symbioticus* was revealed by the combination of qualitative 16S rRNA amplicon data and quantitative qPCR. I suggest the both the persistent core and the stable, dominant symbiont are true and obligate sponge symbionts. The persistent bacteria were found to be associated also with other host organisms including sponges. Thus, I expect mainly

microbe-microbe interactions to be involved in determining their abundance. On the contrary, the dominant symbiont remained overall stable, and bacterial co-occurrence networks showed that it is largely independent of microbial interactions. Thus, I expect the dominant symbiont to be mainly host-driven as a result of specific coevolution. Bacteria-bacteria interactions predicted by co-occurrence networks play an important role in this context. Our study revealed that both positive and negative interactions are involved in healthy sponge microbiomes, while during disturbance the overall complexity increases. Importantly, loss of negative, competitive interactions seems to correlate with dysbiosis and could be a universal indicator of dysbiotic microbiomes.

Two important methodological improvements allowed us to uncover symbiont stability over time. First, a sampling approach with a daily resolution over 2.5 weeks and repeated sampling of the same individuals revealed dynamics in the microbiome that cannot be identified with single time point sampling. Second, during the recolonization experiment, we performed “live-qPCR”, in the sense that sponge tissue was sampled daily in the morning, immediately followed by DNA extractions, qbit measurements and qPCR. In doing so, we could assess abundances of bacteria and the dominant symbiont “live” while the experiment was running.

SYMBIONT PRESENCE DURING SPONGE REPRODUCTION

We could spawn *H. panicea* in the lab in two consecutive years and raise larvae until after metamorphosis (together with Lucía Pita and Tyler Carrier). So far, it was not possible to rear juveniles until they develop into an adult with an osculum, neither in natural maintenance aquaria nor under controlled conditions in artificial seawater. However, a sympatric species, *Haliclona sp.*, did reproduce and settle in maintenance aquaria and animals are viable for >2 years. Thus, I am optimistic that conditions can be tailored towards raising *H. panicea* under laboratory conditions and allow experimentation on all developmental stages in the near future. An extensive bacterial isolate collection from *H. panicea* has been established (lead by Tanja Rahn) and while the dominant symbiont could not be cultivated (as in (Knobloch *et al.*, 2019b)), the broader family *Rhodobacteraceae* was successfully enriched by selective culture media. Especially the nitrogen sources tryptophan and taurine were particularly important to select for *Rhodobacteraceae*. The closest isolated strain to *Ca. H. symbioticus* was an *Amylibacter* isolate, Hal240, that was 90.4 % related to the dominant symbiont. Since the dominant symbiont remains uncultivated, alternative approaches are needed and Hal240 can serve as a model for such, in addition to the total natural community isolated from healthy sponges (as used in this thesis).

ENVIRONMENTAL DRIVERS

Sponges as emerging models have one advantage over long-term laboratory model systems such as *D. melanogaster* or *C. elegans* in that experimental results can be validated in nature, while traditional lab model systems are usually very far away from natural populations (Parker *et al.*, 2018; Morgan *et al.*, 2019). We have conducted experiments on *H. panicea* from the Baltic Sea. This enclosed brackish Sea is a comparatively variable habitat in terms of temperature, pH and oxygen, and most importantly with a strong salinity gradient decreasing from West to East (Hansson and Gustafsson, 2011). Not many sponge species are able to inhabit the low saline Baltic Sea with climate change expected to restrict species distribution even further (Gräwe *et al.*, 2013; Podbielski *et al.*, 2016). *H. panicea* is one of the few sponge species found in coastal shallow water around Kiel, as well as in the low saline White Sea (Gerasimova and Ereskovsky, 2007) while the salinity threshold for *H. panicea* is not known. This aspect makes *H. panicea* additionally attractive to study the effect of environmental variability on microbiome composition and function. Although I detected *Ca. H. symbioticus* in every single *H. panicea* sample analyzed between 2017 and 2020 from different locations in the Baltic and in different seasons, it is not clear what determines *Ca. H. symbioticus* abundance. A sampling effort of different populations along the salinity gradient, as well as monthly sampling of the same sponge individuals over at least one year will allow to determine whether there are naturally occurring habitats with differential symbiont abundance, for example as an adaptation to environmental conditions, and whether symbiont abundance is constant within the same sponge individual over time. *H. panicea* ecology and wide geographic distribution allow for population genetic studies, as well as comparison between sponges adapted to differential environmental conditions and how this affects the symbioses.

IMMUNE GENE EXPRESSION IN AN EARLY DIVERGING METAZOAN

Our study was the first to investigate the *H. panicea* immune system and response to bacterial LPS and thus provided important knowledge on the host-side of the interactions within the holobiont (Schmittmann *et al.*, 2021, Chapter 2). We detected three different levels of immune gene control, which was constitutive expression of PRRs and immune genes, individual-specific expression of PRRs, and induced gene expression in response to LPS. We attribute the different expression patterns to the diverse role innate immunity has in order to maintain a stable microbiome and respond to incoming seawater bacteria and potential pathogens.

Discussion

Immune genes and PRRs were found to be generally elevated in *H. panicea* which is in line with the hypothesis of LMA sponges having an elevated immunity to control their microbiome more closely (Pita *et al.*, 2018a). I emphasize here the importance of not only analyzing the presence/absence of genes and transcripts in reference assemblies, but also of understanding how they are expressed across individuals. The constitutively expressed immune genes identified in *H. panicea* can now give rise to hypothesis which genes are crucial for the baseline sponge immunity that is potentially involved in the constant interaction with the microbiome and maintaining homeostasis. Potential candidate genes from our study include MyD88, as well as a protease, actin-binding genes and a cytokine receptor. Gene expression patterns might translate to other animal phyla and gene expression strategies might be conserved throughout metazoans.

We found no immune receptor genes differentially expressed after exposure to LPS but rather, post-translational mechanisms such as ubiquitination and phosphorylation. A previous study comparing the response of an LMA and a HMA sponge to microbial elicitors also detected a stronger response in the HMA sponge (Pita *et al.*, 2018a). It was hypothesized that LMA sponges rely on a higher constitutive immune gene expression in general and in turn require less gene regulation upon microbe encounter which we supported by our findings. In case of *H. panicea*, the response was mainly in posttranslational mechanisms and thus few direct responses, but rather indirect fine-tuning. This might even be determined on the sponge individual level, since we detected high individual variability in terms of number of differentially expressed genes.

The overall immune repertoire of *H. panicea* included a diversity of PRR classes, GPCRs and cytokine receptors in line with previous studies on sponges (Srivastava *et al.*, 2010; Riesgo *et al.*, 2014; Ryu *et al.*, 2016; Germer *et al.*, 2017; Pita *et al.*, 2018a). Two interesting receptor classes would be interesting candidates for future studies: First, cytokine receptors were diverse in *H. panicea* with almost 200 transcripts. Importantly, this diversity was not detected with the standard annotation pipeline but was only uncovered by the comparison to the proteome of the sponge *Amphimdeon queenslandica*. Most likely the diversity is currently underestimated due to annotation limits and the underrepresentation of sponges in public genomic databases. However, we expect a Porifera-specific superfamily of cytokine receptors that would be worth investigating in the light of symbioses. Cytokine receptors play a role in immunity in other organisms (Darling and Lamb, 2019), while in sponges TGF- β receptors are involved in wounding and Eph receptors in cell-cell communication (Krishnan *et al.*, 2019; Pozzolini *et al.*, 2019). The second receptor class I would suggest important is that of C-type lectin-like domain (CTLN) gene receptors. CTLN receptors are structurally diverse and found in all animals including sponges (Pees *et al.*, 2016) and play a role in interaction with the microbiome (Dierking and Pita, 2020). We discovered 157 different CTLN transcripts while the absolute majority was expressed in a single

sponge clone, while the others expressed < 10 transcripts. This suggests a large plasticity in CTLD expression although we do not know what triggered expression in this clone. Further, it implies a discrepancy between the expressed (transcriptomic) and potential (genomic) repertoire and a context-dependent expression (Pancer, 2000). The comparison between the genomic and transcriptomic repertoire of sponges would reveal if this is true for other receptor classes. Important here is to compare genomic information for the same individuals and not refer only to a reference assembly from several individuals and thus population-wide repertoire.

It should be considered that a differentiation by receptors might not only be an active process initiated by the hosts immune system but also be mediated by microbes. A recent study on sponges has shown that with the help of bacteriophages, bacteria are able to decorate themselves with ankyrin proteins that then enable the bacteria to evade phagocytosis by eukaryotic cells (Jahn *et al.*, 2019). Thus, bacteria would evade immune detection by the host. Similarly, a cyanobacterial sponge symbiont *Ca. Synechococcus spongarium* has a modified LPS structure compared to free-living relatives (Burgsdorf *et al.*, 2015) which could provide a route to evade the sponge immune system.

INDIVIDUALITY AS AN EMERGING PATTERN

All experiments in this thesis were performed on clones of individuals (distinct sponge colonies) and designed so that the same individuals were sampled across several time points and/or treatments. I found individuality on both the host-side as well as on the microbe-side of the sponge holobiont (Chapter 2, 4). The immune repertoire of *H. panicea* and the induced response to LPS revealed gene expression patterns linked to the individual. Further, *Ca. H. symbioticus* absolute abundance was correlated to the sponge individual and successful reduction after antibiotic treatment varied strongly between specimens. Repeated sampling of the same clones within this thesis revealed that variations are not random but determined by the individual. Although sponge individuals in this thesis were not genotyped, I would expect that a single colony refers to one genotype. *A. queenslandica* sponge individuals were found to only fuse during very early larvae stages (Gauthier and Degnan, 2008), so it is expected that *H. panicea* could fuse during early development.

Individual signals might mask overarching patterns and make it difficult to identify a signal in the noise in our experiments. Therefore, it is crucial to understand the interactions of genotype, environment and the microbiome, how they affect each other and how together they determine holobiont stability. Experimentally, individuality is challenging and will additionally complicate controlling or removing bacteria. For example, in the human gut antibiotics have varying effects depending on the initial

Discussion

microbiome composition (Ju *et al.*, 2017; Hildebrand *et al.*, 2019). This is one reason for the increasing effort in personalized medicine (Moyer *et al.*, 2019; Duffy, 2020). Similarly, individual sponge microbiome compositions could effect the outcome of a treatment. Individuality can be reduced or at least accounted for in experiments by working with sponge explants or clones from the same individual, as done in this thesis. Experiments could be performed with clones from only one individual, or with offspring with the same genetic background in an effort to reduce variation.

Variation between sponges has also been demonstrated in physiology, where respiration, feeding and pumping rates were highly variable and attributed to sponge morphology and temporal closing/opening of oscula (Riisgård *et al.*, 2016). To overcome differences in morphology, standardization of sponges is used, which is sponge explants of similar size. Still, variation is large among explant replicates due to osculum size and feeding activity (Kumala *et al.*, 2017, 2021; Kumala and Canfield, 2018). Sponges offer unique experimental opportunities due to their regeneration capacity and thus potential to generating explants and clones. General principles can be discovered that can only be tested experimentally with very few other sexually reproducing organisms (e.g., corals), or cell culture.

Individuality can also be an opportunity to discover important aspects of host-microbe symbioses. For example, individual-specific *Ca. H. symbioticus* strains monitored over time could be used to study ongoing evolution of symbionts within their hosts. I expect that symbiont strains evolve inside a sponge and adapt to environmental conditions. Thus, they could inform about adaptive processes within the sponge microbiome. Additionally, individual immune receptor repertoires could reveal potential innate immune mechanisms of selectivity and reveal whether they translate into different host fitness.

FINAL CONCLUSIONS

Reduction of bacteria in sponges with antibiotics remains difficult. The sponge microbiome could be manipulated with an antibiotic cocktail in a repeatable manner and shifted towards a dysbiotic state, but opportunistic and antibiotic-resistant bacteria increased in relative and absolute abundance. It remains an open question whether the highly diverse sponge microbiome can be reduced or completely eliminated by antibiotic administration. My suggestion for future studies is to continue focusing on the symbiosis with the dominant symbiont *Ca. H. symbioticus* and specifically target its abundance (e.g., increasing it by cultivation of the host sponge under amenable conditions).

The dominant symbiont, *Ca. H. symbioticus*, remains stable during dysbiosis, but varies between individuals. This pattern was only observed by the integration of relative (amplicon sequencing) and absolute (qPCR) bacterial abundance measures. I suggest that the abundance of the dominant symbiont is mainly host-dependent. Hence, future efforts into manipulating *Ca. H. symbioticus* absolute abundances should affect host function.

***H. panicea* has different, context-dependent strategies to regulate immune genes.** The *H. panicea* immune repertoire includes several diverse PRRs, GPCRs and cytokine receptors, which were either expressed constitutively, or were expressed in an individual-specific manner. Induced gene expression was observed in the response to the bacterial elicitor LPS. Together, the three layers of immune gene control (constitutive, individual-specific and induced expression) reflect the complex role of the immune system mediating interactions between sponges and the microbiome, seawater bacteria and potential pathogens.

The *H. panicea* holobiont is an exciting experimental model for sponge-microbe symbioses. The importance of both host-microbe and microbe-microbe interactions during homeostasis and dysbiosis were demonstrated by novel experimental methods. Current limitations lie in an incomplete understanding of the potential hidden diversity within the dominant *Ca. H. symbioticus* clade on the bacteria-side, and in a lack of a sponge phenotype in response to microbes on the host-side.

REFERENCES

OF INTRODUCTION AND DISCUSSION

References

- Abisado, R.G., Benomar, S., Klaus, J.R., Dandekar, A.A., and Chandler, J.R. (2018) Bacterial quorum sensing and microbial community interactions. *MBio* **9**: 1–13.
- Adamska, M. and Degnan, B.M. (2008) Analysis of cell movement in *Amphimedon* embryos by injection of fluorescent tracers. *Cold Spring Harb Protoc* **3**: 1–4.
- Alegado, R.A., Brown, L.W., Cao, S., Dermenjian, R.K., Zuzow, R., Fairclough, S.R., et al. (2012) A bacterial sulfonolipid triggers multicellular development in the closest living relatives of animals. *Elife* **2012**: 1–16.
- Amano, S. (1986) Larval release in response to a light signal by the intertidal sponge *Halichondria panicea*. *Biol Bull* **171**: 371–378.
- Anderson, K. V., Jürgens, G., and Nüsslein-Volhard, C. (1985) Establishment of dorsal-ventral polarity in the *Drosophila* embryo: Genetic studies on the role of the Toll gene product. *Cell* **42**: 779–789.
- Angermeier, H., Glöckner, V., Pawlik, J.R., Lindquist, N.L., and Hentschel, U. (2012) Sponge white patch disease affecting the Caribbean sponge *Amphimedon compressa*. *Dis Aquat Organ* **99**: 95–102.
- Angermeier, H., Kamke, J., Abdelmohsen, U.R., Krohne, G., Pawlik, J.R., Lindquist, N.L., and Hentschel, U. (2011) The pathology of sponge orange band disease affecting the Caribbean barrel sponge *Xestospongia muta*. *FEMS Microbiol Ecol* **75**: 218–230.
- Archibald, J.M. (2015) Endosymbiosis and eukaryotic cell evolution. *Curr Biol* **25**: 911–921.
- Augustin, R., Schröder, K., Murillo Rincón, A.P., Fraune, S., Anton-Erxleben, F., Herbst, E., et al. (2017) A secreted antibacterial neuropeptide shapes the microbiome of *Hydra*. *Nat Commun* **8**: 698.
- Baldassano, S.N. and Bassett, D.S. (2016) Topological distortion and reorganized modular structure of gut microbial co-occurrence networks in inflammatory bowel disease. *Sci Rep* **6**: 1–14.
- Bannister, R.J., Battershill, C.N., and de Nys, R. (2012) Suspended sediment grain size and mineralogy across the continental shelf of the Great Barrier Reef: Impacts on the physiology of a coral reef sponge. *Cont Shelf Res* **32**: 86–95.
- Barthel, D. (1986) On the ecophysiology of the sponge *Halichondria panicea* in Kiel Bight. I. Substrate specificity, growth and reproduction. *Mar Ecol Prog Ser* **32**: 291–298.
- Barthel, D. and Detmer, A. (1990) The spermatogenesis of *Halichondria panicea* (Porifera, Demospongiae). *Zoomorphology* **110**: 9–15.
- Barthel, D. and Theede, H. (1986) A new method for the culture of marine sponges and its application for experimental studies. *OPHELIA* **25**: 75–82.
- Bayer, K., Jahn, M.T., Slaby, B.M., Moitinho-Silva, L., and Hentschel, U. (2018) Marine Sponges as *Chloroflexi* hot spots: genomic insights and high-resolution visualization of an abundant and diverse symbiotic clade. *mSystems* **3**: 1–19.
- Bayer, K., Kamke, J., and Hentschel, U. (2014) Quantification of bacterial and archaeal symbionts in high and low microbial abundance sponges using real-time PCR. *FEMS Microbiol Ecol* **89**: 679–690.
- Bayer, K., Schmitt, S., and Hentschel, U. (2008) Physiology, phylogeny and in situ evidence for bacterial and archaeal nitrifiers in the marine sponge *Aplysina aerophoba*. *Environ Microbiol* **10**: 2942–2955.
- Bell, G. (1998) Model metaorganism. *Science* **282**: 248–248.
- Bell, James J., Bennett, H.M., Rovellini, A., and Webster, N.S. (2018) Sponges to be winners under near-future climate scenarios. *Bioscience* **68**: 955–968.
- Bell, James J., Rovellini, A., Davy, S.K., Taylor, M.W., Fulton, E.A., Dunn, M.R., et al. (2018) Climate change alterations to ecosystem dominance: how might sponge-dominated reefs function? *Ecology*. **99**: 1920–1931
- Bi, W.J., Li, D.X., Xu, Y.H., Xu, S., Li, J., Zhao, X.F., and Wang, J.X. (2015) Scavenger receptor B protects shrimp from bacteria by enhancing phagocytosis and regulating expression of antimicrobial peptides. *Dev Comp Immunol* **51**: 10–21.
- Bosch, T.C.G. (2014) Rethinking the role of immunity: Lessons from *Hydra*. *Trends Immunol* **35**: 495–502.
- Bosch, T.C.G., Guillemin, K., and McFall-Ngai, M. (2019) Evolutionary “experiments” in symbiosis: The study of model animals provides insights into the mechanisms underlying the diversity of host–microbe interactions. *BioEssays* **41**: 1–8.
- Bosch, T.C.G. and McFall-Ngai, M. (2021) Animal development in the microbial world: Re-thinking the conceptual framework. *Curr Top Dev Biol* **141**: 371–397
- Bosch, T.C.G. and Mcfall-ngai, M.J. (2011) Metaorganisms as the new frontier. *Zoology* **114**: 185–190.
- Brennan, J.J. and Gilmore, T.D. (2018) Evolutionary origins of toll-like receptor signaling. *Mol Biol Evol* **35**: 1576–1587.
- Brennan, J.J., Messerschmidt, J.L., Williams, L.M., Matthews, B.J., Reynoso, M., and Gilmore, T.D. (2017) Sea anemone model has a single Toll-like receptor that can function in pathogen detection, NF-κB signal transduction, and development. *Proc Natl Acad Sci* **114**: 10122–10131.

References

- Britstein, M., Cerrano, C., Burgsdorf, I., Zoccarato, L., Kenny, N.J., Riesgo, A., et al. (2020) Sponge microbiome stability during environmental acquisition of highly specific photosymbionts. *Environ Microbiol* **22**: 3593–3607.
- Brown, G.D., Willment, J.A., and Whitehead, L. (2018) C-type lectins in immunity and homeostasis. *Nat Rev Immunol* **18**: 374–389.
- Bucher, M., Wolfowicz, I., Voss, P.A., Hambleton, E.A., and Guse, A. (2016) Development and symbiosis establishment in the cnidarian endosymbiosis model *Aiptasia* sp. *Sci Rep* **6**: 1–11.
- Buckley, K.M. and Rast, J.P. (2015) Diversity of animal immune receptors and the origins of recognition complexity in the deuterostomes. *Dev Comp Immunol* **49**: 179–189.
- Bufe, B. and Zufall, F. (2016) The sensing of bacteria: Emerging principles for the detection of signal sequences by formyl peptide receptors. *Biomol Concepts* **7**: 205–214.
- Burgsdorf, I., Slaby, B.M., Handley, K.M., Haber, M., Blom, J., Marshall, C.W., and Gilbert, J. a (2015) Lifestyle evolution in cyanobacterial symbionts of sponges. *MBio* **6**: 1–14.
- Busch, K., Beazley, L., Kenchington, E., Whoriskey, F., Slaby, B.M., and Hentschel, U. (2020) Microbial diversity of the glass sponge *Vazella pourtalesii* in response to anthropogenic activities. *Conserv Genet* **21**: 1001–1010.
- Calcino, A.D., Fernandez-Valverde, S.L., Taft, R.J., and Degnan, B.M. (2018) Diverse RNA interference strategies in early-branching metazoans. *BMC Evol Biol* **18**: 1–13.
- De Caralt, S., Agell, G., and Uriz, M.J. (2003) Long-term culture of sponge explants: Conditions enhancing survival and growth, and assessment of bioactivity. *Biomol Eng* **20**: 339–347.
- Carrier, T.J. and Reitzel, A.M. (2018) Convergent shifts in host-associated microbial communities across environmentally elicited phenotypes. *Nat Commun* **9**:952.
- Cavalcanti, G.S., Alker, A.T., Delherbe, N., Malter, K.E., and Shikuma, N.J. (2020) The influence of bacteria on animal metamorphosis. *Annu Rev Microbiol* **74**: 137–158.
- Chaib De Mares, M., Sipkema, D., Huang, S., Bunk, B., Overmann, J., van Elsas, J.D., et al. (2017) Host specificity for bacterial, archaeal and fungal communities determined for high- and low-microbial abundance sponge species in two genera. *Front Microbiol* **8**: 1–13.
- Chen, L., Collij, V., Jaeger, M., van den Munckhof, I.C.L., Vich Vila, A., Kurilshikov, A., et al. (2020) Gut microbial co-abundance networks show specificity in inflammatory bowel disease and obesity. *Nat Commun* **11**: 1–12.
- Chu, H. and Mazmanian, S.K. (2013) Innate immune recognition promotes symbiosis. *Nat Immunol* **14**: 668–675.
- Conaco, C., Neveu, P., Zhou, H., Arcila, M.L., Degnan, S.M., Degnan, B.M., and Kosik, K.S. (2012) Transcriptome profiling of the demosponge *Amphimedon queenslandica* reveals genome-wide events that accompany major life cycle transitions. *BMC Genomics* **13**:209.
- Conkling, M., Hesp, K., Munroe, S., Sandoval, K., Martens, D.E., Sipkema, D., et al. (2019) Breakthrough in marine invertebrate cell culture: sponge cells divide rapidly in improved nutrient medium. *Sci Rep* **9**: 1–10.
- Costa, R.M., Cárdenas, A., Loussert-Fonta, C., Toullec, G., Meibom, A., and Voolstra, C.R. (2021) Surface topography, bacterial carrying capacity, and the prospect of microbiome manipulation in the sea anemone coral model *Aiptasia*. *Front Microbiol* **12**: 1–16.
- Coyte, K.Z. and Rakoff-Nahoum, S. (2019) Understanding competition and cooperation within the mammalian gut microbiome. *Curr Biol* **29**: 538–544.
- Coyte, K.Z., Schluter, J., and Foster, K.R. (2015) The ecology of the microbiome: Networks, competition, and stability. *Science* **350**: 663–666.
- Darling, T.K. and Lamb, T.J. (2019) Emerging roles for Eph receptors and ephrin ligands in immunity. *Front Immunol* **10**: 1–15.
- Degnan, B.M., Adamska, M., Craigie, A., Degnan, S.M., Fahey, B., Gauthier, M., et al. (2008) The demosponge *Amphimedon queenslandica*: Reconstructing the ancestral metazoan genome and deciphering the origin of animal multicellularity. *Cold Spring Harb Protoc* **3**: 1–6.
- Degnan, S.M. (2015) The surprisingly complex immune gene repertoire of a simple sponge, exemplified by the NLR genes: A capacity for specificity? *Dev Comp Immunol* **48**: 269–274.
- Degnan, S.M. and Degnan, B.M. (2010) The initiation of metamorphosis as an ancient polyphenic trait and its role in metazoan life-cycle evolution. *Philos Trans R Soc B Biol Sci* **365**: 641–651.
- Dierking, K. and Pita, L. (2020) Receptors mediating host-microbiota communication in the metaorganism: The invertebrate perspective. *Front Immunol* **11**: 1–17.
- Dittami, S.M., Arboleda, E., Auguet, J.-C., Bigalke, A., Briand, E., Cárdenas, P., et al. (2020) A community perspective on the concept of marine holobionts : current status, challenges, and future directions. *PeerJ* **27519**:1-30.
- Domin, H., Zurita-Gutiérrez, Y.H., Scotti, M., Buttlar, J., Hentschel Humeida, U., and Fraune, S. (2018) Predicted

References

- bacterial interactions affect *in vivo* microbial colonization dynamics in *Nematostella*. *Front Microbiol* **9**: 1–12.
- Douglas, A.E. (2019) Simple animal models for microbiome research. *Nat Rev Microbiol* **17**: 764–775.
- Duckworth, A. (2009) Farming sponges to supply bioactive metabolites and bath sponges: A review. *Mar Biotechnol* **11**: 669–679.
- Duckworth, A. and Battershill, C. (2003) Sponge aquaculture for the production of biologically active metabolites: The influence of farming protocols and environment. *Aquaculture* **221**: 311–329.
- Duffy, D. (2020) Understanding immune variation for improved translational medicine. *Curr Opin Immunol* **65**: 83–88.
- Engel, P., Martinson, V.G., and Moran, N.A. (2012) Functional diversity within the simple gut microbiota of the honey bee. *Proc Natl Acad Sci U S A* **109**: 11002–11007.
- Ericson, C.F., Eisenstein, F., Medeiros, J.M., Malter, K.E., Cavalcanti, G.S., Zeller, R.W., et al. (2019) A contractile injection system stimulates tubeworm metamorphosis by translocating a proteinaceous effector. *Elife* **8**: 1–19.
- Erpenbeck, D., Knowlton, A.L., Talbot, S.L., Highsmith, R.C., and Van Soest, R.W. (2004) A molecular comparison of Alaskan and Northeast Atlantic *Halichondria panicea* (Pallas 1766)(Porifera: Demospongiae) populations. *Boll Mus Ist Univ Genova* **61**: 319–325.
- Faith, J.J., Rey, F.E., O'Donnell, D., Karlsson, M., McNulty, N.P., Kallstrom, G., et al. (2010) Creating and characterizing communities of human gut microbes in gnotobiotic mice. *ISME J* **4**: 1094–1098.
- Fan, L., Liu, M., Simister, R., Webster, N.S., and Thomas, T. (2013) Marine microbial symbiosis heats up: the phylogenetic and functional response of a sponge holobiont to thermal stress. *ISME J* **7**: 991–1002.
- Fan, L., Reynolds, D., Liu, M., Stark, M., Kjelleberg, S., Webster, N.S., and Thomas, T. (2012) Functional equivalence and evolutionary convergence in complex communities of microbial sponge symbionts. *Proc Natl Acad Sci* **109**: 1878–1887.
- Faust, K., Sathirapongsasuti, J.F., Izard, J., Segata, N., Gevers, D., Raes, J., and Huttenhower, C. (2012) Microbial co-occurrence relationships in the Human Microbiome. *PLoS Comput Biol* **8**: e1002606.
- Fernandez-Valverde, S.L., Calcino, A.D., and Degnan, B.M. (2015) Deep developmental transcriptome sequencing uncovers numerous new genes and enhances gene annotation in the sponge *Amphimedon queenslandica*. *BMC Genomics* **16**: 1–11.
- Fiebigler, U., Bereswill, S., and Heimesaat, M.M. (2016) Dissecting the interplay between intestinal microbiota and host immunity in health and disease: Lessons learned from germfree and gnotobiotic animal models. *Eur J Microbiol Immunol* **6**: 253–271.
- Fieth, R.A., Gauthier, M.A., Bayes, J., Green, K.M., and Degnan, S.M. (2016) Ontogenetic changes in the bacterial symbiont community of the tropical demosponge *Amphimedon queenslandica*: Metamorphosis is a new beginning. *Front Mar Sci* **3**: 1–20.
- Franklin, C.L. and Ericsson, A.C. (2017) Microbiota and reproducibility of rodent models. *Lab Anim (NY)* **46**: 114–122.
- Franzenburg, S., Fraune, S., Kunzel, S., Baines, J.F., Domazet-Loso, T., and Bosch, T.C.G. (2012) MyD88-deficient *Hydra* reveal an ancient function of TLR signaling in sensing bacterial colonizers. *Proc Natl Acad Sci* **109**: 19374–19379.
- Fraune, S., Anton-Erxleben, F., Augustin, R., Franzenburg, S., Knop, M., Schröder, K., et al. (2015) Bacteria–bacteria interactions within the microbiota of the ancestral metazoan *Hydra* contribute to fungal resistance. *ISME J* **9**: 1543–1556.
- Friedrich, A.B., Fischer, I., and Proksch, P. (2001) Temporal variation of the microbial community associated with the mediterranean sponge *Aplysina aerophoba*. *FEMS Microbiol Ecol* **38**: 105–113.
- Fuqua, W.C., Winans, S.C., and Greenberg, E.P. (1994) Quorum sensing in bacteria: The LuxR-LuxI family of cell density-responsive transcriptional regulators. *J Bacteriol* **176**: 269–275.
- Futo, M., Opašić, L., Koska, S., Corak, N., Široki, T., Ravikumar, V., et al. (2021) Embryo-like features in developing *Bacillus subtilis* biofilms. *Mol Biol Evol* **38**: 31–47.
- Gardères, J., Bourguet-Kondracki, M.L., Hamer, B., Batel, R., Schröder, H.C., and Müller, W.E.G. (2015) Porifera lectins: Diversity, physiological roles and biotechnological potential. *Mar Drugs* **13**: 5059–5101
- Gauthier, M. and Degnan, B.M. (2008) Partitioning of genetically distinct cell populations in chimeric juveniles of the sponge *Amphimedon queenslandica*. *Dev Comp Immunol* **32**: 1270–1280.
- Gauthier, M.A., Watson, J.R., and Degnan, S.M. (2016) Draft genomes shed light on the dual bacterial symbiosis that dominates the microbiome of the coral reef sponge *Amphimedon queenslandica*. *Front Mar Sci* **3**: 1–18.
- Gauthier, M.E.A., Du Pasquier, L., and Degnan, B.M. (2010) The genome of the sponge *Amphimedon*

References

- queenslandica* provides new perspectives into the origin of Toll-like and interleukin 1 receptor pathways. *Evol Dev* **12**: 519–533.
- Geier, B., Sogin, E.M., Michellod, D., Janda, M., Kompauer, M., Spengler, B., et al. (2020) Spatial metabolomics of in situ host–microbe interactions at the micrometre scale. *Nat Microbiol* **5**: 498–510.
- Gerasimova, E. and Ereskovsky, A. (2007) Reproduction of two species of *Halichondria* (Demospongiae: Halichondriidae) in the White Sea. *Porifera Res Biodiversity, Innov Sustain* 327–333.
- Germer, J., Cerveau, N., and Jackson, D.J. (2017) The holo-transcriptome of a calcified early branching metazoan. *Front Mar Sci* **4**: 1–19.
- Gilbert, S.F., Sapp, J., and Tauber, A.I. (2012) A symbiotic view of life: We have never been individuals. *Q Rev Biol* **87**: 325–341.
- Gloeckner, V., Lindquist, N., Schmitt, S., and Hentschel, U. (2013) *Ectyoplasia ferox*, an experimentally tractable model for vertical microbial transmission in marine sponges. *Microb Ecol* **65**: 462–474.
- Gloeckner, V., Wehrl, M., Moitinho-silva, L., Schupp, P., Pawlik, J.R., Lindquist, N.L., et al. (2014) The HMA-LMA dichotomy revisited : an electron microscopical survey of 56 sponge species. *Biol Bull* **227**: 78–88.
- De Goeij, J.M., Van Oevelen, D., Vermeij, M.J.A., Osinga, R., Middelburg, J.J., De Goeij, A.F.P.M., and Admiraal, W. (2013) Surviving in a marine desert: The sponge loop retains resources within coral reefs. *Science* **342**: 108–110.
- Gökalp, M., Mes, D., Nederlof, M., Zhao, H., Merijn de Goeij, J., and Osinga, R. (2021) The potential roles of sponges in integrated mariculture. *Rev Aquac* **13**: 1159–1171.
- Gräwe, U., Friedland, R., and Burchard, H. (2013) The future of the western Baltic Sea: Two possible scenarios. *Ocean Dyn* **63**: 901–921.
- Grice, L.F., Gauthier, M.E.A., Roper, K.E., Fernández-Busquets, X., Degnan, S.M., and Degnan, B.M. (2017) Origin and evolution of the sponge aggregation factor gene family. *Mol Biol Evol* **34**: 1083–1099.
- Gutleben, J., Chaib De Mares, M., van Elsas, J.D., Smidt, H., Overmann, J., and Sipkema, D. (2018) The multi-omics promise in context: from sequence to microbial isolate. *Crit Rev Microbiol* **44**: 212–229.
- Gutleben, J., Loureiro, C., Ramírez Romero, L.A., Shetty, S., Wijffels, R.H., Smidt, H., and Sipkema, D. (2020) Cultivation of bacteria from *Aplysina aerophoba*: effects of oxygen and nutrient gradients. *Front Microbiol* **11**: 1–19.
- Hadas, E., Shpigel, M., and Ilan, M. (2009) Particulate organic matter as a food source for a coral reef sponge. *J Exp Biol* **212**: 3643–3650.
- Hansson, D. and Gustafsson, E. (2011) Salinity and hypoxia in the Baltic Sea since A.D. 1500. *J Geophys Res Ocean* **116**: 1–9.
- Hentschel, U., Fieseler, L., Wehrl, M., Gernert, C., Steinert, M., Hacker, J., and Horn, M. (2003) Microbial diversity of marine sponges. *Prog Mol Subcell Biol* **37**: 59–88.
- Hentschel, U., Piel, J., Degnan, S.M., and Taylor, M.W. (2012) Genomic insights into the marine sponge microbiome. *Nat Rev Microbiol* **10**: 641–654.
- Hentschel, U., Usher, K.M., and Taylor, M.W. (2006) Marine sponges as microbial fermenters. *FEMS Microbiol Ecol* **55**: 167–177.
- Hildebrand, F., Moitinho-Silva, L., Blasche, S., Jahn, M.T., Gossmann, T.I., Huerta-Cepas, J., et al. (2019) Antibiotics-induced monodominance of a novel gut bacterial order. *Gut* **68**: 1781–1790.
- Jackson, D., Leys, S.P., Hinman, V.F., Woods, R., Lavin, M.F., and Degnan, B.M. (2002) Ecological regulation of development: Induction of marine invertebrate metamorphosis. *Int J Dev Biol* **46**: 679–686.
- Jahn, M.T., Arkhipova, K., Markert, S.M., Stigloher, C., Lachnit, T., Pita, L., et al. (2019) A phage protein aids bacterial symbionts in eukaryote immune evasion. *Cell Host Microbe* **26**:1–9.
- Jaspers, C., Weiland-Bräuer, N., Fischer, M.A., Künzel, S., Schmitz, R.A., and Reusch, T.B.H. (2019) Microbiota differences of the comb jelly *Mnemiopsis leidyi* in native and invasive sub-populations. *Front Mar Sci* **6**: 1–9.
- Johnke, J., Dirksen, P., and Schulenburg, H. (2020) Community assembly of the native *C. elegans* microbiome is influenced by time, substrate and individual bacterial taxa. *Environ Microbiol* **22**: 1265–1279.
- de Jonge, P.A., Nobrega, F.L., Brouns, S.J.J., and Dutilh, B.E. (2019) Molecular and evolutionary determinants of bacteriophage host range. *Trends Microbiol* **27**: 51–63.
- Ju, T., Shoblak, Y., Gao, Y., Yang, K., Fohse, J., Finlay, B.B., et al. (2017) Initial gut microbial composition as a key factor driving host response to antibiotic treatment, as exemplified by the presence or absence of commensal *Escherichia coli*. *Appl Environ Microbiol* **83**: 1–15.
- Kauffman, K.M., Hussain, F.A., Yang, J., Arevalo, P., Brown, J.M., Chang, W.K., et al. (2018) A major lineage of non-tailed dsDNA viruses as unrecognized killers of marine bacteria. *Nature* **554**: 118–122.
- Khalaman, V. V, Mukhina, Y.I., and Komendantov, A.Y. (2011) The effects of the excretory – secretory products

References

- of fouling organisms on settlement of larvae of the sponge *Halichondria panicea* (Pallas, 1766) (Porifera: Demospongiae). *Russ J Mar Biol* **37**: 494–500.
- Kim, H.J., Jun, J.W., Giri, S.S., Kim, S.G., Kim, S.W., Kwon, J., et al. (2020) Bacteriophage cocktail for the prevention of multiple-antibiotic-resistant and mono-phage-resistant *Vibrio coralliilyticus* infection in Pacific oyster (*Crassostrea gigas*) larvae. *Pathogens* **9**: 1–10.
- Knobloch, S., Jóhannsson, R., and Marteinson, V. (2019a) Bacterial diversity in the marine sponge *Halichondria panicea* from Icelandic waters and host-specificity of its dominant symbiont “*Candidatus Halichondriabacter symbioticus*.” *FEMS Microbiol Ecol* **95**: 1–13.
- Knobloch, S., Jóhannsson, R., and Marteinson, V. (2019b) Co-cultivation of the marine sponge *Halichondria panicea* and its associated microorganisms. *Sci Rep* **9**: 1–11.
- Knobloch, S., Jóhannsson, R., and Marteinson, V.P. (2020) Genome analysis of sponge symbiont ‘*Candidatus Halichondriabacter symbioticus*’ shows genomic adaptation to a host-dependent lifestyle. *Environ Microbiol* **22**: 483–498.
- Kolodny, O., Callahan, B.J., and Douglas, A.E. (2020) The role of the microbiome in host evolution. *Philos Trans R Soc Lond B Biol Sci* **375**: 20190588.
- Kolodny, O. and Schulenburg, H. (2020) Microbiome-mediated plasticity directs host evolution along several distinct time scales: Microbiome influence on host evolution. *Philos Trans R Soc B Biol Sci* **375**: 20190589.
- Krishnan, A., Degnan, B.M., and Degnan, S.M. (2019) The first identification of complete Eph-ephrin signalling in ctenophores and sponges reveals a role for neofunctionalization in the emergence of signalling domains. *BMC Evol Biol* **19**: 1–17.
- Krishnan, A., Dnyansagar, R., Almén, M.S., Williams, M.J., Fredriksson, R., Manoj, N., and Schiöth, H.B. (2014) The GPCR repertoire in the demosponge *Amphimedon queenslandica*: insights into the GPCR system at the early divergence of animals. *BMC Evol Biol* **14**: 1–16.
- Kumala, L. and Canfield, D.E. (2018) Contraction dynamics and respiration of small single-ostium explants of the demosponge *Halichondria panicea*. *Front Mar Sci* **5**: 1–34.
- Kumala, L., Larsen, M., Glud, R.N., and Canfield, D.E. (2021) Spatial and temporal anoxia in single-ostium *Halichondria panicea* demosponge explants studied with planar optodes. *Mar Biol* **168**: 1–13.
- Kumala, L., Riisgard, H.U., and Canfield, D.E. (2017) Ostium dynamics and filtration activity in small single-ostium explants of the demosponge *Halichondria panicea*. *Mar Ecol Prog Ser* **572**: 117–128.
- Laffy, P.W., Wood-Charlson, E.M., Turaev, D., Jutz, S., Pascelli, C., Botté, E.S., et al. (2018) Reef invertebrate viromics: diversity, host specificity and functional capacity. *Environ Microbiol* **20**: 2125–2141.
- Lavrov, A.I. and Kosevich, I.A. (2016) Sponge cell reaggregation: Cellular structure and morphogenetic potencies of multicellular aggregates. *J Exp Zool Part A Ecol Genet Physiol* **325**: 158–177.
- Lavrov, A.I. and Kosevich, I.A. (2018) Stolonial Movement: A new type of whole-organism behavior in Porifera. *Biol Bull* **234**: 1–10.
- Leigh, B.A., Liberti, A., and Dishaw, L.J. (2016) Generation of germ-free *Ciona intestinalis* for studies of gut-microbe interactions. *Front Microbiol* **7**: 1–8.
- Lesser, M.P., Fiore, C., Slattery, M., and Zaneveld, J. (2016) Climate change stressors destabilize the microbiome of the Caribbean barrel sponge, *Xestospongia muta*. *J Exp Mar Bio Ecol* **475**: 11–18.
- Lewis, W.H., Tahon, G., Geesink, P., Sousa, D.Z., and Ettema, T.J.G. (2020) Innovations to culturing the uncultured microbial majority. *Nat Rev Microbiol* **19**: 225–240.
- Leys, S.P., Larroux, C., Gauthier, M., Adamska, M., Fahey, B., Richards, G.S., et al. (2008) Isolation of *Amphimedon* developmental material. *Cold Spring Harb Protoc* **3**: 1–5.
- Li, C.W., Chen, J.Y., and Hua, T.E. (1998) Precambrian sponges with cellular structures. *Science* **279**: 879–882.
- Luter, H.M. and Webster, N.S. (2017) Sponge disease and climate change. In *Climate Change, Ocean Acidification and Sponges: Impacts Across Multiple Levels of Organization*. Carballo, J.L. and Bell, J.J. (eds). *Springer International Publishing*, pp. 1–452.
- Luter, H.M., Whalan, S., and Webster, N.S. (2012) Thermal and sedimentation stress are unlikely causes of brown spot syndrome in the Coral Reef sponge, *lanthella basta*. *PLoS One* **7**: 1–9.
- Maldonado, M., Aguilar, R., Bannister, R.J., James, J., Conway, K.W., Dayton, P.K., et al. (2016) Sponge grounds as key marine habitats: a synthetic review of types, structure, functional roles and conservation concerns. In: *Marine animal forests: The ecology of benthic biodiversity hotspots*. (Rossi, Bramanti, Gori, Orejas Saco del Valle eds.) *Springer International Publishing*.
- Maldonado, M., Giraud, K., and Carmona, C. (2008) Effects of sediment on the survival of asexually produced sponge recruits. *Mar Biol* **154**: 631–641.
- Margulis, L. (1970) Origin of eukaryotic cells: Evidence and research implications for a theory of the origin and evolution of microbial, plant and animal cells on the precambrian Earth, *Yale University Press*.

References

- Marques, A., Ollevier, F., Verstraete, W., Sorgeloos, P., and Bossier, P. (2006) Gnotobiotically grown aquatic animals: Opportunities to investigate host-microbe interactions. *J Appl Microbiol* **100**: 903–918.
- McFall-Ngai, M., Hadfield, M.G., Bosch, T.C.G., Carey, H. V., Domazet-Lošo, T., Douglas, A.E., et al. (2013) Animals in a bacterial world, a new imperative for the life sciences. *Proc Natl Acad Sci* **110**: 3229–3236.
- Melancon, E., Gomez De La Torre Canny, S., Sichel, S., Kelly, M., Wiles, T.J., Rawls, J.F., et al. (2017) Best practices for germ-free derivation and gnotobiotic zebrafish husbandry. *Methods Cell Biol* **38**: 1–22.
- Mergaert, P. (2018) Role of antimicrobial peptides in controlling symbiotic bacterial populations. *Nat Prod Rep* **35**: 336–356.
- Mohamed, N.M., Cicirelli, E.M., Kan, J., Chen, F., Fuqua, C., and Hill, R.T. (2008) Diversity and quorum-sensing signal production of Proteobacteria associated with marine sponges. *Environ Microbiol* **10**: 75–86.
- Mohamed, N.M., Rao, V., Hamann, M.T., Kelly, M., and Hill, R.T. (2008) Monitoring bacterial diversity of the marine sponge *Ircinia strobilina* upon transfer into aquaculture. *Appl Environ Microbiol* **74**: 4133–4143.
- Moitinho-Silva, L., Steinert, G., Nielsen, S., Hardoim, C.C.P., Wu, Y.C., McCormack, G.P., et al. (2017) Predicting the HMA-LMA status in marine sponges by machine learning. *Front Microbiol* **8**: 1–14.
- Morgan, R., Sundin, J., Finnøen, M.H., Dresler, G., Vendrell, M.M., Dey, A., et al. (2019) Are model organisms representative for climate change research? Testing thermal tolerance in wild and laboratory zebrafish populations. *Conserv Physiol* **7**: 1–11.
- Morganti, T., Coma, R., Yahel, G., and Ribes, M. (2017) Trophic niche separation that facilitates co-existence of high and low microbial abundance sponges is revealed by in situ study of carbon and nitrogen fluxes. *Limnol Oceanogr* **62**: 1963–1983.
- Moroz, L.L., Kocot, K.M., Citarella, M.R., Dosung, S., Norekian, T.P., Povolotskaya, I.S., et al. (2014) The ctenophore genome and the evolutionary origins of neural systems. *Nature* **510**: 109–114.
- Mortzfeld, B.M., Urbanski, S., Reitzel, A.M., Künzel, S., Technau, U., and Fraune, S. (2016) Response of bacterial colonization in *Nematostella vectensis* to development, environment and biogeography. *Environ Microbiol* **18**: 1764–1781.
- Moyer, A.M., Matey, E.T., and Miller, V.M. (2019) Individualized medicine: Sex, hormones, genetics, and adverse drug reactions. *Pharmacol Res Perspect* **7**: e00541.
- Musser, J.M., Schippers, K.J., Nickel, M., Mizzon, G., Kohn, A.B., Pape, C., et al. (2021) Profiling cellular diversity in sponges informs animal cell type and nervous system evolution. *Science* **723**: 717–723.
- Nedashkovskaya, O.I., Kukhlevskiy, A.D., Zhukova, N. V., and Kim, S.B. (2016) *Amylibacter ulvae* sp. nov., a new alphaproteobacterium isolated from the Pacific green alga *Ulva fenestrata*. *Arch Microbiol* **198**: 251–256.
- Ng, K.M., Ferreyra, J.A., Higginbottom, S.K., Lynch, J.B., Kashyap, P.C., Gopinath, S., et al. (2013) Microbiota-liberated host sugars facilitate post-antibiotic expansion of enteric pathogens. *Nature* **502**: 96–99.
- Nielsen, C. (2019) Early animal evolution: A morphologist's view. *R Soc Open Sci* **6**: 190638.
- Nyholm, S. V. and McFall-Ngai, M.J. (2021) A lasting symbiosis: how the Hawaiian bobtail squid finds and keeps its bioluminescent bacterial partner. *Nat Rev Microbiol* **19**: 666–679.
- Nyholm, S. V. and Graf, J. (2012) Knowing your friends : invertebrate innate immunity fosters beneficial bacterial symbioses. *Nat Rev Microbiol* **10**: 815–827.
- Osinga, R., de Beukelaer, P.B., Meijer, E.M., Tramper, J., and Wijffels, R.H. (1999) Growth of the sponge *Pseudosuberites* (aft.) *andrewsi* in a closed system. *Prog Ind Microbiol* **35**: 155–161.
- Osinga, R., Kleijn, R., Groenendijk, E., Niesink, P., Tramper, J., and Wijffels, R.H. (2001) Development of *in vivo* sponge cultures: Particle feeding by the tropical sponge *Pseudosuberites* aff. *andrewsi*. *Mar Biotechnol* **3**: 544–554.
- Osinga, R., Tramper, J., and Wijffels, R.H. (1999) Cultivation of marine sponges. *Mar Biotechnol* **1**: 509–532.
- Pancer, Z. (2000) Dynamic expression of multiple scavenger receptor cysteine-rich genes in coelomocytes of the purple sea urchin. *Proc Natl Acad Sci U S A* **97**: 13156–13161.
- Pande, S. and Kost, C. (2017) Bacterial unculturability and the formation of intercellular metabolic networks. *Trends Microbiol* **25**: 349–361.
- Parker, K.D., Albeke, S.E., Gigley, J.P., Goldstein, A.M., and Ward, N.L. (2018) Microbiome composition in both wild-type and disease model mice is heavily influenced by mouse facility. *Front Microbiol* **9**: 1–13.
- Pees, B., Yang, W., Zárate-Potes, A., Schulenburg, H., and Dierking, K. (2016) High innate immune specificity through diversified C-type lectin-like domain proteins in invertebrates. *J Innate Immun* **8**: 129–142.
- Pham, L.N., Kanther, M., Semova, I., and Rawls, J.F. (2008) Methods for generating and colonizing gnotobiotic zebrafish. *Nat Protoc* **3**: 1862–1875.
- Pita, L., Fraune, S., and Hentschel, U. (2016) Emerging sponge models of animal-microbe symbioses. *Front Microbiol* **7**: 1–8.
- Pita, Lucia, Hoepfner, M.P., Ribes, M., and Hentschel, U. (2018a) Differential expression of immune receptors in

References

- two marine sponges upon exposure to microbial-associated molecular patterns. *Sci Rep* **8**: 1–15.
- Pita, L., Rix, L., Slaby, B.M., Franke, A., and Hentschel, U. (2018b) The sponge holobiont in a changing ocean: from microbes to ecosystems. *Microbiome* **6**: 46.
- Podbielski, I., Bock, C., Lenz, M., and Melzner, F. (2016) Using the critical salinity (S crit) concept to predict invasion potential of the anemone *Diadumene lineata* in the Baltic Sea. *Mar Biol* **163**: 1–15.
- Poppell, E., Weisz, J., Spicer, L., Massaro, A., Hill, A., and Hill, M. (2014) Sponge heterotrophic capacity and bacterial community structure in high- and low-microbial abundance sponges. *Mar Ecol* **35**: 414–424.
- Pozzolini, M., Gallus, L., Ghignone, S., Ferrando, S., Candiani, S., Bozzo, M., et al. (2019) Insights into the evolution of metazoan regenerative mechanisms: Roles of TGF superfamily members in tissue regeneration of the marine sponge *Chondrosia reniformis*. *J Exp Biol* **222**: 1–17.
- Pujol, N., Link, E.M., Liu, L.X., Kurz, C.L., Alloing, G., Tan, M.W., et al. (2001) A reverse genetic analysis of components of the Toll signaling pathway in *Caenorhabditis elegans*. *Curr Biol* **11**: 809–821.
- Rakoff-Nahoum, S., Foster, K.R., and Comstock, L.E. (2016) The evolution of cooperation within the gut microbiota. *Nature* **533**: 255–259.
- Reiswig, H. (1981) Partial carbon and energy budgets of the bacteriosponge *Verongia* in Barbados. *Mar Ecol* **2**: 273–293.
- Reiswig, H. (1971) Particle feeding in natural populations of three marine Demosponges. *Biol Bull* **141**: 568–591.
- Reiswig, H.M. (1971) In situ pumping activities of tropical Demospongiae. *Mar Biol* **9**: 38–50.
- Reiswig, H.M. (1975) The aquiferous systems of three Marine Demospongiae. *Morphology* **145**: 493–502.
- Revilla-I-Domingo, R., Schmidt, C., Zifko, C., and Raible, F. (2018) Establishment of transgenesis in the demosponge *Suberites domuncula*. *Genetics* **210**: 435–443.
- Ribes, M., Coma, R., and Gili, J.M. (1999) Natural diet and grazing rate of the temperate sponge *Dysidea avara* (Demospongiae, Dendroceratida) throughout an annual cycle. *Mar Ecol Prog Ser* **176**: 179–190.
- Richardson, C., Hill, M., Marks, C., Runyen-Janecky, L., and Hill, A. (2012) Experimental manipulation of sponge/bacterial symbiont community composition with antibiotics: Sponge cell aggregates as a unique tool to study animal/microorganism symbiosis. *FEMS Microbiol Ecol* **81**: 407–418.
- Riesgo, A., Farrar, N., Windsor, P.J., Giribet, G., and Leys, S.P. (2014) The analysis of eight transcriptomes from all poriferan classes reveals surprising genetic complexity in sponges. *Mol Biol Evol* **31**: 1102–1120.
- Riisgård, H.U., Kumala, L., and Charitonidou, K. (2016) Using the F/R-ratio for an evaluation of the ability of the demosponge *Halichondria panicea* to nourish solely on phytoplankton versus free-living bacteria in the sea. *Mar Biol Res* **12**: 907–916.
- Rinke, C., Schwientek, P., Sczyrba, A., Ivanova, N.N., Anderson, I.J., Cheng, J.F., et al. (2013) Insights into the phylogeny and coding potential of microbial dark matter. *Nature* **499**: 431–437.
- Rivera, A.S., Hammel, J.U., Haen, K.M., Danka, E.S., Cieniewicz, B., Winters, I.P., et al. (2011) RNA interference in marine and freshwater sponges: Actin knockdown in *Tethya wilhelma* and *Ephydatia muelleri* by ingested dsRNA expressing bacteria. *BMC Biotechnol* **11**: 67.
- Rix, L., Ribes, M., Coma, R., Jahn, M.T., de Goeij, J.M., van Oevelen, D., et al. (2020) Heterotrophy in the earliest gut: a single-cell view of heterotrophic carbon and nitrogen assimilation in sponge-microbe symbioses. *ISME J* **14**: 2554–2567.
- Rosenstiel, P., Philipp, E.E.R., Schreiber, S., and Bosch, T.C.G. (2009) Evolution and function of innate immune receptors - Insights from marine invertebrates. *J Innate Immun* **1**: 291–300.
- Ryu, T., Seridi, L., Moitinho-Silva, L., Oates, M., Liew, Y.J., Mavromatis, C., et al. (2016) Hologenome analysis of two marine sponges with different microbiomes. *BMC Genomics* **17**: 1–11.
- Say, T.E. and Degnan, S.M. (2020) Molecular and behavioural evidence that interdependent photo - and chemosensory systems regulate larval settlement in a marine sponge. *Mol Ecol* **29**: 247–261.
- Schalchian-Tabrizi, K., Minge, M.A., Espelund, M., Orr, R., Ruden, T., Jakobsen, K.S., and Cavalier-Smith, T. (2008) Multigene phylogeny of *Choanozoa* and the origin of animals. *PLoS One* **3**: e2098.
- Schellenberg, J., Reichert, J., Hardt, M., Klingelhöfer, I., Morlock, G., Schubert, P., et al. (2020) The bacterial microbiome of the long-term aquarium cultured high-microbial abundance sponge *Haliclona cnidata* – sustained bioactivity despite community shifts under detrimental conditions. *Front Mar Sci* **7**: 266.
- Schippers, K.J. (2013) Sponge cell culture.
- Schmittmann, L., Jahn, M.T., Pita, L., and Hentschel, U. (2020) Decoding cellular dialogues between sponges, bacteria, and phages. In: Cellular dialogues in the holobiont (Bosch and Hadfield eds.) *CRC Press* 49–63.
- Schmittmann, L., Pita, L., and Franzenburg, S. (2021) Individuality in the immune repertoire and induced response of the sponge *Halichondria panicea*. *Front Immunol* **12**: 1–13.
- Schulenburg, H., Boehnisch, C., and Michiels, N.K. (2007) How do invertebrates generate a highly specific innate immune response? *Mol Immunol* **44**: 3338–3344.

References

- Sebé-Pedrós, A., Chomsky, E., Pang, K., Lara-Astiaso, D., Gaiti, F., Mukamel, Z., et al. (2018) Early metazoan cell type diversity and the evolution of multicellular gene regulation. *Nat Ecol Evol* **2**: 1176–1188.
- Sharon, G., Sampson, T.R., Geschwind, D.H., and Mazmanian, S.K. (2016) The central nervous system and the gut microbiome. *Cell* **167**: 915–932.
- Shikuma, N.J., Antoshechkin, I., Medeiros, J.M., Pilhofer, M., and Newman, D.K. (2016) Stepwise metamorphosis of the tubeworm *Hydroides elegans* is mediated by a bacterial inducer and MAPK signaling. *Proc Natl Acad Sci U S A* **113**: 10097–10102.
- Simion, P., Philippe, H., Baurain, D., Jager, M., Richter, D.J., Di Franco, A., et al. (2017) A large and consistent phylogenomic dataset supports sponges as the sister group to all other animals. *Curr Biol* **27**: 958–967.
- Sipkema, D., M, A.A., and Tramper, J. (2003) Primmorphs from seven marine sponges : formation and structure. *J Biotechnol* **100**: 127–139.
- Sipkema, D., Schippers, K., Maalcke, W.J., Yang, Y., Salim, S., and Blanch, H.W. (2011) Multiple approaches to enhance the cultivability of bacteria associated with the marine sponge *Haliclona* (gellius) sp. *Appl Env Micro* **77**: 2130–2140.
- van Soest, R.W.M., Boury-Esnault, N., Vacelet, J., Dohrmann, M., Erpenbeck, D., de Voogd, N.J., et al. (2012) Global diversity of sponges (Porifera). *PLoS One* **7**: 1–23.
- Sogabe, S., Hatleberg, W., Kocot, K., Say, T., Stoupin, D., Roper, K., et al. (2019) Pluripotency and the origin of animal multicellularity. *Nat Lett* **570**: 519–522.
- Song, H., Hewitt, O.H., and Degnan, S.M. (2020) Bacterial symbionts in animal development: arginine biosynthesis complementation enables larval settlement in a marine sponge. *bioRxiv* 1-14.
- Srivastava, M., Simakov, O., Chapman, J., Fahey, B., Gauthier, M.E.A., Mitros, T., et al. (2010) The *Amphimedon queenslandica* genome and the evolution of animal complexity. *Nature* **466**: 720–726.
- Steindler, L., Huchon, D., Avni, A., and Ilan, M. (2005) 16S rRNA phylogeny of sponge-associated cyanobacteria. *Appl Environ Microbiol* **71**: 4127–4131.
- Steindler, L., Schuster, S., Ilan, M., Avni, A., Cerrano, C., and Beer, S. (2007) Differential gene expression in a marine sponge in relation to its symbiotic state. *Mar Biotechnol* **9**: 543–9.
- Steinert, G., Whitfield, S., Taylor, M.W., Thoms, C., and Schupp, P.J. (2014) Application of diffusion growth chambers for the cultivation of marine sponge-associated bacteria. *Mar Biotechnol* **16**: 594–603.
- Strehlow, B.W., Schuster, A., Francis, W.R., and Canfield, D.E. (2021) Metagenomic data for *Halichondria panicea* from Illumina and Nanopore sequencing and preliminary genome assemblies for the sponge and two microbial symbionts. *bioRxiv* 1–8.
- Tavalire, H.F., Christie, D.M., Leve, L.D., Ting, N., Cresko, W.A., and Bohannon, B.J.M. (2021) Shared environment and genetics shape the gut microbiome after infant adoption. *MBio* **12**: e00548-21.
- Thomas, T., Moitinho-Silva, L., Lurgi, M., Björk, J.R., Easson, C., Astudillo-García, C., et al. (2016) Diversity, structure and convergent evolution of the global sponge microbiome. *Nat Commun* **7**: 11870.
- Thomassen, S. and Riisgard, H.U. (1995) Growth and energetics of the sponge *Halichondria panicea*. *Mar Ecol Prog Ser* **128**: 239–246.
- Van Treeck, P., Eisinger, M., Müller, J., Paster, M., and Schuhmacher, H. (2003) Mariculture trials with Mediterranean sponge species: The exploitation of an old natural resource with sustainable and novel methods. *Aquaculture* **218**: 439–455.
- Turner, E.C. (2021) Possible poriferan body fossils in early Neoproterozoic microbial reefs. *Nature* **596**: 87–91.
- Ueda, N., Richards, G.S., Degnan, B.M., Kranz, A., Adamska, M., Croll, R.P., and Degnan, S.M. (2016) An ancient role for nitric oxide in regulating the animal pelagobenthic life cycle: Evidence from a marine sponge. *Sci Rep* **6**: 1–14.
- Vad, J., Dunnett, F., Liu, F., Montagner, C.C., Roberts, J.M., and Henry, T.B. (2020) Soaking up the oil: Biological impacts of dispersants and crude oil on the sponge *Halichondria panicea*. *Chemosphere* **257**: 127109.
- Versluis, D., de Evgrafov, M.R., Sommer, M.O.A., Sipkema, D., Smidt, H., and van Passel, M.W.J. (2016) Sponge microbiota are a reservoir of functional antibiotic resistance genes. *Front Microbiol* **7**: 1848.
- Visick, K.L., Stabb, E. V., and Ruby, E.G. (2021) A lasting symbiosis: how *Vibrio fischeri* finds a squid partner and persists within its natural host. *Nat Rev Microbiol* **19**: 654-665.
- Wang, D., Wei, Y., Cui, Q., and Li, W. (2017) *Amylibacter cionae* sp. Nov., isolated from the sea squirt *Ciona savignyi*. *Int J Syst Evol Microbiol* **67**: 3462–3466.
- Webster, N.S., Cobb, R.E., Soo, R., Anthony, S.L., Battershill, C.N., Whalan, S., and Evans-Illidge, E. (2011) Bacterial community dynamics in the marine sponge *Rhopaloeides odorabile* under *in situ* and *ex situ* cultivation. *Mar Biotechnol* **13**: 296–304.
- Wehrl, M., Steinert, M., and Hentschel, U. (2007) Bacterial uptake by the marine sponge *Aplysina aerophoba*. *Microb Ecol* **53**: 355–365.

References

- Weiland-Bräuer, N., Fischer, M.A., Pinnow, N., and Schmitz, R.A. (2019) Potential role of host-derived quorum quenching in modulating bacterial colonization in the moon jellyfish *Aurelia aurita*. *Sci Rep* **9**: 1–12.
- Weiland-Bräuer, N., Neulinger, S.C., Pinnow, N., Künzel, S., Baines, J.F., and Schmitz, R.A. (2015) Composition of bacterial communities associated with *Aurelia aurita* changes with compartment, life stage, and population. *Appl Environ Microbiol* **81**: 6038–6052.
- Weisz, J.B., Lindquist, N., and Martens, C.S. (2008) Do associated microbial abundances impact marine demosponge pumping rates and tissue densities? *Oecologia* **155**: 367–376.
- Whalan, S. and Webster, N.S. (2014) Sponge larval settlement cues: The role of microbial biofilms in a warming ocean. *Sci Rep* **4**: 28–32.
- Wiens, M., Korzhev, M., Krasko, A., Thakur, N.L., Perović-Ottstadt, S., Breter, H.J., et al. (2005) Innate immune defense of the sponge *Suberites domuncula* against bacteria involves a MyD88-dependent signaling pathway: Induction of a perforin-like molecule. *J Biol Chem* **280**: 27949–27959.
- Wilkinson, C.R., Garrone, R., and Vacelet, J. (1979) Marine sponges discriminate between food bacteria and bacterial symbionts: electron microscope radioautography and in situ evidence. *Proc R Soc L B* **205**: 519–528.
- Williams, L.M., Inge, M.M., Mansfield, K.M., Rasmussen, A., Afghani, J., Agrba, M., et al. (2020) Transcription factor NF- κ B in a basal metazoan, the sponge, has conserved and unique sequences, activities, and regulation. *Dev Comp Immunol* **104**: 1–14.
- Witte, U. and Barthel, D. (1994) Reproductive cycle and oogenesis of *Halichondria panicea* (Pallas) in Kiel Bight. In *Sponges in Time and Space*. pp. 297–305.
- Witte, U., Barthel, D., and Tendal, O. (1994) The reproductive cycle of the sponge *Halichondria panicea* Pallas (1766) and its relationship to temperature and salinity. *J Exp Mar Bio Ecol* **183**: 41–52.
- Wong, E., Mölter, J., Anggono, V., Degnan, S.M., and Degnan, B.M. (2019) Co-expression of synaptic genes in the sponge *Amphimedon queenslandica* uncovers ancient neural submodules. *Sci Rep* **9**: 1–15.
- Woznica, A., Cantley, A.M., Beemelmans, C., Freinkman, E., Clardy, J., and King, N. (2016) Bacterial lipids activate, synergize, and inhibit a developmental switch in choanoflagellates. *Proc Natl Acad Sci U S A* **113**: 7894–7899.
- Woznica, A., Gerdt, J.P., Hulett, R.E., Clardy, J., and King, N. (2017) Mating in the closest living relatives of animals is induced by a bacterial chondroitinase. *Cell* **170**: 1175–1183.
- Yahel, G., Eerkes-Medrano, D.I., and Leys, S.P. (2006) Size independent selective filtration of ultraplankton by hexactinellid glass sponges. *Aquat Microb Ecol* **45**: 181–194.
- Yatsunenkov, T., Rey, F.E., Manary, M.J., Trehan, I., Dominguez-Bello, M.G., Contreras, M., et al. (2012) Human gut microbiome viewed across age and geography. *Nature* **486**: 222–227.
- Yuen, B. (2016) Deciphering the genomic toolkit underlying animal-bacteria interactions—insights through the demosponge *Amphimedon queenslandica*.
- Yuen, B., Bayes, J.M., and Degnan, S.M. (2014) The characterization of sponge NLRs provides insight into the origin and evolution of this innate immune gene family in animals. *Mol Biol Evol* **31**: 106–120.
- Zhang, M., Shan, C., Tan, F., Limbu, S.M., Chen, L., and Du, Z.Y. (2020) Gnotobiotic models: Powerful tools for deeply understanding intestinal microbiota-host interactions in aquaculture. *Aquaculture* **517**: 734800.
- Zilber-Rosenberg, I. and Rosenberg, E. (2008) Role of microorganisms in the evolution of animals and plants: The hologenome theory of evolution. *FEMS Microbiol Rev* **32**: 723–735.



ACKNOWLEDGEMENTS

The last four years have been a wild ride. I am incredibly grateful to a number of people without whom this document would not be the thesis that I am happy to submit. You helped me fly.

My sincerest thank you to my supervision-dream-team: **Ute** Hentschel and **Lucía** Pita. You made me feel supported and heard, and I value that I could always approach you regardless the topic. Ute, danke für ein spannendes und kreatives Projekt, die Freiheiten und richtungsweisenden Ratschläge. Danke für deine Offenheit, deinen Überblick und großen Ideen. Lucía, thank you for the constant support, elaborate feedback, open ear and pure excitement for your teams' work. One of your many strengths is always being calm and clear-headed; this helped me many times when I had doubts or was intimidated of my project. Muchas gracias!

Ein herzliches Dankeschön an **Sebastian** Fraune, für deine Begleitung von Tag 1 bis zur Verteidigung und deine Hilfe bei der Wegfindung durch ein kompliziertes experimentelles System. Vielen Dank an mein Dissertationskomitee, **Olivia** Roth und **Martin** Frank. Vielen Dank, **Tobias** Lenz, für deine Fragen und deinen anderen Blickwinkel während meiner TAC Treffen.

Experimental and lab work was a huge part of my project, and I am happy to have been part of such a great team. A big thank you to all members of the **RUMS**! Thank you for a great time and making coming to work so pleasant. #teamhalichondria

Andrea Hethke, vielen Dank für deine Hilfe an vielen, langen Experimenttagen, deine Motivation und deine Neugier. Ich freue mich auf spannende Primmorph-Versuche. **Tanja** Rahn, vielen Dank für dein Gefühl für Bakterienisolate und deine Ideen. Ich drücke die Daumen, dass SuSy eines Tages dabei ist. **Ina** Clefsen, danke für deine schnelle und immer freundliche Hilfe in der Amplicon Pipeline. Vielen Dank, **Jule** Böge, für deine Hilfe mit den ersten Schwamm-Dissoziationen und lustige, rosa Stunden im Labor. Danke, **Sabrina** Jung für alle Hilfe rund um qPCR, Labor und Aquarien. **Bettina** Reuter, vielen Dank, dass du immer als Ansprechpartnerin da bist. **Kathrin** Busch, danke für deine Hilfe bei allen Amplicon-relatierten Fragen, aber vor allem für dein Interesse, die vielen, wilden Ideen und den Spaß. Jetzt sind wir beide mit unserer Sch* fertig! **Angela**, thank you for being a great and caring office mate and friend, and for brave snorkel trips in cold water. **Vassia**, I am happy you joined our little team and thank you for your field support. **Kristina** Bayer, danke für deinen Molekularsupport und die Taufe von SuSy. Danke, **Peter** Deines, dass du einen ungewollten Bakterienanstieg in ein interessantes Konzept verwandelt hast. Thank you, **Tyler** Carrier, for introducing developmental work to the group and making me hunt *Halichondria* larvae.



Danke, **Fabian** Wendt für deine Hilfe mit unseren ersten *Halichondria*-Aquarien, dein offenes Ohr bei allen Fragen und dass du immer noch regelmäßig fragst, wie es den Schwämmen geht. **Claas** Hiebenthal, danke für die spontanen Noteinsätze und das gemeinsame Kopfzerbrechen bei bubbeligen Schwämmen. **Ute** Jülly, danke, dass du an mich glaubst, die Motivation und deine kritischen Fragen. **Hanna** Domin, danke für eine schöne Zeit am Bioturm und meine ersten Klonierungserfahrungen. **Julius** Krebs, danke für deine Unterstützung, dass ich deine Betreuerin sein durfte und deine täglichen Gesangseinlagen. **Violeta** Albacete, **Ashley** Coons and **Marvin** Lehmann, thank you for helping with experiments, asking important questions and your diligent work. I want to

thank the **CRC1182** Origin of Metaorganisms for the inspiring community, boosting creativity and supporting my side-project, the sponge pop-up card. Ein riesen Dankeschön an das **Scicomlab** und **Agnes** Piecyk für die großartige Umsetzung meiner Idee. **Sören** Franzenburg, **Corinna** Bang, thank you for sequencing support and making my samples run fast during a difficult time.

Danke, **SuSy und Halichondria**, für die treue, wenn auch nicht immer einfache Zusammenarbeit, die interessanten Ergebnisse und großen Geheimnisse. Ich hoffe, wir sehen uns wieder.

Danke und thank you to my **friends** in Kiel and elsewhere, and my **family**, for making life in- and outside GEOMAR wonderful and letting me forget difficult data sets for a while. Danke, **Mama** und **Papa**, für die bedingungslose Unterstützung und dass ihr euch mit mir freut, ärgert und durchhält. Danke **Felix**, ohne dich geht gar nichts.



APPENDIX

TO CHAPTER 3

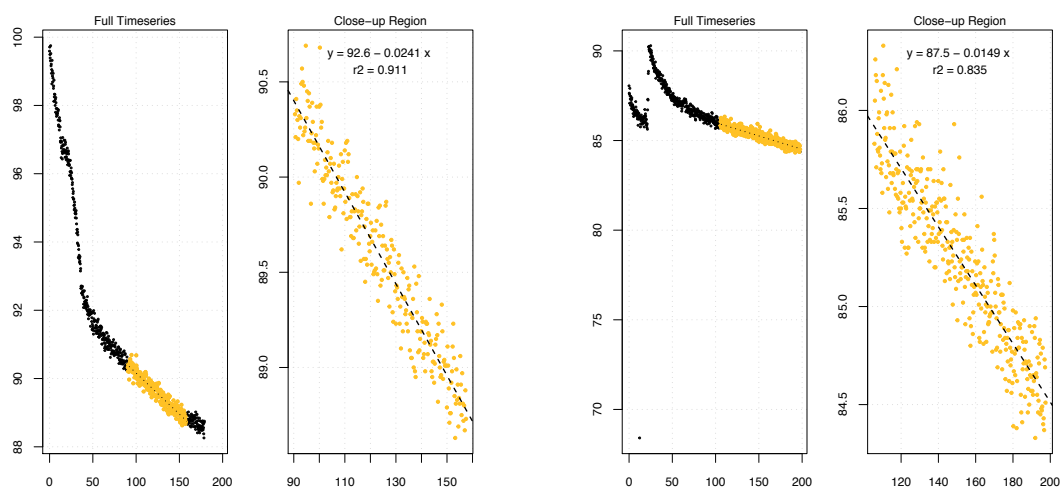
The appendix to chapter 3 includes additional figures, tables and methods, as well as two protocols published on the online platform [protocols.io](https://www.protocols.io).

APPENDIX 3.1 | Differences in beta-diversity between sponge and seawater samples from aquaria and different field locations. PERMANOVA pairwise results of weighted unifrac distances are shown.

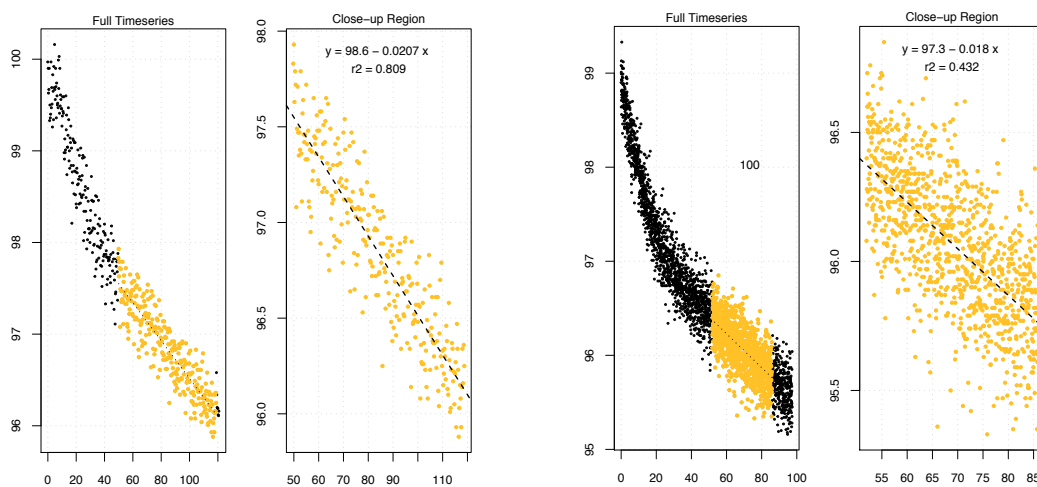
Group 1	Group 2	Sample size	Permutations	pseudo-F	p-value	q-value
aquaria_3months	aquaria_6months	9	999	0.74627	0.655	0.673714
aquaria_3months	sp_Arosund	12	999	3.001797	0.007	0.030462
aquaria_3months	sp_Gelting	11	999	2.028529	0.061	0.08784
aquaria_3months	sp_Laboe	11	999	2.928999	0.011	0.030462
aquaria_3months	sw_Arosund	9	999	11.49216	0.015	0.032571
aquaria_3months	sw_Gelting	9	999	12.10936	0.011	0.030462
aquaria_3months	sw_Laboe	9	999	12.60902	0.011	0.030462
aquaria_3months	sw_aquarium	12	999	11.95893	0.004	0.030462
aquaria_6months	sp_Arosund	9	999	2.801991	0.011	0.030462
aquaria_6months	sp_Gelting	8	999	1.905643	0.156	0.170182
aquaria_6months	sp_Laboe	8	999	2.986411	0.043	0.0645
aquaria_6months	sw_Arosund	6	999	18.65924	0.109	0.1308
aquaria_6months	sw_Gelting	6	999	24.54879	0.099	0.122897
aquaria_6months	sw_Laboe	6	999	25.62469	0.123	0.142839
aquaria_6months	sw_aquarium	9	999	12.50919	0.017	0.032571
sp_Arosund	sp_Gelting	11	999	1.638188	0.149	0.167625
sp_Arosund	sp_Laboe	11	999	2.155631	0.086	0.116
sp_Arosund	sw_Arosund	9	999	9.604433	0.019	0.032571
sp_Arosund	sw_Gelting	9	999	10.42011	0.01	0.030462
sp_Arosund	sw_Laboe	9	999	10.75073	0.01	0.030462
sp_Arosund	sw_aquarium	12	999	10.68402	0.005	0.030462
sp_Gelting	sp_Laboe	10	999	0.569836	0.793	0.793
sp_Gelting	sw_Arosund	8	999	13.8385	0.017	0.032571
sp_Gelting	sw_Gelting	8	999	15.50217	0.02	0.032727
sp_Gelting	sw_Laboe	8	999	16.30802	0.014	0.032571
sp_Gelting	sw_aquarium	11	999	12.91369	0.003	0.030462
sp_Laboe	sw_Arosund	8	999	14.37806	0.019	0.032571
sp_Laboe	sw_Gelting	8	999	16.17029	0.019	0.032571
sp_Laboe	sw_Laboe	8	999	16.79905	0.016	0.032571
sp_Laboe	sw_aquarium	11	999	14.21635	0.006	0.030462
sw_Arosund	sw_Gelting	6	999	1.191105	0.391	0.414
sw_Arosund	sw_Laboe	6	999	2.712651	0.092	0.118286
sw_Arosund	sw_aquarium	9	999	5.842663	0.006	0.030462
sw_Gelting	sw_Laboe	6	999	5.553368	0.087	0.116
sw_Gelting	sw_aquarium	9	999	5.943196	0.022	0.034435
sw_Laboe	sw_aquarium	9	999	6.43357	0.009	0.030462

APPENDIX 3.2 | Oxygen uptake of sponges assessed in experimental aquarium system. The set-up was tested to measure respiration without removing the sponges from the culture bottles, e.g., during a running experiment. Respiration of two sponge individuals was measured twice each as dissolved oxygen decrease over time. While in empty control tanks the oxygen levels remain stable, sponges consume between 0.73-1.35 $\mu\text{mol} / \text{h} / \text{g WW}$. The system is appropriate to perform closed respiration measurements and has to be evaluated during longer experiments. Plots were created with the respR package (R version 4.0.2).

Individual 1

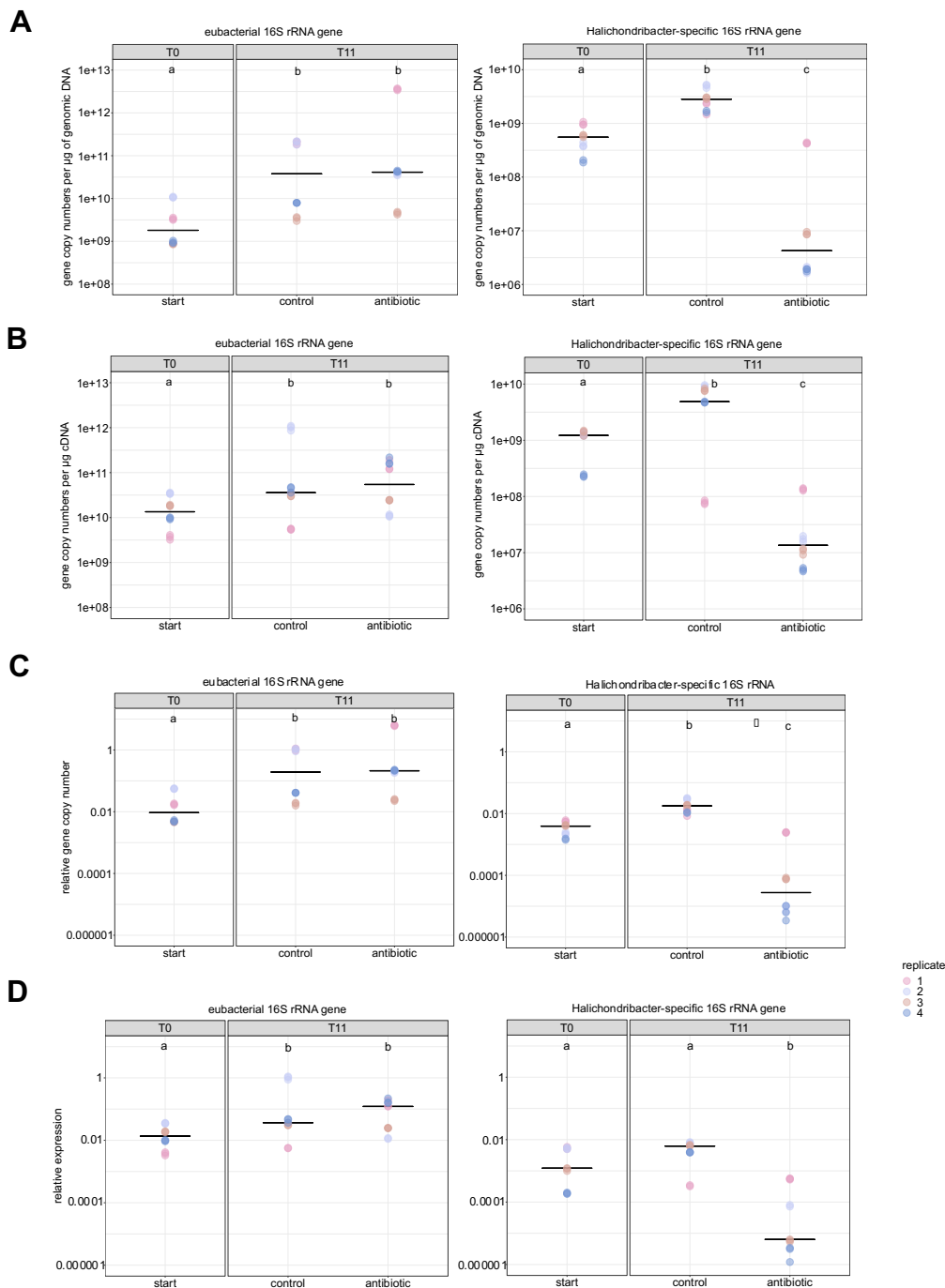


Individual 2



	oxygen consumption ($\mu\text{mol} / \text{h} / \text{g WW}$)
Individual 1 (1st run)	-0.73
Individual 1 (2nd run)	-1.35
Individual 2 (1st run)	-1.08
Individual 2 (2nd run)	-0.91
Empty control (1st run)	-0.00957
Empty control (2nd run)	-0.00398

APPENDIX 3.3 | Absolute bacterial abundance assessed by qPCR. 16S rRNA gene copy numbers per μg genomic DNA (**A**) and per μg cDNA (**B**) at the start (T0) and after the recovery phase (T11). The same data is represented as relative gene copy number (**C**) to the sponge 18S rRNA gene, and as relative gene expression to the sponge β -tubulin gene (**D**). Values with different letters are significantly different ($p > 0.05$), colors indicate individual sponges, and black lines represent median.



APPENDIX 3.4 | Details on ASVs affiliated to the *Amylibacter* family (Rhodobacteraceae, Alphaproteobacteria) that interact with other bacteria in healthy *Halichondria panicea*. Presence/absence of ASVs in healthy sponges from different collections, as well as average relative abundance (%) for one example time point is presented. The sequence difference to the dominant ASV in this study (here with ID A01) is given as number of basepairs (bp).

ID	ASV	bp differences to A01	June 2020	average % June 2020	June 2018	Nov 2018	Nov 2019
A01	350235dc06427f8e808d1bb3452afc91	NA	16/16	54.02	15/15	4/4	6/6
A02	29e6e958f1be8fafde301aa2cc2e9bd1	19 (92.9 %)	9/16	0.12	3/15		4/6
A03	07c400dd2bc35f554fcdd45c1e9b5191	27 (90 %)	16/16	1.39	11/15	4/4	6/6
A04	c2c6c2e06e35ccee422cef2ffce044df	19 (92.9 %)	16/16	0.57	12/15		6/6
A05	54638dc11ebcae9533702e50b14c93b4	26 (90.3 %)	10/16	0.10	1/15	1/4	5/6
A06	0ccbb54ec72c961d809b620a50d80450	1 (99.6 %)	4/16	3.01			2/6
A07	0fb3092d94a80d73b41c9f2bfbec4113	22(91.9 %)	10/16	0.31	9/15		0/6
A08	3669643e8b4488937373c9597bc2e6b9	18 (93.3 %)	8/16	0.19			
A09	864deb0629ed8b73a1e3ac695571e4e9	21 (92.2 %)	7/16	0.18		1/4	1/6
A10	17b2206145c4416446d0f7a7ffa588b	21 (92.2 %)	5/16	0.23			
A11	55cfbabbbbc98af72f8f0c7fdf35888e0	33 (87.7 %)	6/16	0.08		3/4	6/6
A12	fd94d37a46d078210347f8ea89a64cf5	35 (87 %)	5/16	0.08	5/15	2/4	6/6
A13	8f8ce8a50ded37f41e4b6990bb6e5c00	25 (90.7 %)	7/16	0.10	3/15	1/4	2/6
A14	49bd3da753d0337c2787338363c987e5	17 (93.7 %)	7/16	0.25	7/15		
A15	bd1824df81250d36dcc4c302a47caf7f	1 (99.6 %)	1/16	8.35			
A16	ae734ba80649fe89403f245d5bb3e89b	19 (93 %)	4/16	0.18	1/15		
A17	570b6686b13dc3bc7f8af99f20fe16	6 (97.7 %)	3/16	0.14			

APPENDIX 3.5 | Methods: Comparison culture-dependent and culture-independent bacterial abundance

Halichondria panicea individuals were collected by snorkeling at different occasions (Table S1) from Schilksee, Germany. Sponges were individually transported in 500 mL Kautex bottles and brought to Baltic flow-through tanks at the GEOMAR Helmholtz Centre for Ocean Research within 2 hours after collection. Sponge-associated bacteria were isolated in four cultivation efforts on various solid culture media (Table S2, performed by Tanja Rahn). The aim was to create a comprehensive bacterial culture collection with representatives of the different bacterial groups associated to *Halichondria panicea*, with a focus on the bacterial family Rhodobacteraceae (Alphaproteobacteria). For each cultivation effort, approximately 7.5 g sponge tissue was rinsed three times with sterile filtered Baltic seawater to remove loosely attached microbes. The tissue was then homogenized in sterile Baltic seawater for 30 seconds at 17.500 U/min (Ultraturrax). The homogenized sponge tissue was plated in dilutions (10^1 - 10^{-5}). During the first incubation effort, the homogenized tissue was additionally incubated at 25 °C and 1.000 lux for 40 h on a shaker before plating. The base of the media was either the commercially available medium Marine Broth (Difco2216) or sterile filtered Baltic seawater (Table S2). Different carbon or nitrogen sources, supplements or antibiotics were added to provide a variety of growth conditions and increase diversity of bacterial isolates. The plates were incubated at 25°C for days up to weeks and regularly checked for colony growth. Single colonies were picked and streak plated on fresh agar plates, first on the same media they were picked from and later on pure MB agar.

The total genomic DNA was extracted from single colonies using DNeasy Blood & Tissue Kit (Qiagen, Netherlands) DNA extraction kit. following the manufacturer's protocol for gram-positive bacteria and stored at -20 °C before use. Amplification of the 16S rRNA gene (1500 bp) was performed with the primer pairs (concentration: each 10 pmol/ μ L): Eub27f (Noda et al., 2006)/ Univ1492r (Reysenbach et al., 2000); alternative for Univ1492r we used the reverse primer RC1492r (Nathan A. Magarvey et al., 2004) or 1525r (Rainey AF et al. 1996). The PCR products were sequenced at IKMB sequencing facility (now Competence Centre for Genomic Analysis, CCGA, University of Kiel, Germany) or GATC Eurofins Genomics (sequencing primers: 342f (Lane et al., 1991); 534r (G Muyzer et al. 1992); 803f (Rainey AF et al., 1996)). The sequences were processed with the ChromasPro software, and compared to the GenBank database (BLAST tool) and the Ribosomal Database Project (RDP), with and without type strain filter. The sequences are deposited in the NCBI-GenBank under the accession numbers MT406382-MT406727.

The overlap of bacterial diversity identified by cultivation and culture-independent 16S rRNA amplicon sequencing was assessed. Isolates were compared to amplicon data derived from wildtype and

cultured sponges and seawater, as well as experimental sponges (second antibiotic exposure experiment). The 16S rRNA isolate sequences were aligned against the local amplicon sequence database (BLAST) with a minimum sequence similarity of 80 %.

TABLE S1 | Collection time and processing of sponges collected for bacterial isolation. All sponges were collected from Schilksee, Germany (54.424705. 10.175133).

Purpose	Sponge sampling	Processing
Isolation effort 1	10/7/2018	Fresh
Isolation effort 2	2/10/2018	Fresh
Isolation effort 3	2/10/2018	1 month aquarium
Isolation effort 4	3/2/2019	Fresh

TABLE S2 | Solid growth media used in this study and their application during the four cultivation efforts. Abbreviations and applied concentrations: MB = Marine Broth 15g/L (add company); Bac = bacitracin 10 I.E.; DMSO = dimethylsulfoxide 30 μ M; Nalix = nalidixic acid 30 μ g/mL; Thio = sodium thiosulfate 1g/L; OSW = Baltic seawater; NADG = N-Acetyl-D-glucosamine 1g/L; NADM = N-Acetyl-D-mannosamine 1g/L; sponge = sponge tissue in (\sim 5 mm³) autoclaved together with medium; Pen = penicillin 100 μ g/ml; yeast = yeast extract 1 g/L (add company); tryptone 1g/L; Halichondribacter-mix = 10 g/L NaCl + custom vitamins (biotin 20ng/L. folic acid 20ng/L. Thiaminchlorid-hydrochloride 50ng/L. pyridoxamindihydrochloride 100ng/L. riboflavin 50ng/L. B12 50ng/L). trace elements (FeCl₂ x 4 H₂O 1.8mg/L. CoCl₂ x 6 H₂O 250ng/L. NiCl₂ x 6 H₂O 10ng/ml. CuCl₂ x 2 H₂O 10ng/ml. MnCl₂ x 4 H₂O 70ng/L. ZnCl₂ 100ng/L. H₃BO₃ 500ng/L. Na₂MoO₄ x 2 H₂O 30ng/L). NaCl 10g/L. taurine 1g/L. N-Acetyl-D-mannosamin 1g/L; Casa = casaminoacids (add company)1g/L

Medium	Cultivation effort			
	1	2	3	4
MB	x			
MB+Bac	x			
MB+DMSO	x			
MB+Nalix	x			
MB+Nalix+Bac	x			
MB+Thio	x			
MB+Thio+Bac	x			
MB+Thio+DMSO	x			
MB+Thio+Nalix	x			
MB+Thio+Nalix+Bac	x			
OSW	x			
OSW+Bac	x			
OSW+Biotin+Tryptophan				x
OSW+DMSO	x			
OSW+NADG				x
OSW+NADG+Taurine				x
OSW+NADM		x		x
OSW+NADM+DMSO		x		
OSW+NADM+Taurine				x
OSW+Nalix	x			
OSW+Nalix+Bac	x			
OSW+sponge				x
OSW+sponge+Pen				x
OSW+Thio+DMSO	x			
OSW+Thio+Nalix	x			
OSW+Trypton+Yeast		x		
Halichondribacter-mix				x
Halichondribacter-mix+Casa				x
Halichondribacter-mix + Pen				x
Halichondribacter-mix +Casa+Pen				x

APPENDIX 3.6 | Results: Comparison of culture-dependent and culture-independent bacterial abundance

Both the sponge host as well as the symbionts should be experimentally accessible in a model for sponge-symbiosis. An important tool is a symbiont culture collection that can be studied *in vitro* and within the sponge host *in vivo*. Four isolation efforts with 30 culture media (Table S1 and S2) were performed by Tanja Rahn with the aim to isolate sponge symbionts, targeting the *Rhodobacteraceae* family that *Ca. H. symbioticus* is affiliated to. In total, 335 isolates were recovered, representing at least 160 different bacterial strains based on 16S rRNA full length sequencing. Of all isolates, 262 had a match with the amplicon data generated from wildtype and aquarium-maintained sponges or seawater samples (90 % with sponge tissue) (Table S3). Although *Rhodobacteraceae* were by far the most prominent family among the isolates (25 % of the recovered diversity), the dominant symbiont *Ca. H. symbioticus* could not be isolated. Previous efforts were also not successful (Knobloch et al. 2019) suggesting that true and obligate sponge symbionts might not survive outside their sponge host. This poses challenges for experimentation and taking advantage of experimentation with isolates. It has led us to the methodological compromise to use the full natural sponge microbiome for recolonization, instead of pure symbiont isolates (Chapter 4). Bacteria-bacteria co-occurrence networks suggest co-dependence of several bacteria in the sponge microbiome (Figure 6A), many of which probably have a nutritional base. Without exactly knowing the nutritional requirements and understanding the environment within the sponge host completely, it remains difficult to replicate these culture conditions in the lab.

Knobloch, S., R. Jóhannsson, and V. Marteinson. 2019. Co-cultivation of the marine sponge *Halichondria panicea* and its associated microorganisms. *Sci. Rep.* 9:1–11.

Appendix to Chapter 3

TABLE S3 | Bacterial isolates from *H. panicea* that have a match in the amplicon sequences. The relative abundance of the ASVs in sponges and seawater is presented.

Isolate	Closest relative strain (NCBI)	Closest relative ASV	Relative abundance (%)					
			Seawater		Sponge			
			Field	Aquarium	Field	Aquarium	Antibiotic exposure experiment	
							control	antibiotic
Hal001	<i>Shewanella colwelliana</i>	3d56fd9774125a927d7e3142d542144f	0,000	0,000	0,036	0,000	0,043	15,292
Hal002	<i>Shewanella aestuarii</i>	2705081a1229cde6f0b8c7dba4baa644	0,000	0,014	0,000	0,000	0,000	0,000
Hal005	<i>Shewanella aestuarii</i>	2705081a1229cde6f0b8c7dba4baa644	0,000	0,014	0,000	0,000	0,000	0,000
Hal006	<i>Shewanella aestuarii</i>	2705081a1229cde6f0b8c7dba4baa644	0,000	0,014	0,000	0,000	0,000	0,000
Hal007	<i>Shewanella aestuarii</i>	2705081a1229cde6f0b8c7dba4baa644	0,000	0,014	0,000	0,000	0,000	0,000
Hal008	<i>Shewanella aestuarii</i>	1b05768ae6fd9ae2e3dec30e1a97939b	0,000	0,000	0,008	0,000	0,000	0,000
Hal009	<i>Winogradskyella sediminis</i>	1e90951fa54e6f528eba978ae08a5012	0,000	0,000	0,002	0,000	0,000	0,000
Hal018	<i>Thalassomonas ganghwensis</i>	3c296308e35d2f643ec59bd6a9cd0d16	0,000	0,000	0,000	0,000	0,036	0,000
Hal020	<i>Pseudoalteromonas tunicata</i>	abc461ef7de0c8e6afef79ce89077c03	0,000	0,000	0,008	0,007	0,035	0,000
Hal023	<i>Pseudoalteromonas agarivorans</i>	17753a04c358b65972ce4531833fcc1	1,242	0,000	0,073	0,000	2,222	18,789
Hal025	<i>Vibrio artabrorum</i>	f3f91d7ba8978fe66f09c5ac49f0933	0,000	0,000	0,000	0,000	0,358	0,000
Hal026	<i>Vibrio diazotrophicus</i>	aa9f3815f3fe027fbd258723be0b5037	0,000	0,000	0,000	0,024	0,000	0,000
Hal028	<i>Shewanella algae</i>	51cf5ebcb1755ee81f3f9a6bf5d2f04b	0,000	0,013	0,012	0,000	0,000	0,000
Hal030	<i>Flavobacterium jumunjinense</i>	b5f8481ab1741f39cff72fb2289d7c7a	0,000	0,005	0,163	0,000	0,000	0,000
Hal031	<i>Pseudoalteromonas tunicata</i>	abc461ef7de0c8e6afef79ce89077c03	0,000	0,000	0,008	0,007	0,035	0,000
Hal032	<i>Pseudoalteromonas tunicata</i>	abc461ef7de0c8e6afef79ce89077c03	0,000	0,000	0,008	0,007	0,035	0,000
Hal034	<i>Vibrio diazotrophicus</i>	aa9f3815f3fe027fbd258723be0b5037	0,000	0,000	0,000	0,024	0,000	0,000
Hal035	<i>Shewanella colwelliana</i>	3d56fd9774125a927d7e3142d542144f	0,000	0,000	0,036	0,000	0,043	15,292
Hal036	<i>Shewanella algae</i>	51cf5ebcb1755ee81f3f9a6bf5d2f04b	0,000	0,013	0,012	0,000	0,000	0,000
Hal037	<i>Shewanella algae</i>	51cf5ebcb1755ee81f3f9a6bf5d2f04b	0,000	0,013	0,012	0,000	0,000	0,000
Hal041	<i>Vibrio diazotrophicus</i>	aa9f3815f3fe027fbd258723be0b5037	0,000	0,000	0,000	0,024	0,000	0,000
Hal042	<i>Erythrobacter aquimaris</i>	4cdf1d045b71f4ff67c3fbfc3e6e083b	0,000	0,000	0,000	0,188	0,000	0,000
Hal043	<i>Pararhodobacter aggregans</i>	ee5e8a7f3405e15dddc4ccdc541f0792	0,000	0,000	0,003	0,000	0,000	0,000
Hal044	<i>Flavobacterium jumunjinense</i>	b5f8481ab1741f39cff72fb2289d7c7a	0,000	0,005	0,163	0,000	0,000	0,000
Hal046	<i>Erythrobacter aquimaris</i>	4cdf1d045b71f4ff67c3fbfc3e6e083b	0,000	0,000	0,000	0,188	0,000	0,000
Hal047	<i>Nocardia lasii</i>	5e23c4d7da1773d3296164ddc899deda	0,000	0,000	0,000	0,010	0,000	0,000
Hal048	<i>Nocardia lasii</i>	5e23c4d7da1773d3296164ddc899deda	0,000	0,000	0,000	0,010	0,000	0,000
Hal049	<i>Erythrobacter aquimaris</i>	4cdf1d045b71f4ff67c3fbfc3e6e083b	0,000	0,000	0,000	0,188	0,000	0,000
Hal051	<i>Aliikangiella marina</i>	3606d65d63444951e32fcef9c1d05bd2	0,000	0,000	0,000	0,050	0,000	0,000
Hal052	<i>Aliikangiella marina</i>	3606d65d63444951e32fcef9c1d05bd2	0,000	0,000	0,000	0,050	0,000	0,000
Hal053	<i>Vibrio diazotrophicus</i>	aa9f3815f3fe027fbd258723be0b5037	0,000	0,000	0,000	0,024	0,000	0,000
Hal054	<i>Vibrio diazotrophicus</i>	aa9f3815f3fe027fbd258723be0b5037	0,000	0,000	0,000	0,024	0,000	0,000
Hal059	<i>Algoriphagus antarcticus</i>	5a440a7146ad5c536bbf1cb3c66b540d	0,000	0,000	0,001	0,000	0,000	0,000
Hal060	<i>Erythrobacter longus</i>	40377e54010a84dbca9c3914f2969e91	0,013	0,000	0,018	0,032	0,000	0,000
Hal061	<i>Algoriphagus namhaensis sp. nov.</i>	c08f8a35917ae2d30d385b7e15de0082	0,000	0,000	0,007	0,000	0,000	0,000
Hal062	<i>Nocardia lasii</i>	5e23c4d7da1773d3296164ddc899deda	0,000	0,000	0,000	0,010	0,000	0,000
Hal063	<i>Nocardia lasii</i>	5e23c4d7da1773d3296164ddc899deda	0,000	0,000	0,000	0,010	0,000	0,000
Hal064	<i>Nocardia lasii</i>	5e23c4d7da1773d3296164ddc899deda	0,000	0,000	0,000	0,010	0,000	0,000
Hal065	<i>Sediminihabitans luteus</i>	d5584f24ec95081cab72258a1ae40b3b	1,103	0,112	0,156	0,000	0,000	0,000
Hal067	<i>Pseudomonas peli</i>	8e1e8c516edfe371585c23dd1876174a	0,000	0,000	0,003	0,000	0,000	0,000
Hal068	<i>Erythrobacter aquimaris</i>	4cdf1d045b71f4ff67c3fbfc3e6e083b	0,000	0,000	0,000	0,188	0,000	0,000
Hal069	<i>Kiloniella laminariae</i>	d62bf84e66138d9018cb90bd939cccbc	0,000	0,000	0,000	0,049	0,005	0,000
Hal070	<i>Shewanella algae</i>	51cf5ebcb1755ee81f3f9a6bf5d2f04b	0,000	0,013	0,012	0,000	0,000	0,000

Appendix to Chapter 3

Hal071	<i>Nocardia coeliaca</i>	131c1a05f13c52a7efe8aa5ef75997aa	0,000	0,093	0,000	0,028	0,000	0,000
Hal073	<i>Rhodococcus qingshengii</i>	131c1a05f13c52a7efe8aa5ef75997aa	0,000	0,093	0,000	0,028	0,000	0,000
Hal075	<i>Erythrobacter aquimaris</i>	4cdf1d045b71f4ff67c3fbc3e6e083b	0,000	0,000	0,000	0,188	0,000	0,000
Hal076	<i>Sedimentitalea todarodis</i>	abb46bd1cb052cfaef078b2321506018	0,000	0,000	0,007	0,000	0,000	0,000
Hal078	<i>Altererythrobacter luteolus</i>	f63eb003f927def8abd4f4edda1cf3d8	0,000	0,000	0,020	0,000	0,000	0,000
Hal080	<i>Mycolicibacterium conceptionense</i>	0314c5b5c618bf2c53e08b17cf6b5acf	0,000	0,000	0,000	0,005	0,000	0,019
Hal081	<i>Rhodococcus qingshengii</i>	131c1a05f13c52a7efe8aa5ef75997aa	0,000	0,093	0,000	0,028	0,000	0,000
Hal082	<i>Pseudomonas silesiensis</i>	b42f3cba24ee1b0c0f984138fec8a12	0,000	0,463	0,000	0,125	0,000	0,000
Hal083	<i>Rheinheimera hassiensis</i>	88e20bb67048401bc39db0316a6ab4f9	0,022	0,000	0,000	0,000	0,000	0,000
Hal084	<i>Algoriphagus marinus</i>	c08f8a35917ae2d30d385b7e15de0082	0,000	0,000	0,007	0,000	0,000	0,000
Hal085	<i>Erythrobacter longus</i>	8bbaf89045c9cf5720efd5bf2c51cf1a	0,000	0,000	0,044	0,082	0,000	0,000
Hal086	<i>Vibrio calviensis</i>	5a6f6579647b17bc616473c22cad3fce	0,000	0,000	0,011	0,000	0,000	0,000
Hal087	<i>Flagellimonas eckloniae</i>	bc83bf69f8fba0c2c48d44dfed1935fe	0,000	0,000	0,054	0,005	0,000	0,198
Hal087-1	<i>Flagellimonas eckloniae</i>	bc83bf69f8fba0c2c48d44dfed1935fe	0,000	0,000	0,054	0,005	0,000	0,198
Hal087-2	<i>Bacillus marisflavi</i>	ecf69a838b7d63150c042e73e2b50423	0,000	0,216	0,000	0,000	0,000	0,000
Hal088	<i>Mycobacterium peregrinum</i>	0314c5b5c618bf2c53e08b17cf6b5acf	0,000	0,000	0,000	0,005	0,000	0,019
Hal089	<i>Defluviimonas aestarii</i>	b9eb6875cb6b3c9d91aa36411059d61e	0,000	0,000	0,009	0,000	0,000	0,000
Hal090	<i>Pelagibius litoralis</i>	bb8450eea51d38cec0a0e33f70ba605b	0,000	0,000	0,031	0,044	0,014	0,000
Hal091	<i>Pelagibius litoralis</i>	bb8450eea51d38cec0a0e33f70ba605b	0,000	0,000	0,031	0,044	0,014	0,000
Hal092	<i>Pseudomonas peli</i>	8e1e8c516edfe371585c23dd1876174a	0,000	0,000	0,003	0,000	0,000	0,000
Hal095	<i>Pseudomonas peli</i>	8e1e8c516edfe371585c23dd1876174a	0,000	0,000	0,003	0,000	0,000	0,000
Hal096	<i>Erythrobacter aquimaris</i>	4cdf1d045b71f4ff67c3fbc3e6e083b	0,000	0,000	0,000	0,188	0,000	0,000
Hal097	<i>Mycobacterium conceptionense</i>	0314c5b5c618bf2c53e08b17cf6b5acf	0,000	0,000	0,000	0,005	0,000	0,019
Hal099	<i>Pseudoalteromonas agarivorans</i>	17753a04c358b65972ce4531833fcca1	1,242	0,000	0,073	0,000	2,222	18,789
Hal100	<i>Rheinheimera hassiensis</i>	88e20bb67048401bc39db0316a6ab4f9	0,022	0,000	0,000	0,000	0,000	0,000
Hal104	<i>Pseudoalteromonas tunicata</i>	9c2c677d5ad85fe5295e5e8b9e21d340	0,000	0,000	0,013	0,000	0,053	0,000
Hal106	<i>Pseudoalteromonas tunicata</i>	9c2c677d5ad85fe5295e5e8b9e21d340	0,000	0,000	0,013	0,000	0,053	0,000
Hal116	<i>Kiloniella laminariae</i>	d62bf84e66138d9018cb90bd939cccbc	0,000	0,000	0,000	0,049	0,005	0,000
Hal117	<i>Phaeobacter piscinae</i>	becac65900aa499e3678bb6d22ecf290	0,000	0,000	0,000	0,022	0,450	0,000
Hal119	<i>Ruegeria profunda</i>	d8cc70ef719c394a20914cb65fb5b18d	0,000	0,000	0,000	0,027	0,000	0,000
Hal120	<i>Labrenzia marina (Stappia)</i>	51f7c0eca8f0807ca0e3abd71755234	0,000	0,013	0,000	0,000	0,000	0,000
Hal121	<i>Bacillus cereus</i>	ecf69a838b7d63150c042e73e2b50423	0,000	0,216	0,000	0,000	0,000	0,000
Hal122	<i>Bacillus cereus</i>	ecf69a838b7d63150c042e73e2b50423	0,000	0,216	0,000	0,000	0,000	0,000
Hal125	<i>Ruegeria profunda</i>	d8cc70ef719c394a20914cb65fb5b18d	0,000	0,000	0,000	0,027	0,000	0,000
Hal127	<i>Ruegeria profunda</i>	d8cc70ef719c394a20914cb65fb5b18d	0,000	0,000	0,000	0,027	0,000	0,000
Hal129	<i>Ruegeria faecimaris</i>	b8929666c307cf3887a71cd73c66a1ed	0,000	0,000	0,075	0,000	0,000	0,000
Hal131	<i>Rheinheimera baltica</i>	88e20bb67048401bc39db0316a6ab4f9	0,022	0,000	0,000	0,000	0,000	0,000
Hal132	<i>Ruegeria profunda</i>	d8cc70ef719c394a20914cb65fb5b18d	0,000	0,000	0,000	0,027	0,000	0,000
Hal133	<i>Phaeobacter piscinae</i>	becac65900aa499e3678bb6d22ecf290	0,000	0,000	0,000	0,022	0,450	0,000
Hal134	<i>Kiloniella laminariae</i>	d62bf84e66138d9018cb90bd939cccbc	0,000	0,000	0,000	0,049	0,005	0,000
Hal135	<i>Litoreaibacter janthinus</i>	85e255d146bc5f49271dcae6aaf9d9cf	0,000	0,000	0,000	0,037	0,012	0,000
Hal136	<i>Nioella sediminis</i>	c7736d6452dfb2195716f8b07afa4850	0,000	0,000	0,082	0,026	0,000	0,000
Hal137	<i>Erythrobacter seohaensis</i>	561ccfc9d063356c8373a600171733ec	0,028	0,000	0,000	0,000	0,000	0,000
Hal138	<i>Pseudoruegeria sabulilitoris</i>	d212debc9292833f22dec8f201f7ebf	0,000	1,091	0,000	0,000	0,056	0,000
Hal139	<i>Ruegeria profunda</i>	d8cc70ef719c394a20914cb65fb5b18d	0,000	0,000	0,000	0,027	0,000	0,000
Hal140	<i>Sphingopyxis flavimaris</i>	1bc0c22c52d25e72f983b47e38c647c3	0,000	0,000	0,000	0,070	0,000	0,000
Hal141	<i>Tenacibaculum cellulophagum</i>	daadd9b54be62ed453d88a9f50ca5641	0,000	0,000	0,000	0,008	0,000	0,000

Appendix to Chapter 3

Hal142	<i>Neptunomonas concharum</i>	841df60651416535c2c0791b3fc5d71f	0,000	0,023	0,000	0,000	0,000	0,000
Hal143	<i>Pseudohalocynthia bacter aestuarii vivens</i>	21ab9955c5e2ce2b6ce179ffe7d62c90	0,000	0,000	0,010	0,000	0,000	0,000
Hal144	<i>Maribacter dokdonensis</i>	6f07000b878342378ded44ae1096d94b	0,000	0,000	0,069	0,080	0,044	0,042
Hal145	<i>Altererythro bacter ishigakiensis</i>	f63eb003f927def8abddf4edda1cf3d8	0,000	0,000	0,020	0,000	0,000	0,000
Hal146	<i>Bacillus licheniformis</i>	ecf69a838b7d63150c042e73e2b50423	0,000	0,216	0,000	0,000	0,000	0,000
Hal147	<i>Kiloniella laminariae</i>	d62bf84e66138d9018cb90bd939cccbc	0,000	0,000	0,000	0,049	0,005	0,000
Hal148	<i>Pseudooseohaicola caenipelagi</i>	95ed41233edc16cf58d78f9b9ddb186a	0,000	0,000	0,011	0,007	0,000	0,000
Hal149	<i>Defluviimonas aestuarii</i>	b9eb6875cb6b3c9d91aa36411059d61e	0,000	0,000	0,009	0,000	0,000	0,000
Hal150	<i>Defluviimonas aestuarii</i>	8c555f97585f69a60d1a497859badebc	0,000	0,000	0,120	0,148	0,038	0,000
Hal152	<i>Microbulbifer epialgicus</i>	1a50dd4db5ae0206ba073783bb4c5424	0,281	0,000	0,006	0,000	0,000	0,000
Hal153	<i>Pseudooseohaicola caenipelagi</i>	95ed41233edc16cf58d78f9b9ddb186a	0,000	0,000	0,011	0,007	0,000	0,000
Hal154	<i>Tateyamaria omphalii</i>	1967bbafbda8d12891485b3d09cf69a	0,000	0,000	0,000	0,011	0,000	0,000
Hal155	<i>Altererythro bacter ishigakiensis</i>	f63eb003f927def8abddf4edda1cf3d8	0,000	0,000	0,020	0,000	0,000	0,000
Hal156	<i>Micromonospora auratinigra</i>	131c1a05f13c52a7efe8aa5ef75997aa	0,000	0,093	0,000	0,028	0,000	0,000
Hal157	<i>Pseudohalocynthia bacter aestuarii vivens</i>	21ab9955c5e2ce2b6ce179ffe7d62c90	0,000	0,000	0,010	0,000	0,000	0,000
Hal158	<i>Microbulbifer epialgicus</i>	1a50dd4db5ae0206ba073783bb4c5424	0,281	0,000	0,006	0,000	0,000	0,000
Hal159	<i>Sphingopyxis flavimaris</i>	8bbaf89045c9cf5720efd5bf2c51cf1a	0,000	0,000	0,044	0,082	0,000	0,000
Hal161	<i>Pseudorhodobacter wandonensis</i>	22afe9bc34c5c19c0950a9f145355acc	0,000	0,000	0,009	0,004	0,000	0,000
Hal162	<i>Ruegeria mobilis</i>	cc80a7e3bb16a4045179d26baed0b28b	0,000	0,000	0,009	0,000	0,000	0,000
Hal163	<i>Tateyamaria omphalii</i>	1967bbafbda8d12891485b3d09cf69a	0,000	0,000	0,000	0,011	0,000	0,000
Hal164	<i>Microbulbifer epialgicus</i>	1a50dd4db5ae0206ba073783bb4c5424	0,281	0,000	0,006	0,000	0,000	0,000
Hal166	<i>Microbulbifer epialgicus</i>	1a50dd4db5ae0206ba073783bb4c5424	0,281	0,000	0,006	0,000	0,000	0,000
Hal167	<i>Erythro bacter aquimaris</i>	1794674a9cfa68fcd21a4cb40cbcd931	0,000	0,000	0,000	0,000	0,023	0,000
Hal168	<i>Bacillus firmus</i>	8e17d8587b49fd0ba3bd9e53547b8293	0,000	0,008	0,000	0,000	0,000	0,000
Hal169	<i>Bacillus gottheilii</i>	8e17d8587b49fd0ba3bd9e53547b8293	0,000	0,008	0,000	0,000	0,000	0,000
Hal170	<i>Bacillus licheniformis</i>	ecf69a838b7d63150c042e73e2b50423	0,000	0,216	0,000	0,000	0,000	0,000
Hal174	<i>Altererythro bacter ishigakiensis</i>	f63eb003f927def8abddf4edda1cf3d8	0,000	0,000	0,020	0,000	0,000	0,000
Hal175	<i>Roseovarius aestuarii</i>	21ab9955c5e2ce2b6ce179ffe7d62c90	0,000	0,000	0,010	0,000	0,000	0,000
Hal177	<i>Altererythro bacter luteolus</i>	f63eb003f927def8abddf4edda1cf3d8	0,000	0,000	0,020	0,000	0,000	0,000
Hal178	<i>Nocardia coeliaca</i>	131c1a05f13c52a7efe8aa5ef75997aa	0,000	0,093	0,000	0,028	0,000	0,000
Hal179	<i>Rhodococcus qingshengii</i>	131c1a05f13c52a7efe8aa5ef75997aa	0,000	0,093	0,000	0,028	0,000	0,000
Hal180	<i>Nocardia coeliaca</i>	131c1a05f13c52a7efe8aa5ef75997aa	0,000	0,093	0,000	0,028	0,000	0,000
Hal181	<i>Rhodococcus qingshengii</i>	131c1a05f13c52a7efe8aa5ef75997aa	0,000	0,093	0,000	0,028	0,000	0,000
Hal182	<i>Rhodococcus qingshengii</i>	131c1a05f13c52a7efe8aa5ef75997aa	0,000	0,093	0,000	0,028	0,000	0,000
Hal183	<i>Shewanella colwelliana</i>	3d56fd9774125a927d7e3142d542144f	0,000	0,000	0,036	0,000	0,043	15,292
Hal184	<i>Aquimarina muelleri</i>	70efd423a7af9b02278cf10a9e8be033	0,000	0,000	0,219	0,036	0,000	0,000
Hal185	<i>Ruegeria profunda</i>	d8cc70ef719c394a20914cb65fb5b18d	0,000	0,000	0,000	0,027	0,000	0,000
Hal186	<i>Ruegeria profunda</i>	d8cc70ef719c394a20914cb65fb5b18d	0,000	0,000	0,000	0,027	0,000	0,000
Hal187	<i>Ruegeria profunda</i>	d8cc70ef719c394a20914cb65fb5b18d	0,000	0,000	0,000	0,027	0,000	0,000
Hal188	<i>Mycobacterium houstonense</i>	0314c5b5c618bf2c53e08b17cf6b5acf	0,000	0,000	0,000	0,005	0,000	0,019
Hal189	<i>Nocardia lasii</i>	5e23c4d7da1773d3296164ddc899deda	0,000	0,000	0,000	0,010	0,000	0,000
Hal190	<i>Aquimarina muelleri</i>	70efd423a7af9b02278cf10a9e8be033	0,000	0,000	0,219	0,036	0,000	0,000
Hal191	<i>Sphingopyxis flavimaris</i>	8bbaf89045c9cf5720efd5bf2c51cf1a	0,000	0,000	0,044	0,082	0,000	0,000
Hal192	<i>Nocardia coeliaca</i>	131c1a05f13c52a7efe8aa5ef75997aa	0,000	0,093	0,000	0,028	0,000	0,000
Hal193	<i>Mycobacterium peregrinum</i>	0314c5b5c618bf2c53e08b17cf6b5acf	0,000	0,000	0,000	0,005	0,000	0,019
Hal195	<i>Mycobacterium houstonense</i>	0314c5b5c618bf2c53e08b17cf6b5acf	0,000	0,000	0,000	0,005	0,000	0,019

Appendix to Chapter 3

Hal196	<i>Nocardia lasii</i>	5e23c4d7da1773d3296164ddc899deda	0,000	0,000	0,000	0,010	0,000	0,000
Hal197	<i>Aquimarina muelleri</i>	70efd423a7af9b02278cf10a9e8be033	0,000	0,000	0,219	0,036	0,000	0,000
Hal198	<i>Rhodococcus qingshengii</i>	131c1a05f13c52a7efe8aa5ef75997aa	0,000	0,093	0,000	0,028	0,000	0,000
Hal199	<i>Aquimarina muelleri</i>	70efd423a7af9b02278cf10a9e8be033	0,000	0,000	0,219	0,036	0,000	0,000
Hal200	<i>Ruegeria profunda</i>	d8cc70ef719c394a20914cb65fb5b18d	0,000	0,000	0,000	0,027	0,000	0,000
Hal201	<i>Aquimarina muelleri</i>	70efd423a7af9b02278cf10a9e8be033	0,000	0,000	0,219	0,036	0,000	0,000
Hal202	<i>Ruegeria profunda</i>	d8cc70ef719c394a20914cb65fb5b18d	0,000	0,000	0,000	0,027	0,000	0,000
Hal203	<i>Cellulophaga algicola</i>	1bcbd76cf8c24fbb55a1eecd0169b2d3	0,000	0,000	0,019	0,000	0,000	0,000
Hal204	<i>Mycobacterium houstonense</i>	0314c5b5c618bf2c53e08b17cf6b5acf	0,000	0,000	0,000	0,005	0,000	0,019
Hal205	<i>Aquimarina muelleri</i>	70efd423a7af9b02278cf10a9e8be033	0,000	0,000	0,219	0,036	0,000	0,000
Hal206	<i>Mycobacterium houstonense</i>	0314c5b5c618bf2c53e08b17cf6b5acf	0,000	0,000	0,000	0,005	0,000	0,019
Hal207	<i>Mycolicibacterium peregrinum</i>	0314c5b5c618bf2c53e08b17cf6b5acf	0,000	0,000	0,000	0,005	0,000	0,019
Hal208	<i>Mycolicibacterium peregrinum</i>	0314c5b5c618bf2c53e08b17cf6b5acf	0,000	0,000	0,000	0,005	0,000	0,019
Hal209	<i>Mycolicibacterium peregrinum</i>	0314c5b5c618bf2c53e08b17cf6b5acf	0,000	0,000	0,000	0,005	0,000	0,019
Hal210	<i>Mycolicibacterium peregrinum</i>	0314c5b5c618bf2c53e08b17cf6b5acf	0,000	0,000	0,000	0,005	0,000	0,019
Hal211	<i>Mycolicibacterium frederiksbergense</i>	0314c5b5c618bf2c53e08b17cf6b5acf	0,000	0,000	0,000	0,005	0,000	0,019
Hal212	<i>Mycobacterium houstonense</i>	0314c5b5c618bf2c53e08b17cf6b5acf	0,000	0,000	0,000	0,005	0,000	0,019
Hal213	<i>Andersenella baltica</i>	4442113e6729cfe743f976eec78cda01	0,049	0,032	0,217	0,013	0,000	0,000
Hal214	<i>Nocardia fluminea</i>	5e23c4d7da1773d3296164ddc899deda	0,000	0,000	0,000	0,010	0,000	0,000
Hal215	<i>Nocardia lasii</i>	5e23c4d7da1773d3296164ddc899deda	0,000	0,000	0,000	0,010	0,000	0,000
Hal216	<i>Neptunomonas concharum</i>	841df60651416535c2c0791b3fc5d71f	0,000	0,023	0,000	0,000	0,000	0,000
Hal217	<i>Roseovarius aestuarii</i>	21ab9955c5e2ce2b6ce179ffe7d62c90	0,000	0,000	0,010	0,000	0,000	0,000
Hal218	<i>Mycolicibacterium peregrinum</i>	0314c5b5c618bf2c53e08b17cf6b5acf	0,000	0,000	0,000	0,005	0,000	0,019
Hal219	<i>Mycolicibacterium conceptionense</i>	0314c5b5c618bf2c53e08b17cf6b5acf	0,000	0,000	0,000	0,005	0,000	0,019
Hal220	<i>Mycolicibacterium conceptionense</i>	0314c5b5c618bf2c53e08b17cf6b5acf	0,000	0,000	0,000	0,005	0,000	0,019
Hal221	<i>Mycolicibacterium conceptionense</i>	0314c5b5c618bf2c53e08b17cf6b5acf	0,000	0,000	0,000	0,005	0,000	0,019
Hal222	<i>Mycobacterium syngnathidarum</i>	0314c5b5c618bf2c53e08b17cf6b5acf	0,000	0,000	0,000	0,005	0,000	0,019
Hal223	<i>Mycobacterium houstonense</i>	0314c5b5c618bf2c53e08b17cf6b5acf	0,000	0,000	0,000	0,005	0,000	0,019
Hal224	<i>Mycolicibacterium conceptionense</i>	0314c5b5c618bf2c53e08b17cf6b5acf	0,000	0,000	0,000	0,005	0,000	0,019
Hal225	<i>Mycolicibacterium peregrinum</i>	0314c5b5c618bf2c53e08b17cf6b5acf	0,000	0,000	0,000	0,005	0,000	0,019
Hal226	<i>Mycolicibacterium conceptionense</i>	0314c5b5c618bf2c53e08b17cf6b5acf	0,000	0,000	0,000	0,005	0,000	0,019
Hal227	<i>Mycolicibacterium conceptionense</i>	0314c5b5c618bf2c53e08b17cf6b5acf	0,000	0,000	0,000	0,005	0,000	0,019
Hal228	<i>Mycolicibacterium peregrinum</i>	0314c5b5c618bf2c53e08b17cf6b5acf	0,000	0,000	0,000	0,005	0,000	0,019
Hal230	<i>Phaeobacter caeruleus</i>	b8929666c307cf3887a71cd73c66a1ed	0,000	0,000	0,075	0,000	0,000	0,000
Hal231	<i>Microbulbifer epialgicus</i>	1a50dd4db5ae0206ba073783bb4c5424	0,281	0,000	0,006	0,000	0,000	0,000
Hal234	<i>Cellulophaga algicola</i>	1bcbd76cf8c24fbb55a1eecd0169b2d3	0,000	0,000	0,019	0,000	0,000	0,000
Hal235	<i>Cellulophaga algicola</i>	1bcbd76cf8c24fbb55a1eecd0169b2d3	0,000	0,000	0,019	0,000	0,000	0,000
Hal236	<i>Erythrobacter vulgaris</i>	a952451d5eeeb968986dca32fed405bd	0,000	0,000	0,018	0,000	0,000	0,000
Hal237	<i>Mycolicibacterium vanbaalenii</i>	0314c5b5c618bf2c53e08b17cf6b5acf	0,000	0,000	0,000	0,005	0,000	0,019
Hal238	<i>Nocardia lasii</i>	5e23c4d7da1773d3296164ddc899deda	0,000	0,000	0,000	0,010	0,000	0,000
Hal239	<i>Loktanelia cinnabarina</i>	fd2635b6f6dffec9df066d8486b04194	0,000	0,041	0,000	0,000	0,000	0,000

Appendix to Chapter 3

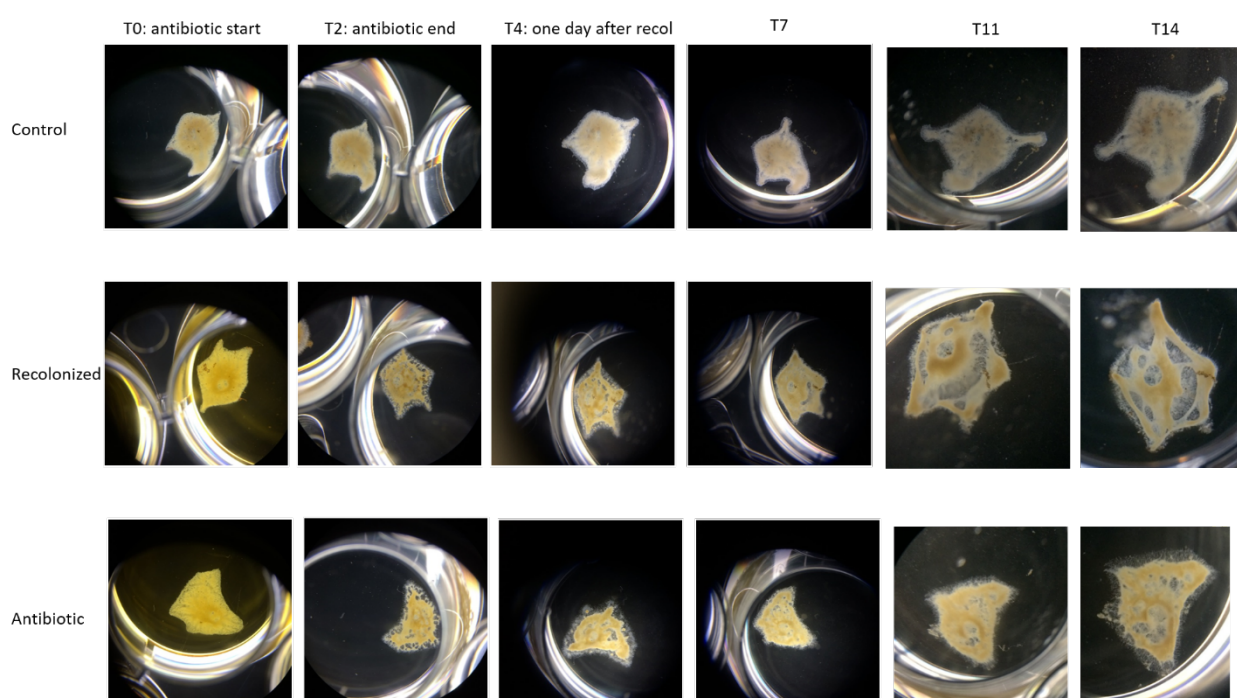
Hal240	<i>Amylibacter cionae</i>	1a53c949d4b9243f52df3e62d1f5e2da	98.889	7.41E-137	0.000	0.000	0.000	0.000
Hal242	<i>Pseudoalteromonas neustonica</i>	db3169a15d59499ad858c9ae2d89ab52	0,000	0,018	0,000	0,000	0,000	0,000
Hal244	<i>Streptomyces fulvissimus</i>	0cac2b97bf85843836a5df531d7b3d42	0,043	0,000	0,061	0,000	0,000	0,080
Hal245	<i>Roseovarius aestuarii</i>	21ab9955c5e2ce2b6ce179ffe7d62c90	0,000	0,000	0,010	0,000	0,000	0,000
Hal246	<i>Loktanella cinnabarina</i>	fd2635b6f6dfec9df066d8486b04194	0,000	0,041	0,000	0,000	0,000	0,000
Hal247	<i>Microbulbifer pacificus</i>	1a50dd4db5ae0206ba073783bb4c5424	0,281	0,000	0,006	0,000	0,000	0,000
Hal249	<i>Maribacter aquivivus</i>	9483ac1d527f5fc7178c60a00dbe9954	0,000	0,000	0,020	0,023	0,000	0,000
Hal250	<i>Shewanella colwelliana</i>	3d56fd9774125a927d7e3142d542144f	0,000	0,000	0,036	0,000	0,043	15,292
Hal251	<i>Ruegeria atlantica</i>	cc80a7e3bb16a4045179d26baed0b28b	0,000	0,000	0,009	0,000	0,000	0,000
Hal252	<i>Streptomyces sampsonii</i>	0cac2b97bf85843836a5df531d7b3d42	0,043	0,000	0,061	0,000	0,000	0,080
Hal253	<i>Maribacter orientalis</i>	9483ac1d527f5fc7178c60a00dbe9954	0,000	0,000	0,020	0,023	0,000	0,000
Hal254	<i>Labrenzia salina</i>	ea0e7f8c1c51ddb7b820fcc75ad94911	0,000	0,000	0,000	0,007	0,000	0,000
Hal255	<i>Pseudomonas cuatrocienegasensis</i>	dca3bdce6abdce3910425b17406b5504	0,000	0,044	0,000	0,000	0,000	0,000
Hal256	<i>Loktanella rosea</i>	e86b6eba9a160bc0f60fa0f317c491a6	0,104	0,000	0,093	0,000	0,000	0,000
Hal257	<i>Nocardioides furvisabuli</i>	225dd6ac7a0a066bb90cd0d85e9d3fa3	0,000	0,011	0,000	0,000	0,000	0,000
Hal259	<i>Hoeflea alexandrii</i>	bd273cfa696cec78f24d2dad6fddd658	0,000	0,000	0,000	0,032	0,000	0,000
Hal260	<i>Shewanella colwelliana</i>	3d56fd9774125a927d7e3142d542144f	0,000	0,000	0,036	0,000	0,043	15,292
Hal261	<i>Sulfitobacter donghicola</i>	663c1d01ebba243a382582b3cc22609d	0,000	0,000	0,000	0,021	0,000	0,000
Hal262	<i>Maribacter aquivivus</i>	9483ac1d527f5fc7178c60a00dbe9954	0,000	0,000	0,020	0,023	0,000	0,000
Hal263	<i>Roseovarius aestuarii</i>	2ae539d64f2f243f3dc7b3117d4bd452	0,000	0,000	0,253	0,000	0,000	0,000
Hal264	<i>Litoreibacter albidus</i>	85e255d146bc5f49271dcae6aaf9d9cf	0,000	0,000	0,000	0,037	0,012	0,000
Hal265	<i>Loktanella rosea</i>	e86b6eba9a160bc0f60fa0f317c491a6	0,104	0,000	0,093	0,000	0,000	0,000
Hal266	<i>Aquimarina muelleri</i>	0c7ef6e17eb811ce6fac4a76fce3a0d4	0,000	0,000	0,067	1,925	0,000	0,000
Hal267	<i>Sedimentitalea todarodis</i>	abb46bd1cb052cfaef078b2321506018	0,000	0,000	0,007	0,000	0,000	0,000
Hal268	<i>Vadicella arenosi</i>	1967bbafbd8d12891485b3d09cfc69a	0,000	0,000	0,000	0,011	0,000	0,000
Hal269	<i>Nocardioides marinisabuli</i>	225dd6ac7a0a066bb90cd0d85e9d3fa3	0,000	0,011	0,000	0,000	0,000	0,000
Hal270	<i>Ruegeria faecimaris</i>	b8929666c307cf3887a71cd73c66a1ed	0,000	0,000	0,075	0,000	0,000	0,000
Hal271	<i>Pseudoalteromonas arctica</i>	17753a04c358b65972ce4531833fcc1	1,242	0,000	0,073	0,000	2,222	18,789
Hal272	<i>Photobacterium halotolerans</i>	5a6f6579647b17bc616473c22cad3fce	0,000	0,000	0,011	0,000	0,000	0,000
Hal273	<i>Pseudoalteromonas arctica</i>	17753a04c358b65972ce4531833fcc1	1,242	0,000	0,073	0,000	2,222	18,789
Hal274	<i>Pseudoalteromonas arctica</i>	6be58fb6b1156724a41b54f979a36802	0,075	0,000	0,000	0,000	0,106	0,000
Hal275	<i>Photobacterium halotolerans</i>	5a6f6579647b17bc616473c22cad3fce	0,000	0,000	0,011	0,000	0,000	0,000
Hal276	<i>Pseudoalteromonas arctica</i>	17753a04c358b65972ce4531833fcc1	1,242	0,000	0,073	0,000	2,222	18,789
Hal277	<i>Pseudoalteromonas arctica</i>	17753a04c358b65972ce4531833fcc1	1,242	0,000	0,073	0,000	2,222	18,789
Hal279	<i>Photobacterium halotolerans</i>	3566bd7e1d47f0cd9a10a70db2138ffb	0,000	0,000	0,000	0,000	0,006	0,000
Hal280	<i>Photobacterium halotolerans</i>	5a6f6579647b17bc616473c22cad3fce	0,000	0,000	0,011	0,000	0,000	0,000
Hal281	<i>Vibrio atlanticus</i>	801f55a4831a1d3ba3eca43803ec88c3	0,080	0,006	0,054	0,005	1,371	19,651
Hal282	<i>Altererythrobacter ishigakiensis</i>	f63eb003f927def8abddf4edda1cf3d8	0,000	0,000	0,020	0,000	0,000	0,000
Hal283	<i>Roseibium sediminis</i>	ea0e7f8c1c51ddb7b820fcc75ad94911	0,000	0,000	0,000	0,007	0,000	0,000
Hal284	<i>Ruegeria profunda</i>	d8cc70ef719c394a20914cb65fb5b18d	0,000	0,000	0,000	0,027	0,000	0,000
Hal285	<i>Roseovarius aestuarii</i>	21ab9955c5e2ce2b6ce179ffe7d62c90	0,000	0,000	0,010	0,000	0,000	0,000
Hal286	<i>Sphingopyxis flavimaris</i>	1bc0c22c52d25e72f983b47e38c647c3	0,000	0,000	0,000	0,070	0,000	0,000
Hal287	<i>Litoreibacter janthinus</i>	4badc41f2833225bbadf7a9dacb12304	0,000	0,000	0,000	0,020	0,000	0,000
Hal288	<i>Microbulbifer pacificus</i>	1a50dd4db5ae0206ba073783bb4c5424	0,281	0,000	0,006	0,000	0,000	0,000
Hal289	<i>Roseovarius aestuarii</i>	21ab9955c5e2ce2b6ce179ffe7d62c90	0,000	0,000	0,010	0,000	0,000	0,000
Hal290	<i>Mycobacterium hodleri</i>	0314c5b5c618bf2c53e08b17cf6b5acf	0,000	0,000	0,000	0,005	0,000	0,019

Appendix to Chapter 3

Hal291	<i>Mycobacterium vanbaalenii</i>	0314c5b5c618bf2c53e08b17cf6b5acf	0,000	0,000	0,000	0,005	0,000	0,019
Hal292	<i>Roseovarius aestuarii</i>	21ab9955c5e2ce2b6ce179ffe7d62c90	0,000	0,000	0,010	0,000	0,000	0,000
Hal293	<i>Litorimonas cladophorae</i>	a67a49dc2c43d45a86fe1c628236920a	0,000	0,000	0,005	0,000	0,000	0,000
Hal294	<i>Mycobacterium arabiense</i>	786e9a3c3f2f362d844d9b78b82c72da	0,241	0,172	0,134	0,073	0,000	0,033
Hal295	<i>Mycobacterium aurum</i>	e074580ef16ef3c53b419ed132365698	0,000	0,006	0,001	0,000	0,000	0,000
Hal296	<i>Streptomyces scabrissporus</i>	0cac2b97bf85843836a5df531d7b3d42	0,043	0,000	0,061	0,000	0,000	0,080
Hal298	<i>Pseudoseohaericola caenipelagi</i>	95ed41233edc16cf58d78f9b9dbd186a	0,000	0,000	0,011	0,007	0,000	0,000
Hal299	<i>Pseudoruegeria lutimaris</i>	d212debc9292833f22dec8f201f7ebf	0,000	1,091	0,000	0,000	0,056	0,000
Hal300	<i>Sphingorhabdus litoris</i>	8bbaf89045c9cf5720efd5bf2c51cf1a	0,000	0,000	0,044	0,082	0,000	0,000
Hal301	<i>Sphingorhabdus flavimaris</i>	40377e54010a84dbca9c3914f2969e91	0,013	0,000	0,018	0,032	0,000	0,000
Hal302	<i>Flavobacterium jumunjinense</i>	b5f8481ab1741f39cff72fb2289d7c7a	0,000	0,005	0,163	0,000	0,000	0,000
Hal303	<i>Seohaericola saemankumensis</i>	f7cda7654affdaccdd18c29edd49c669e	0,000	0,000	0,016	0,000	0,000	0,000
Hal304	<i>Pararhodobacter aggregans</i>	f38ed818f44bd57a3550e22d9ed2ff58	0,000	0,000	0,020	0,000	0,000	0,000
Hal305	<i>Mesorhizobium qingshengii</i>	04598e9ab30714a064c2d81e3f1fb05b	0,000	0,092	0,000	0,000	0,000	0,000
Hal306	<i>Roseovarius aestuarii</i>	c3c2be0957d45403e317997b7d2b7050	0,000	0,000	0,049	0,000	0,000	0,000
Hal307	<i>Pseudohalocynthiibacter aestuariivivens</i>	c21da76cc6133a23af08b1cd52625611	0,000	0,000	0,057	0,000	0,000	0,000
Hal308	<i>Roseovarius aestuarii</i>	c3c2be0957d45403e317997b7d2b7050	0,000	0,000	0,049	0,000	0,000	0,000
Hal309	<i>Roseovarius aestuarii</i>	c3c2be0957d45403e317997b7d2b7050	0,000	0,000	0,049	0,000	0,000	0,000
Hal310	<i>Erythrobacter aquimaris</i>	4cdf1d045b71f4ff67c3bfc3e6e083b	0,000	0,000	0,000	0,188	0,000	0,000
Hal312	<i>Maritalea porphyra</i>	f56c5bf11cf6b1064fed81893f62ed53	0,000	0,006	0,002	0,000	0,000	0,000
Hal313	<i>Sphingorhabdus flavimaris</i>	82b21eb5f09977462412a56550b00e17	0,000	0,000	0,093	0,104	0,053	0,061
Hal314	<i>Mycolicibacterium peregrinum</i>	0314c5b5c618bf2c53e08b17cf6b5acf	0,000	0,000	0,000	0,005	0,000	0,019
Hal315	<i>Mycolicibacterium peregrinum</i>	0314c5b5c618bf2c53e08b17cf6b5acf	0,000	0,000	0,000	0,005	0,000	0,019
Hal317	<i>Aquihabitans daechungensis</i>	00e1515a67205fcb8a0a7feff16a5a06	0,000	0,016	0,126	0,017	0,008	0,000
Hal318	<i>Andersenella sp.</i>	4ca51745563a7826b72a15bace89f4f6	0,000	0,000	0,848	0,430	0,179	0,250
Hal319	<i>Sedimentitalea nanhaiensis</i>	a05c6d1e0255f2e4850182ade942d562	0,177	0,000	0,036	0,000	0,000	0,000
Hal320	<i>Sedimentitalea nanhaiensis</i>	a05c6d1e0255f2e4850182ade942d562	0,177	0,000	0,036	0,000	0,000	0,000
Hal321	<i>Maritalea porphyrae</i>	f56c5bf11cf6b1064fed81893f62ed53	0,000	0,006	0,002	0,000	0,000	0,000
Hal323	<i>Andersenella baltica</i>	4442113e6729cfe743f976eec78cda01	0,049	0,032	0,217	0,013	0,000	0,000
Hal324	<i>Andersenella baltica</i>	4ca51745563a7826b72a15bace89f4f6	0,000	0,000	0,848	0,430	0,179	0,250
Hal325	<i>Pelagicola litorisediminis</i>	a05c6d1e0255f2e4850182ade942d562	0,177	0,000	0,036	0,000	0,000	0,000
Hal326	<i>Andersenella baltica</i>	4442113e6729cfe743f976eec78cda01	0,049	0,032	0,217	0,013	0,000	0,000
Hal327	<i>Halioglobus lutimaris</i>	b58f540777f63002fa0f275b1ab3833b	0,000	0,000	0,010	0,000	0,000	0,000
Hal329	<i>Ruegeria faecimaris</i>	b8929666c307cf3887a71cd73c66a1ed	0,000	0,000	0,075	0,000	0,000	0,000
Hal330	<i>Ruegeria faecimaris</i>	b8929666c307cf3887a71cd73c66a1ed	0,000	0,000	0,075	0,000	0,000	0,000
Hal331	<i>Microbulbifer pacificus</i>	1a50dd4db5ae0206ba073783bb4c5424	0,281	0,000	0,006	0,000	0,000	0,000
Hal332	<i>Ruegeria profunda</i>	d8cc70ef719c394a20914cb65fb5b18d	0,000	0,000	0,000	0,027	0,000	0,000
Hal333	<i>Mycolicibacterium peregrinum</i>	0314c5b5c618bf2c53e08b17cf6b5acf	0,000	0,000	0,000	0,005	0,000	0,019
Hal334	<i>Ruegeria faecimaris</i>	b8929666c307cf3887a71cd73c66a1ed	0,000	0,000	0,075	0,000	0,000	0,000
Hal335	<i>Streptomyces sampsonii</i>	0cac2b97bf85843836a5df531d7b3d42	0,043	0,000	0,061	0,000	0,000	0,080

APPENDIX 3.7 | Growth and morphology of *Haliclona sp.* juveniles after antibiotic treatment and recolonization.

In summer 2019, *Haliclona sp.* spawned coincidentally in the maintenance aquaria. Settled juveniles (1-8 mm diameter) were noticed in August after metamorphosis into functional juveniles with oscula. Spawning and larvae release must have happened earlier, probably around June-July, and over a longer time period judging from the large size differences between juveniles. This species could be interesting for future developmental studies since it shows great potential to reproduce and develop under laboratory conditions. Juveniles of approximately 1-2 month (2-7 mm diameter) were scraped off aquaria walls with a scalpel and transferred to 12-well plates filled with artificial, sterile-filtered seawater. Sponges were either kept under these conditions, treated with antibiotics (rifampicin, ampicillin, nalidixic acid, neomycin and polymyxin B) for two days, or recolonized with the natural sponge microbiome after antibiotic treatment. Water was exchanged manually once a day. A previous test showed fungal growth after antibiotic treatment, and hence the fungicide amphotericin B was added. The figure shows the changes of *Haliclona sp.* juvenile morphology in control, recolonized and antibiotic treatment over time (examples of three individuals).



Sponges in artificial, sterile-filtered seawater grew visibly and changed their morphology. Sponges after antibiotic treatment showed holes in their tissue but organic material visibly grew and changed morphology. Thus, sponges were alive and no mortality was observed until sampling after three weeks

Appendix to Chapter 3

(12 replicates). There was no visible difference between recolonized and non-recolonized sponges. Amphotericin B is known to be cytotoxic not only to fungi but also to other eukaryotic cells. The holes most likely are a result of the Amphotericin B treatment, so other fungicides should be tested in the future.

APPENDIX 3.8 | Schmittmann, L., U. Hentschel. 2021. Antibiotic treatment of the sponge *Halichondria panicea* and subsequent recolonization. [dx.doi.org/10.17504/protocols.io.by7hpzj6](https://doi.org/10.17504/protocols.io.by7hpzj6)



Antibiotic treatment of the breadcrumb sponge *Halichondria panicea* and subsequent recolonization

Lara Schmittmann¹, Ute U Hentschel¹

¹GEOMAR Helmholtz Centre for Ocean Research Kiel

[dx.doi.org/10.17504/protocols.io.by7hpzj6](https://doi.org/10.17504/protocols.io.by7hpzj6)



Lara Schmittmann
GEOMAR Helmholtz Centre for Ocean Research

This protocol generates sponges (*Halichondria panicea*) with a disturbed microbiome under controlled experimental conditions, in order to study bacterial recolonization dynamics. Bacteria-bacteria interactions can be analysed with this set-up within the host environment aiming at a better understanding of sponge-microbe symbiosis *in vivo*.

It is divided into the sections 1) preparation, 2) antibiotic treatment and recovery phase, 3) recolonization with the natural microbiome and 4) sampling.

DOI

[dx.doi.org/10.17504/protocols.io.by7hpzj6](https://doi.org/10.17504/protocols.io.by7hpzj6)

Lara Schmittmann, Ute U Hentschel . Antibiotic treatment of the breadcrumb sponge *Halichondria panicea* and subsequent recolonization. **protocols.io**
<https://dx.doi.org/10.17504/protocols.io.by7hpzj6>



host-microbe interactions, sponge model, symbioses, microbiome, metaorganism, holobiont, antibiotic treatment

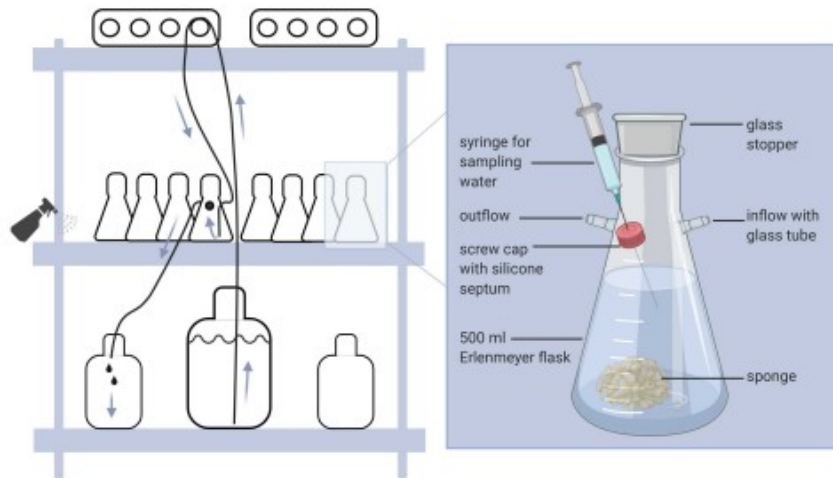


Figure: Experimental set-up in the gnotobiotic chambers in GEOMAR Helmholtz Centre for Ocean Research, Kiel. Four shelves like the one depicted here are available, each holding 8 x 500 mL modified Erlenmeyer flasks, in total 32 flasks.

The flow-through set-up (Figure) consists of 32 x 500 mL modified Erlenmeyer flasks distributed on 4 shelves. Each set of 8 flasks is supplied with fresh, sterile filtered artificial seawater from one 20 L carboy.

The culture flasks are customized flow-through Erlenmeyer flasks (500 mL) that are fully autoclavable and re-usable (Figure). The flasks are closed with a hollow glass stopper. Water is exchanged via a hose barb and attached glass tube reaching near the bottom of the Erlenmeyer flask for water inflow, and a hose barb on the opposite side for water outflow. A thread with a screw cap and silicone septum allows for sampling culture water with a sterile syringe and needle without opening the flasks.

Water flow-through is realized by GHL2 pumps that pump water from a 20 L source tank into the Erlenmeyer flasks; the replaced water is collected in 10 L canisters. Important! Calibrate each pump head prior to an experiment via the GHL software.

The gnotobiotic chambers are equipped with an air filtration system (Expansion Electronic CP500/SNATURE SYSTEM) constantly removing microorganisms from the air. The temperature and light regime can be chosen according to the season. Surface area is minimized and regularly surface sterilized (Curacid Medical wipes). All material is either autoclavable, sterile packed or sterilizable by surface sterilization prior to entering the room. Access is restricted and only allowed with lab coat, gloves and shoe covers. A transitioning zone in front of the gnotobiotic chambers provides space for changing, storage of additional material, cleaning of material etc..

The experiment can be set up one day prior to the start (start = placing sponges in the flasks), but some things have to be prepared 1-2 weeks in advance (start with section "preparation").

Culture:

- Breadcrum sponge *Halichondria panicea* (Pallas) collected from Schilksee, Kiel, Germany 54.424792, 10.175010
- Aqua Medic Seasalt EAN Code: 4025901100075
- *Nannochloropsis salina* freeze dried powder - algova UG
- Stainless steel filter, diameter 142 mm - Sartorius SM 16275
- 0.22 µm PVDF filter, diameter 142 mm
- Silicone tubing - inner diameter 4 mm, outer diameter 6 mm
- Silicone tubing - inner diameter 8 mm, outer diameter 12 mm
- Erlenmeyer - custom built by Eydam, Kiel, Germany
- Waste canisters for chemicals 10 l
- 20 l Nalgene® carboy (PP, for autoclaving)
- 100 l barrel
- Eheim® 1250 universal aquarium pump
- GHX® Doser 2.1
- Curacid® medical soaked whipes for surface sterilization

Antibiotics:

- Rifampicin - CAS :13292-46-1; stock solution as 50 mg/ml in 100 % DMSO
- Ampicillin - CAS :69-52-3; stock solution as 50 mg/ml in MilliQ water
- Nalidixic acid - CAS :389-08-2; stock solution as 50 mg/ml in 0.3 M NaOH
- Neomycin - CAS: 1405-10-3; stock solution as 50 mg/ml in MilliQ water
- Polymyxin B - CAS :1405-20-5; stock solution as 2 mg/ml in MilliQ water

Other chemicals:

- Difco™ Marine Agar
- Difco™ MarineBroth 2216
- RNase AWAY®
- RNAlater
- Ethanol
- Glutaraldehyde 2.5 %, 6.25 % in sterile filtered 1xPBS
- Paraformaldehyde 4 % in sterile filtered 1xPBS
- Glutaraldehyde 0.1 % + Paraformaldehyde 10 % in sterile filtered 1xPBS
- For CMF-ASW: NaCl, Na₂SO₄, KCl, NaHCO₃

Consumables and other material:

- Forceps
- Scalpel
- Sterile plastic petri dishes
- 2 ml polypropylene tubes
- 50 ml polypropylene tubes
- 1.8 ml Cryovials DNase/RNase free
- Corning® cell strainer 40 µm
- Sterile syringes 5 ml
- Sterile needles diameter 0.6 mm, length 80 mm
- 200 ml autoclavable bottles (for food stock)
- 1 l autoclavable bottles
- Bottle top vacuum filter, diameter 47 mm

Appendix to Chapter 3

- Re-usable syringe filter, diameter 25 mm
- 0.22 µm PVDF filter, diameter 25 mm
- 0.22 and 5 µm PVDF filter, diameter 47 mm

Equipment:

- Autoclave
- Fume hood
- Biosafety cabinet
- Orbital shaker
- Climate chamber with controlled light and temperature
- Salinometer
- Water bath
- Centrifuge - for 2 and 50 ml polypropylene tubes
- Vakuum pump

Waste water from the experiment has to be disposed as chemical waste:

- during antibiotic treatment as AVV 20 01 19 toxic pesticides
- after antibiotic treatment as AVV 18 01 03 medical waste for infection prevention (potentially antibiotic resistant bacteria selected by antibiotic treatment)

Work under the fume hood when handling toxic fixatives (Paraformaldehyde, Glutaraldehyde)

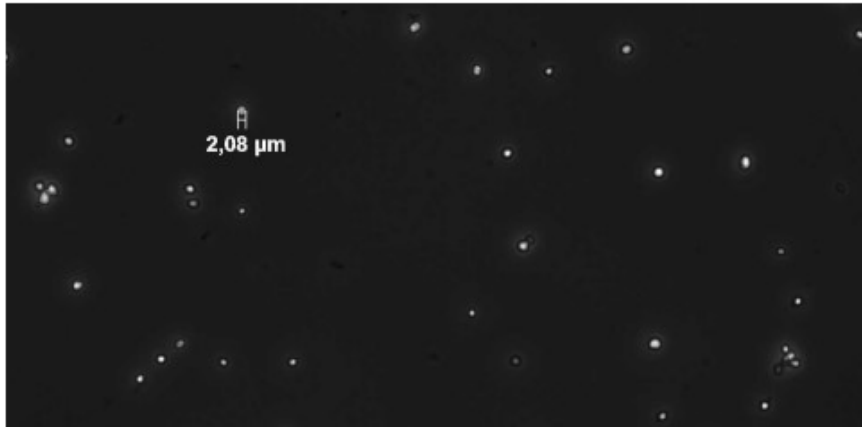
Start with section "preparation" and take ~1-2 weeks to prepare

Preparation 1w 0d 9h

- 1 Autoclaving material prior to use for 15 min at 121°C** 1w
 - culture bottles
 - silicone tubing (in- and outflow tubes can be connected to culture bottles before autoclaving)
 - 20 L carboys with tin foil wrapped around lid but don't close lid! otherwise carboys dent when they cool down
 - filtration unit with inserted filter paper 0.22 µm, diameter 142 mm
 - saline (1.5 % NaCl in MilliQ water)
 - food stock
 - CMF-ASW

- 2 Food stock** 3h

Autoclaved *Nannochloropsis salina* unicellular algae solution



These small (~2 μm) unicellular algae stay intact after autoclaving and retain their chlorophyll fluorescent signal. Also, Dan et al. 2018 showed that the nutritional value of closely related *Nannochloropsis* is not affected by autoclaving

 [Dan2018.pdf](#)

- 2.1 Weigh 16 g *Nannochloropsis salina* powder dried algae and dissolve in 2 L MilliQ water with 30 g artificial seasalt

Shake rigorously for several minutes or use magnetic stirrer

- 2.2 Filter through 40 μm cell strainer to remove algae clumps

- 2.3 Determine concentration in stock (flow cytometer or counting under the microscope)

adjust to a stock solution of 5×10^7 cells/ml (final concentration is 10^5 cells/ml)

- 2.4 Autoclave in 160 mL portions

Store at RT

3 Antibiotic stocks

3h

Per experiment, prepare 350 ml of each of the following antibiotic stocks:

- 50 mg/ml Rifampicin in 100 % DMSO (working conc. 50 mg/l)
- 50 mg/ml Ampicillin in MilliQ water (working conc. 50 mg/l)
- 50 mg/ml Nalidixic acid in 0.3 M NaOH (4.2 g NaOH in 350 ml MilliQ water) (working conc. 50 mg/l)
- 50 mg/ml Neomycin in MilliQ water (working conc. 50 mg/l)

- 2 mg/ml Polymixin B in MilliQ water (working conc. 2 mg/l)

Antibiotics were chosen based on their different mechanisms of actions, compound classes and based on previous studies (Franzenburg et al. 2012 PNAS, Domin et al. 2018 Frontiers in Microbiology, Weiland-Bräuer et al. 2015 AEM).

rifampicin: ansamycine (RNA synthesis inhibition of most Gram +, many Gram-)

nalidixic acid: quinolone (blocks DNA replication of most Gram-, some Gram+)

ampicillin: beta-lactame (inhibits cell wall formation during cell division of Gram+)

neomycin: aminoglycoside (blocks ribosomal subunit of Gram-, some Gram+)

polymixin B: polypeptide (disrupts cell membrane of Gram-)

3.1 Freeze in portions of 20 ml and store at -20°C

3.2 Use freshly thawed solutions, do not re-freeze

4 Sterile filtered artificial seawater (F-ASW)

6h

F-ASW should be prepared every day during the antibiotic treatment and every second day during the recovery phase and recolonization

4.1 Fill a 100 l barrel with distilled water while continuously adding 1.5 kg artificial seasalt
Dissolution can be sped up by adding a water pump into the barrel to mix the water

4.2 Mix well! Check salinity at bottom and top of the barrel and prevent foramtion of a salinity gradient. Slowly add missing salt until the desired salinity is reached

Since the salinity constantly fluctuates in the Baltic Sea, we choose the ambient salinity on the starting day of each experiment (between 14 and 18 PSU)

4.3 Connect autoclaved filter (142 mm) unit to pump and fill 4 autoclaved 20 l carboys with F-ASW

4.4 When all carboys are filled, stop water pump and rinse it in fresh water

Rinse filter unit and change filter paper; autoclave including silicone tube for the next filtration

4.5 Add 40 ml *Nannochloropsis salina* stock solution to each 20 l carboy

During antibiotic treatment, add 20 ml per antibiotic to each 20 l carboy. The final working concentrations will be:

- 50 mg/l Rifampicin
- 50 mg/l Ampicillin
- 50 mg/l Nalidixic acid
- 50 mg/l Neomycin
- 2 mg/l Polymixin B

Mix well (by rolling closed carboys)

4.6 After use, rinse carboys twice with fresh water and autoclave for the next use

5 MB medium

1d

Prepare 15 g/l Difco agar and 37.5 g MarineBroth in 1 l distilled water

Prepare ~350 plates per experiment (= 10 bottles of MB medium) and store at 4°C

5.1 Cook in water bath for 10-15 min to dissolve medium

5.2 Autoclave and store at 60°C until pouring plates

5.3 Pour plates under biosafety cabinet and store upside down at 4°C

6 CMF-ASW (Calcium-Magnesium-free artificial seawater) after Rottmann et al. 1987

Prepare e.g. 10 l as a stock and autoclave in portions of 500 ml



attention! The recipe for CMF-ASW is thought for marine organisms. Since we are working on sponges from brackish water here, dilute the stock 1:1 before autoclaving

6.1 For 1 l stock solution:

- 27 g NaCl
- 1 g Na₂SO₄
- 0.8 g KCl
- 0.18 g NaHCO₃

add 1 l MilliQ water

6.2 Dilute stock 1:1 with MilliQ water and autoclave in portions of 500 ml

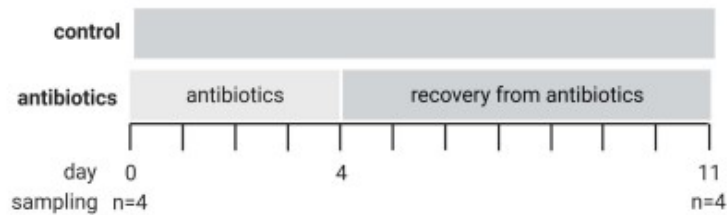
Can be stored at RT, but it is used ice-cold. Put bottles in freezer 1 h before they are needed

Antibiotic treatment and recovery phase 5d

7 Antibiotic treatment

5d

During the first four days of the experiment prepare ASW with antibiotics and change water source daily



Timeline of the antibiotic treatment. T0 = start of the experiment; T4 = end of the antibiotic treatment; T11 = end of the recovery phase and start of the recolonization. Figure created with Biorender.com

7.1 Start pumps on the first day prior to placing sponges in the Erlenmeyer flasks
Set pumps to **150 doses/day of 12 ml** to exchange the volume of each bottle 3.5 times per day

7.2 When Erlenmeyer flasks are filled, add one sponge in each Erlenmeyer flask (about 3x3x3 cm)
Start the experiment early in the morning

- 7.3 Prepare fresh antibiotic water and change carboys daily to prevent degradation and loss of function of antibiotics

8 Antibiotic wash-out

4h

In the afternoon of T4 start wash-out of antibiotics by exchanging the carboys with ASW+antibiotics to carboys with ASW only

- 8.1 Flush the Erlenmeyer flasks several times with 250 ml fresh ASW each (by programming the pumps to dose 250 ml. Attention! The GHL2 pumps are not designed to continuously run; after each flush they need to stop for at least 15 min)

- 8.2 Since Rifampicin is coloured bright orange, you clearly see the reduction of antibiotics in the water by flushing

Aim at completely clear culture water until the next morning to prevent remaining antibiotics at low concentrations

It helps to manually pour out water (without opening the Erlenmeyer; simply tilt the bottle and empty it via the outflow barb) and reduce the water level to about 200 ml before flushing

9 Recovery phase

During the recovery phase, exchange the water source every second day with freshly filtered ASW

Set the pumps to **100 doses/day of 10 ml** to exchange to volume of each bottle twice per day

Recolonization with the natural microbiome

2d

10 Differential centrifugation

3h

To prepare a bacterial inoculum for recolonization with the natural microbiome dissociate fresh, healthy sponges

The volume of sponge tissue should match the volume of sponge that you want to recolonize

- 10.1 Remove large pieces of algae and place sponges in a beaker with sterile, ice-cold CMF-ASW for 5 min to remove loosely attached bacteria

- 10.2 Replace CMF-ASW

- 10.3 Cut sponge tissue with a razor and forceps in a petri dish with sterile, ice-cold CMF-ASW
Only process a small piece at a time and try to keep tissue submerged
Remove algae or other non-sponge material
- 10.4 Transfer the pieces into 50 ml polypropylene tubes filled with ~30 ml sterile, ice-cold CMF-ASW and keep them on ice during the process
Add no more than 10 ml sponge tissue
Top up tubes until 50 ml with sterile, ice-cold CMF-ASW
- 10.5 Incubate tubes on ice on an orbital shaker at 200 rpm for 20 min
- 10.6 Filter through 40 μ m cell strainer in fresh 50 ml polypropylene tubes, squeeze remaining tissue with forceps
Top up until 50 ml with sterile, ice-cold CMF-ASW
- 10.7 Centrifuge for 20 min at 700 g and 4°C to remove sponge cells
- 10.8 Transfer supernatant to a fresh 50 ml polypropylene tube and discard the sponge cell pellet
- 10.9 Centrifuge supernatant for 15 min at 4000 g and 4°C
- 10.10 Resuspend the pellet in ~5 ml CMF-ASW and pool the bacteria fraction from several tubes
This is the recolonization inoculum. Keep on ice!
- 10.11 Proceed as quickly as possible to prevent dying of bacteria. Always keep on ice!

First recolonize, but keep a few milliliters to sample (step 12)

11 Recolonization

30m

Recolonize sponges by injection of 2 ml recolonization mix with sterile syringes and needles
Inject gradually and change location 5 times per sponge to distribute the inoculum throughout the whole animal

- 11.1 For the control treatment, use a sham control with 2 ml sterile CMF-ASW per

sponge

12 Viability and composition of inoculum

30m

Take different samples to ensure viability of inoculum and analyse bacterial composition later with qPCR and amplicon sequencing

- 12.1 Plate 100 µl pure inoculum, 1:10, 1:100 and 1:1000 dilution on MB agar plates at incubate at 25°C for 1 day
Check lower dilutions after 7 days
- 12.2 Freeze several aliquots of 1 ml pure inoculation mix in cryovials and flash freeze in liquid nitrogen
Store at -80°C
- 12.3 Filter 2 x 2 ml inoculum mix onto 0.22 µm filter with a reusable syringe filter (diameter 25 mm), store filter in cryovials and flash freeze in liquid nitrogen
Store at -80°C
- 12.4 Fix 2 x 1.8 ml inoculum mix with 0.2 ml Glutaraldehyde+Paraformaldehyde (final concentration 0.01 % and 1 %)

Fix for 10 min at RT

Freeze at -80°C

13 Repeat recolonization three times within 48 h to ensure transfer of bacteria

2d

Sampling

14 Plating of culture water

To monitor bacterial growth in the Erlenmeyer flasks, culture water is plated every 2-3 days. The sterile filtered ASW and the food stock solutions should be plated before the start and at least once during the experiment to ensure sterility

- 14.1 Sample ~1 ml culture water from 4 replicate tanks per treatment via the silicone septum with a sterile needle and syringe. Rinse syringe once with culture water before taking the sample and take care to do it very slowly, so the sponge does not get kicked around by the water current

Store samples in fridge no longer than 3 h
- 14.2 Under the clean bench: prepare dilution series by pipetting 100 µL culture

water and 900 μ L saline (1:10) and repeat twice until a dilution of 1:1000 that is used for plating

Mix well!

14.3 Plate 100 μ L of the 1:1000 dilution in triplicates on MB agar plates; use glass spatula (sterilize by dipping in ethanol and burning, cool down)

14.4 Wrap plates with parafilm and incubate upside down at 25°C for 7 days

14.5 Count colony forming units (CFUs)

15 Sponge tissue samples

At T0, T11 and after the recolonization take sponge tissue samples and preserve for different analyses

Take a picture of each sponge before sampling

Clean dissection place with ethanol and RNaseaway

Work quickly

15.1 Cut sponge in 6 pieces with sterile forceps and scalpel on a sterile petri dish.

Clean utensils after each sponge with ethanol and RNaseaway and discard petri dish

15.2 DNA/RNA extraction

Preserve two pieces in 2 x cryovials with 1.6 ml RNAlater

Incubate at 4°C overnight and transfer to -80°C the following day

For DNA/RNA extractions and qPCR see protocol:
[dx.doi.org/10.17504/protocols.io.bxwwppfe](https://doi.org/10.17504/protocols.io.bxwwppfe)

15.3 Backup

Flash freeze one piece (or all leftover sponge tissue) in cryovial in liquid nitrogen and store at -80°C

APPENDIX 3.9 | Schmittmann, L, L. Pita. 2021. DNA/RNA extraction and qPCR protocol to assess bacterial abundance in the sponge *Halichondria panicea*. protocols.io dx.doi.org/10.17504/protocols.io.bxwwppfe



DNA/RNA extraction and qPCR protocol to assess bacterial abundance in the sponge *Halichondria panicea*

Lara Schmittmann¹, Lucia Pita²

¹GEOMAR Helmholtz Centre for Ocean Research; ²Institut de Ciències del Mar - CSIC

dx.doi.org/10.17504/protocols.io.bxwwppfe



Lara Schmittmann
GEOMAR Helmholtz Centre for Ocean Research

This protocol summarizes experience and recommendations regarding DNA and RNA extractions from the sponge *Halichondria panicea* and qPCR to quantify bacterial abundance.

We have used both bacterial and sponge DNA and RNA for subsequent qPCR. Further, bacterial 16S rRNA amplicon sequencing was performed on DNA and sponge transcriptomes were sequenced successfully from extracted RNA.

DOI

dx.doi.org/10.17504/protocols.io.bxwwppfe

Lara Schmittmann, Lucia Pita . DNA/RNA extraction and qPCR protocol to assess bacterial abundance in the sponge *Halichondria panicea*. **protocols.io**
<https://dx.doi.org/10.17504/protocols.io.bxwwppfe>

Appendix to Chapter 3

Kits:

- DNA extraction sponge tissue: DNeasy PowerSoil Kit (Qiagen, Netherlands)
- DNA extraction bacterial pellet (inoculum for recolonization): Blood+Tissue Kit (Qiagen, Netherlands)
- RNA extraction sponge tissue and bacterial pellet: RNeasy Mini Kit (Qiagen, Netherlands)
- iScript cDNA synthesis kit (Bio-Rad)
- Marcherey-Nagel Nucleo Spin Clean-up kit (Marcherey-Nagel Düren, Germany)
- DNA-free DNA removal Kit (Thermo Fisher Scientific, USA)
- Qubit DNA and RNA HS Kits (Thermo Fisher Scientific, USA)

Chemicals and reagents:

- DNase/RNase-free water
- +RNase AWAY®
- RNAlater
- Ethanol
- beta-mercaptoethanol (14.3 M)
- SUPERase-IN (Thermo Fisher Scientific, USA)
- nucleic acid stain for gel electrophoresis (e.g. GelGreen, Millipore, USA)
- Maxima SYBR Green 2x Master Mix (Thermo Fisher Scientific, USA)
- tRNA solution (10 ng/µl Sigma Aldrich, Germany)

Consumables and other material:

- forceps
- scalpel
- sterile plastic petri dishes
- 2 ml polypropylene tubes
- Lysing matrix-E tubes
- 1.8 ml Cryovials DNase/RNase free

Equipment:

- Autoclave
- Finescale
- Fume hood
- PowerLyser 24 (MoBio)
- heating block / incubator at 37°C
- Biosafety cabinet (UV sterilization)
- Centrifuge - for 2 polypropylene tubes and PCR plates
- PCR cycler
- Bluelight table
- CFX96 real-time detection system (Bio-Rad, Germany)
- Nanodrop
- Qbit
- qPCR software Bio-Rad CFX Manager Software (version 3.1)

RNA: work under fume hood (beta-mercaptoethanol)

DNA extraction

1 Extract DNA from samples fixed in RNAlater (stored at -80°C) or flash frozen (stored at -80°C) ^{3h}

Qiagen PowerSoil Kit

Input: 70-200 mg tissue

Process max.24 samples at a time, depending on experience

1.1 Follow manufacturers protocol (lysis in PowerBeadTubes and PowerLyzer Bead-Based Homogenizer at 3500 rpm, 2x 30 sec bead beating with 45 sec pause in between)

1.2 We recommend to immediately take a 5 µl aliquot for quality and quantity control (Nanodrop, Qbit, PCR to check contamination presence of 16S DNA). DNA extracts can be frozen at -20°C or for long-term storage at -80°C

2 Extract DNA from bacterial recolonization pellets flash frozen (stored at -80°C) ^{3h}

Qiagen Blood+Tissue kit

Input: cell pellet

Process max.24 samples at a time, depending on experience

No good results were achieved with the Qiagen PowerSoil Kit for cell pellets.

2.1 Follow manufacturers protocol (incubation with proteinase K at 56°C for 30 min)

2.2 We recommend to immediately take a 5 µl aliquot for quality and quantity control (Nanodrop, Qbit, PCR to check contamination presence of 16S DNA). DNA extracts can be frozen at -20°C or for long-term storage at -80°C

3 Dilute DNA extracts for qPCR ^{1h}

Measure DNA extracts of all samples with qbit

3.1 Dilute each extract to a concentration of 6 ng/µl with DNase/RNase-free water. Per qPCR reaction we will use 5 µl template, so the total DNA used per qPCR reaction is 30 ng

4 Extract RNA from sponge samples fixed in RNAlater (stored at -80°C)

- Clean all surfaces and instruments with ethanol and subsequently RNase-Away
- The manufacturers protocol for the RNeasy Mini Kit have been optimized for Halichondria tissue. For more details please refer to the manufacturers protocol
- Work clean and quickly to prevent RNA degradation due to long waiting times. We therefore recommend to not process more than 6-12 samples (depending on the experience of the person) at once



beta-mercaptoethanol is highly toxic. Work under the fume-hood only and dispose contaminated material properly. Use nitril gloves.
Prior to each extraction effort, prepare fresh aliquots from concentrated beta-mercaptoethanol stock (6 µl beta-mercaptoethanol + 594 µl RLT-buffer provided with the extraction kit)

- 4.1 Thaw tissue samples on ice and meanwhile label lysis tubes (label on the side, since during powerlysing step labelling on the lid might disappear!)
- 4.2 Remove first sample from the cryovial (leave others on ice) and cut on a sterile petri dish with sterile forceps into pieces
- 4.3 Tare the lysis tube and load with ~80 mg tissue. Place tube on ice and proceed with the next sample (go back to step 4.2). Use a new petri dish and scalpel to prevent cross-contamination.
- 4.4 Add 600 µl beta-mercaptoethanol/RTL buffer under the hood and disrupt cells in homogenizer for 30 sec at a speed of 3000
- 4.5 Centrifuge for 10 min at maximum speed
- 4.6 Remove supernatant carefully without touching the pellet and transfer it to a 2 ml collection tube. From here on, work at RT
- 4.7 add 1 volume (~370 µl) of 70 % molecular grade ethanol and mix well by pipetting. Proceed immediately to next step
- 4.8 transfer up to 700 µl including any precipitate to RNeasy Spin column placed in a 2 ml collection tube (provided in kit). Close the lid and centrifuge for 30 sec at 10,000 rpm. Discard flow-through and re-use collection tube. Repeat this step if the sample exceeded 700 µl

Appendix to Chapter 3

- 4.9 Add 700 μ l RW1 buffer and centrifuge for 30 sec at 10,000 rpm. Discard the flow-through
- 4.10 Add 500 μ l RPE buffer and centrifuge for 30 sec at 10,000 rpm. Discard the flow-through
- 4.11 Add 500 μ l RPE buffer and centrifuge for 2 min at 10,000 rpm. Carefully remove the spin column and place it in fresh 2 ml collection tube. Centrifuge for 1 min at max speed to remove any remaining buffer
- 4.12 Place the spin column in a fresh 1.5 ml Eppendorf tube and add 60 μ l EB buffer. Take care to place it directly onto the spin column membrane. Close the lid and incubate for 10 min at RT. Centrifuge for 1 min at 10,000 rpm to elute RNA
- 4.13 Keep extracts always on ice! Proceed immediately with RNase inhibition and nuclease treatment.
Already preheat incubator or heating block to 37°C (incubator needs much longer to pre-heat than heating block)



important! The DNase treatment was challenging for *H. panicea* extracts. For other sponge species (*Aplysina aerophoba*, *Dysidea avara*) we have successfully used the TURBO™ DNase (AM2238) kit for DNA removal, but it did not work for *H. panicea*: DNA remained and RNA was degraded, even if we tested different batches of the kit. We also tried unsuccessfully the on-column kit RNase-Free DNase Set (79254).
Finally, **good results** were obtained with the DNA-free™ DNA Removal Kit (AM1906) to remove DNA from *H. panicea* RNA extracts.

- 4.14 Under the clean bench: add 3 μ l SUPERase-IN (0.05 volume of RNA) to 60 μ l RNA. Mix gently
- 4.15 Add 6 μ l (0.1 volume of RNA) 10x DNase I buffer and 1.2 μ l DNase and mix gently
- 4.16 Incubate for 20 min at 37°C, mix frequently
- 4.17 Add 6 μ l resuspended DNase I inactivation reagent and mix well
- 4.18 Incubate for 2-5 min at RT, mix every minute by shortly vortexing

- 4.19 Centrifuge for 1.5 min at 10,300 rpm and transfer supernatant (RNA) to a fresh tube. Take care to not transfer any inactivation reagent (white)
- 4.20 We recommend to immediately take a 5 µl aliquot and a 2 µl aliquot, and freeze all samples at -80°C.
Use the 5 µl aliquot to assess quality and quantity (Nanodrop, Qbit, PCR to check contamination with DNA) and the 2 µl aliquot for capillary electrophoresis (e.g. Experion). To avoid thaw-freeze cycles, the main RNA sample can be split in two equal parts, so that one sample can remain frozen until analysis at -80°C if it is intended for e.g. transcriptomics

cDNA synthesis

5 cDNA synthesis

Use iScript kit and follow manufacturers guidelines. Only thaw reverse transcriptase directly before adding to master mix and keep on ice!

Use 500 ng RNA per reaction and random primers

- 5.1 Dilute cDNA 1:5 with TE buffer and use this dilution for qPCR

- 5.2 Store cDNA dilutions at -20°C

Primers and standard curves

6 Primers

A	B	C	D	E
Specificity	Primer	Sequence	Fragment length (bp)	Reference
eubacterial 16S rRNA	E1052f	TGCATGGYTGTCGTCAGCTCG	141	Wang&Qian 2009
	E1193r	CGTCRTCCCCRCCTTCC		
Ca. H. symbioticus specific 16S rRNA (DNA and cDNA)	Hal_sym F	CGCGGATGGTAGAGATACCG	148	this study
	Hal_sym R	TGTCCCCAACTGAATGCTGG		

Table: qPCR primers to quantify total bacterial 16S rRNA and *Ca. Halichondriabacter symbioticus*. The amplified gene products for the *Ca. H. symbioticus* primers have been sequenced to confirm specificity.

Important: dilute primers in TE buffer

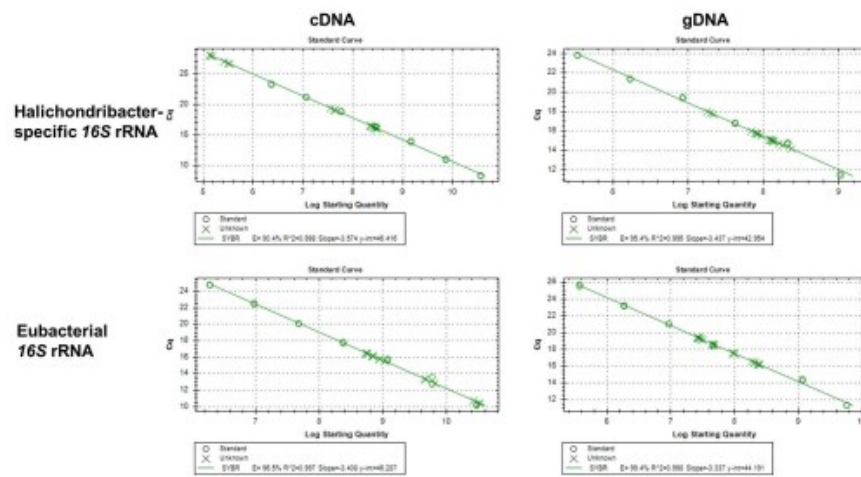
- work under the clean bench and use sterile packed equipment only
- especially eubacterial 16S rRNA primers are prone to contamination. It is recommended to prepare aliquots in advance and thaw a fresh aliquot for each qPCR plate
- prepare 50 μ M stocks in TE buffer as 10 μ l aliquots and freeze at -20°C. Only use once

7 Standard curve preparation

Prepare one DNA and one cDNA standard curve. It is recommended to prepare larger volumes in order to use the same standard curve for a complete experiment, or even several experiments

- 7.1 Run 50 μ l PCRs with primer pair intended for qPCR with DNA from different sponge individuals, e.g. 8 x 50 μ l
- 7.2 Prepare electrophoresis gel with nucleic acid stain (e.g. GelGreen) with large pockets to load 50 μ l/well
- 7.3 Cut out gel bands under blue light table with sterile scalpel. Clean up gel bands (Marcherey Nagel Nucleo Spin Clean-up kit) according to the manufacturers protocol and pool PCR products
- 7.4 Prepare dilution series:
 - Probably, the concentration of the PCR products is way too high for qPCR. Start by preparing a 1:10 dilution by adding 200 μ l PCR product + 1800 μ l tRNA water
 - Then proceed with 1:10 (200+1800 μ l) or 1:5 (400+1600 μ l) dilutions
- 7.5 Measure highest standard in QBIT (high sensitivity kit) and calculate concentration for dilutions (~ 1-5 ng/ μ l)
calculate copy numbers <http://cels.uri.edu/gsc/cndna.html>

7.6



Example standard curves for primer-pairs used with cDNA and gDNA. The efficiencies should be between 90-110 %. During the experiments, the efficiencies were consistent.

qPCR

8 Recommended plate set-up

Important:

have standard curves on each plate

run different primers for a sample within the same plate (= don't run separate plates for total 16S and Halichondribacter)

include negative controls on each plate: just qPCR mix and purified water instead of DNA to control for contamination

9

qPCR preparation

Work under the clean bench.

Prepare master mix for each primer pair:

Appendix to Chapter 3

A	B	C
Template	5 μ L	gDNA: Total 30 ng per reaction, cDNA: 1:5 dilution of cDNA from 500 ng RNA
Primer F (50 μ M)	0.16 μ L	Total 400 nM per reaction
Primer R (50 μ M)	0.16 μ L	Total 400 nM per reaction
qPCR mix (2x)	10 μ L	
H ₂ O	4.68 μ L	
Total	20 μ L	

Table: qPCR master mix

- 9.1 Work in 96-well plate. Pipet 15 μ l master mix per well

- 9.2 Add 5 μ l template per well (use new pipet tip for each well)

- 9.3 Seal plate with optical adhesive foil (check which brand fits your plates and qPCR machine) and spin down plate briefly in plate centrifuge

- 9.4 Run plate immediately, or store plate at 4°C in the dark and run within 24 h

A	B	C
72°C	1 min (plate read)	
96°C	2 min	40x
94°C	30 sec	
60°C	30 sec (plate read)	
60-90°C	0.5 interval, 5 sec Melt curve	

Table: qPCR conditions

- 9.5 Run gel electrophoresis with some qPCR products to check for correct amplification (1 band of correct product length) at least once per experiment

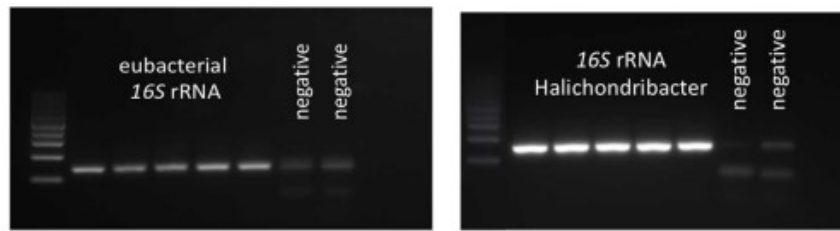
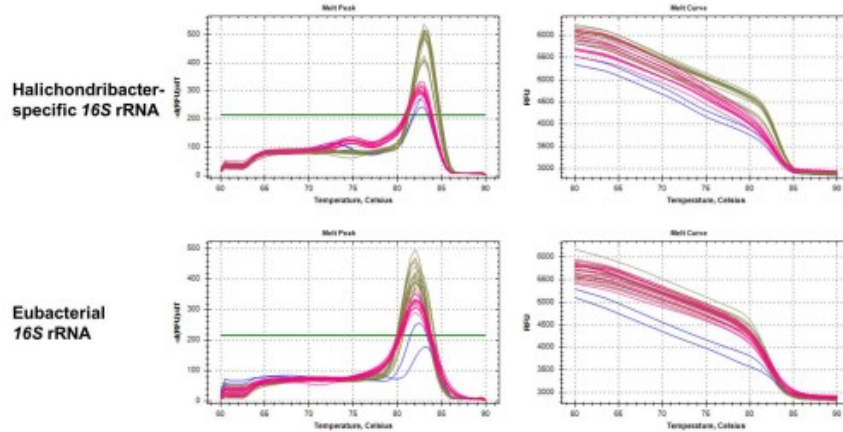
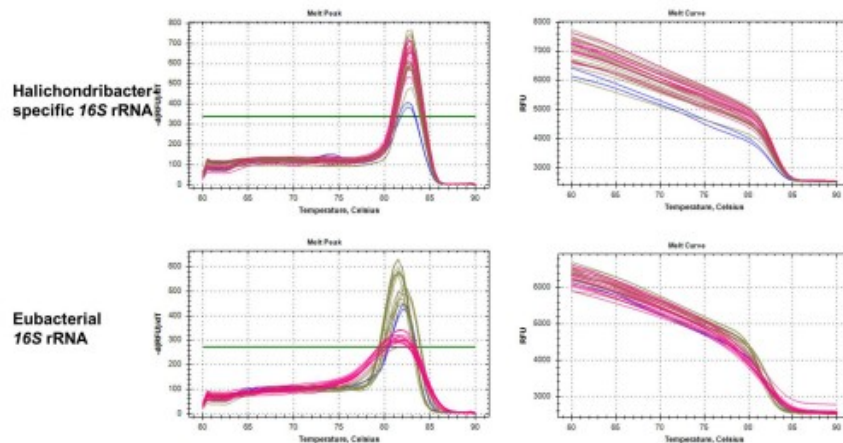


Figure: Example gel electrophoresis of qPCR products. Five replicate products and two negative controls were run per primer pair (eubacterial and Halichondribacter-specific 16S rRNA gene). Specificity of Halichondribacter-primers was confirmed by extraction of the gel band and sequencing of the PCR product. Regularly check qPCR products on a gel to confirm specificity and amplification of one product only.

9.7



Example melt curves for qPCR products from cDNA. Always check melt curves for correct amplification of one qPCR product, and the overlap of melt curves from standard curve samples and experimental samples.



Example melt curves for qPCR products from gDNA. Always check melt curves for correct amplification of one qPCR product, and the overlap of melt curves from standard curve samples and experimental samples.

APPENDIX

TO CHAPTER 4

The appendix to Chapter 4 includes additional methods, figures and tables.

APPENDIX 4.1 | Supplementary methods

EXPERIMENTAL SET-UP: RECOLONIZATION BY INCUBATION

Halichondria panicea individuals were collected by snorkeling from Kiel, Germany (54.424705 N, 10.175133 E) in early November 2019. The experimental set-up, antibiotic treatment, preparation of culture water, water exchange, sample preservation and processing were performed as described in the main text (for details see protocol appendix 3.8 or [dx.doi.org/10.17504/protocols.io.by7hpzj6](https://doi.org/10.17504/protocols.io.by7hpzj6)). See appendix 4.9 for the timeline of the experiment.

Sixteen sponge individuals were each cut in three pieces with a sterile scalpel (each about 4x4x4 cm). One piece of some individuals was immediately preserved in RNAlater as a start sample T0 (n=6) representing the initial conditions. The other two pieces per individual were placed in separate glass beakers and all were treated with the antibiotic cocktail described before. Four sponges were sampled immediately before recolonization on day T11 (n=4). Then, half of the remaining sponges were recolonized by adding 2 ml *H. panicea* symbiont inoculum into the culture bottles. The bacterial inoculum was prepared by differential centrifugation from fresh, healthy sponges as described in the main text. As a control, 2 ml of the medium CMF-ASW (calcium-magnesium-free artificial seawater) was used. The inoculum was plated on MB agar plates and bacterial growth inspected one day after incubation at 25°C. Sponges were sampled one day and seven days after recolonization in RNAlater (n=7).

INOCULUM PREPARATION BY DIFFERENTIAL CELL CENTRIFUGATION

The bacterial inoculum was prepared by differential centrifugation from several fresh and healthy sponges kept in a Baltic flow-through system. The volume of the sponge tissue used to prepare the inoculum was equivalent to the volume of the sponges to be recolonized (estimated by size). Sponge tissue was dissociated with a modified protocol after Wehrl et al. 2007. In short, healthy sponges were washed in sterile filtered, autoclaved, ice-cold CMF-ASW (calcium-magnesium-free artificial seawater) for 5 min to remove loosely attached bacteria. Tissue was transferred to fresh CMF-ASW and cut into small pieces (~2x2x2 mm) while removing any algae pieces from the tissue. Cut sponge tissue was incubated on ice for 20 min while horizontally shaking. The now soft tissue was squeezed through a 40 µm cell strainer and centrifuged for 20 min at 700 g and 4°C to remove sponge cells. The supernatant was centrifuge again for 15 min at 4000 g at 4°C to pellet bacteria. The pellet was resuspended in CMF-ASW and immediately used for recolonization. The inoculum was prepared in <

3 h and kept on ice throughout the process. As a sham control, 2 ml of the medium CMF-ASW was used. The inoculum was plated on MB agar plates and bacterial growth inspected one day after incubation at 25°C. For DNA extraction, the inoculum was pelleted and flash frozen, and filtered 2 ml filtered on a 0.22 µm filter (PVDF 25 mm Merck Millipore, USA) and flash frozen. Samples were stored at -80°C.

BACTERIAL ISOLATION AND ANTIBIOTIC RESISTANCE TESTS

Bacteria were isolated during the recolonization by incubation experiment right after antibiotic treatment (T5). Dilutions from sponge culture water were prepared in sterile 1.5 % NaCl, and 100 µL plated onto MarineBroth (Difco2216) agar plates. Plates were incubated at 25°C for up to two weeks and regularly checked for bacterial growth. Single colonies were picked, and streak plated on fresh agar plates.

The total genomic DNA was extracted from single colonies using DNaeasy Blood & Tissue Kit (Qiagen, Netherlands) DNA extraction kit, following the manufacturer's protocol for gram-positive bacteria and stored at -20 °C before use. Amplification of the 16S rRNA gene (1500 bp) was performed with the primer pairs (concentration: each 10 pmol/µL): Eub27f with the sequence: 5'-GAG TTT GAT CCT GGC TCA G-3' (primer 1) (Noda *et al.*, 2006)/ Univ1492r with the sequence 5'-GGT TAC CTT GTT ACG ACT T-3' (primer 2) (Reysenbach *et al.*, 2000); alternative for Univ1492r we used the reverse primer RC1492r (5'-TAC GGC TAC CTT GTT ACG ACT T-3') (Magarvey *et al.*, 2004) or 1525r (5'-AGA AAG GAG GTG ATC CAG CC-3') (Rainey *et al.*, 1996). The PCR products were sequenced in IKMB sequencing facility (University of Kiel, Germany) or GATC Eurofins Genomics (sequencing primers: 342f (5'-TAC GGG AGG CAG CAG-3') (Lane, 1991); 534r (5'-ATT ACC GCG GCT GCT GG-3') (Muyzer *et al.*, 1993); 803f (5'-ATT AGA TAC CCT GGT AG-3') (Rainey *et al.*, 1996)). The sequences were processed with the ChromasPro software and compared to the GenBank database (BLAST tool) and the Ribosomal Database Project (RDP), with and without type strain filter. The sequences are deposited in the NCBI-GenBank (www.ncbi.nlm.nih.gov).

For antibiotic *in vitro* tests, isolates grown on solid MB medium were resuspended in liquid MB medium, and 100 µl plated on fresh MB agar plates. Two antibiotic test disks (Oxoid, Thermo Fisher Scientific, USA) were placed per agar plate, and the inhibition zones assessed after incubation for 5 days at 25 °C.

Table S1: Constant temperature and salinity settings for the three experiments.

	Temperature	Salinity
Antibiotic exposure experiment	12°C	16 PSU
Recolonization by injection	14°C	15 PSU
Recolonization by incubation	12°C	18 PSU

Tables S2: qPCR primers and qPCR conditions used in this study.

Specificity	Primer	Sequence	Fragment length (bp)	qPCR conditions	Reference
Bacterial 16S rRNA	E1052f E1193r	TGCATGGYGTGTCGTCAGCTCG CGTCRTCCCCRCCTTCC	141	400 nM (30" 94°C, 30" 60°C) 40 cycles	(Wang and Qian, 2009)
Ca. H. symbioticus specific 16S rRNA	Hal_sym F Hal_sym R	CGCGGATGGTAGAGATACCG TGTCCTCAACTGAATGCTGG	148	400 nM (30" 94°C, 30" 60°C) 40 cycles	This study

Table S3: qPCR mastermix used in this study.

Template	5 µL	gDNA: Total 30 ng per reaction, cDNA: 1:5 dilution of cDNA from 500 ng DNA
Primer F (50 µM)	0.16 µL	Total 400 nM per reaction
Primer R (50 µM)	0.16 µL	Total 400 nM per reaction
qPCR mix (2x)	10 µL	
H2O	4.68 µL	
Total	20 µL	

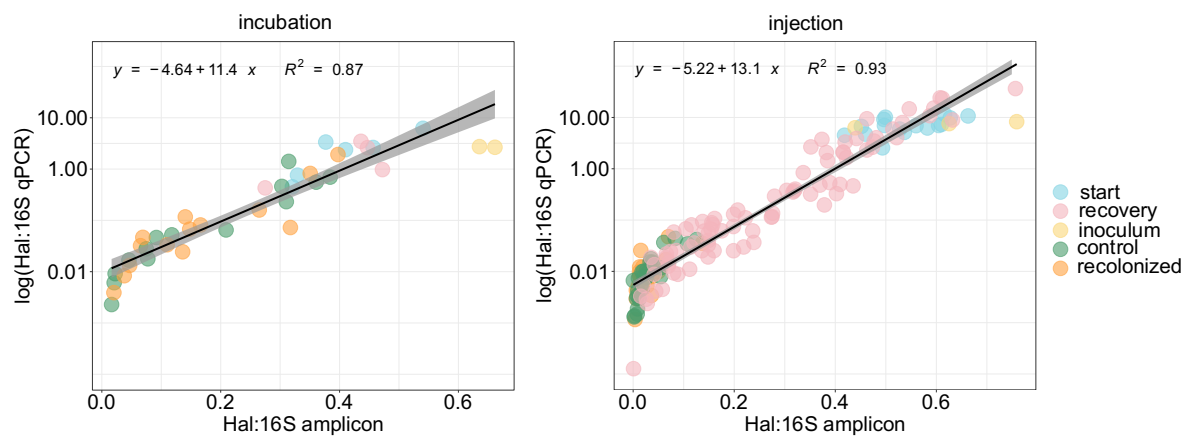
- Lane, D.J. (1991) 16S/23S rRNA sequencing. In *Nucleic acid techniques in bacterial systematics*. Stackebrandt, E. and Goodfellow, M. (eds). John Wiley & Sons, New York, pp. 115–175.
- Magarvey, N.A., Keller, J.M., Bernan, V., Dworkin, M., and Sherman, D.H. (2004) Isolation and characterization of novel marine-derived actinomycete taxa rich in bioactive metabolites. *Appl Environ Microbiol* **70**: 7520–7529.
- Muyzer, G., De Waal, E.C., and Uitterlinden, A.G. (1993) Profiling of complex microbial populations by denaturing gradient gel electrophoresis analysis of polymerase chain reaction-amplified genes coding for 16S rRNA. *Appl Environ Microbiol* **59**: 695–700.
- Noda, S., Inoue, T., Hongoh, Y., Kawai, M., Nalepa, C.A., Vongkaluang, C., et al. (2006) Identification and characterization of ectosymbionts of distinct lineages in Bacteroidales attached to flagellated protists in the gut of termites and a wood-feeding cockroach. *Environ Microbiol* **8**: 11–20.
- Rainey, F.A., Ward-Rainey, N.L., Janssen, P.H., Hippe, H., and Stackebrandt, E. (1996) *Clostridium paradoxum* DSM 7308(T) contains multiple 16S rRNA genes with heterogeneous intervening sequences. *Microbiology* **142**: 2087–2095.
- Reysenbach, A.L., Longnecker, K., and Kirshtein, J. (2000) Novel bacterial and archaeal lineages from an in situ growth chamber deployed at a mid-atlantic ridge hydrothermal vent. *Appl Environ Microbiol* **66**: 3798–3806.
- Wang, Y. and Qian, P.Y. (2009) Conservative fragments in bacterial 16S rRNA genes and primer design for 16S ribosomal DNA amplicons in metagenomic studies. *PLoS One* **4**: e7401.

APPENDIX 4.2 | Supplementary results.**RECOLONIZATION BY INCUBATION EXPERIMENT**

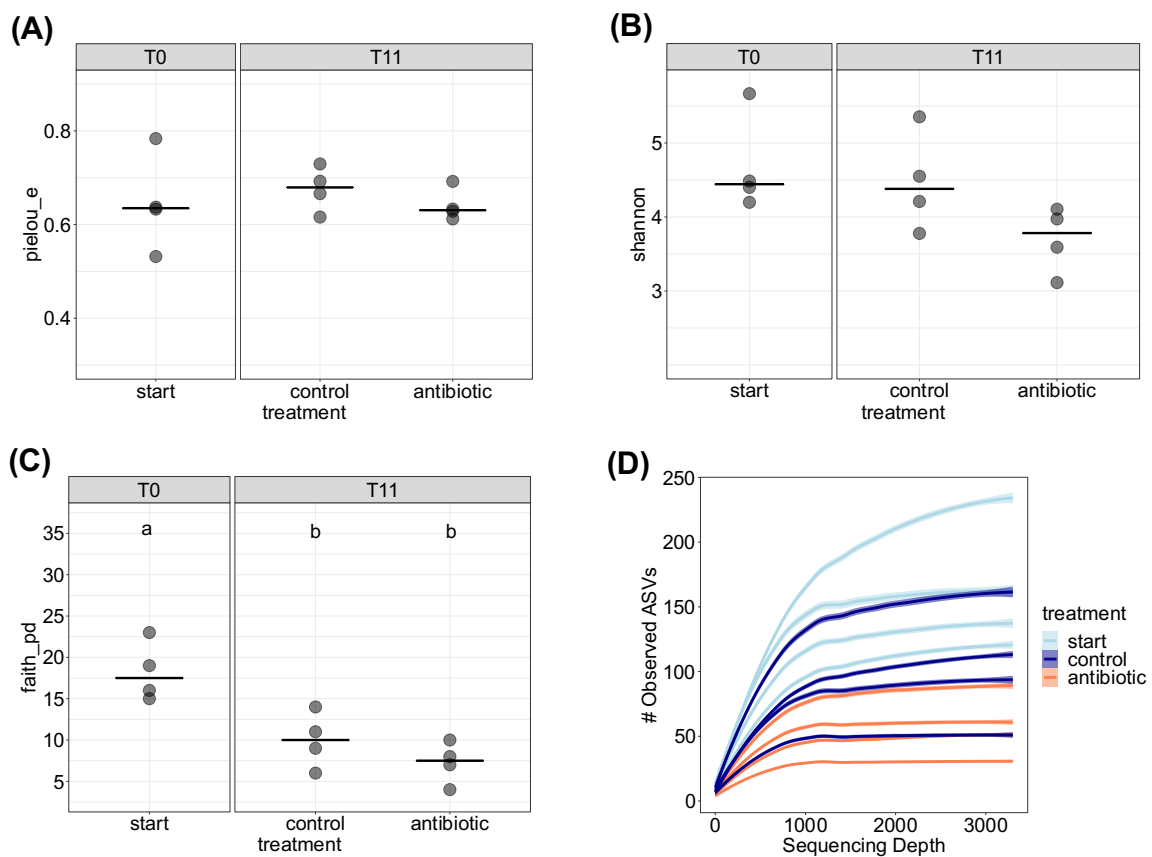
We incubated antibiotic treated sponges with their natural microbiome obtained by differential cell-centrifugation from healthy sponges, or a medium control. The absolute abundance of *Ca. H. symbioticus* remained unchanged compared to T0 (appendix 4.9). The strong decrease observed in the antibiotic test experiment could not be repeated although there was no difference in the application of antibiotics and in the season (both run in November, experiments one year apart). Total bacterial abundance increased over time compared to T0 (both gDNA and cDNA, appendix 4.9). Relative abundance of *Ca. H. symbioticus* decreased over time from 40.6 ± 3.4 % at T0 to 7 ± 1.3 % at T18 (appendix 4.9). Bacterial phyla that were low abundant in healthy sponges at the start T0, increased in abundance after antibiotic treatment, i.e., Desulfobacterota and Firmicutes. Both alpha and beta diversity showed similar trends over time after antibiotic treatment as in the recolonization by injection experiment, and were not affected by recolonization (appendix 4.9, 4.10). Although recolonization did not affect beta-diversity, single ASVs shared between the inoculum (inoculum and start T0) and the recolonized treatment indicate that transfer of microbes is also possible by incubation (data not shown). Nevertheless, mean relative abundance of transferred ASVs did not exceed 0.66 % in contrast to recolonization by injection.

Based on these results, we added the following modifications to the recolonization by injection experiment: increased replication, real-time tracing *Ca. H. symbioticus* abundance on almost all experimental days (with the aim to identify a potentially stronger decrease of *Ca. H. symbioticus* before T11, but that was not the case), recolonization by injection into the tissue instead of incubation, repeated recolonization. The improvements allowed to resolve changes in the bacterial community with high temporal resolution. Overall, the mode of recolonization (incubation vs. injection) did not change the outcome of the experiments. In both cases, single ASVs were transferred while recolonization did not affect alpha- or beta-diversity.

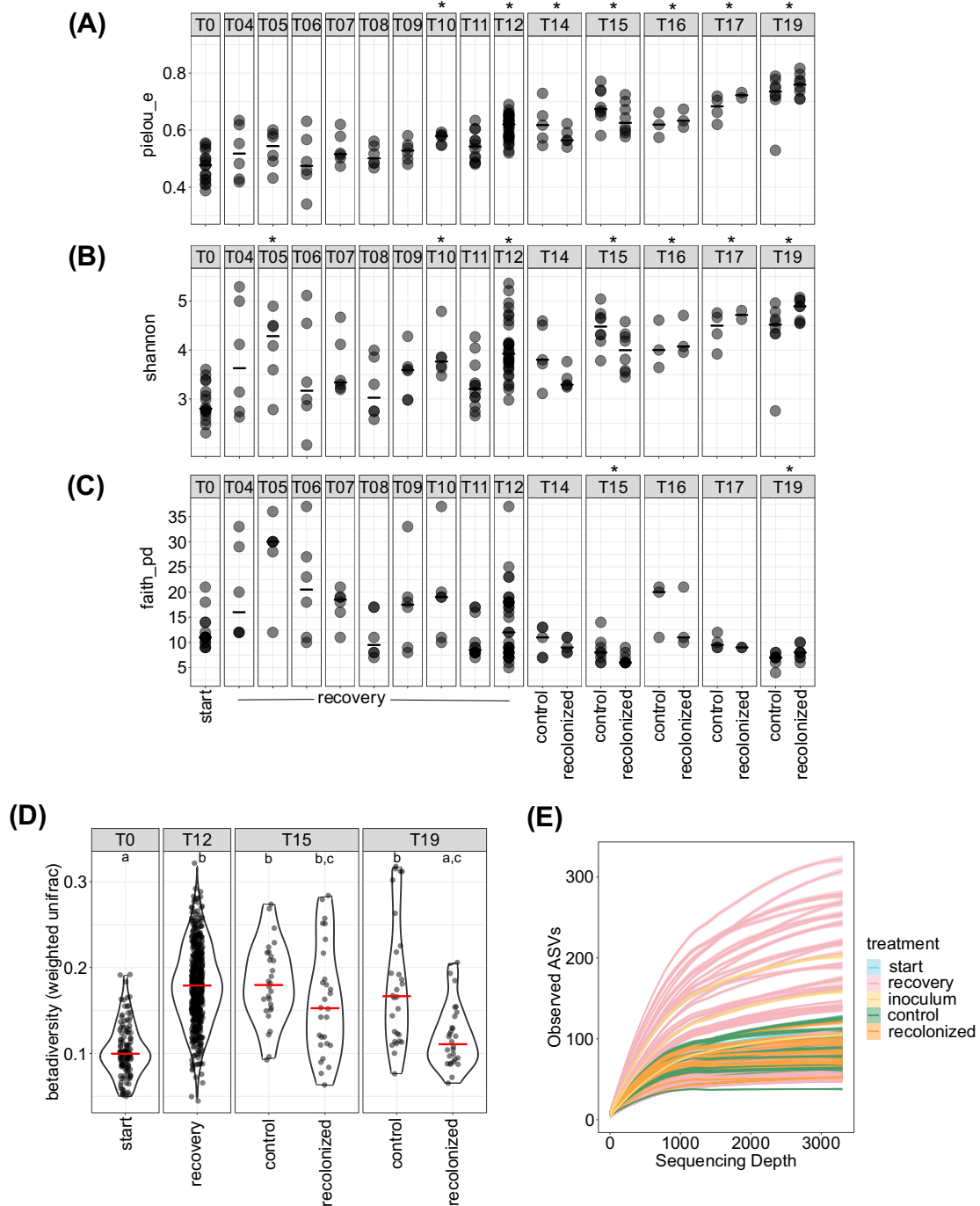
APPENDIX 4.3 | Correlation between relative *Ca. Halichondribacter symbioticus* abundance estimated by 16S rRNA amplicon sequencing (x-axis) and by RT-qPCR (y-axis). Correlations were calculated for samples from the recolonization by incubation (left) and by injection experiment (right). Each dot represents one sample, color depicts the experimental group.



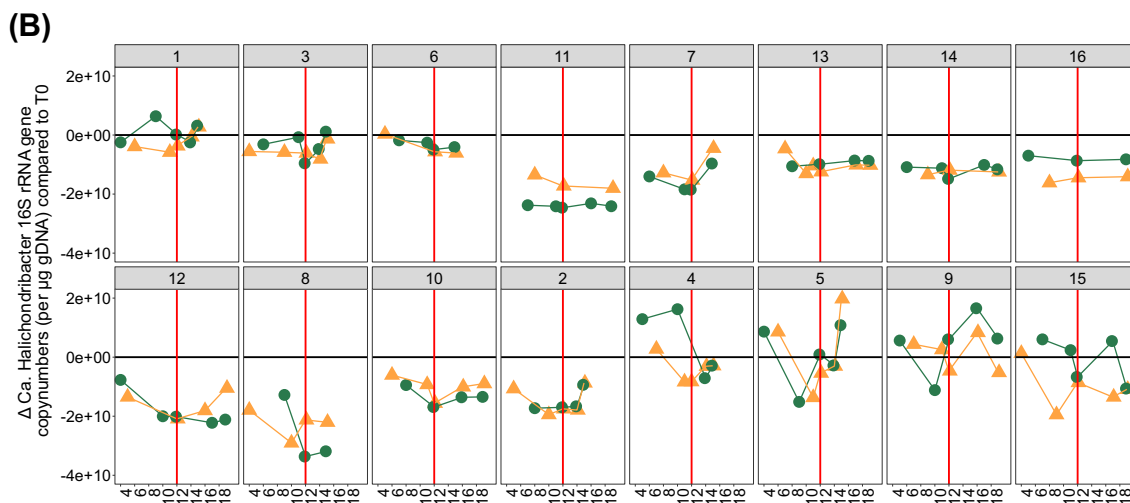
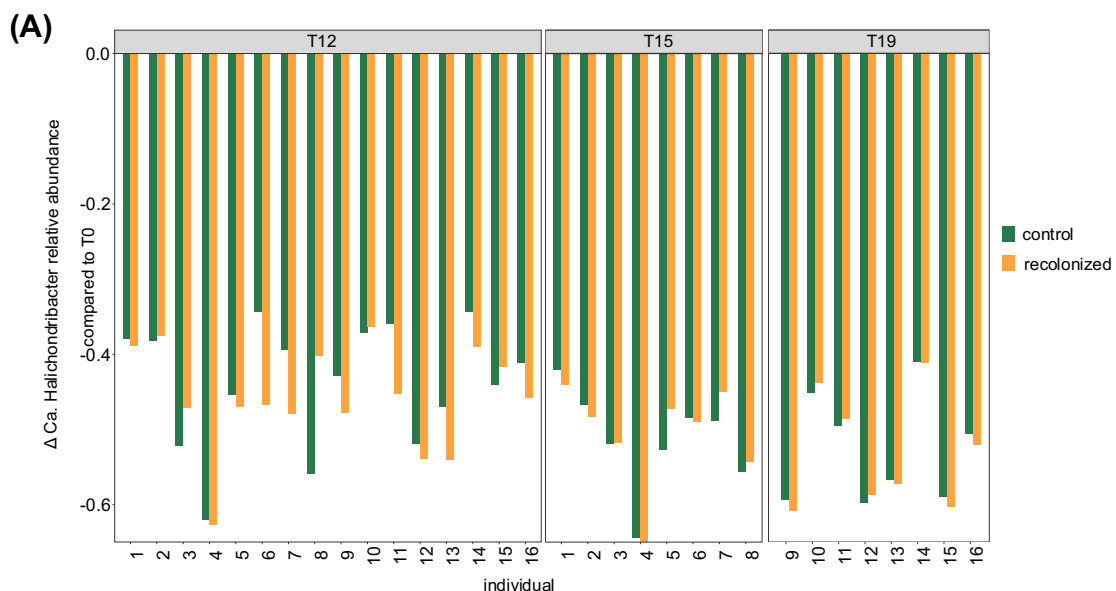
APPENDIX 4.4 | Antibiotic exposure experiment: bacterial alpha diversity before and after antibiotic treatment. **(A)** Pielou evenness **(B)** Shannon index **(C)** Phylogenetic diversity after Faith. Values with different letters are significantly different ($p < 0.05$). **(D)** Rarefaction curves of observed ASVs. Samples subsampled to 3300 reads. Color depicts treatment.



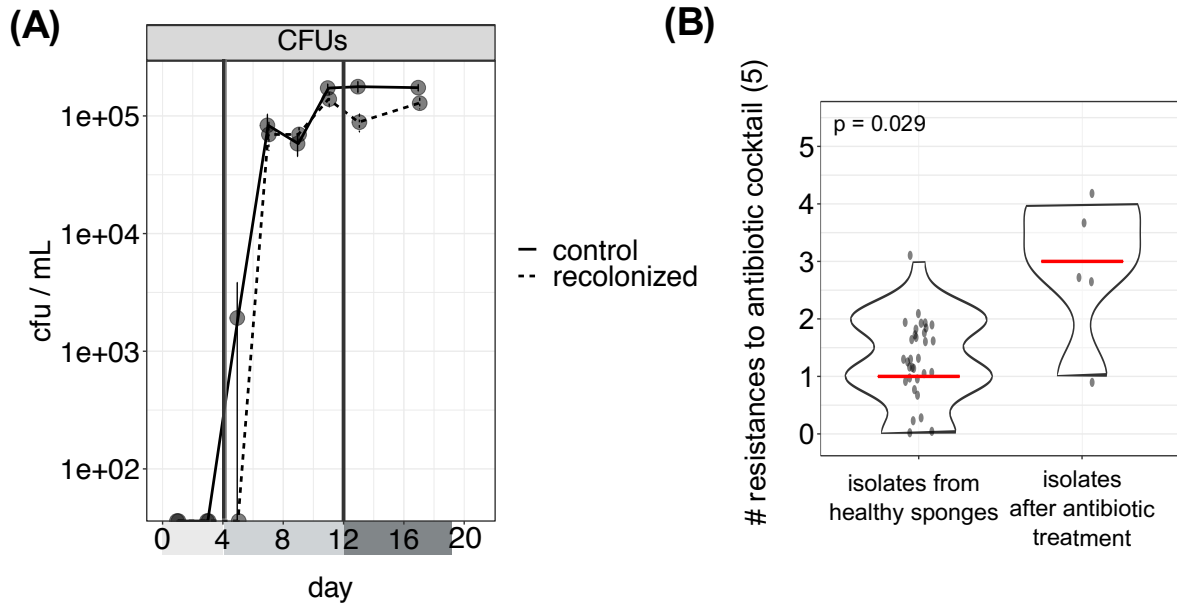
APPENDIX 4.5 | Recolonization experiment: alpha- and beta-diversity before and after recolonization. **(A)** Pielou evenness, **(B)** Shannon index and **(C)** Phylogenetic diversity after Faith. Significant differences between the start (T0) and the respective days are indicated by asterisk above the days (ANOVA or Schreier-Ray-Hare test). There were no significant differences between control and recolonized treatment within days. **(D)** Intra-specific beta-diversity (weighted Unifrac differences). Groups with different letters are significantly different ($p < 0.05$). **(E)** Rarefaction curves of observed ASVs. Samples subsampled to 3300 reads. Color depicts treatment.



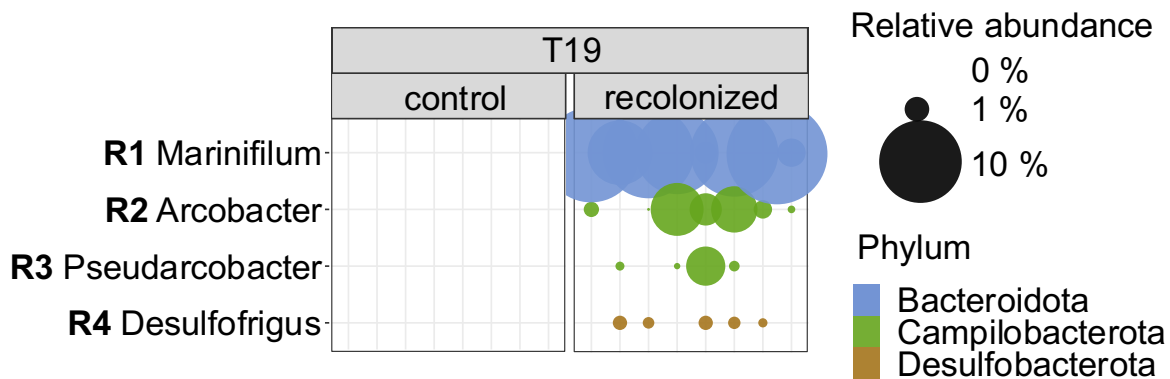
APPENDIX 4.6 | Recolonization experiment: individual-dependent abundance patterns of *Ca. Halichondribacter symbioticus*. **(A)** Difference in relative abundance between T0 and the three main sampling days T12, T15 and T19 separated by sponge individual. **(B)** Difference in absolute abundance between T0 and the respective day on the x axis. Separated by sponge individual and sorted by pattern.



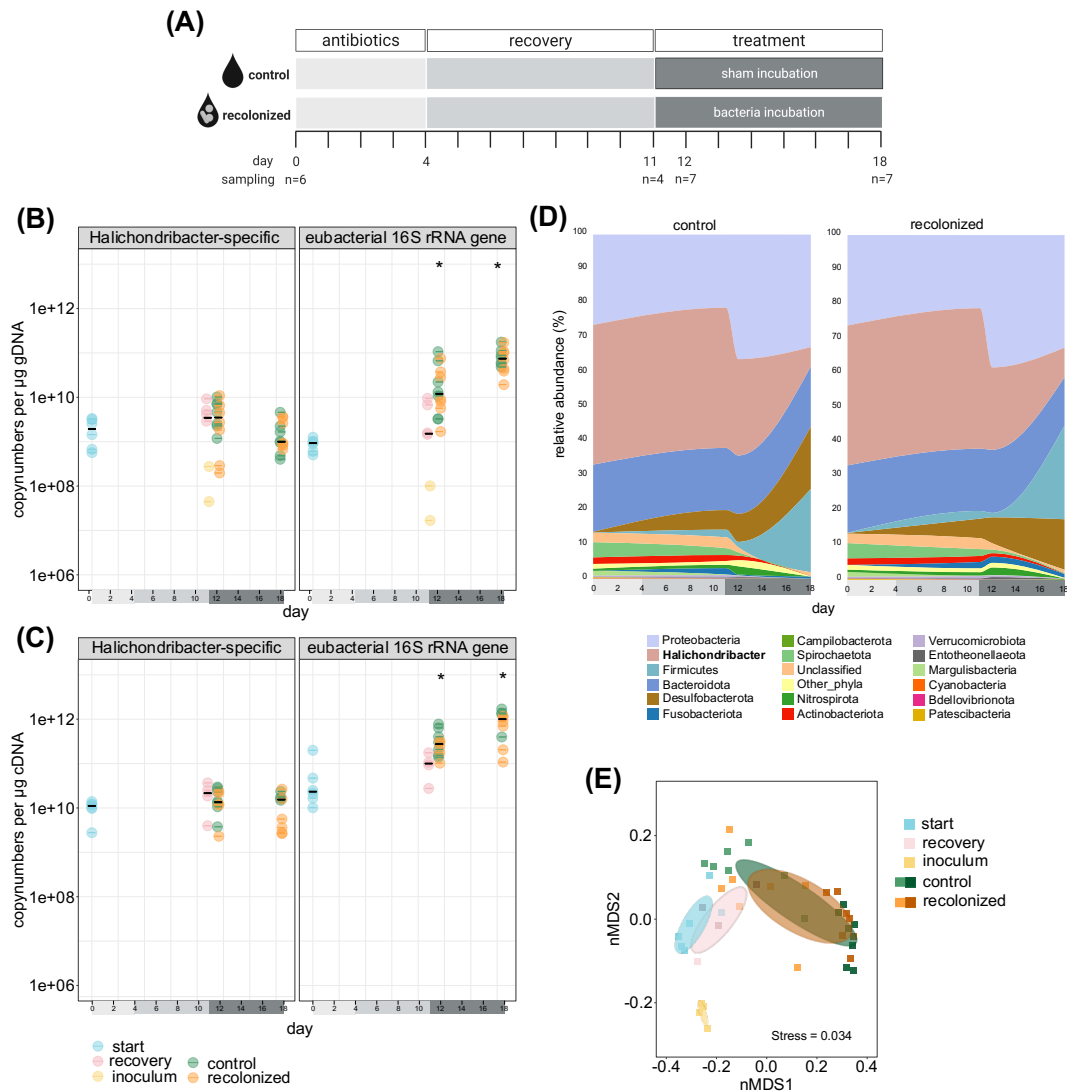
APPENDIX 4.7 | Recolonization experiment: culture-dependent analyses. **(A)** colony forming units in culture water from. CFUs/ml over time are shown (significant increase p -value < 0.0001 for both experiments, Schreier-Ray-Hare test). There were no significant differences between control and recolonized treatment within days. **(B)** Antibiotic resistances of bacterial isolates *in vitro*. Number of resistances to antibiotic cocktail used in experiments. Isolates are separated depending on their source of isolation: isolates from wildtype *Halichondria panicea*; and isolates from antibiotic treated *H. panicea* (recolonization by incubation experiment). Result of t.test in left plot corner, median in red.



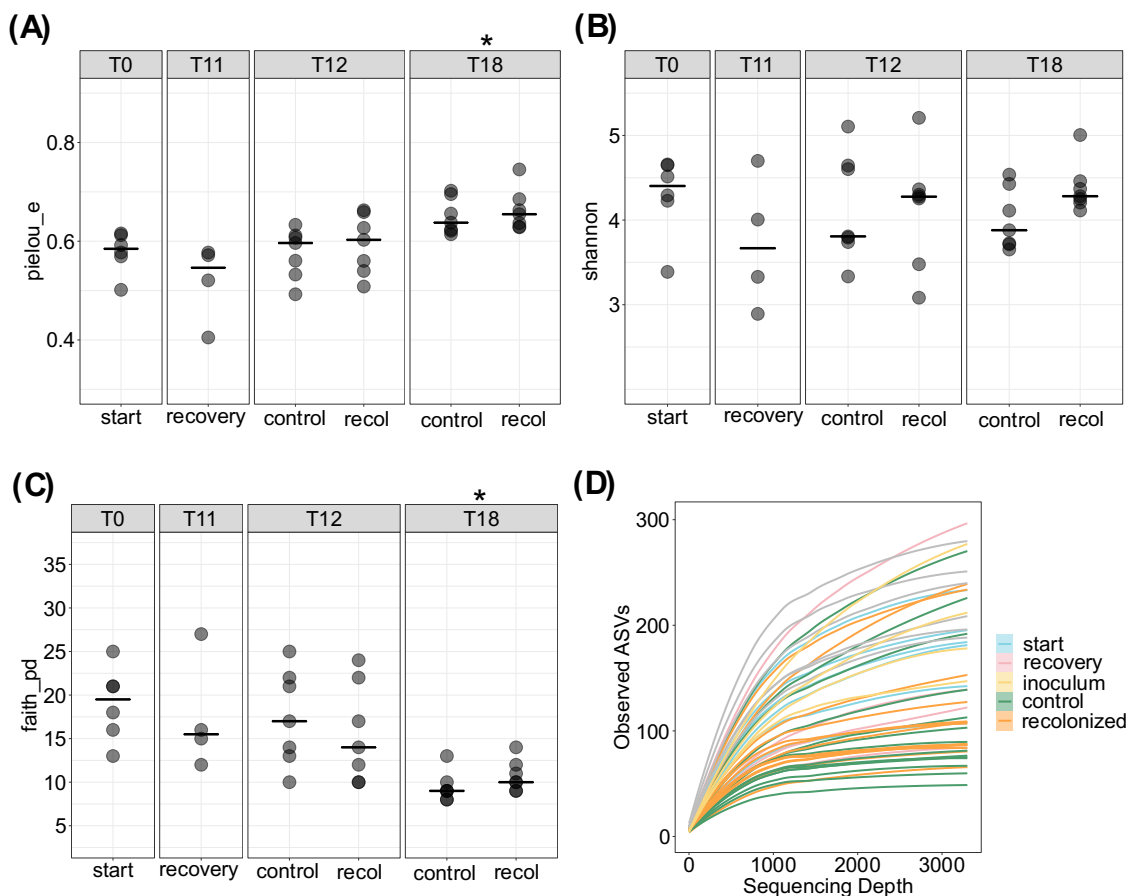
APPENDIX 4.8 | Recolonization experiment: relative abundance of recolonizer ASVs R1-R4 transmitted from inoculum to recolonized sponges (Table 1) is shown. Size of the bubbles represents relative abundances, color depicts phylum affiliation.



APPENDIX 4.9 | Recolonization by incubation experiment: microbial community composition and diversity before and after recolonization by incubating antibiotic treated sponges with the natural microbiome. **(A)** Experimental set-up. All sponges were treated with antibiotics for four days and recovered in sterile filtered artificial seawater for 7 days. Then, sponges were either incubated in a bacterial inoculum, or with a medium control. Samples were taken prior to the experiment at T0 (n=6), after a recovery phase at T11 (n=4), and 1 and 7 days after recolonization (n=7). **(B+C)** Absolute bacterial abundance estimated by RT-qPCR. *16S* rRNA gene copy numbers per μg genomic DNA. *16S* rRNA gene copy numbers per μg genomic DNA **(B)** and cDNA **(C)** throughout the experiment. Results for (left) *Ca. Halichondribacter*-specific *16S* rRNA genes (right), and total *16S* rRNA genes (left). Different experimental groups are indicated by color. Black lines represent median. Significant differences between the start (T0) and the respective days are indicated by asterisk above the days (ANOVA or Schreier-Ray-Hare test). Recolonization and the sponge individual had no effect on copy numbers. **(D)** Relative abundances are shown on phylum level (top 15 phyla), while *Proteobacteria* are resolved in the *Alphaproteobacterium Ca. Halichondribacter symbioticus* and other *Proteobacteria*. **(E)** Betadiversity of microbial communities (non-metric multidimensional scaling plot on weighted UniFrac distances). Treatments are represented by color, with increasing color intensity representing progressing time.



APPENDIX 4.10 | Recolonization by incubation experiment: Alpha diversity before and after recolonization by incubating antibiotic treated sponges with the natural microbiome. **(A)** Pielou evenness **(B)** Shannon index **(C)** Phylogenetic diversity after Faith. Significant differences between the start (T0) and the respective days are indicated by asterisk above the days (ANOVA or Schreier-Ray-Hare test). There were no significant differences between control and recolonized treatment within days. **(D)** Rarefaction curves of observed ASVs. Samples subsampled to 3300 reads. Color depicts treatment.



APPENDIX 4.11 | Antibiotic exposure experiment: results of statistical testing (PERMANOVAs based on weighted UniFrac distances) to assess differences in betadiversity.

Group 1	Group 2	Sample size	Permutations	pseudo-F	p-value	q-value
antibiotic	control	8	999	5.275369	0.03	0.03
antibiotic	start	8	999	14.13381	0.023	0.03
control	start	8	999	2.702103	0.025	0.03

APPENDIX 4.12 | Recolonization by injection experiment: results of statistical testing (BETADISPER analyses and pairwise tests based on weighted UniFrac distances) to assess homogeneity of group dispersion. Only significant pairwise results shown for factors day and treatment.

Subset	Factors	F	p-value
Recolonization	Day	0.774	0.498
	Treatment	0.023	0.887
	Individual	1.878	0.015
Whole dataset	Day	3.572	0.001
	Treatment	28.356	0.001
	Individual	0.221	0.993

Subset	Groups	F	p-value	q-value
Whole dataset	T0-T05	15.75	0.003	0.032
	T0-T06	18.614	0.001	0.018
	T0-T09	14.151	0.001	0.018
	T0-T11	16.908	0.001	0.018
	T0-T12	16.469	0.001	0.018
	T0-T15	17.569	0.001	0.018
	T0-T19	4.508	0.001	0.018
	T05-T10	5.568	0.003	0.032
	T06-T08	6.185	0.002	0.026
	T06-T10	6.129	0.002	0.026
	Recovery – ctrl	14.04	0.001	0.002
	Recovery – inoc	14.79	0.014	0.018
	Recovery – recol	15.621	0.002	0.003
	Recovery – start	69.163	0.001	0.002
	Ctrl – inoc	9.439	0.001	0.002
	Ctrl – start	45.396	0.001	0.002
	Inoc – recol	12.632	0.002	0.003
	Recol – start	56.178	0.001	0.002

APPENDIX 4.13 | Recolonization by injection experiment: results of statistical testing (PERMANOVA analyses and pairwise tests based on weighted UniFrac distances) to assess group dissimilarity. Only significant pairwise results shown for factors day and treatment.

Subset	Factors	F	p-value
Recolonization	Day	8.094	0.001*
	Treatment	0.809	0.519*
	Individual	2.872	0.001
Whole dataset	Day	26.062	0.001
	Treatment	32.813	0.001
	Individual	1.019	0.428*

*homogeneity of variances given (BETADISPER)

Subset	Groups	F	p-value	q-value
Recolonization	T14-T15	3.341	0.001	0.002
	T14-T17	7.647	0.005	0.006
	T14-T19	22.853	0.001	0.002
	T15-T16	3.16	0.003	0.004
	T15-T17	5.42	0.001	0.002
	T15-T19	13.641	0.001	0.002
	T16-T19	9.005	0.001	0.002
	T17-T19	4.64	0.003	0.004
	Whole dataset	T0-T04	4.701	0.003
T0-T05		7.716	0.001	0.002
T0-T06		3.567	0.014	0.016
T0-T07		6.808	0.001	0.002
T0-T08		18.034	0.001	0.002
T0-T09		27.008	0.001	0.002
T0-T10		34.697	0.001	0.002
T0-T11		67.973	0.001	0.002
T0-T12		61.424	0.001	0.002
T0-T14		135.557	0.001	0.002
T0-T15		130.713	0.001	0.002
T0-T16		108.191	0.001	0.002
T0-T17		125.171	0.001	0.002
T0-T19		201.289	0.001	0.002
T04-T08		5.619	0.003	0.004
T04-T09		8.676	0.003	0.004
T04-T10		12.001	0.006	0.007
T04-T11		25.373	0.001	0.002
T04-T12		21.53	0.001	0.002
T04-T14		51.769	0.001	0.002
T04-T15		48.599	0.001	0.002
T04-T16		41.167	0.003	0.004
T04-T17		47.895	0.002	0.003
T04-T19		76.684	0.001	0.002
T05-T08		5.266	0.002	0.003
T05-T09		7.477	0.004	0.005
T05-T10		9.749	0.001	0.002
T05-T11		23.6	0.001	0.002
T05-T12		20.537	0.001	0.002
T05-T14		47.497	0.001	0.002
T05-T15		46.638	0.001	0.002
T05-T16		36.359	0.001	0.002
T05-T17	42.29	0.004	0.005	
T05-T19	71.449	0.001	0.002	
T06-T08	4.522	0.007	0.008	
T06-T09	6.215	0.003	0.004	
T06-T10	7.688	0.004	0.005	
T06-T11	22.501	0.001	0.002	
T06-T12	21.38	0.001	0.002	
T06-T14	44.258	0.001	0.002	

Appendix to Chapter 4

T06-T15	45.72	0.001	0.002
T06-T16	33.891	0.002	0.003
T06-T17	39.028	0.004	0.005
T06-T19	70.186	0.001	0.002
T07-T08	2.482	0.04	0.044
T07-T09	4.633	0.006	0.007
T07-T10	6.494	0.003	0.004
T07-T11	18.08	0.001	0.002
T07-T12	16.271	0.001	0.002
T07-T14	42.761	0.001	0.002
T07-T15	40.939	0.001	0.002
T07-T16	34.388	0.007	0.008
T07-T17	40.826	0.003	0.004
T07-T19	66.817	0.001	0.002
T08-T10	4.322	0.004	0.005
T08-T11	10.998	0.001	0.002
T08-T12	11.565	0.001	0.002
T08-T14	40.375	0.001	0.002
T08-T15	35.923	0.001	0.002
T08-T16	37.73	0.002	0.003
T08-T17	46.222	0.001	0.002
T08-T19	67.809	0.001	0.002
T09-T11	6.988	0.002	0.003
T09-T12	9.969	0.001	0.002
T09-T14	26.378	0.001	0.002
T09-T15	28.594	0.002	0.003
T09-T16	22.893	0.004	0.005
T09-T17	28.115	0.002	0.003
T09-T19	53.811	0.001	0.002
T10-T11	7.788	0.002	0.003
T10-T12	8.235	0.001	0.002
T10-T14	30.402	0.001	0.002
T10-T15	28.039	0.001	0.002
T10-T16	27.809	0.002	0.003
T10-T17	34.795	0.001	0.002
T10-T19	53.813	0.001	0.002
T11-T14	11.395	0.001	0.002
T11-T15	17.214	0.001	0.002
T11-T16	12.723	0.001	0.002
T11-T17	18.643	0.001	0.002
T11-T19	46.16	0.001	0.002
T12-T14	3.348	0.014	0.016
T12-T15	9.242	0.001	0.002
T12-T16	5.035	0.005	0.006
T12-T17	8.314	0.001	0.002
T12-T19	32.012	0.001	0.002
T14-T15	3.09	0.007	0.008
T14-T16	2.592	0.027	0.03
T14-T17	7.788	0.007	0.008
T14-T19	22.251	0.001	0.002
T15-T16	3.382	0.003	0.004
T15-T17	5.142	0.001	0.002
T15-T19	13.342	0.001	0.002
T16-T19	8.571	0.001	0.002
T17-T19	4.009	0.007	0.008
Recovery – ctrl	43.116	0.001	0.001
Recovery – inoc	4.536	0.004	0.004
Recovery – recol	38.233	0.001	0.001
Recovery – start	21.92	0.001	0.001
Ctrl – inoc	24.83	0.002	0.003
Ctrl – start	124.463	0.001	0.001
Inoc – recol	25.393	0.001	0.001
Inoc – start	6.429	0.001	0.001
Recol - start	125.336	0.001	0.001

APPENDIX 4.14 | Recolonization by incubation experiment: results of statistical testing (BETADISPER analyses and pairwise tests based on weighted UniFrac distances) to assess homogeneity of group dispersion. Only significant pairwise results shown for factors day and treatment.

Subset	Factors	F	p-value
Recolonization	Day	13.876	0.001
	Treatment	0.001	0.972
	Individual	< 0.001	0.922
Whole dataset	Day	3.364	0.025
	Treatment	9.322	0.001
	Individual	1.441	0.103

Subset	Groups	F	p-value	q-value
Recolonization	T12-T18	13.876	0.001	0.001
Whole dataset	T11-T18	4.18	0.003	0.009
	T12-T18	13.046	0.001	0.006
	Recovery – inoculum	29.11	0.019	0.035
	Ctrl - inoculum_sponge	14.82	0.001	0.008
	Ctrl – inoculum	34.728	0.002	0.01
	Ctrl – start	14.983	0.001	0.008
	Inoculum_sponge – inoculum	2.5794	0.021	0.035
	Inoculum_sponge – recol	8.508	0.005	0.015
	Inoculum – recol	13.99	0.012	0.026
	Inoculum – start	13.038	0.004	0.015
	Recol – start	7.229	0.008	0.02

APPENDIX 4.15 | Recolonization by incubation experiment: results of statistical testing (PERMANOVA analyses and pairwise tests based on weighted UniFrac distances) to assess group dissimilarity. Only significant pairwise results shown for factors day and treatment.

Subset	Factors	F	p-value
Recolonization	Day	17.922	0.001
	Treatment	0.465	0.83*
	Individual	3.75	0.001*
Whole dataset	Day	19.287	0.001
	Treatment	7.427	0.001
	Individual	6.13	0.001*

*homogeneity of variances given (BETADISPER)

Subset	Groups	F	p-value	q-value
Recolonization	T12-T18	19.287	0.001	0.001
Whole dataset	T0-T12	5.726	0.002	0.0024
	T0-T18	41.351	0.001	0.0015
	T11-T12	9.534	0.001	0.0015
	T11-T12	49.982	0.001	0.0015
	T12-T18	18.465	0.001	0.0015
	Recovery – ctrl	4.376	0.027	0.0368
	Recovery - inoculum_sponge	2.171	0.025	0.0368
	Recovery – inoculum	6.402	0.035	0.0438
	Recovery – recol	4.038	0.014	0.0233
	Recovery – start	1.997	0.042	0.0485
	Ctrl - inoculum_sponge	11.248	0.003	0.0075
	Ctrl – inoculum	13.871	0.001	0.0038
	Ctrl – start	9.746	0.002	0.006
	inoculum_sponge – inoculum	8.731	0.004	0.0086
	inoculum_sponge – recol	11.385	0.001	0.0038
	Inoculum – recol	14.022	0.001	0.0038
	Inoculum – start	11.292	0.006	0.0113
	Recol - start	9.995	0.001	0.0038

APPENDIX 4.16 | Antibiotic exposure experiment: qPCR statistics (ANOVA and Tukey Posthoc tests or Kruskal-Wallice test with Wilcoxon post-hoc test).

DNA Halichondribacter

	Df	Sum Sq	Mean Sq	F	value	Pr(>F)
treatment	2	1.3E+10	6.51E+09	74.81		1.37E-12

	diff	lwr	upr	p adj
control-antibiotic	47154.08	37567.46	56740.69	0
start-antibiotic	16561.33	6974.72	26147.95	0.000517
start-control	-30592.7	-40385.5	-20799.9	0

DNA Eubacteria

	Df	Sum Sq	Mean Sq	F	value	Pr(>F)
treatment	2	76.89	38.45	10.17		0.000363

	diff	lwr	upr	p adj
control-antibiotic	-0.79498	-2.74288	1.152916	0.581168
start-antibiotic	-3.42032	-5.36822	-1.47243	0.000399
start-control	-2.62534	-4.57324	-0.67745	0.006289

RNA Halichondribacter

	Df	Sum Sq	Mean Sq	F	value	Pr(>F)
treatment	2	2.24E+10	1.12E+10	22.98		6.51E-07

	diff	lwr	upr	p adj
control-antibiotic	60793.81	38656.13	82931.49	4E-07
start-antibiotic	25255.71	2620.489	47890.93	0.026116
start-control	-35538.1	-58173.3	-12902.9	0.001473

RNA Eubacteria

	Df	Sum Sq	Mean Sq	F	value	Pr(>F)
treatment	2	16.48	8.239	4.062		0.0265

	diff	lwr	upr	p adj
control-antibiotic	0.025145	-1.40151	1.451796	0.998969
start-antibiotic	-1.42249	-2.84914	0.004164	0.040799
start-control	-1.44763	-2.87428	-0.02098	0.046142

APPENDIX 4.17 | Recolonization by injection experiment: qPCR statistics (2-way ANOVA with Tukey post-hoc test or Scheirer-Ray-Hare test with Dunn post-hoc test; only significant pairwise results shown).

DNA Halichondribacter Whole dataset

	Df	Sum Sq	H	p.value
day	14	77262	38.344	0.00046
individual	15	86096	42.727	0.00017
day:individual	85	112406	55.785	0.99401

Comparison	Z	P.unadj	P.adj
T0 - T10	3.316642	0.000911	0.023915
T0 - T11	3.720113	0.000199	0.010455
T0 - T12	4.764847	1.89E-06	0.000198
T0 - T14	3.566547	0.000362	0.01266

DNA Halichondribacter Recolonization

	Df	Sum Sq	H	p.value
treatment	9	1394.2	5.633	0.77601
individual	14	8252	33.341	0.00257
treatment:individual	30	3471.3	14.026	0.99419

DNA Eubacteria Whole dataset

	Df	Sum Sq	H	p.value
day	14	279621	138.772	0
individual	15	4622	2.294	0.99993
day:individual	85	17101	8.487	1

Comparison	Z	P.unadj	P.adj
T0 - T11	-2.93382	0.003348	0.008789
T0 - T12	-4.60745	4.08E-06	3.29E-05
T0 - T14	-4.41418	1.01E-05	7.6E-05
T0 - T15	-7.00989	2.39E-12	1.25E-10
T10 - T15	-3.69381	0.000221	0.000859
T11 - T15	-3.55607	0.000376	0.001275
T12 - T15	-3.4437	0.000574	0.001721
T0 - T16	-4.87272	1.1E-06	1.28E-05
T10 - T16	-2.81033	0.004949	0.012085
T11 - T16	-2.42453	0.015328	0.03353
T0 - T17	-4.61289	3.97E-06	3.47E-05
T10 - T17	-2.59489	0.009462	0.021598
T0 - T19	-7.52381	5.32E-14	5.59E-12
T10 - T19	-4.07337	4.63E-05	0.00027
T11 - T19	-4.03188	5.53E-05	0.000277
T12 - T19	-4.03396	5.48E-05	0.000288
T11 - T4	2.387403	0.016968	0.035633
T12 - T4	3.344395	0.000825	0.002405
T14 - T4	3.587822	0.000333	0.001207
T15 - T4	5.330326	9.8E-08	1.72E-06
T16 - T4	4.167258	3.08E-05	0.00019
T17 - T4	3.951821	7.76E-05	0.000354
T19 - T4	5.709886	1.13E-08	2.97E-07
T12 - T5	2.836586	0.00456	0.0114
T14 - T5	3.149231	0.001637	0.004646
T15 - T5	4.857208	1.19E-06	1.25E-05
T16 - T5	3.77497	0.00016	0.000672
T17 - T5	3.559533	0.000372	0.0013
T19 - T5	5.236769	1.63E-07	2.45E-06
T11 - T6	2.513642	0.011949	0.026695
T12 - T6	3.485915	0.00049	0.001609
T14 - T6	3.710053	0.000207	0.000837
T15 - T6	5.462178	4.7E-08	9.88E-07
T16 - T6	4.276584	1.9E-05	0.000125
T17 - T6	4.061147	4.88E-05	0.00027
T19 - T6	5.841738	5.17E-09	1.81E-07
T12 - T7	2.72004	0.006527	0.015577
T14 - T7	3.04857	0.002299	0.006191
T15 - T7	4.748624	2.05E-06	1.95E-05
T16 - T7	3.684936	0.000229	0.000858
T17 - T7	3.469499	0.000521	0.001659
T19 - T7	5.128184	2.93E-07	3.84E-06
T14 - T8	2.365518	0.018005	0.037069
T15 - T8	4.011802	6.03E-05	0.000288
T16 - T8	3.073996	0.002112	0.005836
T17 - T8	2.858559	0.004256	0.010899
T19 - T8	4.391362	1.13E-05	7.88E-05
T15 - T9	3.453369	0.000554	0.00171
T16 - T9	2.610967	0.009029	0.021067
T17 - T9	2.39553	0.016596	0.035564
T19 - T9	3.832929	0.000127	0.000554

DNA Eubacteria Recolonization

	Df	Sum Sq	H	p.value
treatment	9	6926.1	27.994	0.00096
individual	14	2808.3	11.351	0.6583
treatment:individual	30	3378.6	13.655	0.9954

Comparison	Z	P.unadj	P.adj
T14Control - T15Recolonization	-2.78238	0.005396	0.040472
T14Recolonization - T15Recolonization	-2.82698	0.004699	0.04229
T14Control - T19Control	-3.38179	0.00072	0.008102
T14Recolonization - T19Control	-3.42639	0.000612	0.009175
T14Control - T19Recolonization	-3.62573	0.000288	0.006483
T14Recolonization - T19Recolonization	-3.67034	0.000242	0.0109

APPENDIX 4.18 | Recolonization by incubation experiment: qPCR statistics (2-way ANOVA with Tukey post-hoc test or Scheirer-Ray-Hare test with Dunn post-hoc test; only significant pairwise results shown).

DNA Halichondribacter Whole dataset

	Df	Sum Sq	H	p.value
day	3	1108.1	8.9727	0.02966
individual	18	2201.4	17.8249	0.46725
day:individual	16	1260	10.2024	0.85585

DNA Halichondribacter Recolonization

	Df	Sum Sq	H	p.value
treatment	3	412.71	6.0992	0.10688
individual	12	890.43	13.159	0.35759
treatment:individual	12	523.86	7.7417	0.80497

DNA Eubacteria Whole dataset

	Df	Sum Sq	H	p.value
day	3	3275.6	26.5228	0.00001
individual	18	817.9	6.6229	0.99294
day:individual	16	476	3.8543	0.99913

Comparison	Z	P.unadj	P.adj
T0 - T12	-2.79254	0.00523	0.010459
T0 - T18	-4.82108	1.43E-06	8.57E-06
T11 - T18	-2.95894	0.003087	0.009261
T12 - T18	-2.61884	0.008823	0.013235

DNA Eubacteria Recolonization

	Df	Sum Sq	H	p.value
treatment	3	768.71	11.3603	0.00993
individual	12	699.43	10.3364	0.58648
treatment:individual	12	358.86	5.3033	0.94707

Comparison	Z	P.unadj	P.adj
T12_recolonized - T18_control	-2.79413	0.005204	0.031223
T12_recolonized - T18_recolonized	-2.30678	0.021067	0.042134

RNA Halichondribacter Whole dataset

	Df	Sum Sq	H	p.value
day	3	325.33	3.697	0.2961
individual	17	1810.17	20.57	0.24611
day:individual	11	592.5	6.733	0.82028

RNA Halichondribacter Recolonization

	Df	Sum Sq	H	p.value
treatment	3	142.12	3.3705	0.33795
individual	11	613.48	14.5489	0.20409
treatment:individual	7	129.9	3.0806	0.87744

RNA Eubacteria Whole dataset

	Df	Sum Sq	H	p.value
day	3	1767.92	20.09	0.00016
individual	17	695.08	7.8987	0.96867
day:individual	11	265	3.0114	0.99057

Comparison	Z	P.unadj	P.adj
T0 - T12	-2.68278	0.007301	0.014603
T0 - T18	-4.09421	4.24E-05	0.000254
T11 - T18	-2.97309	0.002948	0.008844

RNA Eubacteria Recolonization

	Df	Sum Sq	H	p.value
treatment	3	352.2	8.3526	0.03926
individual	11	405.2	9.6094	0.56582
treatment:individual	7	128.1	3.0379	0.88147

Comparison	Z	P.unadj	P.adj
T12_recolonized - T18_control	-2.69741	0.006988	0.041929

APPENDIX 4.19 | Antibiotic exposure experiment: alpha-diversity statistics (ANOVA and Tukey Posthoc tests or Kruskal-Wallis test with Wilcoxon post-hoc test).

Pilou evenness

	Df	Sum Sq	Mean Sq	F	value	Pr(>F)
treatment	2	0.00281	0.001403		0.295	0.751
Residuals	9	0.04275	0.00475			

Shannon diversity

	Df	Sum Sq	Mean Sq	F	value	Pr(>F)
treatment	2	2.255	1.1277		2.952	0.103
Residuals	9	3.439	0.3821			

Faith phylogenetic diversity

	Df	Sum Sq	Mean Sq	F	value	Pr(>F)
treatment	2	262.2	131.08		12.89	0.00228
Residuals	9	91.5	10.17			

	diff	lwr	upr	p adj
control-antibiotic	2.75	-3.54493	9.044925	0.4717729
start-antibiotic	11	4.705075	17.29493	0.0022528
start-control	8.25	1.955075	14.54493	0.0130942

APPENDIX 4.20 | Recolonization by injection experiment: alpha-diversity statistics (ANOVA and Tukey Posthoc tests or Kruskal-Wallis test with Wilcoxon post-hoc test; only significant pairwise results shown).

Pilou evenness Whole dataset

	Df	Sum Sq	Mean Sq	F	value	Pr(>F)
day	14	0.9547	0.06819	21.75		<2e-16

	diff	lwr	upr	p adj
T10-T0	0.098612597	0.006061	0.191164	0.024938
T12-T0	0.136609564	0.077413	0.195806	0
T14-T0	0.126622106	0.048687	0.204558	1.05E-05
T15-T0	0.189625241	0.121271	0.257979	0
T16-T0	0.155579317	0.063028	0.248131	4.2E-06
T17-T0	0.218525354	0.125974	0.311077	0
T19-T0	0.264810254	0.196456	0.333164	0
T12-T04	0.087181874	0.001172	0.173192	0.043472
T15-T04	0.140197552	0.047646	0.232749	5.96E-05
T17-T04	0.169097665	0.057476	0.280719	5.95E-05
T19-T04	0.215382565	0.122831	0.307934	0
T15-T05	0.129721593	0.03717	0.222273	0.000325
T17-T05	0.158621707	0.047	0.270243	0.000244
T19-T05	0.204906606	0.112355	0.297458	0
T12-T06	0.120883972	0.034874	0.206894	0.000307
T14-T06	0.110896515	0.011059	0.210734	0.014922
T15-T06	0.173899649	0.081348	0.266451	1E-07
T16-T06	0.139853725	0.028232	0.251475	0.002552
T17-T06	0.202799763	0.091178	0.314421	4E-07
T19-T06	0.249084663	0.156533	0.341636	0
T15-T07	0.128363678	0.035812	0.220915	0.000401
T17-T07	0.157263791	0.045642	0.268885	0.000292
T19-T07	0.203548691	0.110997	0.2961	0
T12-T08	0.099783179	0.013773	0.185793	0.008289
T15-T08	0.152798856	0.060247	0.24535	6.9E-06
T16-T08	0.118752932	0.007132	0.230374	0.025382
T17-T08	0.181698969	0.070078	0.29332	0.00001
T19-T08	0.227983869	0.135432	0.320535	0
T15-T09	0.135430995	0.042879	0.227983	0.000131
T17-T09	0.164331108	0.05271	0.275953	0.000114
T19-T09	0.210616008	0.118064	0.303168	0
T17-T10	0.119912758	0.008291	0.231534	0.022616
T19-T10	0.166197658	0.073646	0.258749	6E-07
T12-T11	0.066410405	0.000967	0.131854	0.042958
T15-T11	0.119426082	0.045595	0.193257	1.18E-05
T17-T11	0.148326196	0.051659	0.244993	0.000044
T19-T11	0.194611096	0.12078	0.268442	0
T19-T12	0.12820069	0.069004	0.187397	0
T19-T14	0.138188148	0.060253	0.216124	9E-07
T19-T15	0.075185013	0.006831	0.143539	0.016912
T19-T16	0.109230937	0.016679	0.201783	0.006474

Shannon diversity Whole dataset

	Df	Sum Sq	H	p.value
day	12	53586	26.255	0.009877

Comparison	Z	P.unadj	P.adj
T0-T05	-3.08352313	0.002046	0.016523
T0-T10	-2.65196475	0.008002	0.046681

Appendix to Chapter 4

T0-T12	-4.66512126	3.08E-06	8.1E-05
T11-T12	-3.03046271	0.002442	0.018313
T0-T14	-2.28906258	0.022076	0.089152
T0-T15	-4.83248446	1.35E-06	7.08E-05
T08-T15	-2.79742305	0.005151	0.033805
T11-T15	-3.41981102	0.000627	0.007311
T0-T16	-3.48425591	0.000494	0.006477
T0-T17	-4.52461985	6.05E-06	0.000127
T08-T17	-3.11183697	0.001859	0.016269
T11-T17	-3.52683498	0.000421	0.006308
T0-T19	-6.25679567	3.93E-10	4.13E-08
T06-T19	-2.94769784	0.003201	0.02241
T07-T19	-2.73191865	0.006297	0.038891
T08-T19	-3.84934659	0.000118	0.002073
T09-T19	-3.14035783	0.001687	0.016107
T11-T19	-4.73846697	2.15E-06	7.54E-05
T14-T19	-3.19851023	0.001381	0.014505

Faith phylogenetic diversity Whole dataset

	Df	Sum Sq	H	p.value
day	12	88397	43.31	0.00002

Comparison	Z	P.unadj	P.adj
T05-T08	2.709279003	0.006743	0.030783
T04-T11	2.674639498	0.007481	0.030212
T05-T11	3.515767506	0.000438	0.002708
T06-T11	2.68939613	0.007158	0.030064
T07-T11	2.696774446	0.007001	0.030631
T10-T11	2.512316549	0.011994	0.04198
T05-T12	2.909634844	0.003619	0.018093
T04-T14	2.54470121	0.010937	0.0396
T05-T14	3.359119901	0.000782	0.004321
T06-T14	2.558989257	0.010498	0.039366
T07-T14	2.56613328	0.010284	0.039993
T0-T15	3.627298052	0.000286	0.002148
T04-T15	4.229850067	2.34E-05	0.000491
T05-T15	5.108379619	3.25E-07	3.41E-05
T06-T15	4.245262866	2.18E-05	0.000573
T07-T15	4.252969266	2.11E-05	0.000738
T09-T15	3.366733315	0.000761	0.004437
T10-T15	4.060309276	4.9E-05	0.000572
T12-T15	3.759206674	0.00017	0.001627
T15-T16	-3.698108496	0.000217	0.001901
T05-T17	2.766787284	0.005661	0.027019
T0-T19	3.52947448	0.000416	0.002733
T04-T19	4.157602571	3.22E-05	0.000422
T05-T19	5.036132123	4.75E-07	2.49E-05
T06-T19	4.17301537	3.01E-05	0.000451
T07-T19	4.18072177	2.91E-05	0.000509
T09-T19	3.294485819	0.000986	0.005177
T10-T19	3.98806178	6.66E-05	0.000699
T12-T19	3.646249743	0.000266	0.002149
T16-T19	3.625861	0.000288	0.002016

Pilou evenness Recolonization

	Df	Sum Sq	Mean Sq	F	value	Pr(>F)
treatment	9	0.1605	0.017839	5.588		3.99E-05

	diff	lwr	upr	p adj
T19recol-T14ctrl	0.134647	0.02736	0.241934	0.004817
T15ctrl-T14recol	0.109733	0.002446	0.21702	0.041275
T19ctrl-T14recol	0.141729	0.034442	0.249016	0.002486
T19recol-T14recol	0.181212	0.073925	0.288499	4.89E-05
T19recol-T15recol	0.118374	0.024277	0.212471	0.004677
T19recol-T16ctrl	0.139173	0.011765	0.266581	0.022458

Shannon diversity Recolonization

	Df	Sum Sq	Mean Sq	F	value	Pr(>F)
treatment	9	8.44	0.9378		4.644	0.000239

	diff	lwr	upr	p adj
T19recol-T14ctrl	0.878238	0.024943	1.731532	0.039073
T15ctrl-T14recol	1.060971	0.207677	1.914266	0.005402
T17ctrl-T14recol	1.019406	0.015337	2.023474	0.043991
T17recol-T14recol	1.318356	0.066062	2.570649	0.031891
T19ctrl-T14recol	0.955674	0.10238	1.808968	0.017474
T19recol-T14recol	1.42642	0.573126	2.279714	5.93E-05
T19recol-T15recol	0.858126	0.109738	1.606515	0.013658

Faith phylogenetic diversity Recolonization

	Df	Sum Sq	H	p.value
treatment	9	7039	28.441	0.0008

Comparison	Z	P.unadj	P.adj
ctrlT16 - ctrlT19	3.243135	0.001182	0.017733
ctrlT16 - recolT15	3.642169	0.00027	0.012166
ctrlT19 - recolT16	-2.93017	0.003388	0.038113
recolT15 - recolT16	-3.3292	0.000871	0.019597

APPENDIX 4.20 | Recolonization by incubation experiment: alpha-diversity statistics (ANOVA and Tukey Posthoc tests or Kruskal-Wallis test with Wilcoxon post-hoc test; only significant pairwise results shown).

Pilou evenness Whole dataset

	Df	Sum Sq	Mean Sq	F	value	Pr(>F)
day	3	0.07686	0.025621	10.32		5.62E-05

	diff	lwr	upr	p adj
T18-T0	0.078577611	0.01290606	0.14424916	0.0138654
T18-T11	0.137984569	0.06168112	0.21428801	0.0001374
T18-T12	0.071367044	0.02049808	0.12223601	0.0031601

Shannon diversity Whole dataset

	Df	Sum Sq	Mean Sq	F	value	Pr(>F)
day	3	0.841	0.2804	0.948		0.428

Faith phylogenetic diversity Whole dataset

	Df	Sum Sq	H	p.value
day	1	1635.57	13.243	0.000274

Comparison	Z	P.unadj	P.adj
T0 - T18	3.6706938	0.000241893	0.001451358
T11 - T18	2.7095311	0.006737838	0.013475676
T12 - T18	3.6391611	0.000273528	0.000820583

Pilou evenness Recolonization

	Df	Sum Sq	Mean Sq	F	value	Pr(>F)
treatment	3	0.03739	0.012464	5.457		0.00527

	diff	lwr	upr	p adj
T18ctrl-T12ctrl	0.073754	0.003286273	0.14422262	0.0378675
T18recol-T12ctrl	0.086949	0.016481068	0.15741741	0.0116822

Shannon diversity Recolonization

	Df	Sum Sq	Mean Sq	F	value	Pr(>F)
treatment	3	0.518	0.1727	0.633		0.601

Faith phylogenetic diversity Recolonization

	Df	Sum Sq	H	p.value
treatment	3	1086.43	16.056	0.0011

Comparison	Z	P.unadj	P.adj
T12ctrl - T18ctrl	3.606381	0.000310498	0.001862985
T12recol - T18ctrl	3.021562	0.00251474	0.007544219
T12ctrl - T18recol	2.241804	0.024974029	0.049948057

APPENDIX 4.21 | Recolonization by incubation experiment and injection experiment: CFU statistics (2-way ANOVA with Tukey post-hoc test or Scheirer-Ray-Hare test with Dunn post-hoc test; only significant pairwise results shown).

Recolonization by incubation experiment

	Df	Sum Sq	H	p.value
day	8	583467	172.203	0
daytreatment	9	12387	3.656	0.93257
day:daytreatment	198	132619	39.141	1

Comparison	Z	P.unadj	P.adj
10r - 12c	-2.90184848	0.003709679	0.00811
10c - 15c	-2.36531336	0.01801482	0.03489
10r - 15c	-3.39279566	0.000691832	0.00176
10c - 15r	-2.40213439	0.01629972	0.03239
10r - 15r	-3.4296167	0.000604435	0.00157
10c - 1c	3.58917453	0.000331727	0.00091
10r - 1c	2.56169223	0.01041636	0.02125
12c - 1c	5.46354071	4.6673E-08	3.6E-07
12r - 1c	4.15376378	3.27051E-05	0.00013
13c - 1c	4.45008547	8.58361E-06	4.1E-05
13r - 1c	4.0503142	5.11489E-05	0.00018
15c - 1c	5.95448789	2.60888E-09	5E-08
15r - 1c	5.99130892	2.08159E-09	8E-08
10c - 1r	3.1034875	0.001912543	0.00443
12c - 1r	4.97785368	6.42932E-07	4.1E-06
12r - 1r	3.66807675	0.000244382	0.00073
13c - 1r	3.96439844	7.35813E-05	0.00024
13r - 1r	3.56462717	0.000364374	0.00096
15c - 1r	5.46880086	4.53091E-08	4.3E-07
15r - 1r	5.5056219	3.67867E-08	4E-07
10c - 3c	3.3682483	0.000756474	0.0019
10r - 3c	2.340766	0.01924422	0.0368
12c - 3c	5.24261448	1.58317E-07	1.2E-06
12r - 3c	3.93283755	8.3949E-05	0.00027
13c - 3c	4.22915924	2.34566E-05	0.0001
13r - 3c	3.82938797	0.000128462	0.00041
15c - 3c	5.73356166	9.83433E-09	1.5E-07
15r - 3c	5.7703827	7.90917E-09	1.3E-07
10c - 3r	3.58917453	0.000331727	0.00092
10r - 3r	2.56169223	0.01041636	0.02154
12c - 3r	5.46354071	4.6673E-08	3.8E-07
12r - 3r	4.15376378	3.27051E-05	0.00013
13c - 3r	4.45008547	8.58361E-06	4.2E-05
13r - 3r	4.0503142	5.11489E-05	0.00019
15c - 3r	5.95448789	2.60888E-09	5.7E-08
15r - 3r	5.99130892	2.08159E-09	1.1E-07
10c - 4c	3.58917453	0.000331727	0.00094
10r - 4c	2.56169223	0.01041636	0.02183
12c - 4c	5.46354071	4.6673E-08	4E-07
12r - 4c	4.15376378	3.27051E-05	0.00014
13c - 4c	4.45008547	8.58361E-06	4.4E-05
13r - 4c	4.0503142	5.11489E-05	0.00019
15c - 4c	5.95448789	2.60888E-09	6.7E-08
15r - 4c	5.99130892	2.08159E-09	1.6E-07
10c - 4r	3.14732207	0.001647734	0.00394
10r - 4r	2.11983977	0.03401956	0.06426
12c - 4r	5.02168825	5.12193E-07	3.6E-06
12r - 4r	3.71191132	0.0002057	0.00064
13c - 4r	4.00823301	6.11748E-05	0.00021
13r - 4r	3.60846174	0.000308018	0.00091
15c - 4r	5.51263543	3.535E-08	4.5E-07
15r - 4r	5.54945647	2.86559E-08	4E-07

Appendix to Chapter 4

10c - 5c	2.48454338	0.01297177	0.02611
12c - 5c	4.35890957	1.30712E-05	6.1E-05
12r - 5c	3.04913264	0.002295031	0.00524
13c - 5c	3.34545432	0.000821479	0.00203
13r - 5c	2.94568305	0.003222424	0.00715
15c - 5c	4.84985674	1.23551E-06	7.3E-06
15r - 5c	4.88667778	1.02552E-06	6.3E-06
10c - 5r	2.39687425	0.0165356	0.03244
12c - 5r	4.27124043	1.94389E-05	8.7E-05
12r - 5r	2.9614635	0.003061808	0.00689
13c - 5r	3.25778519	0.001122854	0.00273
13r - 5r	2.85801391	0.004263017	0.00919
15c - 5r	4.7621876	1.91506E-06	1E-05
15r - 5r	4.79900864	1.59453E-06	9E-06
10c - 6c	3.58917453	0.000331727	0.00096
10r - 6c	2.56169223	0.01041636	0.02213
12c - 6c	5.46354071	4.6673E-08	4.2E-07
12r - 6c	4.15376378	3.27051E-05	0.00014
13c - 6c	4.45008547	8.58361E-06	4.5E-05
13r - 6c	4.0503142	5.11489E-05	0.0002
15c - 6c	5.95448789	2.60888E-09	8E-08
15r - 6c	5.99130892	2.08159E-09	3.2E-07
10c - 6r	3.1034875	0.001912543	0.0045
12c - 6r	4.97785368	6.42932E-07	4.3E-06
12r - 6r	3.66807675	0.000244382	0.00075
13c - 6r	3.96439844	7.35813E-05	0.00025
13r - 6r	3.56462717	0.000364374	0.00098
15c - 6r	5.46880086	4.53091E-08	4.6E-07
15r - 6r	5.5056219	3.67867E-08	4.3E-07

Recolonization by injection experiment

	Df	Sum Sq	H	p.value
day	7	459704	156.8	0
daytreatment	8	16230	5.536	0.69904
day:daytreatment	176	84035	28.664	1

Comparison	Z	P.unadj	P.adj
11c - 1c	5.64918274	1.61212E-08	1.3E-07
11r - 1c	4.87446999	1.09101E-06	5.7E-06
13c - 1c	5.68499671	1.30815E-08	1.6E-07
13r - 1c	3.76423688	0.000167059	0.00057
17c - 1c	5.71892574	1.072E-08	2.6E-07
17r - 1c	4.73121411	2.23181E-06	9.6E-06
11c - 1r	5.64918274	1.61212E-08	1.4E-07
11r - 1r	4.87446999	1.09101E-06	6E-06
13c - 1r	5.68499671	1.30815E-08	1.7E-07
13r - 1r	3.76423688	0.000167059	0.00059
17c - 1r	5.71892574	1.072E-08	3.2E-07
17r - 1r	4.73121411	2.23181E-06	9.9E-06
11c - 3c	5.64918274	1.61212E-08	1.5E-07
11r - 3c	4.87446999	1.09101E-06	6.2E-06
13c - 3c	5.68499671	1.30815E-08	2E-07
13r - 3c	3.76423688	0.000167059	0.00061
17c - 3c	5.71892574	1.072E-08	4.3E-07
17r - 3c	4.73121411	2.23181E-06	1E-05
11c - 3r	5.64918274	1.61212E-08	1.6E-07
11r - 3r	4.87446999	1.09101E-06	6.5E-06
13c - 3r	5.68499671	1.30815E-08	2.2E-07
13r - 3r	3.76423688	0.000167059	0.00063
17c - 3r	5.71892574	1.072E-08	6.4E-07
17r - 3r	4.73121411	2.23181E-06	1.1E-05
11c - 5c	5.47953761	4.26439E-08	2.8E-07
11r - 5c	4.70482487	2.54084E-06	1.1E-05
13c - 5c	5.51535159	3.48083E-08	2.5E-07
13r - 5c	3.59459175	0.000324901	0.00108

Appendix to Chapter 4

17c - 5c	5.54928061	2.86848E-08	2.2E-07
17r - 5c	4.56156898	5.07728E-06	2E-05
11c - 5r	5.64918274	1.61212E-08	1.8E-07
11r - 5r	4.87446999	1.09101E-06	6.9E-06
13c - 5r	5.68499671	1.30815E-08	2.6E-07
13r - 5r	3.76423688	0.000167059	0.00065
17c - 5r	5.71892574	1.072E-08	1.3E-06
17r - 5r	4.73121411	2.23181E-06	1.1E-05
1c - 7c	-3.59082186	0.000329637	0.00096
1r - 7c	-3.59082186	0.000329637	0.00099
3c - 7c	-3.59082186	0.000329637	0.00101
3r - 7c	-3.59082186	0.000329637	0.00104
5c - 7c	-3.42117674	0.000623508	0.00178
5r - 7c	-3.59082186	0.000329637	0.00107
11c - 7r	2.37691673	0.01745803	0.03174
13c - 7r	2.4127307	0.01583351	0.02923
17c - 7r	2.44665973	0.01441869	0.02704
1c - 7r	-3.27226601	0.001066891	0.00246
1r - 7r	-3.27226601	0.001066891	0.00251
3c - 7r	-3.27226601	0.001066891	0.00256
3r - 7r	-3.27226601	0.001066891	0.00261
5c - 7r	-3.10262088	0.001918152	0.00426
5r - 7r	-3.27226601	0.001066891	0.00267
11c - 9c	2.66908334	0.007605858	0.01449
13c - 9c	2.70489731	0.006832551	0.01322
17c - 9c	2.73882633	0.006165893	0.01213
1c - 9c	-2.9800994	0.002881549	0.00586
1r - 9c	-2.9800994	0.002881549	0.00596
3c - 9c	-2.9800994	0.002881549	0.00607
3r - 9c	-2.9800994	0.002881549	0.00617
5c - 9c	-2.81045428	0.004947162	0.00989
5r - 9c	-2.9800994	0.002881549	0.00629
11c - 9r	2.29397911	0.0217917	0.0379
13c - 9r	2.32979308	0.01981709	0.03497
17c - 9r	2.36372211	0.01809238	0.0324
1c - 9r	-3.35520363	0.000793066	0.00202
1r - 9r	-3.35520363	0.000793066	0.00207
3c - 9r	-3.35520363	0.000793066	0.00211
3r - 9r	-3.35520363	0.000793066	0.00216
5c - 9r	-3.1855585	0.001444749	0.00327
5r - 9r	-3.35520363	0.000793066	0.00221

EIDESSTATTLICHE ERKLÄRUNG

Hiermit erkläre ich, Lara Schmittmann (geboren am 21.05.1991 in Ahlen), dass ich die vorliegende Dissertation bis auf die Beratung durch meine BetreuerIn in Inhalt und Form selbstständig angefertigt habe. Ich versichere, dass ich diese Arbeit unter Einhaltung der Regeln guter wissenschaftlicher Praxis der Deutschen Forschungsgemeinschaft verfasst habe. Alle benutzten Quellen und Hilfsmittel habe ich vollständig angegeben und die Zusammenarbeit mit anderen WissenschaftlerInnen habe ich kenntlich gemacht. Weder diese noch eine ähnliche Arbeit wurden an einer anderen Abteilung oder Hochschule im Rahmen eines Prüfungsverfahrens vorgelegt, veröffentlicht oder zur Veröffentlichung eingereicht. Mir wurde kein akademischer Grad entzogen und dies ist mein erstes und einziges Promotionsverfahren.

Kiel, 15.12.2021 l.schmittmann

Kiel, den 15.12.2021 Lara Schmittmann